

Pyrolysis-Catalysis of Plastic Wastes for Production of Liquid Fuels and Chemicals

By

Chika Muhammad

Submitted in accordance with the requirements for the degree of
Doctor of Philosophy

The University of Leeds
School of Chemical and Process Engineering
Energy Research Institute
October 2015

The candidate confirms that the work submitted is his own, except where work which has formed part of jointly-authored publications has been included. The contribution of the candidate and the other authors to this work has been explicitly indicated below. The candidate confirms that appropriate credit has been given within the thesis where reference has been made to the work of others. *Further details of the jointly-authored publications and the contributions of the candidate and the other authors to the work should be included below this statement.*

This copy has been supplied on the understanding that it is copyright material and that no quotation from the thesis may be published without proper acknowledgement.

Journal Papers

1. Muhammad, C., Onwudili, J.A. and Williams, P.T. (2015). Catalytic pyrolysis of waste plastic from electrical and electronic equipment. *Journal of Analytical and Applied Pyrolysis*, 113, p. 332-339.
2. Muhammad, C., Onwudili, J.A. and Williams, P.T. (2015). Thermal degradation of Real-world Waste Plastics and Simulated Mixed Plastics in a Two-stage Pyrolysis-Catalysis Reactor for Fuel Production. *Energy & Fuels*, 15, 29(4), p. 2601-2609.

The candidate (Chika Muhammad) performed the experimental and analytical work, wrote the initial drafts of the papers along with supporting materials including Tables and Figures, and carried out the calculation and summarization of the results and developed the discussion part.

The co-authors Professor P.T. Williams and Dr J.A. Onwudili supervised and supported the entire research work, proofread the drafts and made suggestions and corrections to the draft papers.

The right of Chika Muhammad to be identified as Author of this work has been asserted by his in accordance with the Copyright, Design and Patents Act 1988

© 2015 The University of Leeds and Chika Muhammad

Acknowledgement

Praise be to Almighty Allah (SWT) my only hope for enabling me to accomplish this studies, May He continue to support me, Ameen.

My sincere gratitude goes to my main supervisor, Professor Paul T. Williams for his effort in getting me to this stage by meaningful criticisms and suggestions. I appreciate him for his caring attitude, patience and for being available at any time.

Similar recognition and appreciation go to Dr Jude A. Onwudili (Co-supervisor), especially for believing in me in times of difficulties and for his patience.

Also to mention are other staff Dr Cunliffe, Sara, Dr Nahil, Dr Wu, David , Ed WoodHouse and James, for their support. I am grateful for all the memorable times spent with my colleagues; Dr Ibrahim, Dr Qari, Dr Paula Blanco, Dr Chidi Efika, Eyup, Amal, Jonathan, Yeshui, Juniza and Ramzi. I also would like to thank Dr Abdulmajeed, Dr Aminu Aliyu Gulmare and their families, as well as my fellow brothers in NMF UK, for their special friendship during my studies.

My gratitude also goes to Professor Abdullahi Abdu Zuru (VC Usmanu Danfodiyo University, Sokoto), Professor U.A. Birnin Yauri, Professor SM Dangwagwo, Professor LG Hassan, B U Bagudo, Associate Professor A Uba, Dr. Dabai, Nuraddeen, Sani, Misbahu, Abdullah and other academic and non-academic staff of the Chemistry Department, Usmanu Danfodiyo University Sokoto. I appreciate you all.

I am also indebted to my employers, Usmanu Danfodiyo University, Sokoto for granting me study leave to pursue this study.

I am particularly grateful to the Petroleum Development Technology Funds (PTDF), Abuja whose scholarship award allowed me to pursue this study. In addition, I also thank the Sokoto State Government for their help through the state scholarships scheme. To my former students, Shehu Umar, Mukhtar and Farooq Atiku, your contributions are appreciated.

Finally, I will like to recognize my family without whom this research work may not have been successful, my wife Shafaatu Magaji Sule, my daughters Hauwau (Walida), Asmau (Aunty), and Sayyada Fatima (Umami), and their junior brothers, Muhammad Salim and Sulaiman (Abba)- a gift from the Almighty while in UK. Many thanks to my brothers; Hamza, Musa, Aliyu, Hamza, Musa, Ahmad (wadata) Yahaya, Aminu, Umar, Badamasi and sisters; Umaima, Halima, Hadiza and Zuwaira, Ummu khairi, Amina, Saudatu, Asmau, Maryam, Saratu. A special mention to our mothers; Hajiya Aishatu (Yaya) and Malama Aishatu (whom we lost recently). My special gratitude goes to Alhaji Ibrahim Dangaskiya and his family for their support. I dedicate this research work to my late parents, Alhaji Muhammadu (Nalailai) Kofar Rini and Hajiya Fatima (Yar-Alkali), all of Sokoto, Nigeria

ABSTRACT

The use of pyrolysis as a waste disposal method for waste plastics has been well established. However, the market value of the recycled plastic products and separate upgrading of the pyrolysis product liquid are some of the challenges facing the process. Therefore, the use of pyrolysis-catalysis of waste plastic in a two-stage pyrolysis-catalysis reactor system could bring a balance between sustainability and market value of the products generated.

Hence, this work investigated the influence of different types of zeolite catalysts on the pyrolysis-catalytic upgrading of waste plastics for quality liquid fuels and valuable chemical production.

Initially, two zeolite Y and ZSM-5 catalysts, in the form of pellets, were used for pyrolysis-catalysis of WEEE. Zeolite catalyst with a lower Si-Al ratio (Y zeolite) produced a higher conversion of the styrene to other aromatic products, particularly benzene and toluene. Thereafter, the influence of six zeolite catalysts with different surface areas and Si: Al ratios was investigated on the catalytic pyrolysis of waste high-density polyethylene (HDPE). Overall, the results suggest that the catalyst properties influenced the conversion of HDPE to more valuable products such as fuel-range hydrocarbons and chemicals. Similarly, pyrolysis of real-world mixed plastics, simulated mixed plastic (SMP), and virgin plastics were investigated in the presence of HZSM-5 catalyst. In addition, a sample of spent FCC catalyst was also tested for the pyrolysis of the plastic samples.

Finally, the influence of spent FCC, fresh zeolite Y and ZSM-5 catalysts was investigated under different bed temperatures from 400 – 600 °C. This final

work confirmed that the choice of a bed temperature of 500 °C, for most of this research was appropriately justified.

Overall, the product oils gave fuel properties similar to gasoline, the aromatic content of the oil make them suitable as chemical feedstocks, the gas products with very high-calorific values can be used as fuel gas.

Table of content

Acknowledgement.....	II
Table of content	VI
List of Tables.....	XVIII
List of equation.....	XX
Abbreviation	XXI
Chapter 1 INTRODUCTION	23
1.1 Introduction	23
1.1.1Plastics.....	23
1.1.2Sources of Plastics waste	24
1.1.2.1 Municipal Plastic Waste	24
1.1.2.2 Industrial Plastic Waste.....	25
1.1.3Plastic Wastes Disposal	25
1.1.3.1 Landfilling.....	25
1.1.3.2 Mechanical recycling.....	25
1.1.3.3 Biological recycling	26
1.1.3.4 Incineration	26
1.1.3.5 Chemical recycling.....	26
1.1.3.6 Cracking/pyrolysis.....	26
1.1.3.7 Pyrolysis.....	27
1.1.3.8 Thermal Degradation of Plastics or Polymer	28
1.1.4Catalysis	29
1.1.4.1 What is catalysis?	29
1.1.4.2 Historical background	30
1.1.4.3 Application	30
1.1.5Description of Catalyst	31
1.1.5.1 Introduction	31
1.1.5.2 Kinetics	32
1.1.5.3 Surfaces.....	34
1.1.6Zeolites	34
1.1.6.1 Structure and composition	34
1.1.6.2 Acidic properties of zeolites	36
1.1.6.3 Synthesis	36
1.1.6.4 Fine turning with addition of modifiers.....	37

1.1.6.5 Zeolite selectivity.....	38
1.1.6.6 Applications of zeolites	40
Reference.....	43
Chapter 2 LITERATURE REVIEW	45
2.1 Thermal Degradation of Plastics	45
2.2 Thermal Degradation of Single Plastics	45
2.2.1 Polyethylene (PE)	45
2.2.2 Polypropylene (PP)	48
2.2.3 Polystyrene (PS)	50
2.2.4 Poly (ethylene terephthalate) (PET)	52
2.2.5 Polyvinyl Chloride (PVC)	55
2.2.6 Acrylonitrile butadiene styrene (ABS).....	56
2.2.7 High Impact Polystyrene (HIPS).....	57
2.3 Thermal Degradation of Mixed Plastics.....	59
2.4 Catalytic Pyrolysis of Plastics.....	60
2.5 Catalytic Degradation of Single Plastics.....	61
2.5.1 Polyethylene.....	61
2.5.2 Polypropylene	63
2.5.3 Polystyrene	64
2.6 Catalytic Degradation of Mixed Plastics	65
2.7 Reactor types	78
2.7.1 Batch/semi-batch reactor	78
2.7.2 Fixed bed reactor	79
2.7.3 Fluidized bed reactor.....	81
2.7.4 Spouted bed reactor.....	84
References.....	87
Chapter 3 MATERIALS AND METHODS	94
3.1 Introduction	94
3.2 Materials	94
3.2.1 Virgin Plastics.....	94
3.2.2 Real-world Mixed Plastics	94
3.2.3 Waste HDPE	94
3.2.4 Simulated mixture of Plastics (SMP)	95
3.2.5 Future Simulated mixture of Plastics (FSMP).....	95
3.2.6 Waste Electrical and Electronic Equipment (WEEE)	95

3.2.7	Catalyst.....	96
3.2.7.1	Pellet Catalysts	96
3.2.7.2	Powdered Catalysts	97
3.2.7.3	Spent FCC	98
3.3	Plastic Sample Characterization	98
3.3.1	Elemental Analysis of Plastics.....	98
3.3.2	Thermogravimetric Analysis (TGA)	99
3.4	Two-stage pyrolysis-catalytic fixed bed bench reactor	101
3.4.1	Reactor Set-up & Experimental procedure.....	101
3.4.2	Experiment Reproducibility and Selection of process conditions	103
3.5	Characterization of materials and products.....	104
3.5.1	Analysis of products gases	104
3.5.2	Permanent gases	105
3.5.3	Hydrocarbon gases	106
3.5.4	Calibration of Gas Chromatography (GC) Analysis...	107
3.5.5	Reproducibility of the standard gas injection.....	109
3.5.5.1	Permanent Gases	109
3.5.5.2	Hydrocarbon gases.....	110
3.5.6	Calculation of Gas Concentration.....	111
3.5.7	Liquid Products Analysis	113
3.5.7.1	Sample Preparation	113
3.5.7.2	Gas Chromatography/ Mass Spectrometry (GC-MS).....	113
3.5.7.3	Gas Chromatography FID Liquid Injection..	115
3.5.7.4	Simulated Distillation.....	118
3.5.8	Characterization of Catalysts	119
3.5.8.1	Surface Area by Brunauer-Emmet-Teller (BET) Method.....	119
3.5.8.2	Determination of microspore volume by Dubinin-Radushkevich (DR) method.....	121
3.5.8.3	Barrett, Joyner & Halenda (BJH) method for total pore volume and pore diameter.....	122
3.5.8.4	Temperature Programmed oxidation (TGA-TPO).....	123
3.5.8.5	Scanning Electron Microscopy (SEM).....	124
	References.....	127

Chapter 4 THERMAL AND CATALYTIC PYROLYSIS OF WASTE PLASTIC FROM ELECTRICAL AND ELECTRONIC EQUIPMENT	129
4.1 Introduction	129
4.2 Elemental composition of the WEEE and characteristic of catalyst.....	129
4.2.1 Elemental composition of the WEEE.....	130
4.2.2 Characteristic properties of the zeolite catalysts	131
4.3 Pyrolysis-catalysis results	131
4.3.1 Product Yields and Gas composition	131
4.4 Oil Composition.....	138
4.5 Summary	152
References.....	154
Chapter 5 : INFLUENCE OF ZEOLITE CATALYST CHARACTERISTICS ON THE CATALYTIC PYROLYSIS OF WASTE HIGH-DENSITY POLYETHYLENE.....	158
5.1 Introduction	158
5.2 Influence of Zeolite Y characteristics on the catalytic degradation of HDPE wastes	163
5.2.1 Influence of zeolite Y catalysts surface area on the catalytic degradation of waste HDPE	163
5.2.1.1 Product Yields.....	163
5.2.1.2 Gas composition	165
5.2.1.3 Oil composition	167
5.2.1.4 Summary.....	173
5.2.2 Influence of silica: alumina ratio of the Y zeolite on catalytic degradation of waste HDPE	173
5.2.2.1 Gas Composition	174
5.2.2.2 Summary.....	181
5.2.3 Influence of silica: alumina ratio of the ZSM-5 zeolite on catalytic degradation of waste HDPE.....	181
5.2.3.1 Products Yield.....	181
5.2.3.2 Gas Composition	182
5.2.3.3 Summary.....	189
5.3 Comparing influence of Zeolite Y and ZSM-5 catalysts.....	190
5.3.1 Gas Composition.....	191
5.4 Summary	196
References.....	198

Chapter 6 : THERMAL DEGRADATION OF REAL-WORLD WASTE PLASTICS AND SIMULATED MIXED PLASTIC FOR FUEL PRODUCTION	200
6.1 Introduction	200
6.2 Mixed plastic Characterization	202
6.3 Product Yield.....	204
6.4 Gas Composition:.....	209
6.5 Oil Composition:.....	213
Summary	231
References.....	232
Chapter 7 : PYROLYSIS-CATALYSIS OF REAL-WORLD WASTE PLASTICS AND FUTURE SIMULATED MIXED PLASTIC FOR VALUABLE PRODUCTION FUELS AND CHEMICAL FEEDSTOCK.....	235
7.1 Introduction	235
7.2 Product Yields.....	238
Summary	255
References.....	256
Chapter 8 : INFLUENCE OF CATALYST BED TEMPERATURE AND CATALYST TYPE ON PYROLYSIS OF FUTURE SIMULATED MIXED PLASTICS (FSMP).....	259
8.1 Introduction	259
8.2 Influence of FCC bed temperature.....	261
8.2.1Product Yields.....	261
8.2.2Gas composition	264
8.3 The influence of catalyst type and bed temperatures for the pyrolysis-catalysis on the future simulated mixed plastic.....	270
8.3.1Product Yields.....	271
8.3.2Gas composition	273
8.3.3Product oils composition	277
Summary	285
References.....	287
Chapter 9 CONCLUSIONS AND SUGGESTIONS FOR FUTURE WORK.....	290
9.1 General conclusion	290
9.1.1Thermal and Catalytic Pyrolysis of Waste Plastic from Electrical and Electronic Equipment.....	290

9.1.2	Influence of Zeolite Catalysts Characteristics on the Catalytic Pyrolysis of Waste High-Density Polyethylene.....	291
9.1.3	Thermal degradation of real-world waste plastics and simulated mixed plastic for fuel production.....	293
9.1.4	Pyrolysis-Catalysis of real-world waste plastics and future simulated mixed plastic (FSMP) for valuable production fuels and chemical feedstock	294
9.1.5	Influence of catalyst bed temperature and catalyst type on pyrolysis of future simulated mixed plastics (FSMP).....	295
9.1.6	General remarks	296
9.2	Future work	297
9.2.1	Life cycle studies of the catalysts used	297
9.2.2	Use of mesoporous zeolite catalyst and metallic doping of the catalyst	298
9.2.3	Pyrolysis-catalysis of contaminated plastics and co-pyrolysis of biomass and plastics.....	298

Figure 1.1-2 Three temperature ranges of pyrolysis	27
Figure 1.1-2 Energy profile	33
Figure 1.1-3 Zeolite structure	35
Figure 3.3-1 The Flash 2000 CHNS-O Analyzer.....	99
Figure 3.3-2 The 50A Thermogravimetric Analyzer Instrument.....	100
Figure 3.3-3 A typical TGA-DTG plot of Polyethylene	100
Figure 3.4-1 Schematic diagram for two stage Pyrolysis-catalysis reactor.....	102
Figure 3.4-2 Assembled and main part of the pyrolysis-catalysis reactor.....	103
Figure 3.5-1 General schematic diagram for typical GC	105
Figure 3.5-2 GC-/TCD for CO ₂ gas analysis.....	106
Figure 3.5-3 GC-FID for Hydrocarbon gases analysis.....	107
Figure 3.5-4 A GC response peaks for a standard gas mixture of hydrocarbon (alkane) gases.....	108
Figure 3.5-5 A GC response peaks for a standard gas mixture of hydrocarbon (alkene) gases.....	108
Figure 3.5-6 A GC response peaks for a standard gas mixture of permanent gases (H ₂ , O ₂ , N ₂ and CO).....	109
Figure 3.5-7 GC-MS chromatogram for thermal Pyrolysis of PE.....	114
Figure 3.5-8 Calibration curve for the standard aromatic and PAH injected into GC-FID.....	117
Figure 3.5-9 Peak response for standard aromatic and PAH injected into GC-FID.....	118
Figure 3.5-10 BET surface area and pore size analyzer NOVA 2200e	121
Figure 3.5-11 Toledo Mettler TGA-DTS.....	124
Figure 3.5-12 Schematic diagrams for SEM.....	125
Figure 3.5-13 (a) Coater and (b) LEO SEM	126
Figure 4.3-1 Product yield from the pyrolysis and pyrolysis-catalysis of CRT and Fridge plastics with Zeolite Y and ZSM-5 catalysts.....	132
Figure 4.3-2 Product yield from the pyrolysis and pyrolysis-catalysis of HIPS and ABS plastics with Zeolite Y and ZSM-5 catalysts.....	132
Figure 4.3-3 Degradation or transformation of Polystyrene scheme 1	133
Figure 4.3-4 Degradation or transformation of Polystyrene scheme 2	134

Figure 4.4-1 Aromatic compounds (AR) composition for oil from pyrolysis of CRT and Fridge plastics (1R = single ring; 2R = two rings; 3R = three rings; 4R = four rings aromatic compounds).....	139
Figure 4.4-2 Aromatic compounds (AR) composition for oil from pyrolysis of HIPS.....	140
Figure 4.4-3 Relative proportions of the main aromatic compounds in the oil derived from the pyrolysis of CRT and Fridge plastics.....	141
Figure 4.4-4 Relative proportions of the main aromatic compounds in the oil derived from the pyrolysis of HIPS and ABS plastic	142
Figure 4.4-5 Gas Chromatograms for (a) the product oil from pyrolysis catalysis of HIPS with ZSM-5 zeolite catalyst, (b) the product oil from pyrolysis catalysis of HIPS with Y zeolite catalyst and (c) the pyrolysis oil derived from uncatalysed pyrolysis of HIP	143
Figure 4.4-6 Gas Chromatograms for (a) the product oil from pyrolysis catalysis of ABS with ZSM-5 zeolite catalyst, (b) the product oil from pyrolysis catalysis of ABS with Y zeolite catalyst and (c) the pyrolysis oil derived from uncatalysed pyrolysis of ABS	144
Figure 4.4-7 Catalytic addition of H on aromatic ring give rise to two ions (a) and (b); after β -scission of ion (b) benzene is produced and polymer ion (I)[31]	150
Figure 4.4-8 The ion (a) undergo β -scission or internal rearrangement by H ⁻ ion shift follows by β -scission to produced styrene or and α -methyl styrene respectively.[31].....	151
Figure 5.2-1 Gases produced from non-catalytic and catalytic pyrolysis of HDPE waste with Y zeolite with varying surface area.....	165
Figure 5.2-2 Fuel range (C ₅ – C ₁₅) and high molecular weight (C ₁₆₊) hydrocarbons from the pyrolysis-catalysis of HDPE in relation to surface areas of Y-zeolite catalysts	167
Figure 5.2-3 Aliphatic and aromatic content of the product oil from the pyrolysis-catalysis of HDPE in relation to surface areas of Y-zeolite catalysts	168
Figure 5.2-4 Yields of selected aromatic compounds in the oils produced from the pyrolysis-catalysis of HDPE in relation to surface areas of Y-zeolite catalysts.....	169
Figure 5.2-5 Reaction pathways for the catalytic cracking of waste plastics [1]	171
Figure 5.2-6 Simulated distillation of pyrolysis oils from the pyrolysis-catalysis of HDPE in relation to surface areas of Y-zeolite catalysts.....	172

Figure 5.2-7 Gases produced from non-catalytic and catalytic pyrolysis of HDPE with Y zeolite with varying Si: Al ratio.....	174
Figure 5.2-8 Fuel range (C ₅ – C ₁₅) and high molecular weight (C ₁₆₊) hydrocarbons from HDPE in relation to Si:Al ratio of zeolite Y catalysts	176
Figure 5.2-9 Aliphatic and aromatic content of the product oils from HDPE in relation to Si:Al ratio of zeolite Y catalysts.....	178
Figure 5.2-10 Yields of selected aromatic compounds in the oils from HDPE in relation to Si:Al ratio of zeolite Y catalysts.....	179
Figure 5.2-11 Simulated distillation of uncatalyzed pyrolysis oils from the pyrolysis-catalysis of HDPE in relation to Si:Al ratio of Y-zeolite catalysts.....	180
Figure 5.2-12 Gases produced from non-catalytic and catalytic pyrolysis of HDPE waste with ZSM-5 with varying Si: Al ratio....	183
Figure 5.2-13 Fuel range (C ₅ – C ₁₅) and high molecular weight (C ₁₆₊) hydrocarbons from the pyrolysis-catalysis of HDPE in relation to Si:Al ratio of ZSM-5 zeolite catalysts	184
Figure 5.2-14 Aliphatic and aromatic content of the product oil from the pyrolysis-catalysis of HDPE in relation to Si:Al ratio of ZSM-5 zeolite catalysts.....	186
Figure 5.2-15 Yields of selected aromatic compounds in the oils produced from the pyrolysis-catalysis of HDPE in relation to Si:Al ratio of ZSM-5 zeolite catalysts.....	187
Figure 5.2-16 Mechanistic diagram for catalytic degradation of HDPE	188
Figure 5.2-17 Simulated distillation of uncatalyzed pyrolysis oil and pyrolysis-catalysis derived the oil from the pyrolysis-catalysis of HDPE in relation to Si:Al ratio of ZSM-5 zeolite catalysts.....	189
Figure 5.3-1 Gases produced from non-catalytic and catalytic pyrolysis of HDPE waste with Y zeolite and ZSM-5	191
Figure 5.3-2 Fuel range (C ₅ – C ₁₅) and high molecular weight (C ₁₆₊) hydrocarbons from the pyrolysis-catalysis of HDPE in relation to zeolite structure	192
Figure 5.3-3 Aliphatic and aromatic content of the product oil from the pyrolysis-catalysis of HDPE in relation to zeolite structure	193
Figure 5.3-4 Yields of selected aromatic compounds in the oils produced from the pyrolysis of HDPE in relation to zeolite structure	194
Figure 5.3-5 Simulated distillation of uncatalyzed pyrolysis oil and pyrolysis-catalysis derived the oil from the pyrolysis-catalysis of HDPE in relation to zeolite structure.....	195

Figure 6.2-1 Thermogravimetric Analysis for (a) Virgin Plastics, (b) Real-world mixed plastics (MP) and(c) Simulated mixed plastic (SMP).....	203
Figure 6.3-1 Product yield and mass balance (MB) for non-catalytic (a) and catalytic (b) pyrolysis of real world plastics (MP), the simulated mixture of plastics (SMP) and virgin plastics (PE, PP, PS, PET).....	205
Figure 6.3-2 SEM analysis of the fresh and reacted HZSM-5 after pyrolysis for the plastic samples.....	208
Figure 6.4-1 Gases produced from (a) non-catalytic (b) catalytic pyrolysis of real world plastics (MP), the simulated mixture of plastics (SMP) and virgin plastics (PE, PP, PS, PET).....	209
Figure 6.5-1 Influence of HZSM-5 on the distribution of fuel range (F.R.) and high molecular weight (HMWt) compounds in non-catalysed (a) and catalysed (b) product oil from processing MP, SMP and virgin plastics (PE, PP, PS, PET) in comparison to gasoline.....	213
Figure 6.5-2 Simulated distillation of (a) the uncatalyzed pyrolysis oil and (b) the pyrolysis-catalysis product oils.	215
Figure 6.5-3 Distribution of aliphatic and aromatics hydrocarbons in (a) non-catalysed and (b) catalysed (b) product oil from processing of real world plastics (MP), the simulated mixture of plastics (SMP) and virgin plastics (PE, PP, PS, PET).	216
Figure 6.5-4 Jing et. al.[18] proposed interaction scheme by enhanced intermolecular hydrogen transfer.	218
Figure 6.5-5 Initiation mechanism of HDPE via carbenium ion [15]... 	221
Figure 6.5-6 Cyclization and aromatization as termination step for degradation mechanism of the polymer	224
Figure 6.5-7 Yields of some selected aromatic compounds in (a) non-catalysed and (b) catalysed (b) product oil from processing of real world plastics (MP), the simulated mixture of plastics (SMP) and, virgin plastics (PE, PP, PS, PET).	227
Figure 6.5-8 Aguado et. al,[30] proposed reaction pathways in the (catalytic) conversion of polyolefins mixtures	230
Figure 7.2-1 Product yield for (a) FCC1 and (b) FCC2 catalytic pyrolysis of real-world (MP), the future simulated mixture of plastics (SMP), and virgin plastics (HDPE, LDPE,PP,PS and PET).....	239
Figure 7.2-2 Gases produced from non-catalytic (a) FCC1 (b) and FCC2 catalyzed (c) pyrolysis of real-world (MP), the future simulated mixture of plastics (FSMP), and virgin plastics (HDPE,LDPE,PP,PS and PET)	244

Figure 7.2-3 Distribution of fuel range and high molecular weight hydrocarbons for (a) non-catalytic (b) FCC1 and (c) FCC2 catalytic pyrolysis of MP, FSMP and virgin plastics	246
Figure 7.2-4 Distribution of aliphatic and aromatic hydrocarbons for (a) non-catalytic (b) FCC1 (c) FCC2 pyrolysis of MP, SMP, and virgin plastics (HDPE,LDPE,PP,PS and PET).....	248
Figure 7.2-5 Yield of some selected aromatic compounds for (a) non-catalytic (b) FCC1 (c) FCC2 pyrolysis of real-world (MP), the future simulated mixture of plastics (FSMP), and virgin plastics (HDPE,LDPE,PP,PS and PET)	250
Figure 7.2-6 Simulated distillation of for (a) non-catalytic (b) FCC1 (c) FCC2 pyrolysis of real-world (MP), the future simulated mixture of plastics (FSMP), and virgin plastics (HDPE,LDPE,PP,PS and PET)	253
Figure 8.2-1 Product yield for non-catalytic and catalytic pyrolysis of the future simulated mixture of plastics (FSMP) at 400 °C.....	262
Figure 8.2-2 A schematic representation of two stage reaction system by Aguado et al.	263
Figure 8.2-3 Gas composition from non-catalytic (a) and catalytic (b) pyrolysis of the future simulated mixture of plastics (FSMP).....	265
Figure 8.2-4 Distribution of Fuel range (C₅ – C₁₅) and high molecular weight (C₁₆₊) hydrocarbons for (a) non-catalytic and (b) catalytic pyrolysis of the future simulated mixture of plastics (FSMP) at 400 °C	267
Figure 8.2-5 Distribution of aliphatic and aromatics hydrocarbon for (a)non-catalytic and (b) catalytic pyrolysis of the future simulated mixture of plastics (FSMP)	268
Figure 8.2-6 Simulated distillation of (a) thermal and (b) catalytic pyrolysis product oils from FSMP.....	270
Figure 8.3-1 Product yield for non-catalytic and catalytic pyrolysis of the future simulated mixture of plastics (FSMP) at (a) 500 °C and (b) 600 °C catalyst bed temperature	271
Figure 8.3-2 Gas composition from non-catalytic and catalytic pyrolysis of the future simulated mixture of plastics (SMP) at (a) 500 °C and (b) 600 °C catalyst bed temperature.....	275
Figure 8.3-3 Distribution of Fuel range (C₅ – C₁₅) and high molecular weight (C₁₆₊) hydrocarbons for non-catalytic and catalytic pyrolysis of the future simulated mixture of plastics (FSMP) at (a) 500 °C and (b) 600 °C catalyst bed temperature	278
Figure 8.3-4 Distribution of aliphatic and aromatics hydrocarbon for non-catalytic and catalytic pyrolysis of the future simulated mixture of plastics (FSMP) at (a) 500 °C and (b) 600 °C catalyst/sand bed temperature	280

Figure 8.3-5 Yield of some selected aromatic compounds for non-catalytic and catalytic pyrolysis of the future simulated mixture of plastics (FSMP) at (a) 500 °C and (b) 600 °C catalyst/sand bed temperature	282
Figure 8.3-6 Diels-Alder reaction of alkenes	283
Figure 8.3-7 Simulated distillation of (a) 500 °C and (b) 600 °C bed temperature thermal and catalytic pyrolysis product oils from FSMP	284

List of Tables

Table 3.2-1 Zeolite Y and ZSM-5 Catalysts used in the research work.....	97
Table 3.2-2 Characteristic of spent FCC catalyst by Hall et al.	98
Table 3.5-1 Peak Area values for the standard of permanent gases .	110
Table 3.5-2 Peak Area values for the standard of hydrocarbon gases.....	111
Table 3.5-3 the various standard aromatic and PAH compounds used with their retention time	115
Table 4.2-1 Elemental analysis of the plastics (wt. %)	130
Table 4.3-1 Gas composition for the pyrolysis and pyrolysis-catalysis of HIPS and ABS plastic waste with Zeolite Y and ZSM-5 catalysts.....	135
Table 4.3-2 Gas composition for the pyrolysis and pyrolysis-catalysis of CRT and Fridge plastic wastes with Zeolite Y and ZSM-5 catalysts.....	136
Table 5.1-1 Characteristics of zeolite catalysts used.....	160
Table 5.1-2 Product yield and gas composition from the pyrolysis-catalysis of waste HDPE with different zeolite catalysts.....	162
Table 5.2-1 Gas composition from Y zeolite with varying surface area.....	165
Table 5.2-2 Gas composition from HDPE pyrolysis using Y zeolite catalysts with varying Si: Al ratio area.....	174
Table 5.2-3 Gas composition from ZSM-5 with varying Si: Al ratio catalyzed degradation of HDPE waste	182
Table 5.3-1 Gas composition from Y zeolite and ZSM-5 catalysed degradation of HDPE waste	191
Table 6.1-1 Composition of waste plastics used for research	201
Table 6.4-1 Possible Interaction of plastics during pyrolysis of the simulated mixture of plastics compared with the expected gas composition based on the proportions of the individual plastics.....	211
Table 6.5-1 Evaluation of possible Interaction of plastics during pyrolysis of the simulated mixture of plastics using aliphatic and aromatic components.....	226
Table 7.1-1 Characteristics of spent FCC and the zeolite catalysts used.....	237
Table 7.1-2 Catalyst and quartz sand mixing proportion.....	238
Table 7.2-1 Products Yields for FSMP, HDPE and LDPE thermal pyrolysis	239

Table 7.2-2 Gas Product composition for thermal pyrolysis of FSMP, HDPE and LDPE plastics	241
Table 7.2-3 Gas Product composition for FCC1 catalyzed pyrolysis of MP, FSMP and five virgin plastics	242
Table 7.2-4 Gas Product composition for FCC2 catalyzed pyrolysis of MP, FSMP and five virgin plastics	243
Table 8.1-1 Catalyst and quartz sand mixing proportion.....	261
Table 8.2-1 Gas Product composition for FCC catalyzed pyrolysis of FSMP at different catalyst bed temperature	265
Table 8.3-1 Gas Product composition for thermal and catalytic pyrolysis of FSMP with different catalyst type at 500 °C bed temperature	273
Table 8.3-2 Gas Product composition for thermal and catalytic pyrolysis of FSMP with different catalyst type at 600 °C bed temperature	274

List of equation

Equation 3.5-1.....	112
Equation 3.5-2.....	112
Equation 3.5-3.....	112
Equation 3.5-4.....	120
Equation 3.5-5.....	121
Equation 3.5-6.....	122
Equation 3.5-7.....	123

Abbreviation

ABS	Acrylonitrile-Butadiene-Styrene
ASTM	American Society for Testing Materials
BET	Brunnauer-Emmet-Teller
BJH	Barrett, Joyner and Haleda method for surface area and porous determination
BTX	Benzene Toluene Xylene
CV	Calorific Value
DCM	Dichloromethane
DBF	Dibenzofurans
DR	Dubin-Radushkevich method for microspore volume determination
CRT	Cathode Ray Tube
DTG	Differential Thermogravimetry
EtOH	Ethanol
EPA	US Environmental Protection Agency
EIA	US Energy Information Administration
(EDXS)	Energy Dispersed X-Ray Spectrometer
FID	Flame Ionization Detector
TCD	Thermal Conductivity Detector (TCD)
GC	Gas Chromatography
GC-MS	Gas Chromatography-Mass Spectrometer/ Gas Chromatography-Mass Spectrometry
(HIPS)	High Impact Polystyrene
LDPE	Low-Density Polyethylene
LLDPE	Linear Low-Density Polyethylene
MSW	Municipal Solid Waste
PE	Polyethylene
PP	Polypropylene
PS	Polystyrene

PET	Polyethylene Terephthalate
PDMT	Poly Decamethylene Terephthalate
PBT	Polybutylene Terephthalate
PVC	Polyvinyl chloride
PSW	Plastic Solid Waste
OECD	Organization for Economic Cooperation and Development
R	Universal gas constant
RON	Research Octane Number
SEM	Scanning Electron Microscopy
TCD	Thermal Conductivity Detector
TGA	Thermogravimetric Analysis
TPO	Temperature Programmed Oxidation
WtE	Waste to Energy
WEEE	Waste Electric and Electric Equipment

Chapter 1 INTRODUCTION

1.1 Introduction

1.1.1 Plastics

Plastics are lightweight, resistant to rust or rot, cheap in price, reusable and durable. These are common reasons for the popularity of plastics in many applications [1]. Global plastics production has risen by almost 10% every year to reach 245 million tonnes in 2006. Panda et al. [1], reported that plastic consumption on a per capita basis has grown to over 100 kg/y in North America and Western Europe, with the potential to grow to up to 130 kg/y per capita in the future. The USA has the highest annual plastics consumption with 27.3 million tonnes. Also, the rapidly developing part of Asia (excluding Japan) has the highest potential for growth in per capita consumption.

The rise in plastics consumption has led to the creation of massive amounts of plastic waste and in turn poses greater difficulties for its disposal. The problem is compounded by the fact that the service life of some plastic wastes is very small as 40% at less than 1 month [2], whereas the service life of other plastics ranges from 1-35 years [3]. These service lives differ from country to country, in Germany plastic has 14 years average service life while India it is eight years [3].

The main forms of plastics are thermosets and thermoplastics. The thermosets plastics are those plastics which harden by curing and cannot be remoulded while thermoplastics are those which soften when heated and harden again when cooled. Thermoplastics are the most common types of

plastics accounting for almost 80 percent of the plastics used in Western Europe [4]. Waste from service industries or manufacturing industries may contain much higher proportions of plastics.

Municipal solid waste (MSW) contains a wide range of plastics and makeup 7-9% of the weight of MSW, which is about 20-30% by volume of the MSW. For sorted municipal solid waste, the plastic content increases to about 9-12% by weight [5]. Sorted waste is waste sorted according to their usage.

In Europe (West Europe countries), the main plastic components of municipal solid waste are high-density polyethylene (HDPE), low density polyethylene (LDPE), polypropylene (PP), polystyrene (PS), polyvinylchloride (PVC) and polyethylene terephthalate (PET) [4, 6]

1.1.2 Sources of Plastics waste

Plastic wastes may be classified as municipal and industrial plastics according to their origin.

1.1.2.1 Municipal Plastic Waste

Municipal plastic waste are discarded and collected as part of municipal solid waste (MSW). Municipal solid waste plastic include domestic items (food containers, packaging foam, disposable cups, plates, cutlery, CD and cassette boxes, fridge liner, vending cups, electronic equipment cases, drainage pipes, carbonated drinks bottles, plumbing pipes and guttering, flooring, cushioning foams, thermal insulation foams and surface coating). Therefore, MSW is a mixture of plastic with major components being polyethylene, polypropylene, polystyrene, polyvinyl chloride and polyethylene terephthalate [1].

1.1.2.2 Industrial Plastic Waste

The industrial plastic wastes are mainly homogenous and are wastes arising from the large processing, packaging and manufacturing industry. These waste plastics arise from the electric industries (e.g. TV screen, cassette boxes, switch boxes, cable sheaths), the automotive industries (spare parts for cars e.g. fan blades, battery containers and seat cover) and construction and demolition companies (e.g. polyvinyl chloride pipes, and fitting, tiles and sheets).

1.1.3 Plastic Wastes Disposal

Plastic wastes are classified as solid waste. Thus, their disposal may involve already established methods of solid waste disposal. However, there are many methods of solid waste disposal, since plastic is mainly non-biodegradable the methods most suited for its disposal are landfilling, incineration, recycling and chemical recovery.

1.1.3.1 Landfilling

The landfill is the oldest waste disposal method, but undesirable for plastic which is mainly non-biodegradable and poses a problem with recent legislations. However, the plastic wastes have a high volume to weight ratio; appropriate landfill space is both scarce and expensive. Thus, other disposal methods should be preferred as alternatives [2].

1.1.3.2 Mechanical recycling

Mechanical recycling is a type of recycling where the homogenous waste plastics are converted into products with nearly the same or lower performance level than the original product. However, practical experience has shown that reprocessing of mixed contaminated plastic produce polymer

poly-blends that are inferior mechanically and lacking in durability compared with those produced by virgin polymer [7].

1.1.3.3 Biological recycling

Biological recycling methods are only applicable to biodegradable plastics which are currently less than 2% of plastic products. In biological recycling, living organisms degrade the organic matter into its raw monomers.

1.1.3.4 Incineration

Incineration is a waste-to-energy (WtE) technology for energy recovery from combustible materials including plastics. Plastic waste generates thermal energy in the same order as that used in its manufacture [8]. Public distrust in developed countries at present limit the use of incineration technology as it can produce greenhouse gases and some highly toxic pollutants.

1.1.3.5 Chemical recycling

Chemical recycling or tertiary recycling is a process to convert polymer waste into the original monomer or other valuable chemicals that can serve as feedstock for a variety of downstream industrial processes. Three main types of chemical recycling are; depolymerisation (alcoholysis, glycolysis and hydrolysis to yield their raw monomer), partial oxidation (gasification) and cracking (thermal, catalytic and hydrocracking) [2].

1.1.3.6 Cracking/pyrolysis

The cracking process shown in Figure 1.1.1 below includes processes that break down the polymer chain into useful lower molecular weight compounds [1]. Cracking or pyrolysis processes are of three types i.e. thermal, catalytic and hydrocracking.

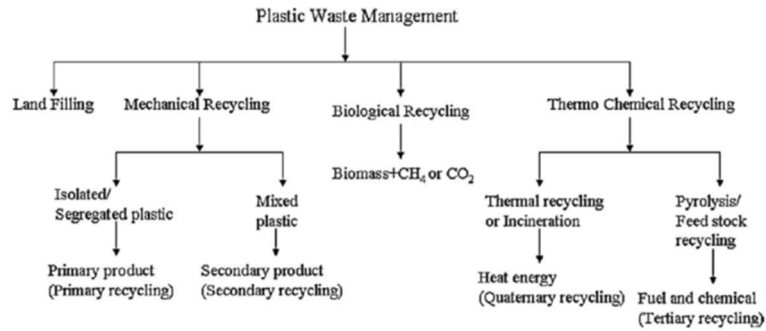


Figure 1.1-1 the different routes for plastic managements [1]

1.1.3.7 Pyrolysis

Pyrolysis can be classified into low, medium and high temperature processes, based on the range of temperature used to degrade the polymer structure as shown in Figure 1.1-2. Several researchers [9] [10] [11] [12] [13] have described the three ranges as follows:

- i) High-temperature pyrolysis the process involves thermal degradation of polymer/organic materials at temperatures higher than 800 °C and produces a mainly gas product.
- ii) Medium temperature pyrolysis process is carried out at a temperature between 550-800 °C to produce a mainly oil and gas product and in some cases char.
- iii) Low-temperature pyrolysis is performed at temperatures lower than 500 °C to produce mostly oils.

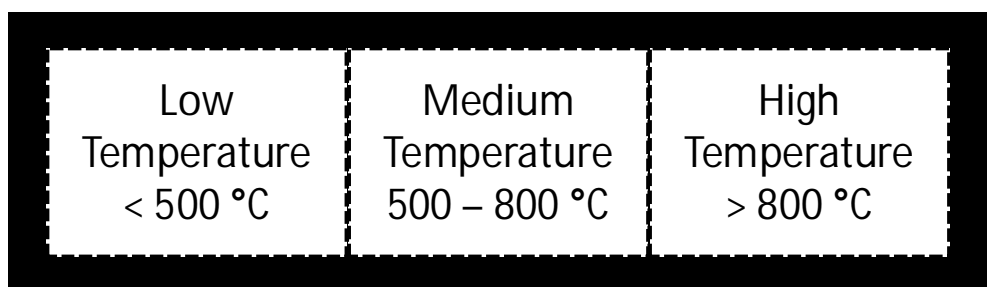


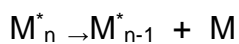
Figure 1.1-2 Three temperature ranges of pyrolysis [13]

Use of pyrolysis as a means of waste management should be economically viable to produce marketable products at a saleable price.

1.1.3.8 Thermal Degradation of Plastics or Polymer

There are two distinct reactions in thermal degradation of plastics or polymer; these reactions normally occur simultaneously in the reactor. The first reaction involves a random scission of chemical bonds, causing a molecular weight reduction of the polymer compound, and the second is a chain –end scission of C-C bonds, producing volatile products. The composition and type of pyrolysis give useful information about mechanisms of thermal degradation [14]. Thermal degradation of the polymers follows either chain end degradation (unzipping route) or random degradation route [15].

Chain end degradation or unzipping route



Random degradation route



Chain-end degradation involves the continuous release of monomer units from the chain ends and also known as a depolymerization reaction. The reaction occurs through free radical mechanisms and is the opposite of the propagation step in addition polymerization. The molecular weights of the polymer decrease slowly and simultaneously, and a great number of monomers are liberated. Thus, in general, the chain end degradation occurs when the backbone bonds are weaker than the bonds of the side groups and only with polymer molecules, carrying active chain ends with a free radical, cation, anion etc. [14].

Random degradation is the opposite of the polycondensation process, it occurs at any random point along the polymer chain, and practically no monomer is liberated. Carrying an active site by the polymer is not prerequisite for random degradation to occur.

The degradation of plastics has been conducted by numerous researchers for decades, and has involved thermal and catalytic degradation and has been performed on single and mixed plastics.

1.1.4 Catalysis

1.1.4.1 What is catalysis?

The word catalysis originates from the Greek which means to split or breakdown. Catalysis is an increase in the rate of a chemical reaction as a result of the action or use of a catalyst. A catalyst is a substance that increases the rate of a chemical reaction without itself undergoing any change at the end of the reaction. In a better perspective, a catalyst can speed up reactions by orders of magnitude, enabling them to be carried out under the auspicious thermodynamic regime, and at a much lower temperature and pressure [16]. Two types of catalysis are known i.e. homogeneous and heterogeneous catalysis. In homogeneous catalysis both the catalysts and the reactants are in the same phase, i.e., all molecules are in the gas phase or all molecules are in the liquid phase. Heterogeneous catalysis means the catalyst is in a different phase of the reaction mixture it is catalysing. In heterogeneous catalysis, solid catalysed reactions can occur in gas molecules or solution.

1.1.4.2 Historical background

Berzelius in 1836 coined the name catalysis. Egyptians of 2000 BC used yeast to catalysed fruits into alcoholic beverages. It has been applied for thousands of years in the process of fermentation. The influence of metal and oxides on the decomposition of several substances was studied at the end of the eighteenth and the beginning of the nineteenth century. Thernard in 1813 found that dissociation of ammonia occurs over various metals provided they are hot.

1.1.4.3 Application

Catalysts improve a large number of reactions, principally in organic synthesis and reformation. The petroleum and petrochemical industries use a variety of catalysts in processing crude oil and other secondary raw materials for the production of fuels and chemicals. Some of the uses of catalyst in the industry include [17] catalytic;

(i) hydrodesulfurization (ii) cracking (iii) reforming

(v) dehydrogenation and dehydrocyclization

(vi) oxidative condensation and (vii) isomerization [17].

Catalytic cracking is an extremely important process that was estimated to generate financial benefit in 1992 to the US economy to the tune of \$8 billion dollars [18]. Catalytic reforming in the petroleum industry is used to improve products by catalytic cracking. Catalytic reforming changes straight chain alkanes into branched and aromatic molecules [19].

1.1.5 Description of Catalyst

1.1.5.1 Introduction

The most familiar forms of catalyst are metals and their oxide. Mostly numerous metal catalysts are involved in different areas from everyday life to large industrial processes. Transition metals have the upper hand in the catalysis process because of the presence of vacant d or f orbital in their atoms. Some metal oxides such as V_2O_5 , TiO_2 , SiO_2 and Al_2O_3 and their mixtures are widely used to promote dehydration, isomerization and oligomerization reactions.

For a catalyst the desired properties are

- high and stable activity
- high and stable selectivity
- controlled surface area and porosity
- good resistance to poisons
- good resistance to high temperatures and temperature fluctuations.
- high mechanical strength
- no uncontrollable hazards

1.1.5.2 Kinetics

Catalysts are vital to non-equilibrium reactions as it improves the yield of products but do not affect the equilibrium of products in ideal equilibrium systems.

In essence, a catalyst performs its function by increasing the rate at which reactions take place without affecting the equilibrium conditions. Thus, use of catalysts in industrial processes usually yields more products at higher rates and lower temperatures.

Activation energy is the energy needed to make molecules of a substance take part in a chemical reaction. Essentially activation energy exists because of the numerous bond breaking and dissociation that occurs for a specific reaction. The chemical reaction must overcome activation energy barrier to convert reactants to products. The catalyst function by lowering activation energy as demonstrated in Figure 1.2-1.

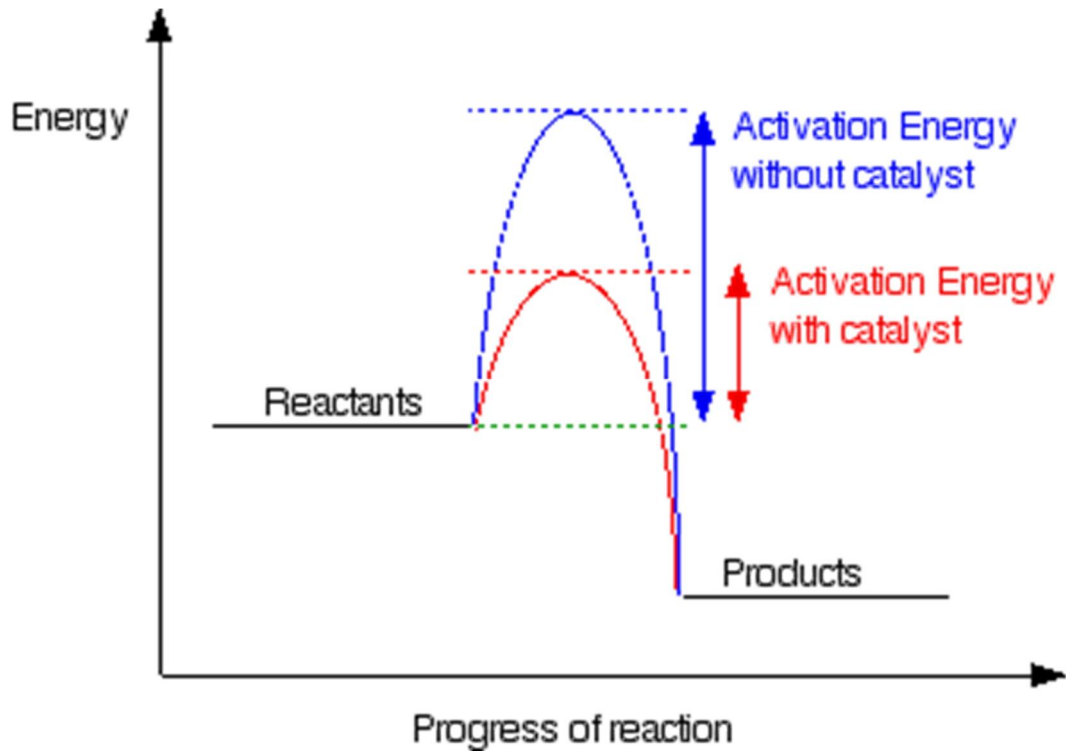


Figure 1.1-2 Energy profile

Three different aspects of kinetics studies identified are as follows;

(i) Kinetics studies for design purpose; as kinetic expressions are useful for the design of chemical reactors, quality control in catalyst production, and comparison of different brands of catalysts, studies of deactivation and poisoning of catalysts.

(ii) Kinetics studies of mechanistic detail, for a simple reaction kinetic study, may be used to determine detailed mechanisms.

(iii) Kinetics as a consequence of a reaction mechanism; kinetics is usually deduced from proposed reaction mechanisms [16].

1.1.5.3 Surfaces

Accessibility of free bonding sites on the catalyst is crucial for the catalytic process to proceed. The initial step involves the adsorption of the reactant molecular species onto the catalyst. There are two types of adsorptions; physisorption embraces the forces of molecular interaction such as dipole, naked dipole and quadrupole attraction; and chemisorption when the molecule forms actual bonds with the catalytic surface [20]. The Higher enthalpy changes are associated with chemisorption than physisorption, but the chemisorbed intermediates have greater stability.

1.1.6 Zeolites

Zeolites are a class of oxides consisting of microporous crystalline aluminosilicates that can either be found in nature or synthesized artificially [16]. The zeolite catalyst was discovered by Swedish mineralogist Alex Frederick Cronstedt. The zeolite framework is very open and contains channels and cages where cations, water and adsorbed molecules may reside and react

1.1.6.1 Structure and composition

Natural zeolites typically bear the name of the mineral (mordenite, faujasite, ferrierite, silicate) or person that discovered e.g. Barrerite after Professor Barrer or place of discovery e.g. Bikitaite from Bikita, Zimbabwe.

Synthetic zeolites bear the name of the industry synthesizing the catalyst e.g. ZSM stands for Zeolite Socony Mobil or university e.g. VPI Virginia Polytechnic Institute.

Essentially zeolites consist of SiO_4 and AlO_4 tetrahedral ions which can be arranged by sharing O-corner atoms in many different ways to build a

crystalline lattice. The SiO_4 can be arranged into several silicate units e.g. square (four), 6 or 8-membered rings called secondary building blocks. The zeolite structures are built up by joining a selection of building blocks into recurring structures.

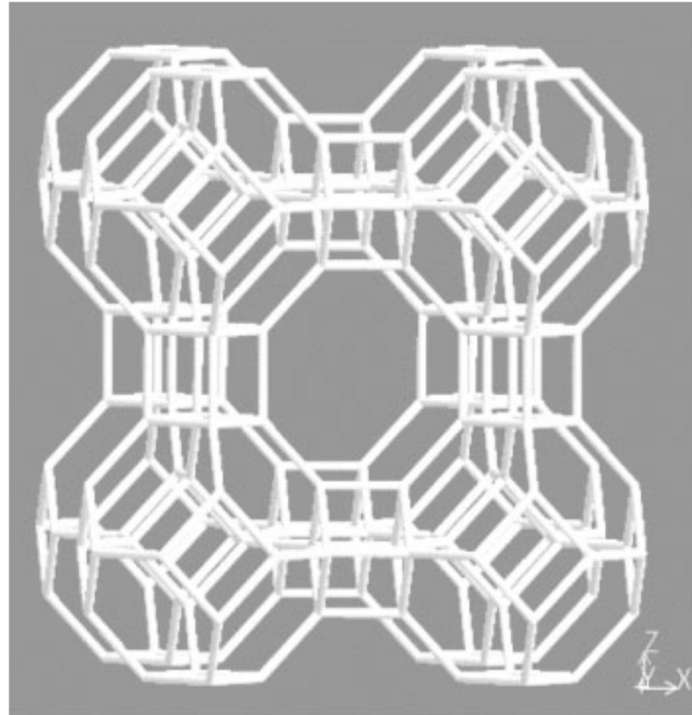


Figure 1.1-3 Zeolite structure [16]

As soon as Al^{3+} replaces Si^{4+} ions atoms in the tetrahedral, the net unit charge will be -1, and thus cations such as Na^+ are needed to neutralize the charge. Hence, the number of cations present within in a zeolite structure equals the number of alumina tetrahedral in the framework. However, when a proton replaces sodium (yielding HX^- , H-ZSM-5, etc.), the zeolites become a very large poly acid. For being a proton donor, the site at which H located, is called a Brønsted acid. Its strength depends on the local environment of the proton, in particular on the number of other aluminium ions in the environment

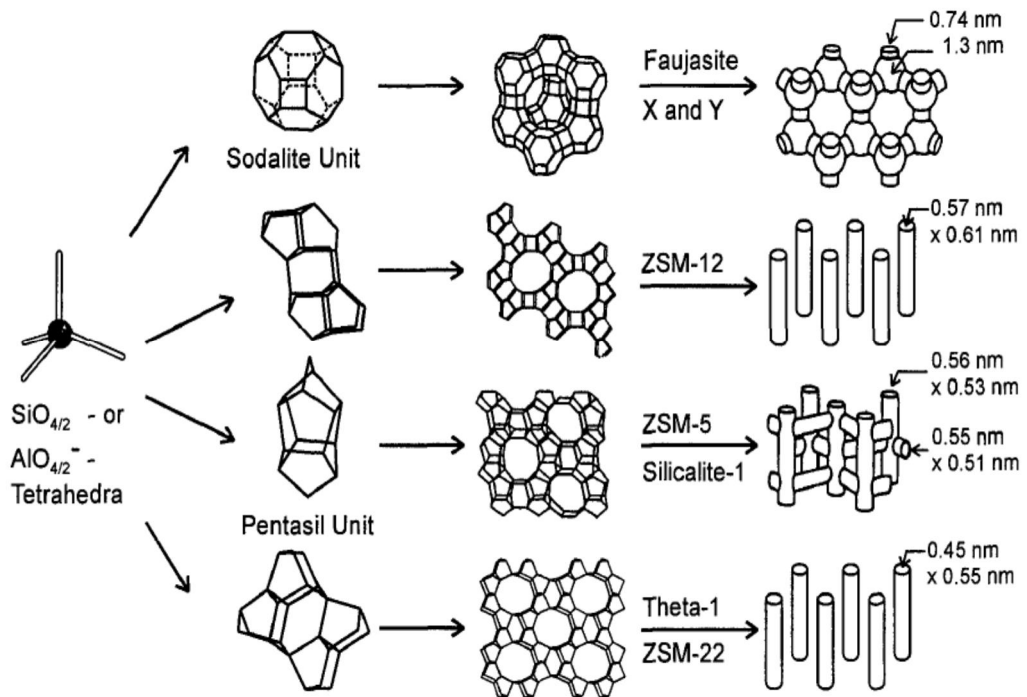


Figure 1.2-3 Structures four selected zeolite (from top to bottom; faujasite or zeolite, zeolite ZSM-12, zeolite ZSM-5 or silicate zeolite[21])

1.1.6.2 Acidic properties of zeolites

Two acid sites are present in the zeolite structure, Lewis and Bronsted sites. The Bronsted acidic character occurs from a positive ions excess of an ion with a formal negative charge while Lewis acid character arises from positives ions excess on an ion with a formal positive charge. A Lewis base character occurs from a negative ion excess of a negative ion with formal negative charge, but a Bronsted basic character arises from negative ion excess on an ion of formal positive charge.

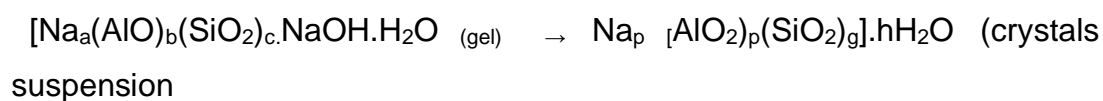
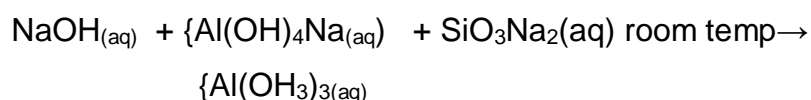
1.1.6.3 Synthesis

Zeolites are prepared by hydrothermal synthesis under pressure in autoclaves, in the presence of template molecules such as tetramethylammonium, which act as structure directing agents.

Basic preparatory materials for the process are alumina and silicate gels prepared from aqueous solutions of sodium silicate, sodium aluminates and NaOH. The typical process conditions or preparation of standard A, X and Y zeolites are summarized below;

Table 1.2-1 Summarized typical composition of material for synthesis of zeolite catalysts[22]

Zeolite	Na/Si molar ratio	Si/Al molar ratio	H ₂ O/Si molar ratio	Process time (Hours)
A	0.5	1.0	17	3
X	0.9	1.5	48	8
Y	0.2	10	16	8



Formation of Y-zeolite[22].

1.1.6.4 Fine tuning with addition of modifiers

Wojciechowski and Corma [23], reported that increasing the silica: alumina ratio of 2.5-5.5 increases thermal stability from 820 °C to 860 °C. Use of ions such other simple sodium or ammonium do have far reaching effects on the properties and structures of the zeolites. The increase in atomic cation size will increase thermal stability. The thermal stability of cations is in order of; monovalent<divalent<trivalent.

Ward [24] investigated the effect of cation-exchange using divalent cations and concluded that Bronsted acidity is increased with increasing ionic radius, and consequently catalytic activity.

1.1.6.5 Zeolite selectivity

The diameter of the zeolite pore (0.3 to 5.0 nm) is similar to those of regular molecules used in fuel or chemical industry feedstocks, thus a molecular sieving effect can be achieved with selection of an appropriate zeolite. The regular pore, cage, super cage, crystallinity, and channel of a zeolite make it unique amongst porous solids

Csicsery [25], articulate four types of zeolite selectivity namely;

- (i) Reactant selectivity occurs when only part of the reactant molecules are small enough to diffuse through the catalyst pores.
- (ii) Product selectivity, this occurs when some of the products formed within the pores are too bulky to diffuse out as observed products. They are either converted to a less bulky molecule (e.g. equilibration) or eventually deactivate the catalyst by blocking the pores.
- (iii) Restricted transition state selectivity which occurs when some reactions are prevented because the corresponding transition state would require more space than available in the cavities.

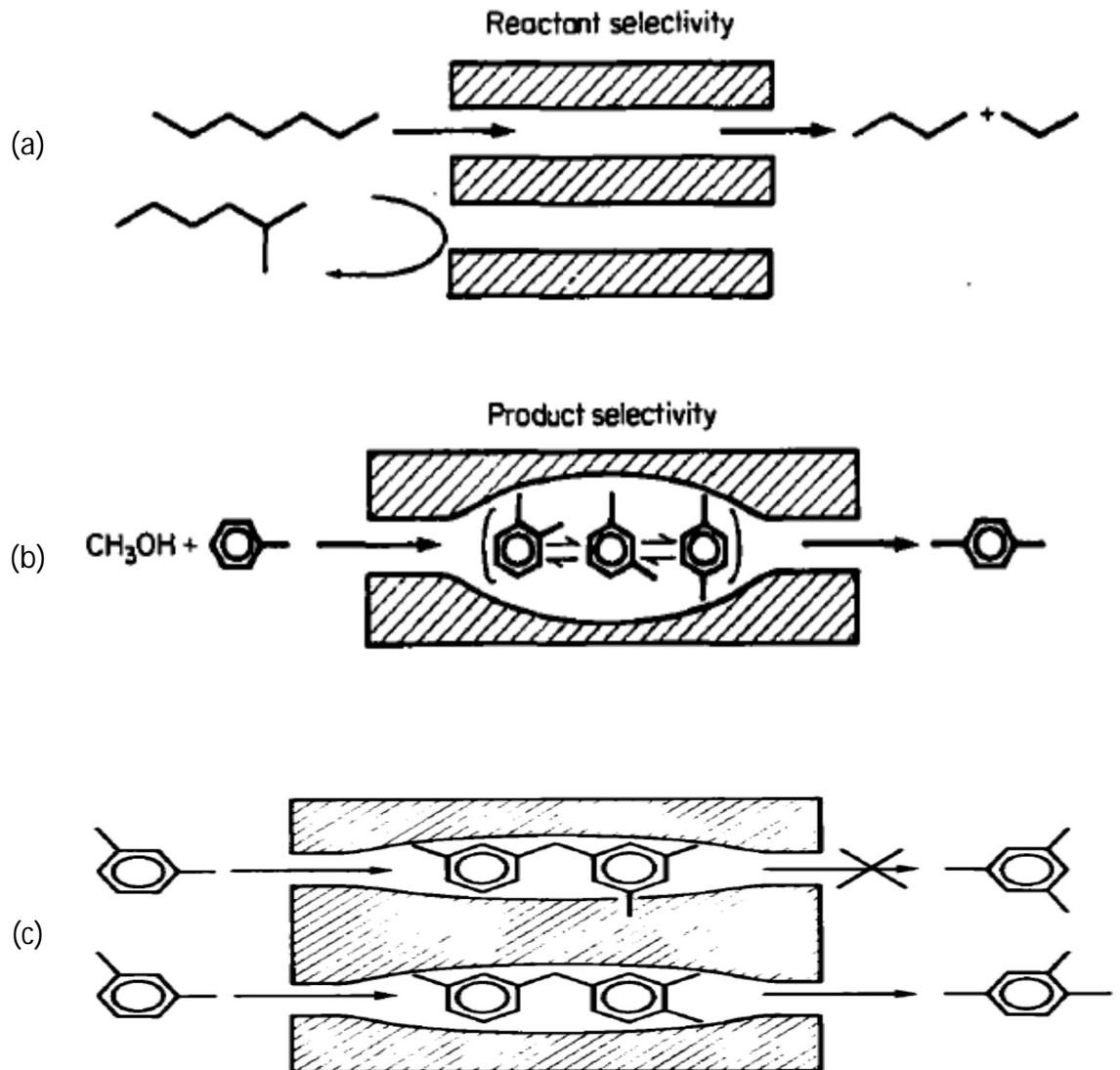


Figure 1.2-4 shows zeolite selectivity for (a) Reactant (b) Product and (c) Restricted

- (iv) Molecular traffic control may take place in zeolites with more than one type of pore system. Reactant molecules may preferentially enter the catalyst through one of the pore systems while the products diffuse out by the other. Counter diffusion is thereby minimized at this point.

1.1.6.6 Applications of zeolites

There are three main uses of zeolites in industry: catalysis, gas separation and ion exchange.

Catalysis: Zeolites are extremely useful as catalysts for several important reactions involving organic molecules. The most important are cracking, isomerization and hydrocarbon synthesis. Zeolites can promote a diverse range of catalytic reactions including acid-base and metal induced reactions. Zeolites can also be acid catalysts and utilized as supports for active metals or reagents. Zeolites can be shape-selective catalysts either by transition state selectivity or by the exclusion of competing reactants on the basis of molecular diameter. They have also been used as oxidation catalysts. The reactions can take place within the pores of the zeolite, which allows a greater degree of product control. The main industrial application areas are petroleum refining, synfuels production, and petrochemical production. Synthetic zeolites are the most important catalysts in petrochemical refineries.

Adsorption: Zeolites are used to adsorb a variety of materials, this includes applications in drying, purification, and separation. They can remove water to very low partial pressures and are very effective desiccants, with a capacity of up to more than 25% of their weight in water. They can remove volatile organic chemicals from air streams, separate isomers and mixtures of gases. A widely used property of zeolites is that of gas separation. The porous structure of zeolites can be used to "sieve" molecules having certain dimensions and allow them to enter the pores. This property can be fine-tuned by varying the structure or by changing the size and number of cation around

the pores. Other applications that can take place within the pore include polymerization of semiconducting materials and conducting polymers to produce materials having unusual physical and electrical attributes.

Ion exchange: Hydrated cations within the zeolite pores are bound loosely to the zeolite framework, and can readily exchange with other cations when in aqueous media. Applications of zeolite for ion exchange can be seen in water softening devices, and the use of zeolites in detergents and soaps. The largest volume use for zeolites is in detergent formulations where they have replaced phosphates as water-softening agents. They do this by exchanging the sodium in the zeolite for the calcium and magnesium present in the water. It is even possible to remove radioactive ions from contaminated water

1.2 Aims and Objectives

This research work aim at converting plastics waste into valuable liquid resources (liquid fuels) via thermal and catalytic pyrolysis processes. The plastic waste used are commonly available plastic, such as polyethylene, polypropylene, PET, polystyrene, Laboratory prepared or simulated mixtures of virgin plastics (e.g. PE/PP, PE/PS, PP/PS, PE/PP/PS etc.), real world plastic wastes or mixed plastics, Waste electric and electronic equipment (WEEE) such as CRT, fridge, ABS and HIPS etc. Elemental analysis technique will be use to characterize plastic samples. TGA studies on plastic samples will be conducted to ascertain the degradation pattern of the plastic by varying temperature conditions under inert nitrogen flow. Some catalysts will be selected base on their properties and performance for initial pyrolysis experiments. Zeolite Y and ZSM-5 will be used for preliminary work, later stage spent FCC catalyst (Fluid Cracking Catalyst from the petroleum

industry) will be used for catalytic pyrolysis. Thermal and catalytic pyrolysis will be carried out at varying reaction conditions, catalyst type and plastic to catalyst ratios using novel two-stage pyrolysis-catalysis downdraft batch reactor.

The various products of pyrolysis; gas, liquid or oil and char (solid) are to be analysed. Gas will be analysed for hydrocarbon gases (hydrogen and C₁-C₄ hydrocarbons) and permanent gases (carbon monoxide, carbon dioxide, oxygen and nitrogen) by gas chromatography. Liquid or oil products will be analysed using both gas chromatography mass spectrometer (GCMS/MS) and GC-FID for aliphatic and aromatic hydrocarbons. The liquid product simulated distillation properties will be quantified using GC studies.

The catalysts, both fresh and spent will be characterized using the following techniques: TGA, scanning electron microscopy (SEM), Electron diffraction X-ray EDX and XRD.

Reference

1. Panda, A.K., Singh, R.K. and Mishra, D.K., *Thermolysis of waste plastics to liquid fuel A suitable method for plastic waste management and manufacture of value-added products-A world perspective*. Renewable & Sustainable Energy Reviews, 2010. **14**(1).
2. Achilias, D.S., Roupakias, C., Megalokononimos, P., Lappas, A.A. and Antonakou., D.S., *Chemical recycling of plastic wastes made from polyethylene (LDPE and HDPE) and polypropylene (PP)*. J Hazard Mater, 2007. **149**(3): p. 536-42.
3. Mutha, N.H., Patel, M. and Premnath, V., *Plastics materials flow analysis for India*. Resources, conservation and recycling, 2006. **47**(3): p. 222-244.
4. Bajus, M. and Hajekova, E., *Thermal Cracking of The Model Seven Componentsmixed Plastics Into Oils/Waxes*. Petroleum & Coal, 2010. **52**(3): p. 8.
5. Scott, D.S., Czernik, S.R., Piskorz, J. and Radlein, D.S.G., *Fast Pyrolysis of Plastic Wastes*. Energy & Fuels, 1990. **4**(4).
6. Marcilla, A., Gomez, S.A., Quesada, J.C.G. and Berenguer, D., *Characterization of high-impact polystyrene by catalytic pyrolysis over Al-MCM-41: Study of the influence of the contact between polymer and catalyst*. Polymer Degradation and Stability, 2007. **92**(10).
7. Scott, G., 'Green polymer'. Polymer degradation and stability, 2000. **68**(1): p. 1-7.
8. Scott, D.S., Majerski, P., Piskorz, J. and Radlein, D., *A second look at fast pyrolysis of biomass—the RTI process*. Journal of Analytical and Applied Pyrolysis, 1999. **51**(1): p. 23-37.
9. Marcilla, A., Beltrán, M. and Navarro, R., *Evolution of products generated during the dynamic pyrolysis of LDPE and HDPE over HZSM5*. Energy & Fuels, 2008. **22**(5): p. 2917-2924.
10. Ciliz, N.K., Ekinici, E., and Snape, C.E., *Pyrolysis of virgin and waste polypropylene and its mixtures with waste polyethylene and polystyrene*. Waste Management, 2004. **24**(2): p. 173-181.
11. Elordi, G., Lopez, G., Aguado, R., Olazar, M. and Bilbao, J., *Catalytic pyrolysis of high-density polyethylene on an HZSM-5 zeolite catalyst in a conical spouted bed reactor*. International Journal of Chemical Reactor Engineering, 2007. **5**.

12. González, Y.S., Costa, C., Marquez, M.C. and Ramos, P., *Thermal and catalytic degradation of polyethylene wastes in the presence of silica gel, 5A molecular sieve and activated carbon*. Journal of hazardous materials, 2011. **187**(1): p. 101-112.
13. Balek, V. and de Koranyi, A., *Diagnostics of structural alterations in coal: Porosity changes with pyrolysis temperature*. Fuel, 1990. **69**(12): p. 1502-1506.
14. Murata, K., Hirono, Y., Sakata Y. and Azhar Uddin, Md., a *Basic study on a continuous flow reactor for thermal degradation of polymers*. Journal of Analytical and Applied Pyrolysis, 2002. **65**(1).
15. Singh, B. and Sharma, N., *Mechanistic implications of plastic degradation*. Polymer Degradation and Stability, 2008. **93**(3): p. 561-584.
16. Chorkendorff, I. and Niemantsverdriet, J., *Concepts of Modern Catalysis and Kinetics*. 2003, 2003, Weinheim: Wiley-VCH.
17. Olah, G.A. and Molnar, A., *Hydrocarbon chemistry*2003: Wiley-Interscience.New York
18. Farrauto, R. and Bartholomew, C., *Introduction to Industrial Catalytic Processes, Fundamentals and Practice*, 1997, Chapman & Hall, London.
19. McMurry, J., *Fundamentals of Organic Chemistry*. Brooks, 1992, Cole Publishing Company.
20. Thomas, J.M. and Thomas W.J., *Principles and practice of heterogeneous catalysis*. Vol. 638. 1997: VCH New York.
21. Weitkamp, J., *Zeolites and catalysis*. Solid State Ionics, 2000. **131**(1): p. 175-188.
22. Wojciechowski, B.W. and Corma, A., *Catalytic cracking: catalysts, chemistry, and kinetics*. 1986.
23. Wojciechowski, B.W. and Corma, A., *Catalytic cracking: catalysts, chemistry, and kinetics*1996.
24. Ward, J.W., *The nature of active sites on zeolites: IV. The influence of water on the acidity of X and Y type zeolites*. Journal of Catalysis, 1968. **11**(3): p. 238-250.
25. Csicsery, S.M., *Shape-selective catalysis in zeolites*. Zeolites, 1984. **4**(3): p. 202-213.

Chapter 2 LITERATURE REVIEW

2.1 Thermal Degradation of Plastics

In this section, thermal degradation is discussed for both single and mixed plastics.

2.2 Thermal Degradation of Single Plastics

The thermal degradation or pyrolysis of single (individual) plastics has been performed by several researchers using different reactor designs, reaction conditions and reaction times. The following are some cited research work reported for some selected single plastics.

2.2.1 Polyethylene (PE)

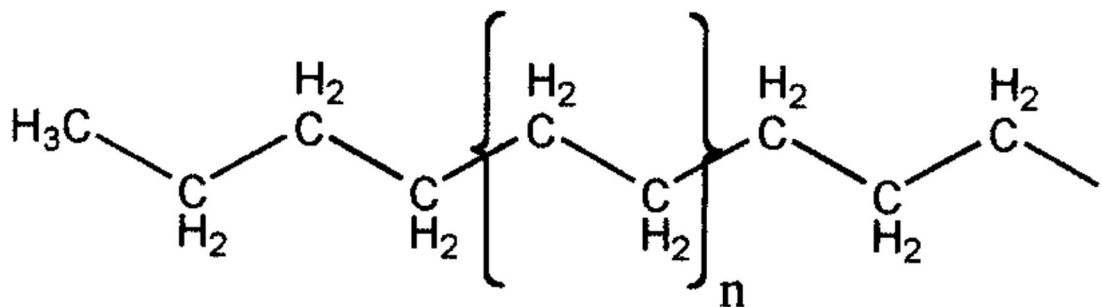


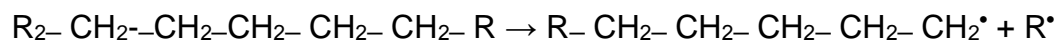
Figure 2.1- 1 Polyethylene structure

Polyethylene is the commonest polymer compound produced. Polyethylene is made from pure ethylene as a result of polymerization either by the high or low-pressure method. The polyethylene produced by the high-pressure method possesses a low density, also known as high-pressure or low-density polyethylene (LDPE). However, the polyethylene produced by the low-pressure method possesses a high density and is known as high-density polyethylene (HDPE).

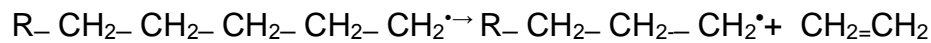
Polyethylene is used for the injection moulding of housewares and toys, containers, and bottles. The high-density polyethylene utilized for in packaging. Accordingly unpigmented HDPE are used for milk, juice, water and laundry product containers, whereas pigmented HDPE are used for margarine tubs, yogurt containers and for bottling detergent and bleach.

The degradation of polyethylene is considered to be a free radical chain reaction in a sequence involving initiation, propagation, intermolecular hydrogen transfer, and termination. Siddiqui and Redhwi [1], suggested that the depolymerization of polyalkenes such as polyethylene occurs using radical mechanisms. The reaction has activation energies of between 188-251 kJ mol⁻¹ and significant degradation occurring only above 370 °C [2].

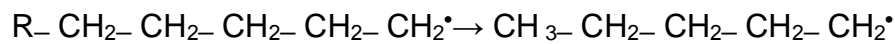
Initiation;



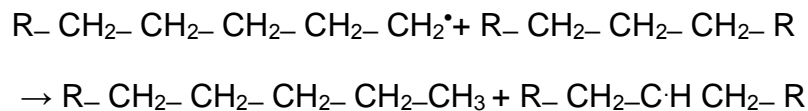
β-Scission propagation;



Random propagation;



Intermolecular hydrogen transfer;



Termination;



However, the type of polyethylene high density, low density or linear low density; the thermal degradation temperature and its molecular weight, dictate the reaction products as reported by Xanthos and Leidner [3].

Seo and Shin [4], reported that the pyrolysis reaction at a high temperature of around 600-800 °C is capable of reducing reaction time, but produced more light hydrocarbons as well as gaseous materials. However, low-temperature pyrolysis 400-500 °C produces oily material while consuming less energy.

Researchers have worked with different types of reactors for both thermal and catalytic pyrolysis of polyethylene. Miskolczi et al. [5], reported the thermal degradation of polyethylene and polystyrene from the packaging industry over different catalysts into fuel-like feedstocks using a batch reactor at a temperature range of 410 - 450 °C. The liquid products were mainly alkene and alkane hydrocarbons while the aromatic content was higher at lower temperatures. The gas yield increased with temperature.

Gonzalez et al. [6], performed work on the thermal degradation of polyethylene in a batch reactor at the reaction temperatures of 450, 500 and 700 °C. But, a full range of hydrocarbons was observed in the gas products with the number of carbon in the range of C₄-C₁₀, linear and branched hydrocarbon and benzene. The products obtained in the studies could be used as feedstock for the chemical industry or energy production.

Williams and Williams [7], pyrolysed low-density polyethylene in a fluidized bed reactor at a temperature range of 500-650 °C. Gas production showed an increase as the temperature was increased, as a result of liquid products being cracked to gas. The liquid product yield increased with an increase in temperature from 500 & 560 °C; these might be ascribed to the wax product being cracked to oil at medium temperature. However, the liquid fraction decreased with temperatures as the temperature rose to 600, 650 & 700 °C,

whereas the liquids were further cracked into gas. The primary gas products were H₂, CH₄ and ethane, ethene, propane, propene, butane and butene. Single ring aromatic and polycyclic aromatic hydrocarbons of significant concentration formed at 700 °C. Consequently, the rise in the reaction temperature also enhanced the yield of gas. Thus, the gas yield reaches 71% at 700 °C, and their main compositions were methane (11.7%), ethane (26.8%) and propene (18.6%). Conesa [8], pyrolysed polyethylene at temperatures range 500 & 900 °C, and Kaminsky et al. [9], pyrolysed polyethylene at temperature 760 °C both work in fluidized bed reactors.

Serrano et al. [10], worked with a screw kiln reactor for converting low-density polyethylene (LDPE) into petrochemical feedstock. They placed two furnaces to heat the reactor tube to heat the plastic, creating two different heating areas of 450 °C and 550 °C. The thermal treatment led mainly to gasoline range hydrocarbons (C₅-C₁₂) and middle distillates (C₁₃-C₃₃) with the selectivity of ~25 and 55 wt. % respectively. Alkenes and n-alkanes were the principal products of the middle distillate and gasoline range hydrocarbons respectively.

2.2.2 Polypropylene (PP)

The production of polypropylene is through the polymerization of propylene in a batch reactor at 20-120 °C temperature and 1 - 40 atmospheres pressure in the presence of triethyl aluminum and titanium tetrachloride catalyst dispersed in n-heptane in an inert solvent. The crystalline polymer is insoluble and precipitates as finely granular solid, propylene addition is continued until the slurry becomes quite thick. The catalyst is recovered by adding a suitable reagent, and the polymer is separated from the solvent and dried.

Polypropylene has a melting point of 160-170 °C due to its crystalline structure. Polypropylenes are known to be used in making automobile components, stationery, containers of various types, plastic components, and laboratory equipment.

Pyrolysis of polypropylene waste plays a significant role in converting the waste into an economically valuable hydrocarbon, which can be used either as feedstock in the petrochemical industry or as fuels. Kruse et al. [11], reported work on the pyrolysis of polypropylene at different pyrolysis temperatures; i.e. 350, 380, and 420 °C. Hence, they proposed a mechanistic model using free radical reactions types. The reactions include; intermolecular hydrogen abstraction, radical addition or recombination, bond fission, mid/end-chain β -scission and disproportion to predict the formation of low molecular weight (C_1 - C_{15}) hydrocarbon products. Thermal decomposition of polypropylene proceeds essentially by random scission mechanisms. The way in which a molecule fragments during pyrolysis and the identity of the fragments evolved depend on the type of chemical bonds involved and the stability of the resulting smaller molecules [12].

Hujuri et al. [13], studied the temperature-dependent pyrolytic product evolution profiles for polypropylene at a different temperatures; these are 200, 300, 400, 446, 500 or 600 °C. The samples were heated from ambient temperature at a heating rate of $10^{\circ}\text{C min}^{-1}$ under a constant flow of argon (flow rate $40\text{-}50\text{ ml min}^{-1}$). The yield of light liquid hydrocarbon (C_5 - C_{10}) was small at a pyrolysis temperature of 200-300 °C, and gradually increased up to the maximum decomposition temperature of 446 °C and decreased afterward.

Shah et al. [14], performed the catalytic pyrolysis of low-density polyethylene in a batch reactor. Approximately 5 g of polyethylene heated at different temperatures 250, 300, 350 and 400 °C. The products of the thermal degradation of each cracking temperature collected separately. The total conversion to gas and liquid products improved from 10.52 ± 0.45 to 25.36 ± 0.52 % as the temperature was increased.

2.2.3 Polystyrene (PS)

Polystyrene polymer usually produced by polymerization of the monomer, styrene. Styrene polymerized by radical, coordination, cationic or anionic polymerization mechanism.

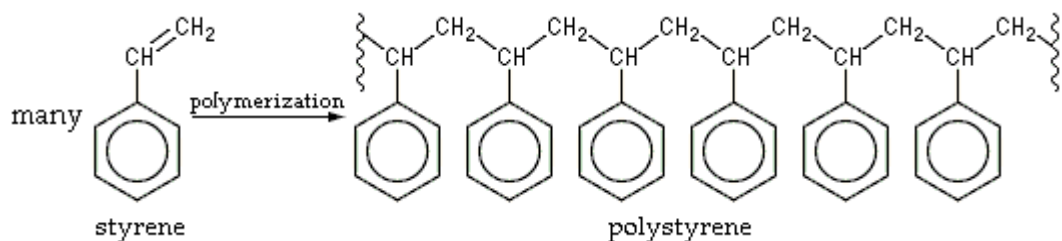
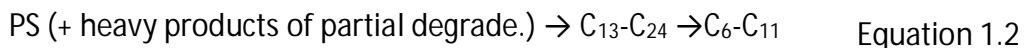


Figure 2.1- 2 Polymerization reaction for polystyrene

The Figure depicts a typical polymerization process of styrene. Polystyrene is used in making disposable cutlery, plastic models, CD and DVD cases, and smoke detector housing, packing materials and foam drink cups. Polystyrene has poor biodegradability and its waste generated from both household and industry causes significant impact to the environment.

The thermal degradation of polystyrene was investigated by Carniti et al. [15], and they suggested the degradation was through consecutive reactions as follows;



Madorsky et al. [16], reported an investigation on the vacuum degradation of polystyrene at a set of two different temperatures. The temperatures are lower set at 400 °C and 500 °C for 30 min and a higher set at temperatures between 800 °C and 1200 °C for 5 min. The major composition of the degradation products was styrene that decreased with higher temperatures due to secondary decomposition into benzene and lower molecular weight alkanes. The authors work was similar to the work of Jianfeng et al. [17], who reported a 61.1 % yield of styrene from the thermal pyrolysis of polystyrene. The polystyrene was pyrolyzed in the temperature range of 370-430 °C, but styrene yield improved slowly at a temperature higher than 410 °C.

Bajus and Hajekova [18], investigated polystyrene that produced an oil yield which consisted almost wholly of aromatic compounds particularly toluene, ethylbenzene and styrene over the range of temperatures. The polystyrene produced a mainly dark-coloured viscous oil at 350 °C and char formation was significantly enriched at higher temperatures 450 °C and 500 °C, up to 30% [18].

2.2.4 Poly (ethylene terephthalate) (PET)

Poly (ethylene terephthalate) (PET) produced from ethylene glycol and dimethyl terephthalate or terephthalic acid. The monomer for PET is bis (2-hydroxyethyl) terephthalate.

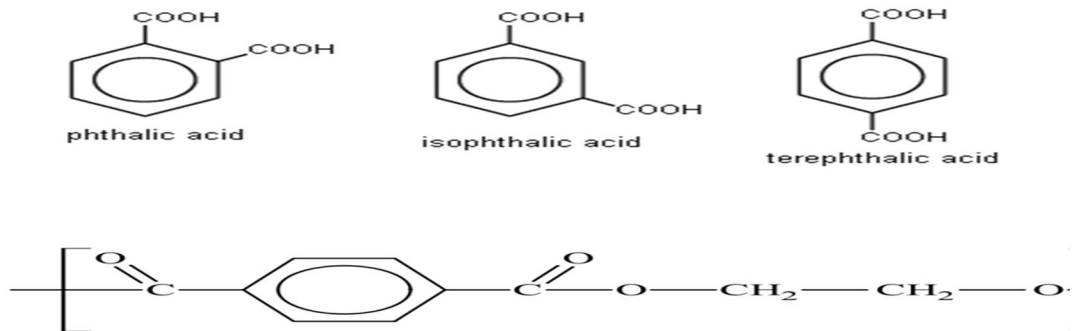
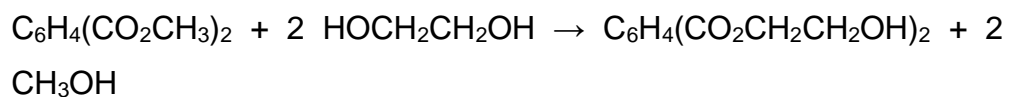


Figure 2.1-3 PET monomers and the polymer

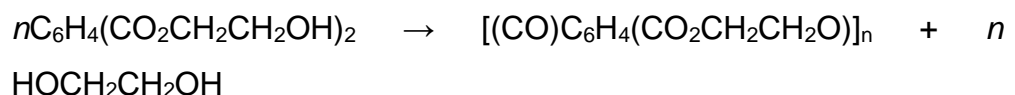
In this process, the excess ethylene glycol and dimethyl terephthalate are reacted at a temperature of 150-200 °C with methanol as a basic catalyst. The catalyst (methanol) is distilled off to help drive the reaction forward. Another trans-esterification reaction will proceed at 270-280 °C, and excess ethylene glycol are distilled off in both steps

The two steps for the reactions are as follows:

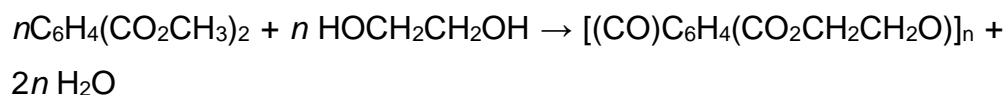
First step



Second step



In the esterification process ethylene glycol and the terephthalic acid reacted at moderate pressure (2.7-5.5 bars) and temperature (220 - 260 °C). A continuous distillation process is used to remove water.



PET is mainly used to package consumer items such as soft drinks, water, beer, mouthwash, food containers, and for oven-proof film and food trays. Some other use includes chemical drums, carpeting, and pipes and tubing for gas, water, etc. due to its strength, toughness, and transparency.

Thermogravimetric degradation curves of polyethylene terephthalate (PET), polybutylene terephthalate (PBT) and poly Deca methylene terephthalate (PDMT) produced by McNeil & Bounekhel [19], showed a single stage decomposition. The onset of degradation was above 300 °C, the maximum rate of weight loss being in the range 400-450 °C. The amount of residue at 500 °C was relatively small, particularly for PBT and PDMT. Carbon monoxide was detected in all the three polymers in the non-condensable gases. Traces of methane were also detected only in PET, which was presumed to originate from the methyl ester end groups present. However, three main fractions obtained from the condensable gases and volatile liquids in PET products; the first fraction consisted of carbon dioxide together with traces of alkenes. But the second fraction was acetaldehyde, and the third fraction collected a liquid which characterized as vinyl benzoate and dioxane with traces of benzaldehyde, toluene, and divinyl terephthalate.

Montaudo et al. [20], reported on the thermal degradation of PET and PBT and concluded that the primary step is an ionic process. In the ionic process, a β -CH hydrogen transfer leading to the formation of the oligomer with an olefin and carboxylic end groups was suggested.

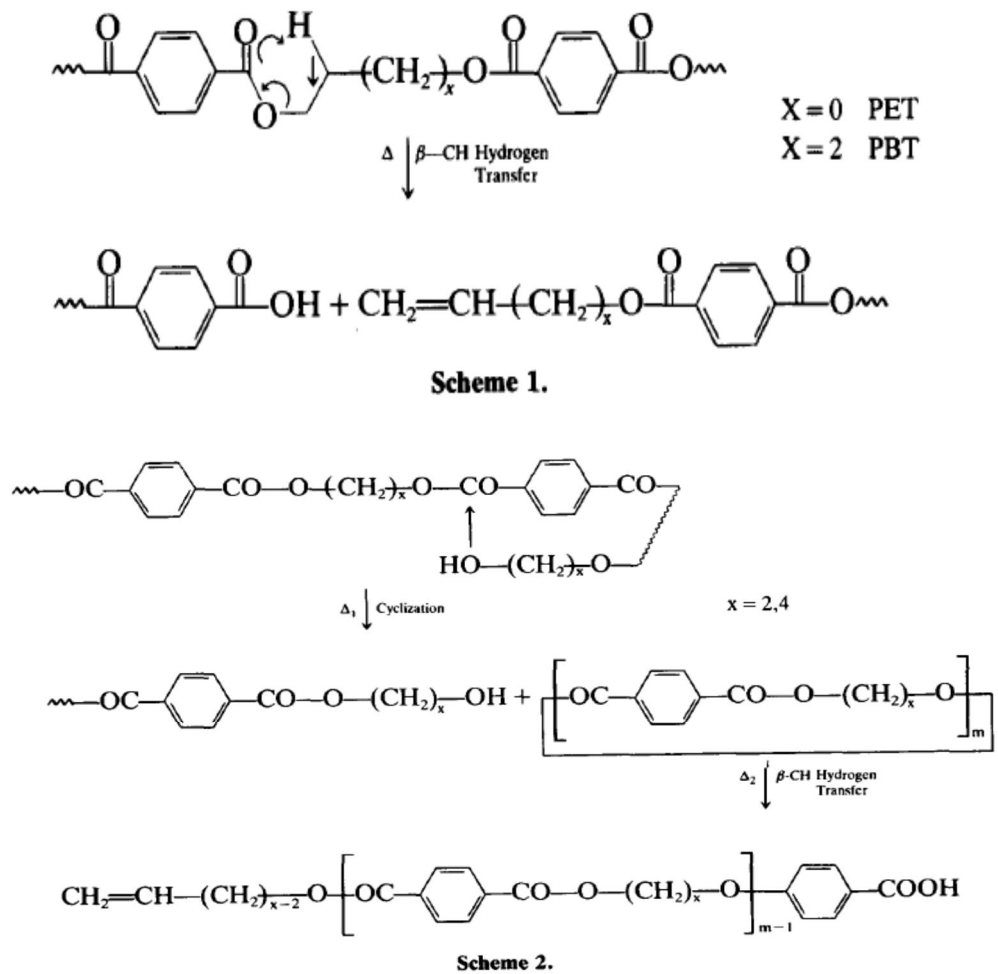


Figure 2.1- 4 Thermal degradations of PET and PBT (a) Scheme 1
(b)Scheme 2 [20]

The Scheme 2 proposed by Montaudo et al. [20], involved an intramolecular exchange process that leads to the formation of the cyclic oligomer. The Scheme 2 is based on an on-line analysis that prevents thermally labile compounds with short lifetimes at high temperatures to escape the reactor. Montaudo et al. [20], reported that several studies have ascertained that the cyclization occurs in PET through an intramolecular alcoholysis reaction (ionic). The intramolecular alcoholysis is usually activated at a temperature range of 250-300 °C, involving the attack of hydroxyl ends on the inner group of the polyester chain as scheme.

2.2.5 Polyvinyl Chloride (PVC)

Polyvinyl chloride (PVC) produced by polymerization of the monomer, vinyl chloride. The monomer vinyl chloride is prepared using various methods;

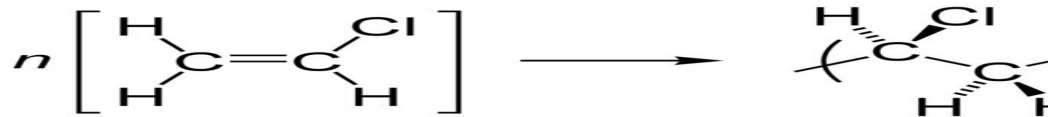
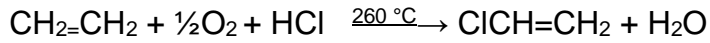


Figure 2.1- 5 Polymerization of vinyl chloride to polyvinyl chloride

Polyvinyl chloride used in sewage piping and other piping applications when cost or vulnerability to corrosion limits the use of metal. In the thermal degradation of the polymer, polyvinyl chloride degrades by a different mechanism compared to other common polymers such as PE, PP and PS with a two-stage mechanism. Dehydrochlorination (DHC) is the first stage in which more than 99 wt. % of the initial chlorine content in PVC released as HCl in the temperature range of between 200-360 °C that is lower than the usual decomposition temperature of polyethylene, polypropylene, and polystyrene [21].

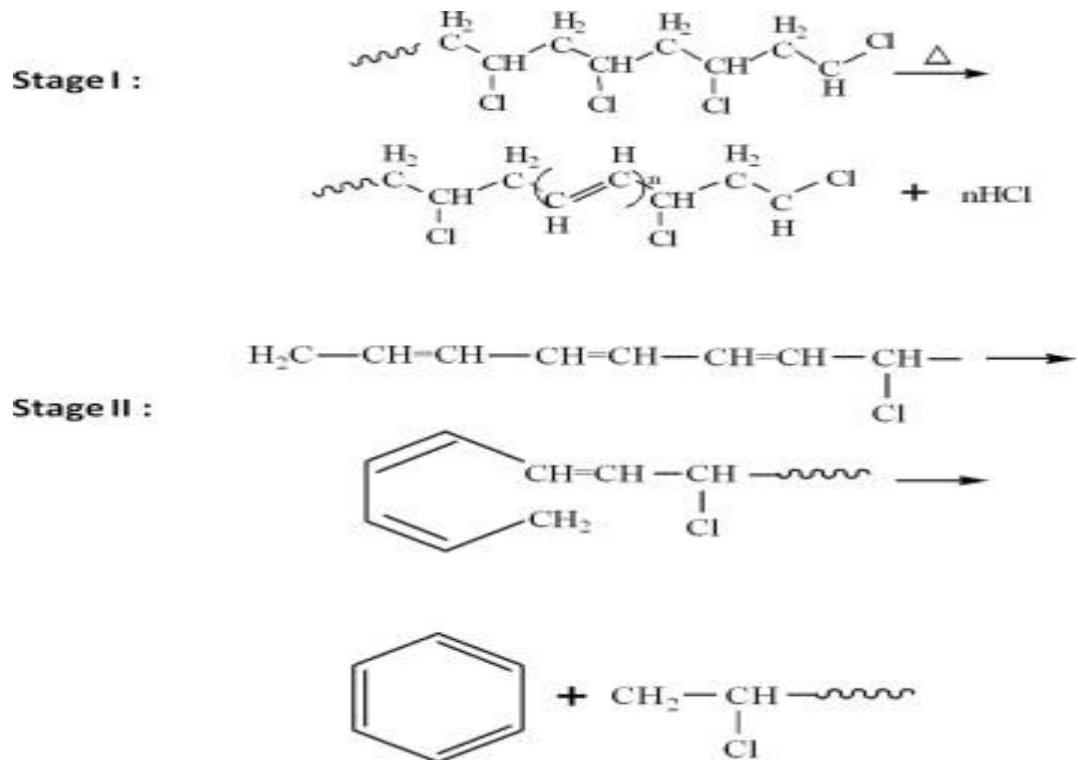


Figure 2.1- 6 Two stage degradation of PVC stage: Elimination of HCl and stage 2: Decomposition of unsaturated hydrocarbons and benzene formation [21]

The emission of HCl accompanied by the evolution of small amounts of C_1 - C_4 hydrocarbons, C_6H_6 and some unsaturated aromatic compounds [22, 23]. Aromatization and chain scission dominate degradation at higher temperature giving large amounts of carbonaceous residue whereas liquid products are formed in low amounts [21, 24]. Williams and Williams [25], reported on the pyrolysis of PVC at a heating rate of $25\text{ }^\circ\text{C min}^{-1}$ to a maximum temperature of $700\text{ }^\circ\text{C}$ in the fixed bed batch reactor. They recorded product yields of 2.47% permanent and hydrocarbon gas, 31.69% oil, 13.78% char and 52.93% as HCl gas. However, other researchers recorded much higher char values up to 20% [26].

2.2.6 Acrylonitrile butadiene styrene (ABS)

Acrylonitrile butadiene styrene (ABS) is a copolymer made by polymerization of styrene, and acrylonitrile in the presence of polybutadiene. Acrylonitrile is a

synthetic monomer produced from propylene and ammonia, and styrene obtained by dehydrogenation of ethylbenzene. ABS is used to make light, rigid molded products such as piping, musical instruments, golf club heads, automotive body parts, wheel covers, enclosures, protective head gear and toys.

Jung et al. [27], reported on the thermal degradation of ABS in a bench scale pyrolysis plant equipped with a fluidized bed reactor constructed with a char separation system. Pyrolysis was carried out over a temperature range of 430–510 °C. The oil produced was in the range of 64.11-77.41 wt. %, gas was 1.12-3.4 wt. % while char products were 6.36-21.21 wt. %. The addition of calcium based additives decreases oil yield and increased char formation. The major compounds formed were ethyl benzene, toluene, and styrene, with also appreciable N-compounds in the heteroatom fraction identified. The acetonitrile, propene-nitrile, propane-nitrile and benzene butane-nitrile were the predominant aliphatic and aromatic nitriles amongst the nitrogenised compounds. The reaction between acrylonitrile and styrene might be the source of benzene butane-nitrile [28]. The maximum styrene yields were recorded at reaction temperatures ranging between 460 and 480 °C. The hydrogenation of styrene at higher temperature might have stimulated the production of ethylbenzene [27].

2.2.7 High Impact Polystyrene (HIPS)

High impact polystyrene (HIPS) is prepared by free radical polymerization of styrene in the presence of dissolved rubber such as polybutadiene (PB), to improve the impact strength and toughness of the glassy polystyrene.

HIPS commonly produced by the introduction of PB before the free radical polymerization of styrene with a variable content PB (3-10 mol %); the PB then compatibilized by the grafting of styrene units [29].

High impact polystyrene mainly used in making packaging, containers, appliance parts, housewares, refrigerator interiors, toys and interior parts in household electronics. HIPS composed of multiphase and multicomponent polymeric materials, with glass and rubber phases. End use properties are dependent on many variables such as the molecular weight and the distribution of the polymerized polystyrene and rubber used [30].

Some synergic combination of polybrominated compounds and antimony trioxide (Sb_2O_3) are used as flame retardants sometimes added to HIPS [31]. The polybrominated flame retardants are thermally labile and release Br radicals that extinguish the radical chain reactions of combustion and fire spreading processes. The antimony trioxide accelerates the rate of halogen release from aromatic halides via the formation of antimony halides and oxyhalides during combustion [32] [33]. Polybrominated diphenyl ethers (DPE) were known to produce brominated dioxins and dibenzofurans (DBF) during combustion [34]. Accordingly, Dumler [35], studied the formation of polybrominated DBFs from decabromodiphenyl ether (Br_{10} -DPE) in a polybutylene-terephthalate- Sb_2O_3 matrix. They observed that high-temperature degradation (500–700 °C) resulted in a high yield of tetrabromo dibenzofurans. Likewise, numerous brominated benzene, toluene, and styrene derivatives have also been identified by [36] through combustion of HIPS- Br_{10} -DPE- Sb_2O_3 composite.

2.3 Thermal Degradation of Mixed Plastics

The processing of highly commingled plastics with different compositions of plastics represents a significant technical challenge [37]. This challenge is as a result of the different degradation pattern and possibility of interaction of plastics degradation product. For example, the presence of polyvinyl chloride in a mixture of plastic wastes which undergoes pyrolysis always is accompanied by releases of hydrogen chloride. The hydrogen chloride released by PVC can cause not only a corrosion of the equipment but, also the formation of chloro-organic compounds in the product hydrocarbon oil [38].

Mlynková et al. [39], reported work on the thermal pyrolysis of several mixtures of commonly found plastic wastes. The mixture consists of high-density polyethylene (HDPE), low-density polyethylene (LDPE), linear low-density polyethylene (LLDPE), polypropylene (PP), polyvinyl chloride (PVC), polyethylene terephthalate (PET) and polystyrene (PS). The reactor used was a batch reactor system at temperatures from 350 to 500 °C at atmospheric pressure. The low carbon number fractions in the gasoline range were the primary yield, and there was a small yield fraction of heavy oil. The predicted polystyrene, polyvinyl chloride and polyethylene terephthalate in the feedstock had a significant effect on the formation and yields of gases and oil/waxes in comparison with thermal cracking of individual and mixed polymers. The authors found that the presence of polystyrene, polyvinyl chloride and polyethylene terephthalate increased the formation of carbon monoxide and carbon dioxide in the gas and benzene, toluene, xylenes, styrene in the liquid (oil/waxes) products [39].

Bhaskar [40], investigated the influence of the presence of PET in a mixture of PP/PE/PS/PVC/HIPS-Br plastics, during pyrolysis. The author reported a significant influence on the product yield and composition. For example, both the gaseous products and chlorinated branched alkanes yields increased in the presence of PET, with a waxy residue formed. On the other hand, liquid yield decreased.

Ballice [41], reported work on the co-pyrolysis of low-density polyethylene with polypropylene, and the authors found that conversion of the mixture into volatile hydrocarbons was higher with the mixture. However conversion rise with increasing amount of polypropylene ratio in the co-pyrolysis operation. The work showed that n-alkane hydrocarbon gas yield (C₁-C₄) improved with the increase in polypropylene in the mixture. The formation rate of n-alkenes was lower than n-alkanes. Jung et al. [42], reported work on pyrolysis of a fraction of waste PP and PE for the recovery of BTX aromatics using fluidized bed reactor. They suggested that the ease with which propene formed in polypropylene pyrolysis enabled subsequent participation in Diels–Alder reactions for benzene, toluene and xylene production. The propene formation was as a result of sequence reactions; random chain scission of polypropylene produces both primary and secondary radicals, and afterward, tertiary radicals were formed by intramolecular transfer reactions. Thus, the beta cleavage of the tertiary radicals led to the easier formation of propene [43].

2.4 Catalytic Pyrolysis of Plastics

In this section, catalytic pyrolysis is discussed for both single and mixed plastics. The yield and composition of pyrolysis products greatly influenced

by a range of process parameters. These parameters include the type of waste plastic, reactor system, the gas residence time, temperature and pressure ranges, the presence of a catalyst and or hydrogen gas or hydrogen donor compounds [44] [39] [5] [45].

2.5 Catalytic Degradation of Single Plastics

Single plastics were pyrolyzed using various catalysts type, amounts, and reactor type and reaction condition as reported by researchers.

2.5.1 Polyethylene

Gonzalez et al. [6], investigated the thermal and catalytic degradation of polyethylene wastes in the presence of silica gel, 5A molecular sieve and activated carbon in a batch reactor at 450, 500 and 700 °C temperature for 2 h. The catalytic degradation showed a higher conversion of PE waste than the thermal degradation for all the temperature ranges. They found that the silica gel conversion rate decreased with increasing temperature. The 5A molecular sieve conversion of PE increased with temperature and activated carbon recorded the highest conversion at the lower temperature of 450 °C. Buekens and Huang [46], reported work on the catalytic and thermal degradation of PE to a broad range of products. The authors reported that activated carbon as a catalyst gave the highest quantity of aromatics compounds, while the silica gel produced a greater amount of methane.

Shah et al. [14], performed catalytic pyrolysis using a wide range of acidic and basic catalysts; silica (SiO_2), calcium carbide (CaC_2), alumina (Al_2O_3), magnesia (MgO), zinc oxide (ZnO), and homogeneous mixture of silica and alumina. The authors based temperature optimization as the suitable

temperature at which maximum liquid could be obtained. But, the total conversion was based on the amount of liquid, and gas formed during catalytic pyrolysis. Thus, MgO, CaC₂, SiO₂ and Al₂O₃ optimum was obtained at 350 °C. But, ZnO and mixture of silica and alumina optimum was obtained at 400 °C temperatures. Shah et al. [14], found that beyond the optimum temperature a decrease in the liquid fraction, and associated that with further conversion of a liquid into volatile product leading to higher gases and decrease in liquid fraction. Shah et al. [14], conclude from the physical test results, that the liquid fractions are comparable with the standard results of the physical test for gasoline, kerosene and diesel fuel oil.

Olazar et al. [47], reported the influence of FCC catalyst steaming on HDPE pyrolysis product distribution, using a conical spouted bed reactor provided with a feeding system for continuous operation to maximize the diesel -oil fraction. They used commercial FCC catalysts based on active zeolite phase for the pyrolysis of HDPE, and also different treatment applied to improved catalyst behavior. Thus separately from the fresh catalyst, the two different steaming treatment have been applied to the catalyst. The treatment is mild steaming carried out at 760 °C for 5 h and severe steaming at 816 °C for 8 h. The pyrolysis runs have been carried out at 500 °C with the fresh and mildly steamed catalysts while a reduced temperature of 475 °C was used for severely steamed catalyst to improve product distribution. The catalyst used by Olazar et al. [47], has the following characteristic properties as shown in Table 2.2-1.

Table 2.2-1 Properties of the fresh and equilibrated FCC commercial catalysts used [47]

	<i>Fresh</i>	<i>Equilibrated at 750 °C</i>	<i>Equilibrated at 816 °C</i>
<i>BET surface area (m²/g)</i>	338	192	187
<i>Micropore Volume (cm³/g)</i>	0.116	0.061	0.061
<i>Mesopore volume (cm³/g)</i>	0.070	0.078	0.099
<i>Acid strength (kJ/mmol NH₃)</i>	123.2	99.2	87.9
<i>Total acidity (mmol NH₃/g cat)</i>	0.598	0.057	0.039

The fresh catalyst yielded 52 wt. % gas, 35 wt. % light liquid fraction and; low C₁₀⁺ fraction (13 wt. %). However, after the author performed mildly steaming the results show a significant change in product distribution. Consequently, product gas yield decreases to 22 wt. %, light liquid fraction yield is similar to that of the fresh one (38 wt. %), but the desired C₁₀⁺ fraction rose to 38 wt. %. However, the best results concerning aim of the work were obtained with severe streamed catalyst. Thus, the gas fraction was decreased (8 wt. %), the light liquid fraction also reduced to 22 wt. % and the yield of diesel fraction rose to 69 wt. %).

2.5.2 Polypropylene

Lin and Yen [48], performed work on the fluidized bed pyrolysis of polypropylene over a zeolite cracking catalyst for the production of

hydrocarbons at a temperature range 290-430 °C in a varying nitrogen flow (270-900 mL/min). But, the authors used three zeolite catalysts; HZSM-5, H-ultra stabilised Y-zeolite (HUSY) and H-mordenite (HMOR) and non-zeolite; amorphous SiO₂-Al₂O₃ (SAHA) and mesoporous-Mobile crystalline materials (MCM-41). Lin and Yen [48] found that the zeolite catalyst (in order HZSM-5>HUSY ≈HMOR) recorded a higher volatile hydrocarbon yield than the non-zeolite catalyst (SAHA ≈MCM-41). Equally, zeolite catalysts produced more alkane hydrocarbon while the non-zeolite catalyst produced more alkene hydrocarbons. Lin and Yen [48], found that HZSM-5 catalyzed show product distribution contained more olefinic materials with about 60 wt.% in the range of C₃-C₅. However, other two zeolite catalyst HMOR and HUSY produced more paraffin streams with large amounts of isobutene (i-C₄). The non-zeolite SAHA and MCM-41 gave the lowest conversion and produced an olefin-rich product with the rise to the broadest carbon range C₃-C₇. The authors suggested that under suitable reaction conditions, a catalyst can have the ability to control both the product yield and product distribution from polymer degradation, potentially leading to a cheaper process with more valuable products.

2.5.3 Polystyrene

Pyrolysis of polystyrene produces a high concentration (>70%) of styrene and other styrene oligomers compared to catalytic pyrolysis which shows a marked reduction in styrene content in the product oil [49, 50]. Lower yields of styrene from catalytic degradation of polystyrene on solid acid catalysts have been attributed to further cracking of styrene into either toluene or benzene and further hydrogenation of styrene into ethylbenzene [51].

Bagri and Williams [50], investigated the catalytic pyrolysis of polystyrene over fluidized bed reactor. They used ZSM-5 catalyst to study the effect of catalyst bed loading and particle size on product yields and composition of the derived oils and waxes. Bagri and Williams [50], found gas yield increased with the addition of ZSM-5 catalyst and further increased with increasing catalyst loading. However, the wax/oil yield decreases with the catalyst loading. They also found that reduction of catalyst particles size had the same effect as catalyst loading. The hydrocarbon gases produced are mainly C₁, and C₄, ethane and propene gases are dominant. Bagri and Williams [50], found that the product oils for non-catalyzed pyrolysis run contain a large amount of styrene and a small quantity of non-styrene single ring aromatic and PAH. But, they found a reduction in styrene concentration and increase in non-styrene single ring aromatic and PAH with the introduction of catalyst and rose with catalyst loading.

2.6 Catalytic Degradation of Mixed Plastics

Lin [52], performed a pyrolysis of a post-consumer plastic waste (PE /PP /PS/ PVC) over a wide range catalysts (FCC-R1, HUSY, ZSM-5, and SAHA), using a fluid catalytic cracking (FCC) process operating at ambient pressure. The product distribution at 390 °C was dependent on the type of catalyst used. For example, the zeolitic catalysts (ZSM-5 ≈ HUSY) gave a higher yield of volatile hydrocarbons than non-zeolitic catalysts (SAHA) and the zeolite based equilibrium FCC catalyst (FCC-R1). The zeolitic catalyst ZSM-5 gave the highest volatile hydrocarbon yields (83.3 wt. %). The bulk of products obtained with the acidic cracking catalysts (FCC-R1, HUSY, ZSM-5, and SAHA) were in the gas phase with less than four wt. % liquid collected.

The significant difference in the products between the acidic catalysts observed with ZSM-5 producing a much higher C₁–C₄ hydrocarbon gas yield (~55 wt. %) than HUSY, SAHA, and FCC-R1 catalysts. However, some similarities were observed between SAHA and FCC-R1 with C₁-C₄ and C₅-C₉ yields, which were approximately 24 - 30 wt. % and 52-55 wt. % respectively. However, both acidity and diffusion constraints within individual microspores of each catalyst may play significant roles in the observed products distribution confirmed by Lin, [52].

Bhaskar et al. [40], reported on catalytic experiments in the presence of Ca-C catalyst on the effect of PET in a mixture of PP/PE/PS/PVC/HIPS-Br, using semi-batch operation for pyrolysis at 430 °C temperature. The use of calcium carbonate (Ca-C) without PET entirely removed Cl and Br. But for the liquid products trace amounts of Cl and Br (20 ppm and 310 ppm respectively) were detected in the presence of PET. The chlorine-containing compounds detected in the liquid products were mono-chlorinated branched alkanes (2-chloro-2-methylpropane, 2-chloro-2-methylpentane, and 2-chloro-2, 4-dimethylheptane). The addition of the released HCl during PVC pyrolysis on products of polypropylene decomposition forms the basis for the formation of the chlorine compounds. The tertiary carbon atoms of PP are more prone to Cl addition than secondary C-atoms of n-alkenes and n-alkadienes, the main unsaturated products of PE decomposition. Thus, the HCl furthermore reacts with styrene monomer and dimer to formed a significant amount of 1-chloro-ethylbenzene and a smaller amount of chlorinated diphenyl butane and pentane [40]. The catalytic decomposition of HIPS-Br evolves a significant quantity of hydrogen bromide. HBr reacts primarily with branched alkenes and

styrene as indicated by the evolution of 2-bromo 2-methyl pentane, and 1-bromo ethyl benzene in the study reported Bhaskar et al. [40].

Tang et al. [53], published work on the catalytic degradation of the mixed polymer systems, PE/PVC at 420 °C, PP/PVC at 380 °C and PS/PVC at 360 °C was reported. The work was carried out in a glass reactor under atmospheric pressure by the batch operation. For thermal degradation of the mixed polymer systems, the liquid yield was highest (72.7%) for PP/PVC and lowest (60.5%) for PS/PVC. The char product was highest (19.3%) for the PS/PVC mixture with PP/PVC recording the lowest (8.55%). Consequently, the chlorine distribution in various phases showed 88 – 96 wt.% of chlorine content of the sample evolved as gaseous HCl, and in the liquid, 3 -12wt.% and less than 2 wt.% in the residue. The liquid yield was highest (64.38%) for the PP/PVC mixture and lowest (59.85%) for the PS/PVC. However, for catalytic degradation the liquid yield was lower than thermal degradation, this might be due to further cracking of some long chain hydrocarbons. This argument further demonstrated with high gas yield for the catalytic degradation. The char products were highest (23.56%) for the PS/PVC while the mixture of PP/PVC gave the lowest liquid phase (8.02%). However, except for the PS/PVC mixture the char produced by catalytic degradation was higher than thermal. The chlorine distribution in various phases showed a sharp decrease in both liquid and gas phases while char (residue) recorded the highest yield for all samples

Hung et al. [54], studied the pyrolysis of post-consumer polymer waste (HDPE/LDPE/PP/PS) in a fluidized bed reactor operating isothermally at

ambient pressure over various catalysts over range of a reaction temperature 290-420 °C. The acidic zeolite catalyst yielded higher volatile hydrocarbons in the order of ZSM-5>MOR>USY than non-zeolite catalyst MCM-41>ASA over a range of reaction conditions. The majority of the products were gas with less than 6 wt. % liquids. The non-zeolite catalyst ASA with the low surface ($274 \text{ m}^2 \text{ g}^{-1}$) and Si: Al ratio (2.6), produced a highest unconverted polymer. But, the zeolite catalyst USY with high surface area ($603 \text{ m}^2 \text{ g}^{-1}$) and Si: Al ratio (6.6) yielded the highest coke as solid products. For USY, the gas phase and solid residue production increased with increased temperature. Similarly, faster rates of hydrocarbon production were observed at a higher temperature. The time for the polymers to be degraded lengthened, and the initial rate of hydrocarbon production dropped as the temperature decreased. The ZSM-5 cracking catalyst exhibited greater selectivity for the product yields, with about 60% of the products in the range of $\text{C}_3\text{-C}_5$.

Zhou [55], performed a catalytic degradation of polyvinyl chloride (PVC) containing polymer mixtures. The polymer mixture includes polypropylene (PP)/PVC, low-density polyethylene (LDPE)/PVC, polystyrene (PS)/PVC and LDPE/PP/PS/PVC. Accordingly, for LDPE/PVC thermal degradation, the wt.% distribution of Cl was that the bulk amount (95.89%) was in the gas phase products with less than 4% in liquid products and the residue contained only trace amounts (0.16%).

Lopez et al. [56], worked on catalytic pyrolysis of packaging plastic waste using semi-batch reactor. The researchers explored three methods. Hence, the first method was "Conventional catalytic pyrolysis" where the plastic sample mixed with the catalyst and the system heated at a rate of $20 \text{ }^\circ\text{C min}^{-1}$

¹ to 400 °C and maintained there for 30 min. The second method "Catalytic stepwise pyrolysis" where plastic sample mixed with a catalyst, then a dechlorination was carried out at a temperature of 300 °C for 60 min before the temperature was raised at 20 °C min⁻¹ to 440 °C to complete the pyrolysis process. The third method was "Non-catalytic dechlorination step+ catalytic pyrolysis". In which the dechlorination step was applied to the plastic sample alone (without catalyst) and then the catalyst was added and then carry out the final pyrolysis as in the other methods. The zeolite catalyst ZSM-5 with the following properties; BET S.A. (m² g⁻¹) 412.0, external S.A. (m² g⁻¹) 65.88, micropore volume (cm³ g⁻¹) 0.100, total pore volume (cm³ g⁻¹) 0.397, and total acidity (mmol NH₃ g⁻¹) 0.176 was used. Five plastic samples used for the mixture are polyethylene (40%), polypropylene (35%), polystyrene (18%), PET (4%) and polyvinyl chloride (3%).

They observed that the catalyst played an important role in pyrolysis product distribution, producing more gas and lower liquid than in the thermal run. However, zeolite catalysts show losses in activity with an increase in liquid yield and a reduced in gas yield when a dechlorination step is carried out in the presence of a catalyst. Lopez et al. [56], preferred that the decreased in gas yield owing to the loss of activity of the catalyst seemed to be greater than the increase due to the dechlorination step. Thus, the catalyst might have lost its activity because the plastic sample melted during the dechlorination step, then cracked, and the melted fragment may physically block the catalyst pores. Therefore, the effect of the catalyst in the subsequent pyrolysis step could be hindered.

The characteristic of the pyrolysis liquids in the three different methods used by Lopez et al. [56], show variation in their composition. The liquid was characterized using GC-MS analysis and reported as area % calculated with respect to total ion. Conventional catalytic run shows the low molecular weight C₅-C₉ as the main fraction, amounting to more than 80% area. However, when they carried out dechlorination step in the presence of the zeolite. The percentage of light (C₅-C₉) and medium (C₁₀-C₁₃) hydrocarbons significantly decrease (to 70.4 and 1.5 % area respectively), and the yield of heavy hydrocarbons increases up to 9.5 % area. These further strengthen the argument, which that the catalyst loses its activity with dechlorination step. But when compared the conventional catalytic run with non-catalytic dechlorination step + catalytic pyrolysis, the catalyst works well with both runs recorded nearly equal amount of C₅-C₉ yields (81.5 and 82 %area respectively). However, they observed the difference in the C₁₀-C₁₃ and >C₁₃ yield, which are lower and higher respectively than in the conventional catalytic run. The authors reported similar trend found in their previous work [57] for non-catalytic pyrolysis run as the stepwise pyrolysis compared to conventional thermal run. They suggested that some degradation and rearrangement of polymer structure are taken place during the dechlorination step, leading to different pyrolysis pathways and consequently to various pyrolysis products.

Likewise, the authors reported the distribution of aromatics show similar trend as observed in the composition of light, medium and heavy hydrocarbons. The conventional catalytic (>95%) and non-catalytic dechlorination + catalytic pyrolysis run (94.2%) are similar. But as the dechlorination step was carried

out with the catalyst mixed with the sample, the production of aromatic was lowered (80.6%). The high yield of aromatic came as a surprise to the authors since the plastic sample used in the work mainly composed of a polyolefin. However, they revealed that there was evidence in the literature that high content of aromatic could be obtained from the pyrolysis of the polyolefin. The use of ZSM-5 in the pyrolysis of the polymer was reported by the authors to obtain liquids with a high level of aromatics. They attributed this to the high number of Bronsted acid sites contained within the zeolite, which promote aromatization reactions. The distribution of the main aromatic compounds shows a similar trend for the conventional catalytic run and the non-catalytic dechlorination + catalytic pyrolysis run. Both produced more than 30% area of styrene, and around 10% area of toluene, ethyl benzene, and xylenes. But the stepwise catalytic pyrolysis run produced higher styrene ($\approx 45\%$ area) and other less than 10%. The authors were able to reduce the chlorine content with the addition of dechlorination step to about 75 wt. % reduction in the liquid fraction.

Antonakou et al. [58] performed pyrolysis and catalytic pyrolysis as a recycling method of waste CDs originating from polycarbonate and HIPS in a bench fixed bed reactor. The two catalysts used included ZSM-5 based catalyst with properties as follows, BET surface area $127 \text{ m}^2 \text{ g}^{-1}$, the total number of acid sites $0.14 \text{ mmol NH}_3 \text{ g}^{-1}$ and Bronsted to Lewis acid sites ratio 1.8. The other catalyst was MgO catalyst with properties as follows, the surface area of $62 \text{ m}^2 \text{ g}^{-1}$ and negligible acidity of $<0.01 \text{ mmol NH}_3 \text{ g}^{-1}$ and contained basic sites $0.24 \text{ mmol NH}_3 \text{ g}^{-1}$. The samples used for the work were commercial poly(bisphenol A carbonate) and HIPS; and two commercial CDs

which were CD-PC (polycarbonate base) and CD-PS (polystyrene base). The plastic to catalyst/silica ratio used was 2:1. The solid feedstock fed from the top of the reactor and was pushed down instantaneously with the aid of a piston in the reactor hot zone (at 600 °C). The produced pyrolysis vapour was swept through the catalyst bed with flowing N₂ (100 ml min⁻¹) for 15 min while an additional purging with N₂ (50 ml min⁻¹) performed for another 10 min. The authors observed that the nature of polymer had a dramatic effect on the pyrolysis product yields. However, the use of both catalysts did not seem to have a significant additional effect on the product yields compared to those of thermal pyrolysis run. The product yield for both thermal and catalytic run for PC (both CD-PC and PC), showed liquid products yield between 50 and 60 wt, %, gas yield 15-20 wt. % and solid products 20-30 wt. % the original polymer. The polystyrene raw material (HIPS and CD-PS) both pyrolysis runs showed liquid fraction was the main pyrolysis products, with more than 90 wt. % of the original polymer. Likewise, a similar behavior was observed for the model and commercial polymers (with the same chemical origin) in terms of pyrolysis product distribution under same experimental conditions. Antonakou et al. [58] had an astonishing findings in terms of the high selectivity of the valuable chemicals in the pyrolysis liquid fractions (up to 93 and 95 area % observed for phenol and aromatic respectively). The use of catalysts had showed a negligible effect on the liquid fraction composition, with only a noticeable small increase in the yield of phenols with the use of basic MgO catalysts in the pyrolysis of PC polymer. Then, Antonakou et al.[58], suggested that the decrease in a monomer for catalytic pyrolysis of both polymers was because selected catalysts favour the polymer decomposition into lower molecular weight compounds (mainly single ring phenols and

hydrocarbon). Thus, for these mention reason the liquid fraction coming from catalytic pyrolysis run contain less of the initial monomer. The two catalysts used did not differ in terms of recovery of monomer in the polymer studied, and thermal pyrolysis was a better option as a recycling method for recovery of the monomers. Benzene was detected in the catalytic run of polystyrene raw materials, as rightly reported by other researchers [58].

Lee [59], performed work on the composition of aromatic products in the degradation of the mixture of wastes PS and HDPE using spent FCC catalyst in a semi-batch reactor at 400 °C. The study used 10:1 reactant to catalyst ratio, N₂ stream 20 ml/min, a heating rate of about 9 °C/min to 400 °C and stirring speed of 200 rpm. The characteristic of the FCC used in the research was summarized as follows; BET surface area 151 m²g⁻¹. Then the micropore area 76 m²g⁻¹, mesopore area 75 m²g⁻¹, total volume 0.25 cm³g⁻¹, micropore volume area 0.03 cm³g⁻¹ and average pore diameter 6.7nm. The experimental system used by Lee [59] shown in Figure 2.2-1

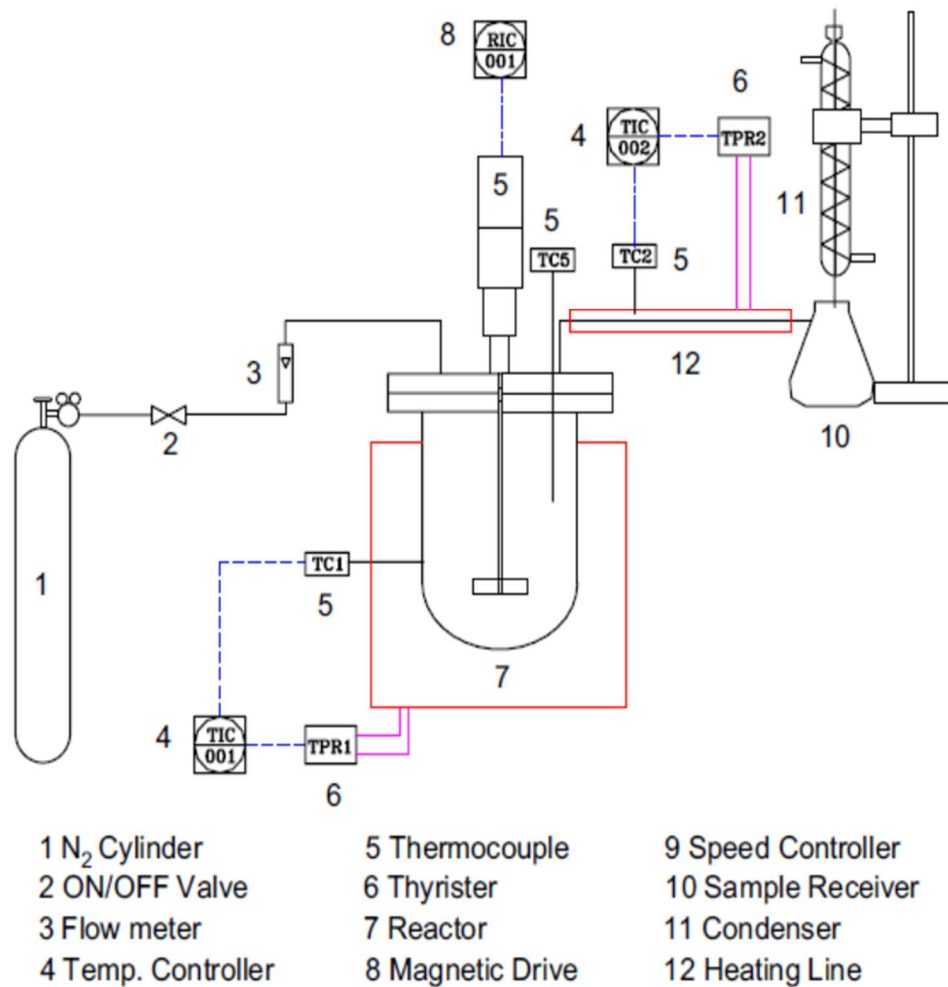


Figure 2.2-1 Schematic diagram of the experiment [59]

The author obtained in the initial (short) reaction time the fraction of gasoline range components (C₆-C₁₂) in liquid products was 90 wt.% or more, irrespective of weight proportion of HDPE and PS. Then during the prolong reaction time the fraction gasoline range components was reduced, whereas the kerosene and diesel compounds (>C₁₃) rose. These results obtained were suggested to be due to different degradation characteristic of PS and HDPE [59, 60]. Consequently, Lee [59] noted that degradation of PS mainly influenced carbon number distribution of oil product obtained at initial (short)

reaction time. But with a prolonging in reaction time the effect of HDPE with relatively difficult degradation become apparent. The composition of the degraded product obtained strongly depended on the chemical properties of the plastic type in waste plastic as observed by the other authors. Thus, the styrene monomer and alkyl-styrene content in degraded products had risen with the increase in the PS content in plastic mixtures. Lee [59] noted from Boxiong et al. [61], that the concentration of aromatic hydrocarbons obtained from the degradation of the waste polymer using USY catalyst with large pore size was much higher than that for ZSM-5 with small pore size. Therefore, the size of zeolite aperture plays a crucial role in the aromatic product distribution. Lee [59], showed that the distribution of styrene and ethylbenzene product highly influenced by the proportion of both HDPE and PS. While, he observed benzene and toluene products were 10% or less, and these are less than styrene and ethylbenzene product obtained. The author [59], concluded that the distribution C₉-C₁₂ alkyl aromatic components as by-products, methyl styrene, (C₁-styrene) and isopropylbenzene (C₃-benzene) components were the primary products formed by β -scission and hydrogen transfer of PS while the rest of alkylation products showed very low fraction being 1% or less.

Lin and Yang [62], reported work on catalytic conversion of commingled polymer waste into chemical and fuels over spent FCC commercial catalyst in a fluidized-bed reactor Figure 2.2-2. The commingled polymer waste (CPW#1) used is composed of HDPE=38 wt.%, LDPE= 24 wt.%, PP = 30 wt.%, PS = 7 wt.% and PVC =1 wt.%.

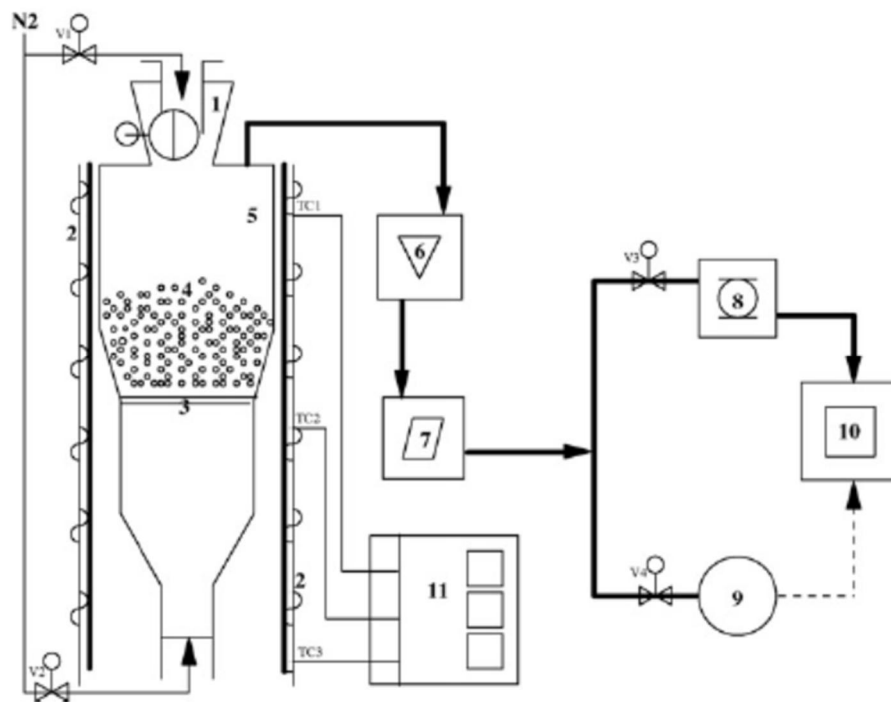


Figure 2.2-2 Schematic diagram of a fluidized bed reactor system : (1) Feed (2) Furnace (3) sintered distributor (4) fluidized catalyst (5) reactor (6) condenser (7) de-ionized water trap (8) 16-loop automated sample system (9) gas bag (10) GC and (11) digital controller for three=zone furnace[62].

Six catalysts used for the pyrolysis of the commingled polymer are as follows; ECat-1, USY, ZSM-5, ASA, and silicates. The catalysts characteristic properties are shown in Table 2.2-2 [62].

Table 2.2-2 Catalysts used in commingled polymer waste degradation [62]

Catalyst	Si/Al	Surface area	Surface area (cm^2g^{-1})	Surface area (cm^2g^{-1})	Metal (ppm)		Commercial name
		(cm^2g^{-1})	microspore	External	V	Ni	
ECat-1	ND ^b	147	103	44	2560	870	Equilibrium catalyst
Silicates	>1000		ND		-		Synthesized in-house
USY	5.7	547	421	126	-		Ultrastabilised Y-Zeolite ^c
ZSM-5	17.5	391	263	128	-		ZSM-5 zeolitic ^d
ASA	3.6	268	21	247	-		Amorphous Si:Al ^c

The carbon number distribution of the products of CPW#1 cracking at 400 °C over the six catalysts used by Lin and Yang [62], and nature of the product distribution found to vary with the catalyst used. The yield of volatile hydrocarbon for zeolite catalyst (ZSM-5 ≈ USY) gave higher than spent FCC commercial catalysts (ECat-1), and non-zeolitic catalysts (ECat-1 ≈ ASA). But the highest yield was obtained for ZSM-5 (≈ 86 wt.%). However, the work showed the bulk of the product obtained with these acidic cracking catalysts (ECat-1, ZSM-5, USY, and ASA) in the as phase with less than 6 wt.% Liquid collected. The significant difference in the product distribution between the catalysts used was found to be a high yield of C₁-C₄ hydrocarbon in ZSM-5 (53 wt.%) than ECat-1, USY and ASA catalysts. However, the authors observed some close similarity between ECat-1 and ASA with C₁-C₄ and C₅-C₉ yields, which were approximately 24-27 wt.% and 50-54 wt.% respectively. Lin and Yang conclude that the experiments carried out with differing

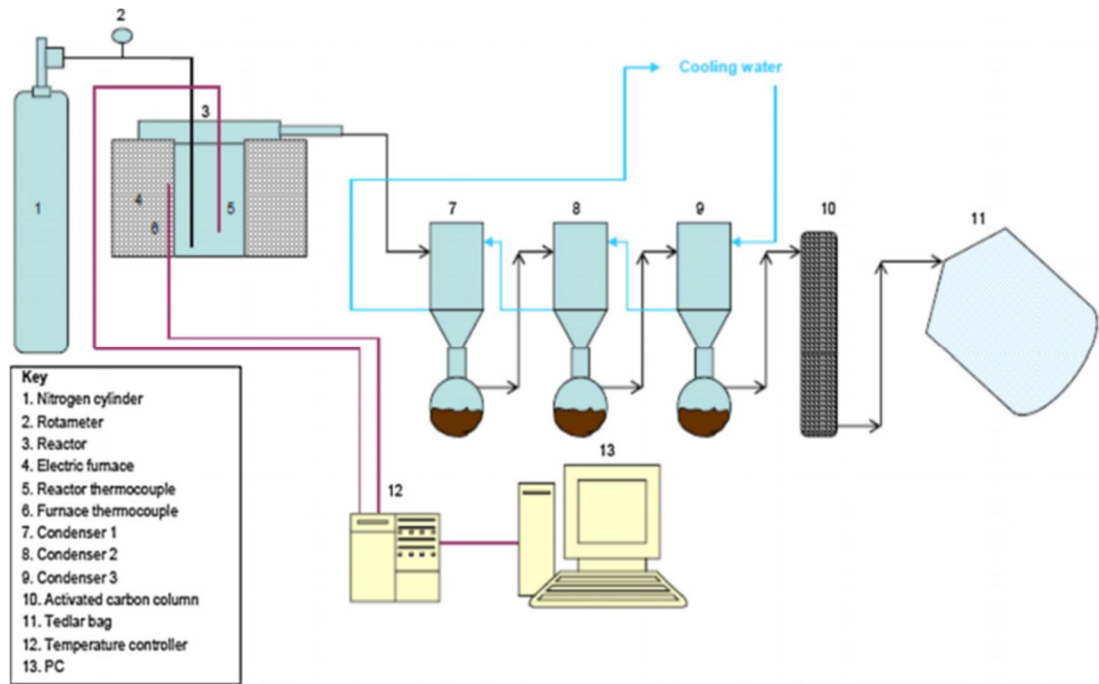
selectivity in the final products depend on reaction condition. Likewise, the selectivity could be further influenced by changes in operating conditions; in particular, olefins and iso-olefins were produced by low temperature and short contact time.

2.7 Reactor types

There are various types of reactor used in the pyrolysis of plastic materials. However, the most widely used are batch/semi-batch, fixed bed, fluidized bed, spouted bed and screw kiln reactors [63].

2.7.1 Batch/semi-batch reactor

The main reason for the use of batch/semi-batch reactor in the pyrolysis of plastics is the ease of their design and operation [63]. In some cases, a purge gas is used which removes the volatile products from the reactor that consequently reduces the extent of the secondary reactions of the primary pyrolysis products. There is voluminous literature that have reported on the use of either batch reactor [43, 64-67] or semi-batch reactor [49, 57, 68, 69].



2.3- 1 Schematic diagram of semi-batch reactor [57]

For example, Lopez et al. [57], work on the catalytic pyrolysis of a plastic mixture using a ZSM-5 zeolite catalyst. The study was carried out in a semi-batch reactor (Figure 2.3-1) at 440 °C. They proved that after one pyrolysis experiment the catalyst rapidly lost its activity. But the deactivation was found to be reversible via regeneration by heating at 550 °C in an oxygen atmosphere.

2.7.2 Fixed bed reactor

Fixed-bed reactors have been used for thermal cracking of the plastic, followed by feeding the liquid or gaseous products into the fixed catalyst bed as shown in Figure 2.3-2 [70-72].

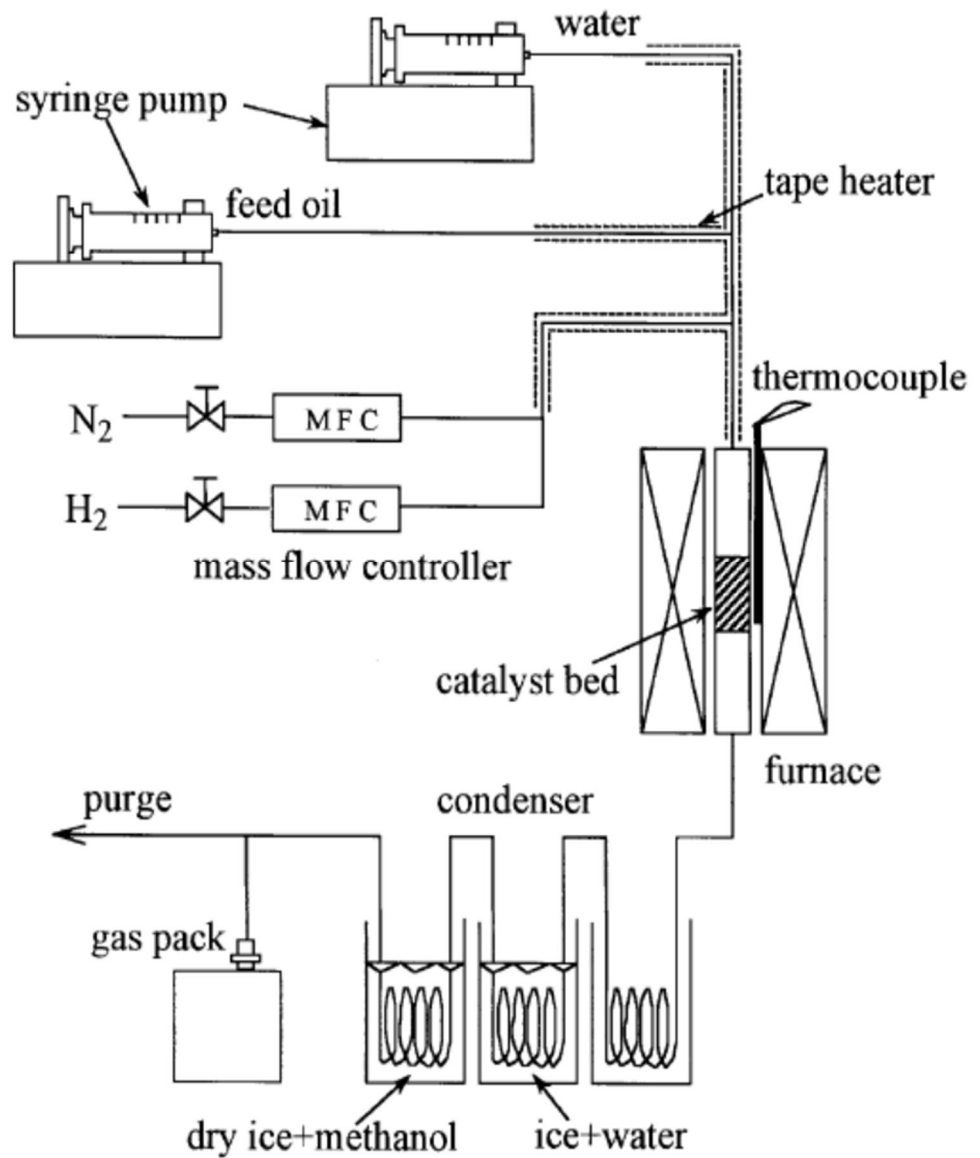


Figure 2.3- 2. Schematic diagram of fixed bed reactor [73]

For example, Masuda et al. [73], produced high-quality gasoline from waste PE derived heavy oil over a Raney-Ni catalyst, in a steam atmosphere using a fixed bed reactor.

2.7.3 Fluidized bed reactor

The use of fluidized bed reactors in plastic pyrolysis helps to eliminate the temperature gradients observed in other reaction systems [63]. Hence, both temperature and composition homogeneity are achieved with ease using fluidized bed reactors. Fluidized bed reactor also promotes the possibility of secondary reactions in the gas phase due to high gas flow rates of up to 25 L min⁻¹.

Umberto and Maria [74] quoted the following advantage of fluidized bed pyrolysis by Kunii and Lever [75];

- (i) The rapid and good mixing of solids, this allows virtually uniform isothermal condition throughout the bed i.e. reliable process control.
- (ii) The entire reactor of well-mixed solids represents a large thermal flywheel that resists to rapid temperature changes and avoids the formation of cold or hot spots.
- (iii) The range of operating temperature is usually lower than that of other gas-solid reactors.
- (iv) Heat and mass transfer between gas and particle are high when comparing with those of other gas-solid reactors and there is enough quality contact between reactants of a gas-solid reactor.
- (v) The liquid-like flow of particles allows continuously controlled operations with easy handling.

- (vi) The high process flexibility makes possible to utilize different fluidizing agents, operating temperature and gas residence times and to operate with or without a specific catalyst.
- (vii) The lower maintenance times and costs, the absence of moving parts in the hot region and lower operating temperature.

The authors [74] also enumerate the following disadvantages or shortcoming for fluidized bed reactor.

- (i) Friable solids are pulverized and entrained by the gas.
- (ii) For non-catalytic thermal treatment of waste, the agglomeration and sintering of fine or sticky particles can require a lowering use in operating temperature or a continuous withdrawal of bed materials that must be substituted with a make-up of fresh materials.
- (iii) The intensive rapid solid mixing in the reactor leads to a wide range of residence times of individual particles in the reactor; for continuous operation this gives poorer performance.
- (iv) Erosion of pipes and vessels by abrasion of bed particles can be serious
- (v) Scale-up is not always easy to realize in pilot plants, which is often necessary to verify the validity of laboratory scale test.

Kaminsky et al. [9], used a fluidized bed reactor which was shown in Figure 2.3-3 to investigate the thermal degradation of the plastic. The plastics degraded to monomers and oil, and syngas.

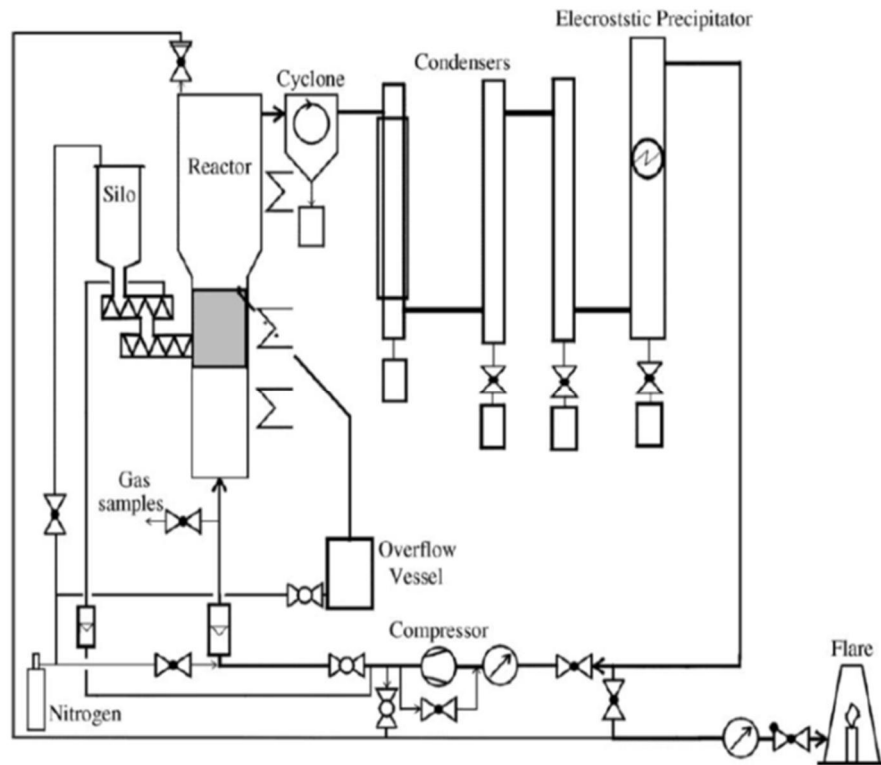


Figure 2.3- 3 Schematic diagram of Fluidized bed reactor [9]

The fluidized reactor used by Kaminsky et al. [9] had an interior diameter of 450 mm; the plastic was introduced by a screw or a double lock into an auxiliary fluidized bed of quartz sand at temperatures of between 600 and 900 °C. The fluidizing gas was preheated with pyrolysis gas at 400 °C. The various products obtained were separated in several stages comprising a cyclone, condensers, and electrostatic separators. The oil products were distilled in two packed column. The authors found that polystyrene as feed produced up to 75% styrene and 10% of oligomers, using fluidized bed reactor indicating that secondary reactions were well eliminated.

2.7.4 Spouted bed reactor

Elordi et al. [76], used a conical spouted bed reaction for the catalytic pyrolysis of HDPE on a ZSM-5 catalyst. The reactor presented in Figure 2.3-4 and showed that the conical shape is the principal component of an upper cylindrical section. The height of the reactor (H_T) 340 mm; Conical section (H_c) 205 mm the angle of the conical section (γ) is 28° . The cylinder dimensions (diameter (D_c) 123 mm; diameter base (D_i) 20 mm; and gas inlet diameter (D_o) 10 mm) guarantee bed stability in a wide range of process condition. The reactor was provided with a continuous solid-fed system and consisting of a hopper. The hopper was a hollow ball valve where the plastic to be pulse-fed is located with an inlet tube cooled by water.

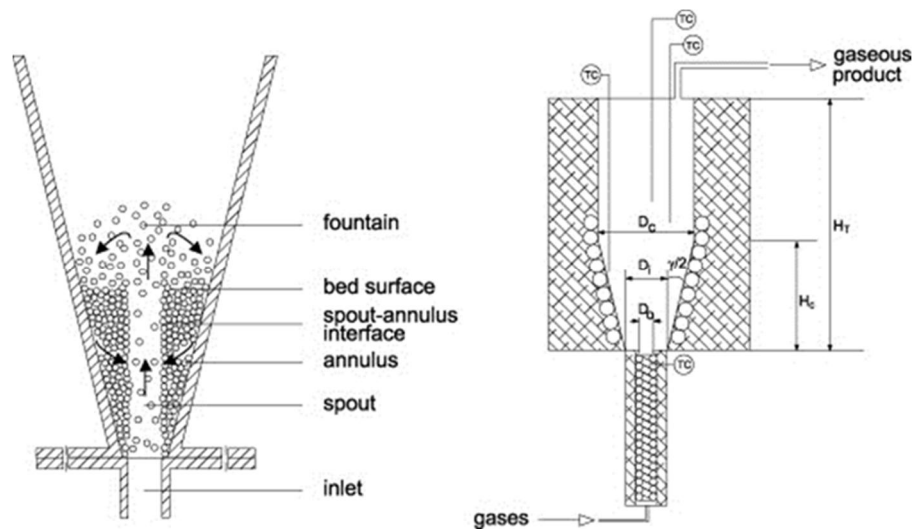


Figure 2.3- 4 Schematic diagram of a conical spouted bed reactor by Elordi et al. [76]

Screw kiln reactor

The screw kiln reactor mainly designed for thermal and or catalytic degradation of plastics and plastic oil mixtures [10 63 77 78]. The reactor as reported by Aguado et al. [64], was built with a hopper where raw plastics

were melted and fed by gravity into the screw. The stirring and mixing of the melted materials in the hopper was achieved by means of an electric motor and an anchor mixer. Nitrogen was employed to provide an inert atmosphere as the hopper was hermetically closed. The two furnaces F_A and F_B heated the hopper for the materials to be melted. A screw auger located inside a 52 cm long stainless steel tube with an i.d. of 2 cm in the second heating zone. The speed rate and residence time in the screw adjusted in a range 0.5-2.5 r.p.m. Three furnaces (F_C , F_D , and F_E) were used to heat the tube reactor, inside which is the screw. The F_C furnace kept at a temperature of melted plastics same as that existing inside the hopper. Hence, the furnace F_D and F_E allowed a combination of two different reaction temperatures set along the screw. Various thermocouples located inside the tube were used to measure the temperature at different points of the reaction zone.

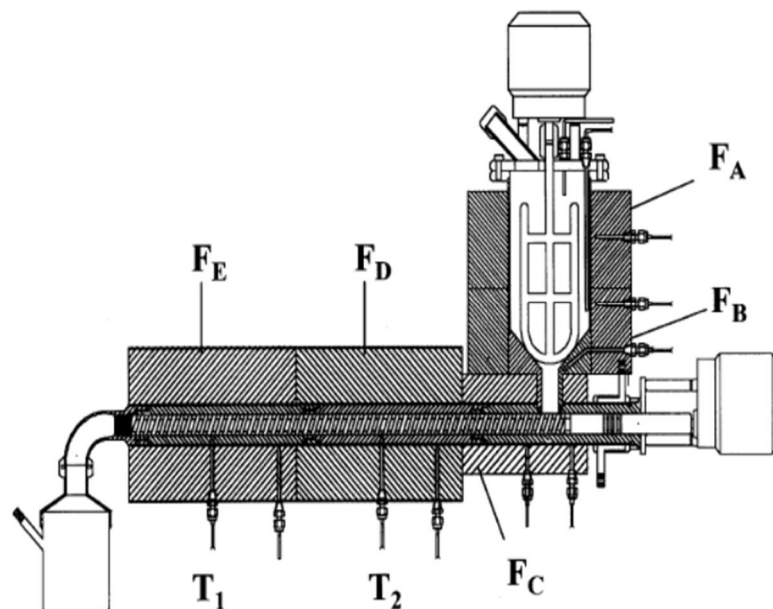


Figure 2.3- 5 Schematic diagram of screw kiln reactor [64]

The work showed that the thermal pyrolysis carried out at different temperature and screw speed in a continuous system was suitable for LDPE. High gasoline range hydrocarbons ($C_5 - C_{12}$) has been obtained using the reactor in the presence of mesoporous catalyst MCM-41.

References

1. Siddiqui, M.N. and H.H. Redhwi, *Pyrolysis of mixed plastics for the recovery of useful products*. Fuel Processing Technology, 2009. **90**(4): p. 545-552.
2. Doyle, C., *Estimating thermal stability of experimental polymers by empirical thermogravimetric analysis*. Analytical Chemistry, 1961. **33**(1): p. 77-79.
3. Xanthos, M. and J. Leidner, *Thermolytic Processes*, in *Frontiers in the Science and Technology of Polymer Recycling*1998, Springer. p. 407-423.
4. Seo, Y.H. and D.H. Shin, *Determination of paraffin and aromatic hydrocarbon type chemicals in liquid distillates produced from the pyrolysis process of waste plastics by isotope-dilution mass spectrometry*. Fuel, 2002. **81**(16).
5. Miskolczi, N., L. Bartha, and G. Deák, *Thermal degradation of polyethylene and polystyrene from the packaging industry over different catalysts into fuel-like feedstocks*. Polymer Degradation and Stability, 2006. **91**(3): p. 517-526.
6. González, Y.S., Costa, C., Marquez, M.C. and Romos, P., *Thermal and catalytic degradation of polyethylene wastes in the presence of silica gel, 5A molecular sieve and activated carbon*. Journal of hazardous materials, 2011. **187**(1): p. 101-112.
7. Williams, P.T. and E.A. Williams, *Fluidised bed pyrolysis of low-density polyethylene to produce petrochemical feedstock*. Journal of Analytical and Applied Pyrolysis, 1999. **51**(1-2): p. 107-126.
8. Conesa, J., Font, R., Marcilla, A., and Cabellero, JA, *Kinetic model for the continuous pyrolysis of two types of polyethylene in a fluidized bed reactor*. Journal of analytical and applied pyrolysis, 1997. **40**: p. 419-431.
9. Kaminsky, W., M. Predel, and A. Sadiki, *Feedstock recycling of polymers by pyrolysis in a fluidised bed*. Polymer Degradation and Stability, 2004. **85**(3): p. 1045-1050.
10. Serrano, D.P., Aguado, J., Escola, J.M. and Garagorri, E., *Conversion of low-density polyethylene into petrochemical feedstocks using a continuous screw kiln reactor*. Journal of Analytical and Applied Pyrolysis, 2001. **58**.
11. Kruse, T.M., H.-W. Wong, and L.J. Broadbelt, *Mechanistic modeling of polymer pyrolysis: polypropylene*. Macromolecules, 2003. **36**(25): p. 9594-9607.

12. Wampler, T.P., *Applied Pyrolysis handbook* 2006 CRC.
13. Hujuri, U., A.K. Ghoshal, and S. Gumma, *Temperature-Dependent Pyrolytic Product Evolution Profile for Polypropylene*. Journal of Applied Polymer Science, 2011. **119**(4).
14. Shah, J., Jan, M.R., Mabood, F. and Jabeen, F., *Catalytic pyrolysis of LDPE leads to valuable resource recovery and reduction of waste problems*. Energy Conversion and Management, 2010. **51**(12).
15. Carniti, P., Beltrame, P.L., Armanda, M., Gervasini, A. and Audisio, G., *Polystyrene thermodegradation. 2. Kinetics of the formation of volatile products*. Industrial & Engineering Chemistry Research, 1991. **30**(7): p. 1624-1629.
16. S.L., M., McIntyre, D., O'Mara, H. and Straus, S., *Thermal degradation of fractionated high and low molecular weight polystyrenes*. J. Res. Natl. Bur. Stand, 1962. 66A(4).
17. Jianfeng, L., Fusheng, L., Shitao, Y., Xiaoping, G. and Xin, Z., *Pyrolysis of Waste Polystyrene to Recover Styrene over Alkaline Mesoporous Molecular Sieve K₂O-BaO/MCM-41*. in *Digital Manufacturing and Automation (ICDMA), 2010 International Conference on*. 2010. IEEE.
18. Bajus, M. and E. Hájeková, *Thermal cracking of the model seven components mixed plastics into oils/waxes*. Petroleum & Coal, 2010. **52**(3): p. 164-172.
19. McNeill, I. and M. Bounekhel, *Thermal degradation studies of terephthalate polyesters: 1. Poly (alkylene terephthalates)*. Polymer Degradation and Stability, 1991. **34**(1): p. 187-204.
20. Montaudo, G., C. Puglisi, and F. Samperi, *Primary thermal degradation mechanisms of PET and PBT*. Polymer degradation and stability, 1993. **42**(1): p. 13-28.
21. Murata, K., M. Brebu, and Y. Sakata, *The effect of PVC on thermal and catalytic degradation of polyethylene, polypropylene and polystyrene by a continuous flow reactor*. Journal of Analytical and Applied Pyrolysis, 2009. **86**(1): p. 33-38.
22. Ma, S., J. Lu, and J. Gao, *Study of the low-temperature pyrolysis of PVC*. Energy & Fuels, 2002. **16**(2): p. 338-342.
23. Sun, Q.-L., Shi, XG, Lin, YL, He, Z., Xiao, W., Cheng, CG and Liu, JH., *Thermogravimetric-mass spectrometric study of the pyrolysis behavior of PVC*. Journal of China University of Mining and Technology, 2007. **17**(2): p. 242-245.

24. Bounekhel, M. and I.C. McNeill, *Thermal-Degradation Studies Of Terephthalate Polyesters .2. Poly(Ether-Esters)* . Polymer Degradation and Stability, 1995. **49**(3).
25. Williams, E.A. and Williams, P.T., *The Pyrolysis of Individual Plastics and a Plastic Mixture in a Fixed Bed Reactor* J. Chem. Tech. Biotechnol, 1997. **70**: p. 9-20.
26. P., W.H., *The VEBA OEL Technologie pyrolysis process*. Journal of Analytical and Applied Pyrolysis, 1993. **25**: p. 301-310.
27. Su-Hwa Jung, S.-J.K., Joo-Sik Kim, *Thermal degradation of acrylonitrile–butadiene–styrene (ABS) containing flame retardants using a fluidized bed reactor: The effects of Ca-based additives on halogen removal* Fuel Processing Technology, 2012. **96**: p. 265–270.
28. M. Brebu, T.B., K. Murai, A. Muto, Y. Sakata, Md.A. Uddin, *Removal of nitrogen, bromine, and chlorine from PP/PE/PS/PVC/ABS–Br pyrolysis liquid products using Fe- and Ca-based catalysts*. Polymer Degradation and Stability, 2005. **87**: p. 225–230.
29. Israeli, Y., Lacoste, J., Lemaire, J., Singh, RP and Sivaram, S., *Photo-and them initiated oxidation of high-impact polystyrene. I. Characterization by FT-IR spectroscopy*. Journal of Polymer Science Part A: Polymer Chemistry, 1994. **32**(3): p. 485-493.
30. Marcilla, A., Gomez, SA, Quesada, JCG and Berenguer, D., *Characterization of high-impact polystyrene by catalytic pyrolysis over Al-MCM-41: Study of the influence of the contact between polymer and catalyst*. Polymer Degradation and Stability, 2007. **92**(10).
31. R. Gachter and H. Muller, *Plastics Additives Handbook*, ed. H.M. R. Gachter 1990, Munich: Hanser Publishers.
32. Jakab, E., Uddin, MA., Bhaskar, T., and Sakat, Y., *Thermal decomposition of flame-retarded high-impact polystyrene*. Journal of analytical and applied pyrolysis, 2003. **68**: p. 83-99.
33. Zhang, P. Song, L., Lu, H., Wang, J. and Hu, Y., *The influence of expanded graphite on thermal properties for paraffin/high-density polyethylene/chlorinated paraffin/antimony trioxide as a flame retardant phase change material*. Energy Conversion and Management, 2010. **51**(12): p. 2733-2737.
34. Thoma, H., Hauschulz, G., Knorr, E. and Hutzinger, O , *Polybrominated dibenzofurans (PBDF) and dibenzodioxins (PBDD) from the pyrolysis of neat brominated diphenyl ethers, biphenyls and plastic mixtures of these compounds*. Chemosphere, 1987. **16**(1): p. 277-285.

35. Dumler, R., Thoma, H., Hutzinger, O, *Content and Formation of toxic products in flame retardants*, in *Workshop on Brominated aromatic flame retardants 1989*: Skokloster, Sweden
36. Klusmeier, W., Sonnemann, R, Ohrbach, KH and Kettrup, A., *Investigations of the combustion products of flame-protected impact resistant polystyrene*. *Thermochimica Acta*, 1987. **112**(1): p. 75-79.
37. Aguado, J., D.P. Serrano, and J.M. Escola, *Fuels from Waste Plastics by Thermal and Catalytic Processes: A Review*. *Industrial & Engineering Chemistry Research*, 2008. **47**(21): p. 7982-7992.
38. Aguado, J., D.P. Serrano, and J.M. Escola, *Fuels from Waste Plastics by Thermal and Catalytic Processes: A Review*. *Industrial & Engineering Chemistry Research*, 2008. **47**(21).
39. Mlynková, B., Bajus, M., Hajekova, E., Kostrab, G., and Mravec, D., *Fuels obtained by thermal cracking of individual and mixed polymers*. *Chemical Papers*, 2010. **64**(1): p. 15-24.
40. Bhaskar, T., Kaneko, J., Muto, Akinori, Sakata, Y., Jakab, Emma, Matsui, Toshiki and Uddin, MA., *Pyrolysis studies of PP/PE/PS/PVC/HIPS-Br plastics mixed with PET and dehalogenation (Br, Cl) of the liquid products*. *Journal of Analytical and Applied Pyrolysis*, 2004. **72**(1).
41. Levent, B., *Classification of volatile products evolved during temperature programmed co-pyrolysis of low-density polyethylene (LDPE) with polypropylene*. *Fuel*, 2002. **81**(9): p. 1233-1240.
42. Jung, S.-H., Cho, MH, Kang, BS and Kim, JS ., *Pyrolysis of a fraction of waste polypropylene and polyethylene for the recovery of BTX aromatics using a fluidized bed reactor*. *Fuel Processing Technology*, 2010. **91**(3): p. 277-284.
43. Aguado, J. and D.P. Serrano, *Feedstock recycling of plastic wastes*. Vol. 1. 1999: Royal society of chemistry.
44. Mlynková, B., E. Hájeková, and M. Bajus, *Copyrolysis of oils/waxes of individual and mixed polyalkenes cracking products with petroleum fraction*. *Fuel Processing Technology*, 2008. **89**(11): p. 1047-1055.
45. Onwudili, J.A., Insura, N. and Williams, P.T., *Composition of products from the pyrolysis of polyethylene and polystyrene in a closed batch reactor: Effects of temperature and residence time*. *Journal of Analytical and Applied Pyrolysis*, 2009. **86**(2): p. 293-303.

46. Buekens, A. and Huang, H., *Catalytic plastics cracking for recovery of gasoline-range hydrocarbons from municipal plastic wastes*. Resources, Conservation and Recycling, 1998. **23**(3): p. 163-181.
47. Olazar, M., Lopez, G., Amutio, M., Elordi, G., Aguado, R. and Bilbao, J., *Influence of FCC catalyst steaming on HDPE pyrolysis product distribution*. Journal of Analytical and Applied Pyrolysis, 2009. **85**(1): p. 359-365.
48. Lin, Y.H. and Yen, H.Y., *Fluidised bed pyrolysis of polypropylene over cracking catalysts for producing hydrocarbons*. Polymer Degradation and Stability, 2005. **89**(1).
49. Lee, K.-H., Shin, D.-H. and Seo, Y.-H., *Liquid-phase catalytic degradation of mixtures of waste high-density polyethylene and polystyrene over spent FCC catalyst. Effect of mixing proportions of reactants*. Polymer degradation and stability, 2004. **84**(1): p. 123-127.
50. Bagri, R. and Williams, P.T., *Fluidised-bed catalytic pyrolysis of polystyrene*. Journal of the Institute of Energy, 2002. **75**(505): p. 117-123.
51. Zhibo Zhang, T.H., Nishio, S., Morioka, Y., Azuma, N., Akifumi, U., Ohkita, H. and Okada, M., *Chemical Recycling of Waste Polystyrene Acids and Bases*. Znd. Eng. Chem. Res, 1995. **34**: p. 4514-4519.
52. Lin, Y.H. and Yang, M.H., *Tertiary recycling of commingled polymer waste over commercial FCC equilibrium catalysts for producing hydrocarbons*. Polymer Degradation and Stability, 2009. **94**(1): p. 25-33.
53. Tang, C., Wang, Y.-Z., Zhou, Q. and Zheng, L. *Catalytic effect of Al-Zn composite catalyst on the degradation of PVC-containing polymer mixtures into pyrolysis oil* Polymer Degradation and Stability, 2003. **81**: p. 6.
54. Huang, W.-C., Huang, M.S., Huang, C.F., Chen, C.C. and Ou, K.L., *Thermochemical conversion of polymer wastes into hydrocarbon fuels over various fluidizing cracking catalysts*. Fuel, 2010. **89**(9).
55. Zhou, Q., Tang, C., Wang, Y.-Z. and Zheng, L. *Catalytic degradation and dechlorination of PVC-containing mixed plastics via Al-Mg composite oxide catalysts*. Fuel, 2004. **83**: p. 6.
56. Lopez-Urionabarrenechea, A., and de Marco, I., Caballero, B.M., Laresgoiti, M.F. and Adrados, A., *Catalytic stepwise pyrolysis of packaging plastic waste*. Journal of Analytical and Applied Pyrolysis, 2012. **96**(0): p. 54-62.
57. Lopez, A., de Marco, I., Caballero, B.M., Adrados, A. and Laresgoiti, M.F., *Deactivation and Regeneration of ZSM-5 zeolite in the catalytic*

- pyrolysis of plastic wastes*. Waste Management, 2011. **31**(8): p. 1852-1858.
58. Antonakou, E., Kogiannis, K.G., Stephanidis, S.D., Triantafyllidis, K.S., Lappas, A.A. and Achilias, D.S., *Pyrolysis and catalytic pyrolysis as a recycling method of waste CDs originating from polycarbonate and HIPS*. Waste Management, 2014. **34**(12): p. 2487-2493.
 59. Lee, K.-H., *Composition of aromatic products in the catalytic degradation of the mixture of waste polystyrene and high-density polyethylene using spent FCC catalyst*. Polymer Degradation and Stability, 2008. **93**(7): p. 1284-1289.
 60. Lee, K.-H., *Effects of the types of zeolites on the catalytic upgrading of pyrolysis wax oil*. Journal of Analytical and Applied Pyrolysis, 2012. **94**.
 61. Boxiong, S., Wu.C., Binbin,G. and Rui, W., *Pyrolysis of waste tyres with zeolite USY and ZSM-5 catalysts*. Applied Catalysis B: Environmental, 2007. **73**(1): p. 150-157.
 62. Lin, Y.-H. and M.-H. Yang, *Catalytic conversion of commingled polymer waste into chemicals and fuels over spent FCC commercial catalyst in a fluidised-bed reactor*. Applied Catalysis B: Environmental, 2007. **69**(3): p. 145-153.
 63. Aguado, J., D., Serrano, and J. Escola, *Catalytic Upgrading of Plastic Wastes*. Feedstock Recycling and Pyrolysis of Waste Plastics: Converting Waste Plastics into Diesel and Other Fuels, 2006: p. 73-110.
 64. Aguado, J., Serrano, D.P., Sotelo, J.L., Van Grieken, R. and Escola, J.M., *Influence of the operating variables on the catalytic conversion of a polyolefin mixture over HMCM-41 and nanosized HZSM-5*. Industrial & engineering chemistry research, 2001. **40**(24): p. 5696-5704.
 65. Aguado, J., Serrano, D.P., Escola, J.M. and Peral, A., *Catalytic cracking of polyethylene over zeolite mordenite with enhanced textural properties*. Journal of Analytical and Applied Pyrolysis, 2009. **85**(1): p. 352-358.
 66. Serrano, D., Aguado, J., Escola, J.M., Garagorri, E., Morselli, L., Palazzi, G. and Orsi., R., *Feedstock recycling of agriculture plastic film wastes by catalytic cracking*. Applied Catalysis B: Environmental, 2004. **49**(4): p. 257-265.
 67. Mordi, R.C., Fields, R. and Dwyer, J., *Gasoline range chemicals from zeolite-catalysed thermal degradation of polypropylene*. J. Chem. Soc., Chem. Commun., 1992(4): p. 374-375.

68. Cardona, S.C. and Corma, A. *Tertiary recycling of polypropylene by catalytic cracking in a semi batch stirred reactor: use of spent equilibrium FCC commercial catalyst*. Applied Catalysis B: Environmental, 2000. **25**(2): p. 151-162.
69. Lee, K.-H., Noh, N.S., Shin, D.H. and Seo, Y., *Comparison of plastic types for catalytic degradation of waste plastics into a liquid product with spent FCC catalyst*. Polymer Degradation and Stability, 2002. **78**(3): p. 539-544.
70. Vasile, C., Onu, P., Barboiu, V., Sabliovachi, M. and Morai, G., *Catalytic decomposition of polyolefins. III. Decomposition over the ZSM-5 catalyst*. Acta polymeric, 1988. **39**(6): p. 306-310.
71. Bagri, R. and Williams, P.T., *Catalytic pyrolysis of polyethylene*. Journal of analytical and applied pyrolysis, 2002. **63**(1): p. 29-41.
72. Songip, A.R., Masuda, T., Kuwahara, H. and Hishimoto, K., *Production of High-Quality Gasoline by Catalytic Cracking over Rare-Earth-Metal Exchanged Y-Type Zeolites of Heavy Oil from Waste Plastics*. Energy & Fuels, 1994. **8**(1): p. 136-140.
73. Masuda, T., Kuwahara, H., Mukai, S.R., and Hishimoto, K., *Production of high-quality gasoline from waste polyethylene derived heavy oil over Ni-REY catalyst in a steam atmosphere*. Chemical engineering science, 1999. **54**(13): p. 2773-2779.
74. Arena, U. and Mastellone, M.L., *Fluidized bed pyrolysis of plastic wastes*. Feedstock Recycling and Pyrolysis of Waste Plastics: Converting Waste Plastics into Diesel and Other Fuels, 2006: p. 435-474.
75. Levenspiel, O., *Fluidization engineering* 1991: Butterworth-Heinemann.
76. Elordi, G., Lopez, G., Aguado, R., Olazar, M. and Bilbao, J., *Catalytic pyrolysis of high-density polyethylene on a HZSM-5 zeolite catalyst in a conical spouted bed reactor*. International Journal of Chemical Reactor Engineering, 2007. **5**.
77. Aguado, J., Serrano, D.P., Escola, J.M. and Garagorri, E., *Catalytic conversion of low-density polyethylene using a continuous screw kiln reactor*. Catalysis today, 2002. **75**(1): p. 257-262.
78. Serrano, D., Aguado, J., Escola, J.M., Morselli, L. and Orsi, R., *Thermal and catalytic cracking of a LDPE-EVA copolymer mixture*. Journal of Analytical and Applied Pyrolysis, 2003. **68**: p. 481-494.

Chapter 3 MATERIALS AND METHODS

3.1 Introduction

This chapter discusses the materials and experimental systems used to investigate the pyrolysis and catalytic pyrolysis of waste plastics. Also, the analytical techniques used to characterise the different raw materials, catalysts, and products of pyrolysis and catalytic pyrolysis.

3.2 Materials

3.2.1 Virgin Plastics

Polyethylene (3mm), polypropylene (3mm), Polystyrene (3.5mm) and PET (3mm) supplied as virgin polymer provided by Good Fellow Ltd, UK. Samples of virgin high-impact polystyrene (HIPS) and acrylonitrile –butadiene-styrene (ABS) were obtained from Atofina and Vamptech United Kingdom, respectively.

3.2.2 Real-world Mixed Plastics

Real-world, post-consumer, municipal solid waste mixed plastic obtained from Belgium collected and recycled by Fost Plus. The collected plastic waste fraction was flaked, and air separated to produce a sample containing mainly PE, PP, and PET with a sample size of approximately 5mm.

3.2.3 Waste HDPE

Waste high-density polyethylene (HDPE) was in 2mm pellet form supplied by Regain Polymers Limited, UK.

3.2.4 Simulated mixture of Plastics (SMP)

A simulated mixture of plastics (SMP) was prepared to consist of a blended mixture of virgin plastics and consisted of 60.0 wt. % Polyethylene, 13.0wt. % Polypropylene, 18.0 wt. % Polystyrene, and 9.00 wt. % PET. The proportions based on data obtained from a short review of the literature.

3.2.5 Future Simulated mixture of Plastics (FSMP)

A future simulated mixed plastic (FSMP) was prepared to consist of a blended mixture of virgin plastics and consisted of 62.0 wt.% Polyethylene (HDPE=19% + LDPE=43%), 8 wt.% polypropylene, 15 wt.% Polystyrene and 15 wt.% PET. The proportions of the plastics in the mixtures adopted from Delgado [1] and represented a projection of the future range of plastics that would be found in future MSW plastic fractions.

3.2.6 Waste Electrical and Electronic Equipment (WEEE)

The waste electrical and electronic equipment feedstock consisted of plastics collected from a waste electrical and electronic equipment recycling plant that separately recovered the plastics. Plastics from waste refrigerators and freezers and plastic from waste cathode ray tubes (televisions and computer monitors) were collected. For the refrigerator and freezer waste (designated as 'Fridge'), the compressors were first removed followed by shredding before various WEEE fraction were separated. Foam insulation removed by air blowing; ferrous metals removed by electromagnets and non-ferrous metals and plastics are separated by cyclones. However, complete separation could not be achieved, and a significant proportion of non-ferrous metal pieces remained in the sample. The second WEEE sample collected from the recycling unit that handled the waste cathode ray tubes from old style waste television sets and computer monitors (designated as CRT). The plastic outer

casings were removed before the separation of the glass screen from the electronic components. The circuit board and glass are separated from the CRT equipment, and the plastic fraction is ground into small flakes of approximately 10-20mm in size. Representative one kg samples of the two types of the shredded WEEE plastics were taken using standard sampling procedures [2].

3.2.7 Catalyst

This section described the various catalysts used; catalysts were grouped into pellets and powdered as commercial zeolite catalysts mainly used, and a powdered spent FCC catalyst. Table 3.3.1 shows the various commercial catalysts used, and Table 3.3.2 shows the spent FCC catalyst used

3.2.7.1 Pellet Catalysts

Zeolites Y and ZSM-5 were in pellet form of approximate size, 1 mm by 5 mm obtained from Zeolyst International (USA) and the BDH United Kingdom.

3.2.7.2 Powdered Catalysts

Powdered zeolite Y and ZSM5 catalyst used for the research were all supplied by Alfa Aesar, United Kingdom. Powdered spent FCC catalyst provided by the University of Pannonia, Hungary.

Table 3.2-1 Zeolite Y and ZSM-5 Catalysts used in the research work

SN	Physical state	Zeolite structure	Surface area m^2g^{-1}	Si: Al ratio	Cation	Na_2O (%)	Microspore Volume $(\text{cm}^3\text{g}^{-1})$	Mesopore Volume $(\text{cm}^3\text{g}^{-1})$	Pore radius (\AA)
1	Pellets	Y-Zeolite	-	5.4	-	-	-	-	7.8
2	Pellets	ZSM-5	-	40	-	-	-	-	5.6
3	Powdered	Y-Zeolite	705	5.1:1	H^+	0.15	0.321	0.163	7.55
4	Powdered	Y-Zeolite	853	5.1:1	NH_4^+	0.14	0.189	0.100	7.15
5	Powdered	Y-Zeolite	935	5.2:1	NH_4^+	2.93	0.340	0.040	7.62
6	Powdered	Y-Zeolite	937	30:1	H^+	0.02	0.390	0.220	7.39
7	Powdered	Y-Zeolite	888	80:1	H^+	0.02	0.315	0.221	7.05
8	Powdered	ZSM-5	450	23:1	NH_4^+	0.03	0.064	0.060	7.21
9	Powdered	ZSM-5	452	50:1	NH_4^+	0.00	0.167	0.134	7.40
10	Powdered	ZSM-5	467	80:1	NH_4^+	0.00	0.204	0.117	7.50

3.2.7.3 Spent FCC

The spent Fluid Catalytic Cracker (FCC) catalyst used was obtained from the Department of Hydrocarbon and Coal Processing, the University of Pannonia, Hungary, which was obtained from a petrochemical refinery. Hall et al. [3], characterized the spent FCC catalyst using X-ray spectrometry for Si:Al, Micrometric ASAP 2000 for BET surface area; and Analysette 22 grain analyser for pore size distribution. The detail characteristics of the spent FCC as determined are shown in Table 3.3.2.

Table 3.2-2 Characteristic of spent FCC catalyst by Hall et al.[3]

	FCC catalyst
Average grain size (μm)	59.7
Si/Al ratio	16.4
BET area (m^2/g)	148.1
Micropore area (m^2/g)	78.9
Micropore area 1.7-300 nm (m^2/g)	83.6
Micropore volume 1.7-300 nm (m^3/g)	0.155
Micropore volume (m^3/g)	0.032

3.3 Plastic Sample Characterization

3.3.1 Elemental Analysis of Plastics

The elemental compositions of the plastic sample were carried out using a CE Instrument (Wigan, United Kingdom) CHNS-O analyser to determine carbon (C), hydrogen (H), nitrogen (N) and sulphur. However, oxygen (O) was calculated by weight difference.



Figure 3.3-1 The Flash 2000 CHNS-O Analyzer

3.3.2 Thermogravimetric Analysis (TGA)

The temperature indicates the nature and amount of products obtained by thermal degradation of polymers. Accordingly TGA studies were carried out to investigate the degradation pattern of the plastic materials under the reaction conditions to be used for pyrolysis. Therefore, the TGA study was carried out at medium reaction temperatures of 500 °C with 30 minutes hold time under nitrogen flow. It was carried out to determine the weight loss of the plastic as a function of temperature and time. The core components of a thermogravimetric analyser are a controlled ceramic furnace coupled to microbalance, and a data recorder [4].

Thermogravimetric analysis (TGA) of the plastic samples were performed on a Shimadzu 50A TGA instrument to determine the thermal degradation characteristics of the plastics via plastic weight loss of the sample in relation to increasing temperature. The procedure involved heating approximately 15 mg of the plastics (in nitrogen) at 10 °C min⁻¹ to a final temperature of 500 °C;

the sample held at the temperature for 30 min. For the TGA, the plastic samples were pulverized into 500 nm particles in a cryogenic mill to ensure that a representative, homogeneous sample was presented to the TGA.



Figure 3.3-2 The 50A Thermogravimetric Analyzer Instrument

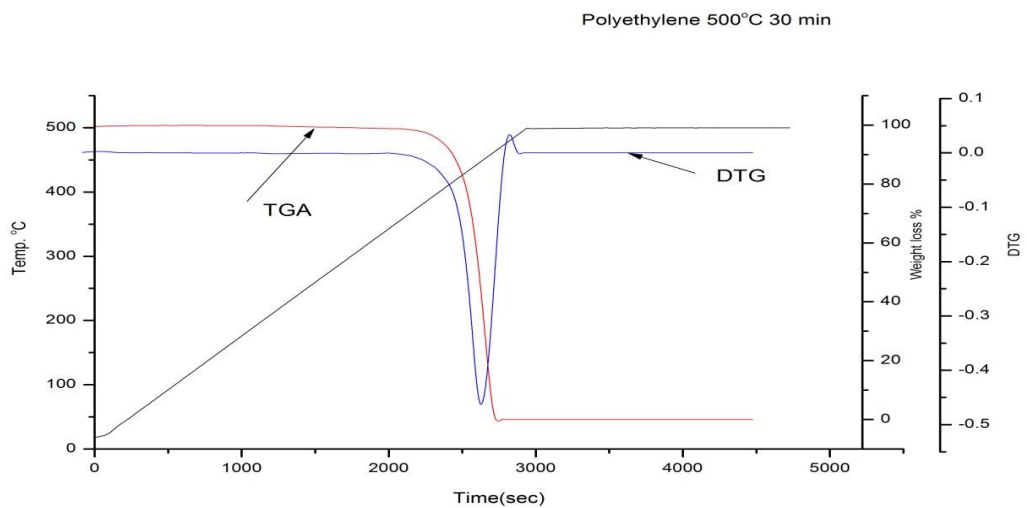


Figure 3.3-3 A typical TGA-DTG plot of Polyethylene

3.4 Two-stage pyrolysis-catalytic fixed bed bench reactor

A two-stage pyrolysis-catalytic fixed bed bench reactor was used in this study to conduct the pyrolysis-catalysis of the various waste plastics.

3.4.1 Reactor Set-up & Experimental procedure

The reactor consisted of two stages with a downdraft configuration. The reactor was designed to test pyrolysis-catalysis process of the different plastic samples. The pyrolysis process takes place within the first stage; while the catalysis was carried out downdraft in a second stage. The reactor was made up of a vertical stainless steel cylindrical tube of length 480 mm and an internal diameter 39 mm and both stages were thermally heated independently by two 1.5 kW tube furnaces. The reactor divided into two section; with pyrolysis heated zone, and catalyst heated zones. Two thermocouples were located via the reactor cover lid to allowed control of the temperature; the heat transfer between the two stages was negligible. The two furnaces were mounted in a vertical arrangement with pyrolysis in the upper stage and catalysis in the lower stage. The catalytic section contained stainless steel mesh supporting quartz wool on top of which was weighed an amount of sand for thermal pyrolysis or catalyst for catalytic pyrolysis. The plastic sample was weighed into a stainless steel crucible (78 mm length and 24 mm diameter) which was suspended inside the pyrolysis reactor. A schematic diagram of the laboratory bench scale two stage fixed bed pyrolysis-catalysis reactor system is shown in Figure 3.5-1.

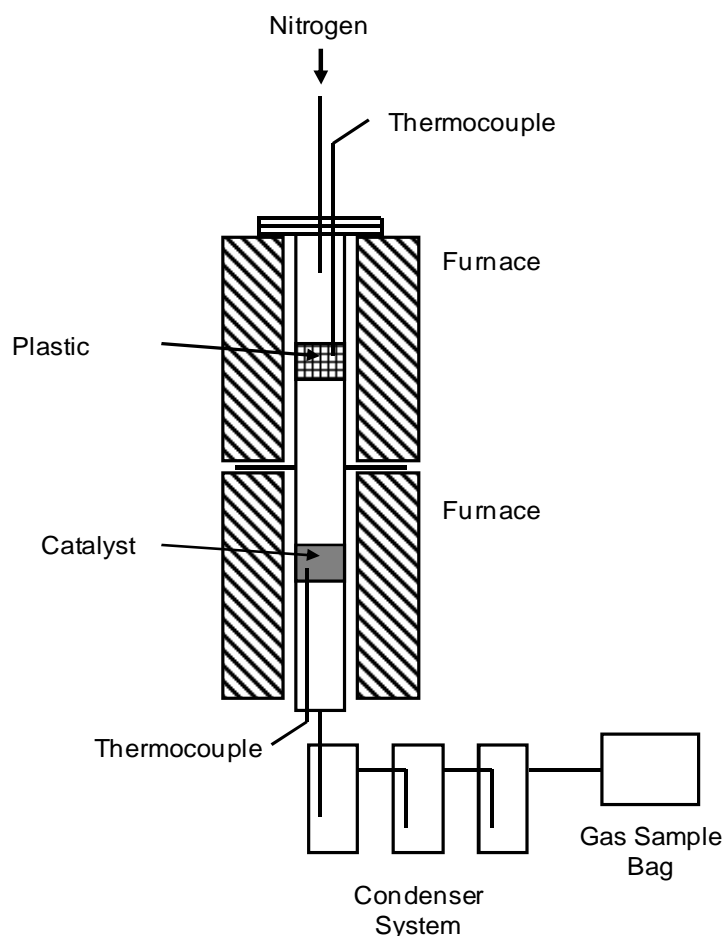


Figure 3.4-1 Schematic diagram for two stage Pyrolysis-catalysis reactor

In the experimental procedure, the bottom catalyst furnace was controlled and heated to 500 °C (or varying temperature) and kept constant at that temperature. Then the top pyrolysis furnace was switched on and the plastic sample was heated at a heating rate of 20 °C min⁻¹ to a temperature of 500 °C and then held constant for a 30 minutes hold time and followed by 20 minutes gas collection time. Nitrogen (200ml min⁻¹ flow rate) was used as the carrier gas to provide an inert atmosphere and to sweep the evolved pyrolysis gases from the reactor. Hence, it also served to curtail any minor reactions of the gaseous products. Condenser system: three condenser system consisting of solid dry ice-cooled condensers. The condenser system was connected to a gas sample bag. The loss of volatiles was prevented by sealing the

condenser and tubes with parafilm at the end of the experiment; and condensers are weighed immediately the experiment finished.

The gas bag was taken immediately at an end of each experiment for gas analysis by gas chromatography (GC) [5].



Figure 3.4-2 Assembled and main part of the pyrolysis-catalysis reactor

3.4.2 Experiment Reproducibility and Selection of process conditions

The reactor was fabricated in-house (internally) at the Energy Research Institute Leeds University, and some test experiments were performed for initial validation and optimization in order to establish the most suitable operational condition for the pyrolysis-catalysis process. During the test experiments virgin plastic samples and a bed of sand was initially used. The amount of plastic sample was varied between 2 and 4 grams; an amount was established considering the high density of the plastic material and the size of

the bolt\crucible. The heating rate of $10\text{ }^{\circ}\text{C min}^{-1}$ and $20\text{ }^{\circ}\text{C min}^{-1}$ was tested under a nitrogen flow rate of 200ml min^{-1} .

3.5 Characterization of materials and products

3.5.1 Analysis of products gases

The gas products collected in the gas bag were routinely and immediately used for both permanent and hydrocarbon gas analyses. The purpose of using the analytical technique was to acquire qualitative and quantitative information about the product gas composition. The gas chromatography technique involved an injection of the sample into the GC via an injection port. A carrier gas chemically inert (argon, helium or nitrogen) was used to transport the sample through the oven and via suitable analytical column packed with a mesh of specific characteristics. Lastly, the eluted sample reached the detection system which was either a flame ionization (FID) or thermal conductivity detector (TCD). The major constituents of a GC comprise a sample injection system, column, oven, thermostat, data interpretation system, and a flow meter; are shown in Figure [6].

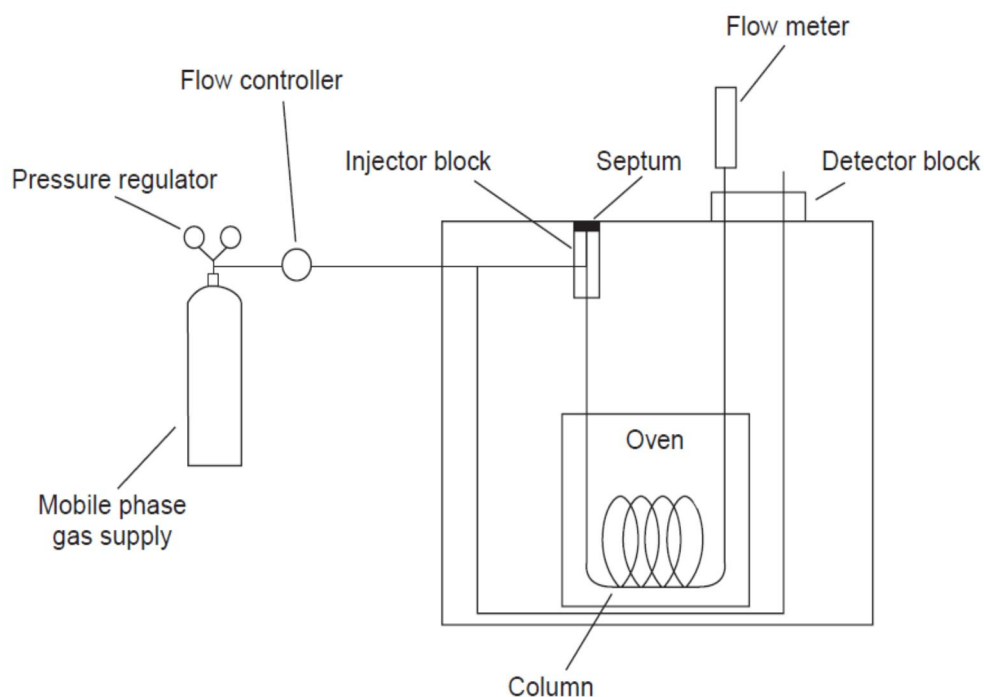


Figure 3.5-1 General schematic diagram for typical GC [7]

3.5.2 Permanent gases

For permanent gases, the analysis was performed using a Varian CP-3380 GC with thermal conductivity detector (TCD) equipped with a 2m-long column with a 2 mm diameter packed with 60-80 mesh molecular sieve. The carrier gas for the GC/TCD was argon gas. The column oven temperature was held constant at 40 °C during the analysis, and the temperature of the injector and detector was 120 and 160 °C respectively. The GC oven temperature was isothermally held at 30 °C; the injector and detector temperature were set at 120 °C and the filament temperature at 160 °C.

Carbon dioxide was analysed on a Hysep 80–100 mesh column with argon carrier gas. The temperature of the detector and the filament was 120 °C and 160 °C respectively.



Figure 3.5-2 GC-/TCD for CO₂ gas analysis

3.5.3 Hydrocarbon gases

Hydrocarbon gases from C₁ to C₄ were analysed using a Varian CP 3380 GC with a flame ionization detector (FID) equipped with a 2m long column with a diameter of 2mm and packed with 80-100 mesh size Haysep was used. The injector was set and held at 150 °C while the detector temperature was 200 °C. The oven temperature was programmed to be held at 60 °C for 3 minutes, then heating up to 100 °C with a rate of 10 °C min⁻¹, further held for 3 minutes and finally ramped to at 20 °C min⁻¹. The oven temperature was set at 60 °C for 3 minutes, then the temperature was increased up to 100 °C at 5 °C min⁻¹ heating rate and held for 3 more minutes; lastly the temperature was ramped up to 120 °C at 20 °C min⁻¹ heating rate and held for 17 minutes.

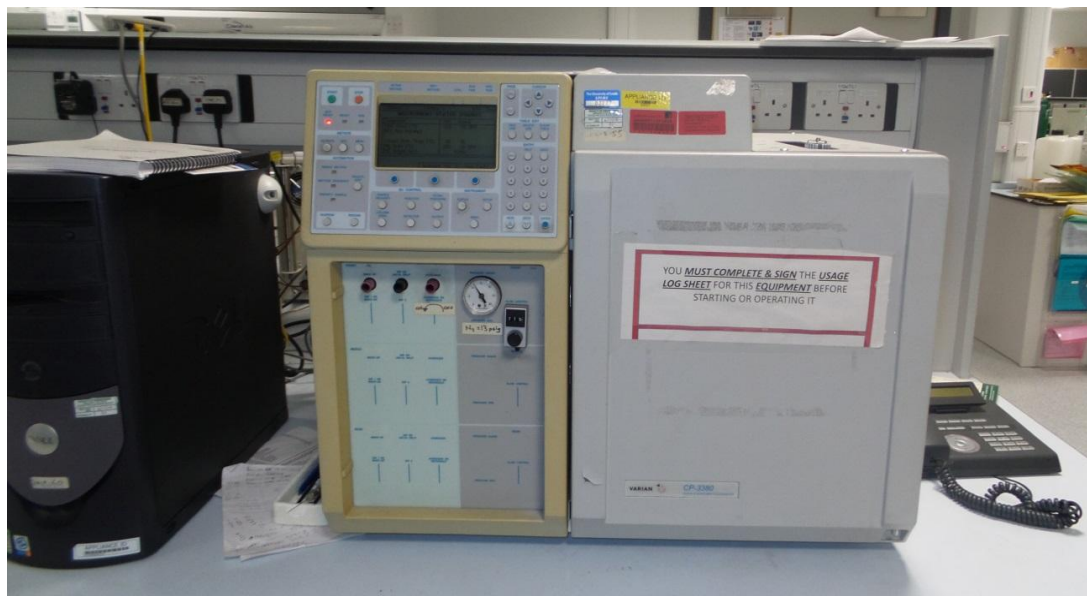


Figure 3.5-3 GC-FID for Hydrocarbon gases analysis

3.5.4 Calibration of Gas Chromatography (GC) Analysis

The standard gas mixture was used to calibrate the gas chromatography to ensure accurate quantitation. The standard gases were used to make calibration curves and used as a reference for compositional calculation of each gas. Thus, for hydrocarbons the calibration curve was made using two standard gas for saturated (alkanes) and unsaturated (alkenes) hydrocarbons both balanced with nitrogen. Accordingly, the standard alkane's mixture contains approximately 1 vol. % each of CH_4 , C_2H_6 , C_3H_8 and C_4H_{10} . The standard alkenes mixture contains 1 vol. % each of ethane (C_2H_4), propene (C_3H_6) and 2vol. % 1-3 butene-butadiene (C_4H_8).

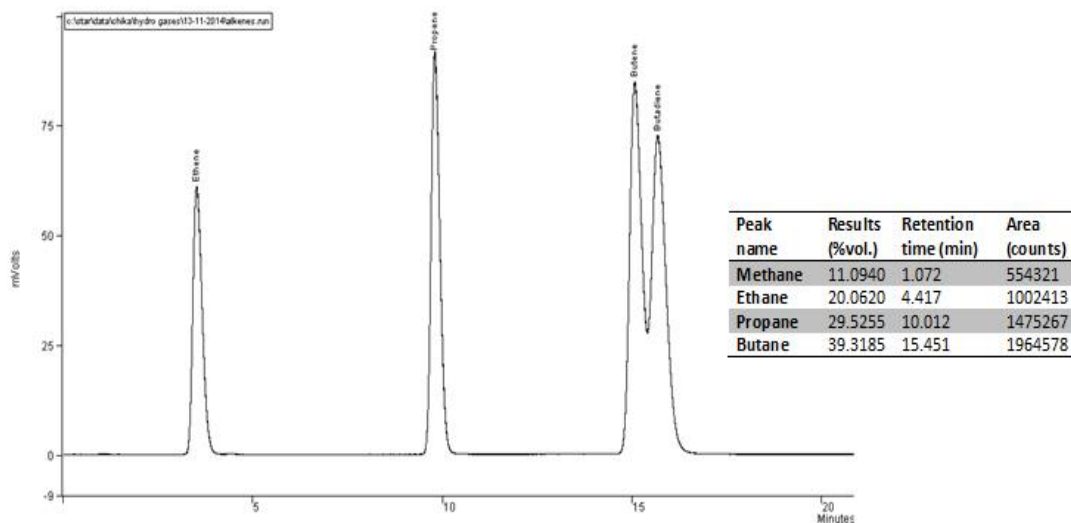


Figure 3.5-4 A GC response peaks for a standard gas mixture of hydrocarbon (alkane) gases.

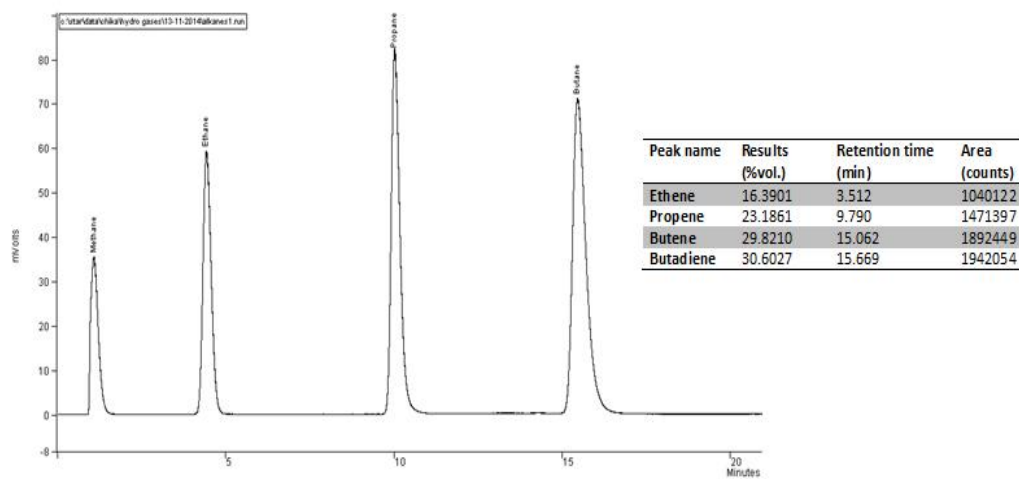


Figure 3.5-5 A GC response peaks for a standard gas mixture of hydrocarbon (alkene) gases.

However, for permanent gases the calibration curve was created by using the standard gas mixture containing 1 vol. % each of H₂, O₂, CO, CO₂ and 96 vol. % N₂.

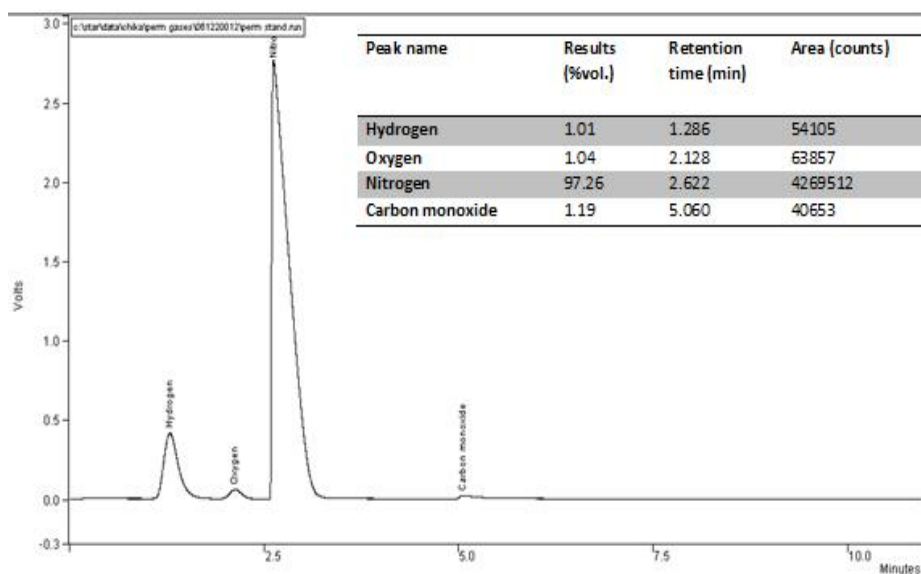


Figure 3.5-6 A GC response peaks for a standard gas mixture of permanent gases (H₂, O₂, N₂ and CO).

The procedure for injection of standard gas was the same as describe in the sections 3.6.1.1 and 3.6.1.2 using appropriate the GC for hydrocarbon and permanent gases separately. Hence, 1 ml of each standard was injected into the GC. The voltage signal obtained for each gas component was fed manually into the GC software (a digital integrator); which in turn gave a response factor for each component.

3.5.5 Reproducibility of the standard gas injection

3.5.5.1 Permanent Gases

Permanent gases standard injection is shown in the table 3.6.1. The percentage standard deviation shows the values are with minimal errors.

Table 3.5-1 Peak Area values for the standard of permanent gases

Run	Hydrogen	Nitrogen	CO
1	595068	4457732	48776
2	595068	4457732	48776
3	595068	4457732	48776
4	595068	4457732	48776
5	595068	4457732	48776
6	586410	4669621	48370
7	595068	4457732	48776
8	595068	4457732	48776
9	595068	4457732	48776
Mean	594106	4481275	48730.89
Rel. Standard Deviation (%)	0.49	1.58	0.28

3.5.5.2 Hydrocarbon gases

Similarly, the two separate standard hydrocarbon gases were injected. The Table shows the injection of the standard gases; the mean values and percent standard deviation indicate the minimal error.

Table 3.5-2 Peak Area values for the standard of hydrocarbon gases

Run	Methane	Ethene	Ethane	Propene	Propane	Butene+Butadiene	Butane
1	543760	933754	970690	1310338	1405587	3277859	1842283
2	543760	933754	970690	1310338	1405587	3277859	1842283
3	543760	933754	970690	1310338	1405587	3277859	1842283
4	543760	933754	970690	1310338	1405587	3277859	1842283
5	543760	933754	970690	1310338	1405587	3277859	1842283
6	511183	853996	895441	1178473	1295293	3057853	1707504
7	511183	853996	895441	1178473	1295293	3057853	1707504
8	543760	933754	970690	1310338	1405587	3277859	1842283
9	543760	933754	970690	1310338	1405587	3277859	1842283
Mean	536520.7	916030	953968	1281035	1381077	3228969	1812332
Rel. Std Deviation (%)	2.68	3.84	3.48	0.45	3.52	3.00	3.28

3.5.6 Calculation of Gas Concentration

The calculation of the volume percentage of the gas products was made using the results produced by the analysis of standard gases. The area values recognized by the digital integrator by converting the electrical signal from the detector were used to obtain response factors (RFs) for each species in the

standard gases. The following equation was used to calculate response factors;

$$RF = \frac{\text{Peak area of standard gas}}{\text{Volume \% standard gas}} \quad \text{Equation 3.5-1}$$

After obtaining RFs for all the gases, the volume percentages of each species in the gas effluent obtained from the experiments can be calculated as;

$$\text{Volume \% of the gas} = \frac{\text{peak area of each anal. gas}}{\text{RF of the standard gas}} \quad \text{Equation 3.5-2}$$

After the volume % of each gas, species were obtained the ideal gas equation was used to calculate the mole of each gas.

$$n = \frac{PV}{RT} \quad \text{Equation 3.5-3}$$

Where n is the number of moles (mol.); V is the volume obtained; P and T are pressure and temperature respectively; R is gas constant (8.3144 J K⁻¹mol⁻¹ [8]). A spreadsheet was developed to calculate accurately results and corrected values for the large amount data collected. The spreadsheet was designed to make gas data analysis easy and error free. The various parameters included in the spreadsheet were; calculation of gas concentration, corrected nitrogen values, oxygen correction, and mass balance. Hence, the sheet gave useful information from data input such as; volumes, ratio of different gases, moles and, weight emitted for individual and total gases.

3.5.7 Liquid Products Analysis

The condensed liquid products of plastic pyrolysis were collected in the three condenser system. The liquid product weight was obtained by weight difference, i.e. weight of the three empty condensers subtracted from the weight of the condenser with the liquid products.

3.5.7.1 Sample Preparation

The liquid product was dissolved in a dichloromethane (DCM) solvent and stored in a freezer at end of the experiment or analysed immediately with liquid injection using a Varian 430 GC.

3.5.7.2 Gas Chromatography/ Mass Spectrometry (GC-MS)

The liquid product i.e, oil or wax dissolve in dichloromethane were qualitatively analysed using a gas chromatography coupled to a mass spectrometer (GC-MS). This device combines the benefit of the high resolution separation components from GC with the very sensitive and selective detector of the mass spectrometer. Principally GC acts as the separation technique, whereas MS identifies the compounds eluted from the column [9].The mass spectrometer measures the relation of mass and charge ratio of the eluted samples. The interaction between the GC and the mass spectrometer proceeds via an inlet system (interface) that must provide a suitable pressure (10^{-5} to 10^{-8} torr) by using a vacuum system.

The identification of individual components is achieved by ionising and fragmenting them. Thus, ionisation of the molecule is vital for detection since the analyser separates ions using their charges. For example, ethyl benzene would generate four major ions to be detected. So, the first would be the ionic form of ethyl benzene itself, the parent species, this would give an MW

spectrum line 106. Fragmentation would likely break the ethyl benzene up into a variety of species. These species are a benzyl ion (MW of 77), an ethyl ion (MW of 29) and methyl ion (MW of 15). Therefore, these ions and their relative concentrations are entirely indicative of the ethyl benzene species [9]. The detailed description of how this technique works is reported in Skoog [10]

GC-MS analyses were carried out using a Varian CP3800 gas chromatograph coupled to a Varian Saturn 2200 GC-MS mass spectrometer. An aliquot of 2 μ L of liquid sample dissolved in DCM injected via autosampler system into the GC injection port at a temperature of 290 °C. The oven programme temperature was 40 °C for 2 minutes, and then the temperature ramped into 280 °C at 5 °C min⁻¹ heating rate and held for 10 minutes. The transfer line temperature maintained at 280 °C; the manifold was 120 °C, and the oil trap temperature was kept at 200 °C. A typical chromatogram for thermal pyrolysis of pure HDPE shown in Figure 3.5-7.

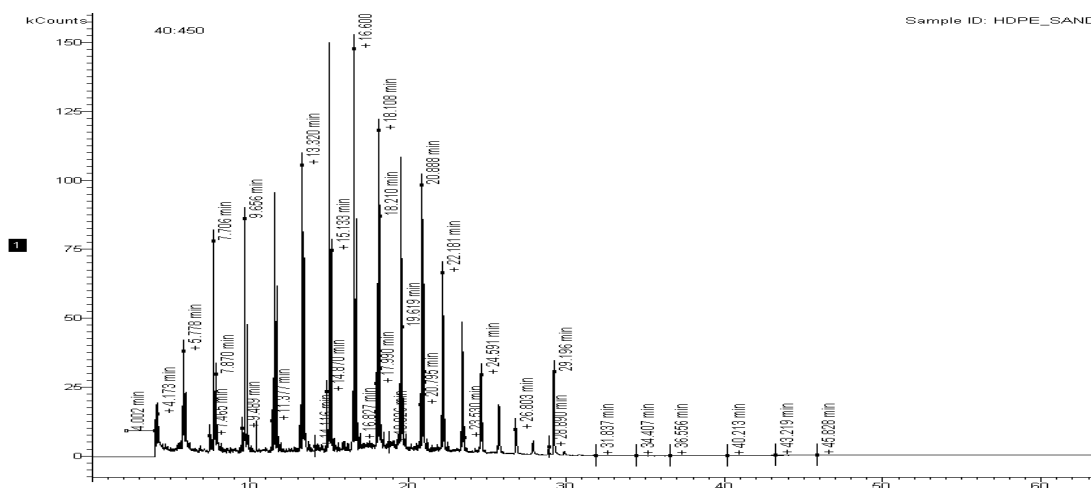


Figure 3.5-7 GC-MS chromatogram for thermal Pyrolysis of PE

3.5.7.3 Gas Chromatography FID Liquid Injection

The use of gas chromatography FID has wider acceptance as an analytical technique. It used for identification and quantification of the array of compounds identified in the plastic pyrolysis oils. Moreover, use of capillary column gas-liquid chromatography was well established [11].

The external standard method was used for identification and quantification of organic compounds. Skoog [11], reported that quantitative chromatography is built upon a comparison of either the height or the area of an analyte peak with that of one or more standard g [10]. Hence, both of these parameters vary linearly with concentration provided the conditions are adequately controlled. A range of the standard was prepared; this was done as the high-value chemicals in the sample had been known. The standard helps to quantify the high-value chemicals. Hence, the standard for a range of simple aliphatic and aromatics were obtained commercially from Aldrich, Poole, UK.

The pure aromatic standards prepared from the compound that were found or known to be in a significant amount and indicative of a group of compounds. The Table 3.6.3 shows the various standard aromatic and PAH compounds used with their retention times.

Table 3.5-3 the various standard aromatic and PAH compounds used with their retention time

Compound	formula	Molar mass g mol. ⁻¹	Retention time (min)
Benzene	C ₆ H ₆	78.112	4.476
Toluene	C ₇ H ₈	92.138	8.728
Ethylbenzene	C ₈ H ₁₀	106.165	12.450
m/p-Xylene	C ₈ H ₁₀	106.165	12.897
Styrene	C ₈ H ₈	104.149	13.647
o-Xylene	C ₈ H ₁₀	106.165	13.813
Alphamethylstyrene	C ₉ H ₁₀	118.176	16.925
Betamethylstyrene	C ₉ H ₁₀	118.176	17.491
s-Limonene	C ₁₀ H ₁₆	136.234	18.941

Compound	formula	Molar mass g mol. ⁻¹	Retention time (min)
Indane	C ₉ H ₁₀	118.176	21.050
1,2,3,4 Tetra methylbenzene	C ₁₀ H ₁₄	134.218	23.382
Naphthalene	C ₁₀ H ₈	128.171	26.635
2-Methylnaphthalene	C ₁₁ H ₁₀	142.197	28.825
Biphenyl	C ₁₂ H ₁₀	154.208	29.333
2-ethylnaphthalene	C ₁₂ H ₁₂	156.224	29.617
1,4-dimethylnaphthalene	C ₁₂ H ₁₂	156.224	30.433
2,6,-demethylnaphthalene	C ₁₂ H ₁₂	156.224	30.498
2,2-diphenylpropane	C ₁₅ H ₁₆	196.292	33.002
Bibenzyl	C ₁₄ H ₁₄	182.261	33.953
Fluorene	C ₁₃ H ₁₀	166.219	35.534
1,3-diphenylpropane	C ₁₅ H ₁₆	196.288	38.315
Phenanthrene	C ₁₀ H ₁₄	178.229	39.856
1-Phenylnaphthalene	C ₁₆ H ₁₂	204.094	40.481
o-Terphenyl	C ₁₈ H ₁₄	230.304	43.928
Fluoranthene	C ₁₆ H ₁₀	202.251	44.906
Pyrene	C ₁₆ H ₁₀	202.251	45.396
m-terphenyl	C ₁₈ H ₁₄	230.304	53.988
1-3-5-triphenylbenzene	C ₂₄ H ₁₈	306.420	59.434

Therefore, to obtain a calibration curve, the standards were accurately diluted to the range 50-1000 ppm. All prepared standard were from Aldrich. The calibration curve was produced for each compound by injecting 2 μ L of each concentration (20 ppm, 40 ppm, 80 ppm, 100 ppm) into the GC-FID equipment. An example of a calibration curve plot for the standard compound injected is shown in Figure 3.6.8.

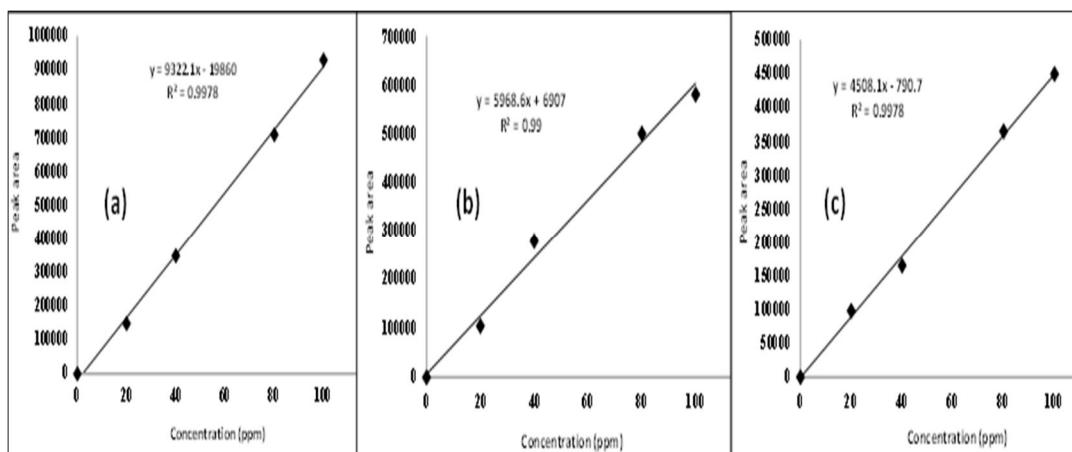


Figure 3.5-8 Calibration curve for the standard aromatic and PAH injected into GC-FID

The oil was quantitatively analysed by liquid injection GC using a Varian 430 Liquid GC with flame ionization detector (FID). The gas chromatograph was equipped with a split/split less injection port. The analysis was carried out on a ZB-1 capillary column (30 m × 0.53 mm i.d., 0.5 μm ;). The liquid phase was 100% Dimethyl siloxane. Nitrogen was used as carrier gas with a constant flow of 1.0 mL min⁻¹. The injection volume was 2.0 μL. The column was temperature programmed from 40 to 310 at 5 °C min⁻¹ heating rate. The system was calibrated with aromatic and polycyclic standards for aromatic and PAH analysis, while prepared aliphatic hydrocarbons standard was used for aliphatic hydrocarbon analysis.

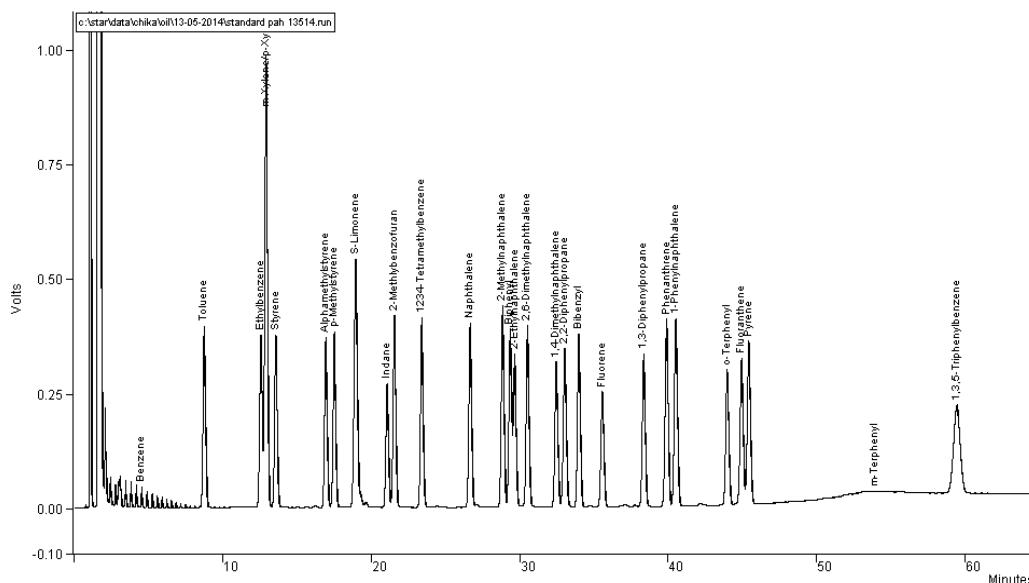


Figure 3.5-9 Peak response for standard aromatic and PAH injected into GC-FID

The oil sample was prepared using dichloromethane (analytical reagent grade) to approximately 2000 ppm [5].

The GC-FID system used was controlled by computer with the aid of software. On-column split less injection system was used. Grob and Eugen [12] reported that the on-column injection system greatly reduces errors associated with the other injection methods. The reduction in error is achieved by inserting the sample directly onto the column.

3.5.7.4 Simulated Distillation

Boiling point distribution properties of plastic pyrolysed oil is essential for its potential use as fuels. Hence, the distribution of oil with increasing temperature indicate the amount of oil distributed between the range of distillation appropriate for processing of different oil based products. The use of simulated distillation for pyrolysis oil has been reported by a number of authors [5, 13-16].

The distillation curve provides a platform for comparative fuel analysis of commercial fuel and pyrolysed oil. Although the method has a limitation it helps in the study of the fuel properties of the pyrolysis oil. Commercial unleaded gasoline was used for comparison.

The simulated distillation was determined using the GC-FID Varian 430 analysis data described above. The computation uses the retention time for all n-alkanes in the analytical range, and the boiling point of the n-alkanes. The combined peak areas for all peaks with retention times between the n-alkanes were used as an estimation of the products with same carbon number as alkanes. Therefore, by estimating a constant response factor for all the compounds integrated and the boiling point of the n-alkanes, the concentration was calculated. A normalised simulated distillation curve, showing the quantity of the oil distilled against the temperature was produced for comparison with the fuel oils [9].

3.5.8 Characterization of Catalysts

This section describes the various techniques used to characterize the reacted and /or fresh catalyst. Thus, some of the techniques were used to characterize reacted catalyst and compare some properties before and after the pyrolysis-catalysis process. The various analytical techniques used in this research work were as follows;

3.5.8.1 Surface Area by Brunauer-Emmet-Teller (BET) Method

The BET method determination of surface area was carried out only for fresh catalysts. The fresh catalysts were analysed to determine their surface area and porous properties via nitrogen adsorption at liquid gas temperature.

Likewise, the surface area might be also studied using other techniques such as adsorption from solution and by the heat of adsorption [17]

The ultra-fine powders and porous materials surface area are analysed using Brunauer-Emmet-Teller linear equation which was as follows ; [18] [19].

$$\frac{1}{(V(p^{\circ} - 1))} = \frac{1}{V_m} + \left(\frac{(C - 1)}{V_m C} \cdot \left(\frac{p}{p^{\circ}} \right) \right) \quad \text{Equation 3.5-4}$$

Where p_0 refers to the saturation pressure, V is the amount of gas adsorbed at the determined P/P_0 pressure; V_m is the monolayer capacity and C is an empirical constant. Therefore a linear trend can be built using point-by-point adsorption data from the multipoint analysis.

The surface area analysis was carried out using a NOVA 2200e series instruments. The samples were degassed using a degassing unit of the instrument. About 100mg of each sample was degassed for 3h at 300 °C under N_2 atmosphere. The degassing was carried out in order to remove all previously physisorbed matter from the adsorbent surface [18]. A full isotherm was carried out for each sample.



Figure 3.5-10 BET surface area and pore size analyzer NOVA 2200e

3.5.8.2 Determination of micropore volume by Dubinin-Radushkevich (DR) method

Further information apart from the BET linear equation might be obtained from adsorption-desorption studies, using other calculation methods. The Dubinin-Radushkevich (DR) method, relates the temperature, relative pressure and energy with the adsorbed amount of gas per unit of micropore volume. The calculation of micropore volumes, uses the equation below [20, 21].

$$W/W_0 = \exp[-(AE)^2]$$

Equation 3.5-5

$$W/W_0 = \exp - [RT (\ln(x))/E]^2 \quad \text{Equation 3.5-6}$$

With $x = p/p^0$, characteristic energy for a given fluid system (E), the amount of gas adsorbed (W), micropore volume (W_0), temperature in kelvin (T) and universal gas constant (R). Moreover, the adsorbed volume (V_{ads} ; $\text{cm}^3 \text{ STP g}^{-1}$) could be plotted against the $\{\log(x)\}^2$ or $\{\log(p/p_0)\}^2$. Hence, the relationship gives a typical straight line from which the volume of gas adsorbed can be obtained.

Thus, from the Figure the 'Y intercept' is usually used to compute the micropore volume [V_{micro}]. Hence, the quantity of gas adsorbed at relative pressures closer to one correspond to the total amount adsorbed at both micropores (generally filled at low relative pressure), and mesopore volume (generally filled at relative pressure above 0.2) [22]. Hence, the mesopore volume value can be computed by subtracting the micropore volume (calculated from DR equation) from total amount of gas adsorbed at relative pressure p/p^0 [22].

3.5.8.3 Barrett, Joyner & Halenda (BJH) method for total pore volume and pore diameter

The Barrett, Joyner & Halenda (BJH) method is used to determine the total pore volume and pore diameter. The method is aimed at securing information about porous adsorbents with a wide range of pore size. The technique accounts for capillary condensation in pores, based on the Kelvin equation. The total excess adsorption in each pore is given by a surface layer $t(P)$ plus a pore-filling terms; Thus the pore is filled as the pressure satisfied the following expression in equation [23].

$$\ln \frac{p}{p^0} \geq \frac{(-2\gamma VL)}{RT} * \frac{1}{rc}$$
Equation 3.5-7

Where $rc = r-t(p)$ and r is the radius of the pore. VL is the molar volume of the liquid, γ is the surface tension, and p^0 is the vapour pressure [23].

3.5.8.4 Temperature Programmed oxidation (TGA-TPO)

The reacted catalysts from the pyrolysis-catalysis of plastics were analysed using thermogravimetric method known as temperature programme oxidation (TGA-TPO). The analytical technique is suitable for analysis of the reacted catalyst and coke deposited using TGA method which was described previously in section 3.4.2 for plastic characterization. In this work a thermogravimetric Mettler Toledo (TGA\DSC) instrument was used; about 20 mg of the reacted catalysts was weighted into the alumina crucible which was transferred into auto sampler. The TGA was programmed to heat-up at heating rate $15 \text{ }^\circ\text{C min}^{-1}$ to a temperature of $800 \text{ }^\circ\text{C}$ using air with a flow rate of 50 ml min^{-1} and dwell time of 10 min. The change in catalyst weight denoted the combustion of coke deposited over the catalyst surface used. The variation of weight was detected by the ultra-microbalance and recorded by the computer using software. Thus, with the aid of the software, both the thermo gravimetric (TGA-TPO) curve and differential gravimetric (DTG-TPO) were obtained. Two main stages were identified from TPO studies, around $80\text{-}100 \text{ }^\circ\text{C}$ moisture volatile are lost and above $390 \text{ }^\circ\text{C}$ might be the identified carbon combustion depending on the sample studied.

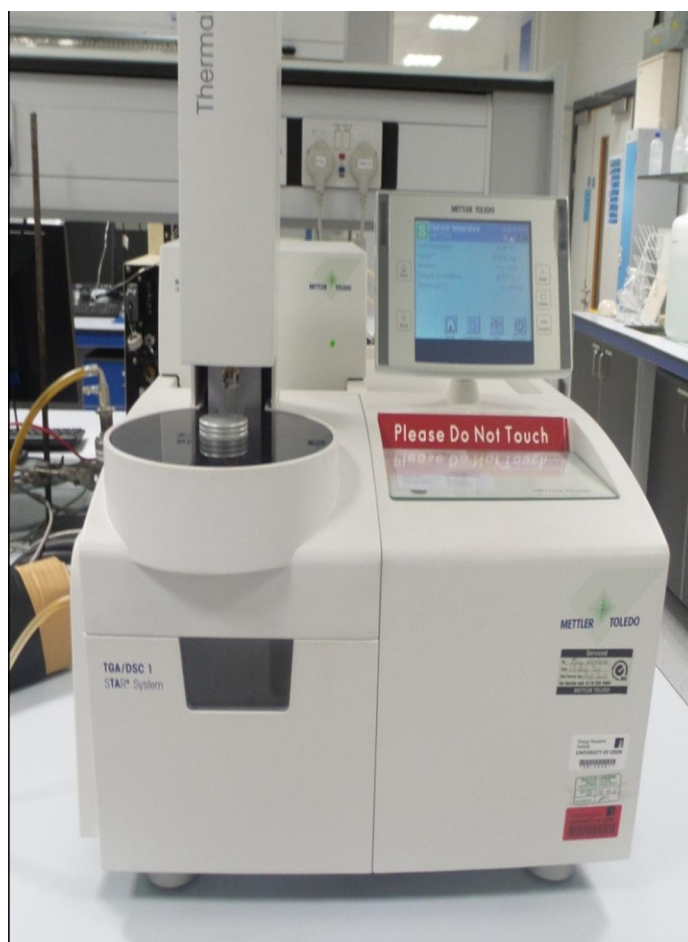


Figure 3.5-11 Toledo Mettler TGA-DTS

3.5.8.5 Scanning Electron Microscopy (SEM)

The microscopic technique was used to characterize both fresh and reacted catalyst. The image of morphologies before and after reaction was used to further characterize the catalyst. The major component of scanning electron microscope (SEM) technique is the electron column which consists of an electron gun and mainly two electron lenses, other components include the control console consisting of a cathode ray tube (CRT), screen, and computer system that allows the control the electron beams. An energy filter might be used, allowing the electron beam to be dispersed according to the electron energy. Thus electrons can pass through a diaphragm to form the final image [24].

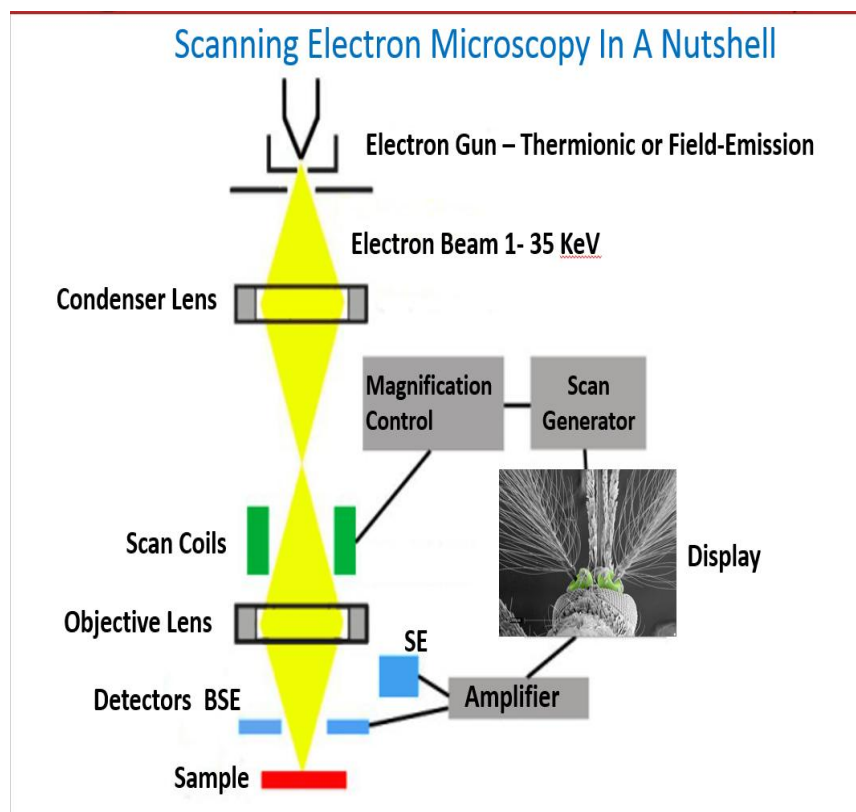


Figure 3.5-12 Schematic diagrams for SEM

<http://zenofstem.com/project/using-the-sem/03-05-2015> 22:22

In this work a high resolution scanning electron microscope (LEO 1530), coupled to an energy dispersed X-ray spectrometer (EDXS) was used to carry out SEM and SEM-EDXS studies. The catalyst sample was prepared by applying a metallic coating which was reported to be necessary for charge dissipation to improve [25]. Thus, the catalyst was coated with Pt/Pd to produce a 5.0nm layer.



(a) Coater



(b) LEO SEM

Figure 3.5-13 (a) Coater and (b) LEO SEM

References

1. Delgado, C., Barretabena, L., Salas, O. and Wolf, O., *Assessment of the Environmental Advantage and Drawbacks of Existing and Emerging Polymers Recovery Processes*. Join Research Center Scientific and Technical Report, 2007. jrc37456: p. 264.
2. Muhammad, C., Onwudili, J.A. and Williams, P.T., *Catalytic Pyrolysis of Waste Plastic from Electrical and Electronic Equipment*. Journal of Analytical and Applied Pyrolysis, 2015.
3. Hall, W.J., Miskolczi, N., Onwudili, J.A. and Williams, P.T., *Thermal processing of toxic flame-retarded polymers using a waste fluidized catalytic cracker (FCC) catalyst*. Energy & Fuels, 2008. **22**(3): p. 1691-1697.
4. McDougall, F.R., White, P.R., Franke, M. and Hindle, P., *Integrated solid waste management: a life cycle inventory 2008*: John Wiley & Sons.
5. Muhammad, C., Onwudili, J.A. and Williams, P.T., *Thermal Degradation of Real-World Waste Plastics and Simulated Mixed Plastics in a Two-Stage Pyrolysis-Catalytic Reactor for Fuel Production*. Energy & Fuels, 2015. **29**(4): p. 1601-1609.
6. Skoog, D., West, D.M., Holler, F.J. and Crouch, S.R., *Fundamentals of Analytical Chemistry*, Brooks Cole, Belmont, CA, USA, 2004: p. 795.
7. Harvey, D., *Modern analytical chemistry*. Vol. 798. 2000: McGraw-Hill New York.
8. Nag, P., *Engineering thermodynamics* 2008: Tata McGraw-Hill Education.
9. Brindle, A.J., *High Value Chemicals from the Pyrolysis of Scrap Tyres*, 2000, University of Leeds.
10. Skoog, D., West, D., and Holler, F., *Fundamentals of Analytical Chemistry*, 1996.
11. Skoog, D. and West, D., Holler, F., *Fundamentals of analytical Chemistry*, 1997.
12. Grob, K. and Müller, E., *Sample reconcentration by column-external solvent evaporation or injection of large volumes into gas chromatographic capillary columns?* Journal of Chromatography A, 1987. **404**: p. 297-305.
13. Sharma, B.K., Moser, B.R., Vermillon, K.E., Doll, K.M. and Rajagopalan, N., *Production, characterization and fuel properties of alternative diesel fuel from pyrolysis of waste plastic grocery bags*. Fuel Processing Technology, 2014. **122**: p. 79-90.

14. Lima, A.D.M., Cantoa, E.M., De Souza, M.B. and Valleb,M.LM., *Using Simulated Distillation or Density to Maximize Lubricants Production from Low Density Polyethylene (LDPE) Pyrolysis*. Chemical Engineering, 2012. **26**.
15. Arabiourrutia, M., Elordi, G., Lopez, G., Borsella, E., Bilbao, J. and Olazar,M., *Characterization of the waxes obtained by the pyrolysis of polyolefin plastics in a conical spouted bed reactor*. Journal of Analytical and Applied Pyrolysis, 2012. **94**: p. 230-237.
16. Csukás, B., Varga, M., Miskolczi, N., Balogh, S., Angyal, A. and Bartha, L., *Simplified dynamic simulation model of plastic waste pyrolysis in laboratory and pilot scale tubular reactor*. Fuel Processing Technology, 2013. **106**: p. 186-200.
17. Allen, T., *Particle Size Measurement: Volume 2: Surface Area and Pore Size Determination*. Vol. 2. 1997: Springer Science & Business Media.
18. Wagner, L., *Waste-to-energy (WtE) technology*. Analyst, 2007.
19. Merritt, J.A., *Waste-to-Energy: Comprehensive Recycling's Best Chance? Recovering Energy from Waste: Various Aspects*, 2002: p. 15.
20. Nguyen, C. and Do, D. *The Dubinin–Radushkevich equation and the underlying microscopic adsorption description*. Carbon, 2001. **39**(9): p. 1327-1336.
21. Amphlett, J., Creber, K., Davis, J.M., Mann, R.F., Peppley, B.A. and Stokes, D.M. and Stokes, D.M., *Hydrogen production by steam reforming of methanol for polymer electrolyte fuel cells*. International Journal of Hydrogen Energy, 1994. **19**(2): p. 131-137.
22. Blanco Sanchez, P.H., *Nickel based catalysts for hydrogen production from the pyrolysis/gasification of refuse derived fuel (RDF)*, 2014, University of Leeds.
23. Gelb, L.D. and Gubbins, K. *Characterization of porous glasses: simulation models, adsorption isotherms, and the Brunauer-Emmett-Teller analysis method*. Langmuir, 1998. **14**(8): p. 2097-2111.
24. Watt, I.M., *The principles and practice of electron microscopy*1997: Cambridge University Press.
25. Datye, A.K., *Electron microscopy of catalysts: recent achievements and future prospects*. Journal of Catalysis, 2003. **216**(1): p. 144-154.

Chapter 4 THERMAL AND CATALYTIC PYROLYSIS OF WASTE PLASTIC FROM ELECTRICAL AND ELECTRONIC EQUIPMENT

This chapter describes the thermal and catalytic pyrolysis of waste plastic from electrical and electronic equipment in two stage catalysis-pyrolysis reaction system.

4.1 Introduction

A two stage down draft pyrolysis-catalysis fixed bed batch reactor was used to carry out a series of experiments. The experiments were carried out using pyrolysis or pyrolysis-catalysis reaction system as described in Chapter 3, Section 3.3. Waste electric and electric equipment (WEEE) whose preparation was described in Chapter 3, section 3.2.6 and; two major component of WEEE plastic HIPS and ABS in section 3.2.1. These materials were used as raw material for the work. However, two zeolite catalysts; zeolite Y and ZSM-5 catalysts were tested during the catalytic cracking stage to promote cracking/reforming reactions. Hence, the activities of the two zeolite catalysts were measured in terms of their influence on the product yields as well as gas and liquid compositions. However, the results obtained were compared with non-catalytic pyrolysis experiment carried out using a bed of sand.

4.2 Elemental composition of the WEEE and characteristic of catalyst

This section describes both the elemental composition of WEEE plastic used and, characteristic properties of the two zeolite catalysts tested.

4.2.1 Elemental composition of the WEEE

The elemental analysis of WEEE plastic was carried out with CE Instrument Flash EA 1112 Elemental Analyzer as described in Chapter 3 Section 3.4.1. The result of the elemental analyses for the four plastic represented in Table 4.2-1

Table 4.2-1 Elemental analysis of the plastics (wt. %)

	High impact polystyrene (HIPS)	Acrylonitrile-butadiene-styrene (ABS)	Plastics from Waste Cathode Ray Tubes (CRT)	Plastics from Waste refrigerators (Fridge)
Carbon	80.5	72.3	81.6	71.4
Hydrogen	7.30	6.40	7.50	7.00
Nitrogen	0.20	4.10	5.50	1.80
Oxygen	0.80	2.80	3.90	4.70
Bromine	7.60	11.2	<0.01	<0.01
Chlorine	-	-	0.26	1.30
Antimony	3.60	3.20	-	-
Ash	-	-	1.30	13.8

The halogen elements (Br and Cl) and antimony were detected in all or two of the plastic samples. The high bromine content of the HIPS and ABS plastic samples reflects the high content of brominated flame retardant added to the plastic. The use of brominated compounds in flame retarder is well known and reported [1, 2]. However, antimony is added as antimony trioxide as a synergist to aid the effectiveness of the flame retardant. Zhang et al. [1], highlighted that a series of reaction between antimony trioxide and hydrogen halide produce

antimony trihalide and various antimony oxygen halide compounds. Thus, oxygen is excluded from the front of the flame, and the antimony oxygen halides absorb the quantity of heat. Interestingly, the bromine content of the plastics from the waste televisions and computer monitors and fridge and freezers plastics samples was very low, below the detection limit of the analysis procedure. This was most likely due to dilution of the brominated plastic waste with non-brominated Fire-retardant plastics. The ash content of the plastics derived from the recycled WEEE was high, particularly from the plastic sample produced from waste fridges and freezers. The plastic from fridge and freezer commonly consisted of mainly metals carried over from poor separation of the materials and plastics.

4.2.2 Characteristic properties of the zeolite catalysts

The characteristic properties of catalysts play a vital role in the catalytic pyrolysis of polymeric materials [3, 4]. The catalysts used were Y zeolite and ZSM-5 zeolite which were in pellet form of approximate size, 1 mm by 5 mm. The Y zeolite catalyst had a Si-Al ratio of 5.4, the pore size of 7.8 Å and high acidity, the ZSM-5 zeolite catalyst had a Si-Al ratio of 40, the pore size of 5.6 Å and lower acidity.

4.3 Pyrolysis-catalysis results

4.3.1 Product Yields and Gas composition

The mass balance of the products was calculated using the Excel spreadsheet developed and described in Chapter 3 Section 3.6.1.4. The results for the mass balance and product yields (gas, liquid and char) presented in Figure 4.3-1 and Figure 4.3-2.

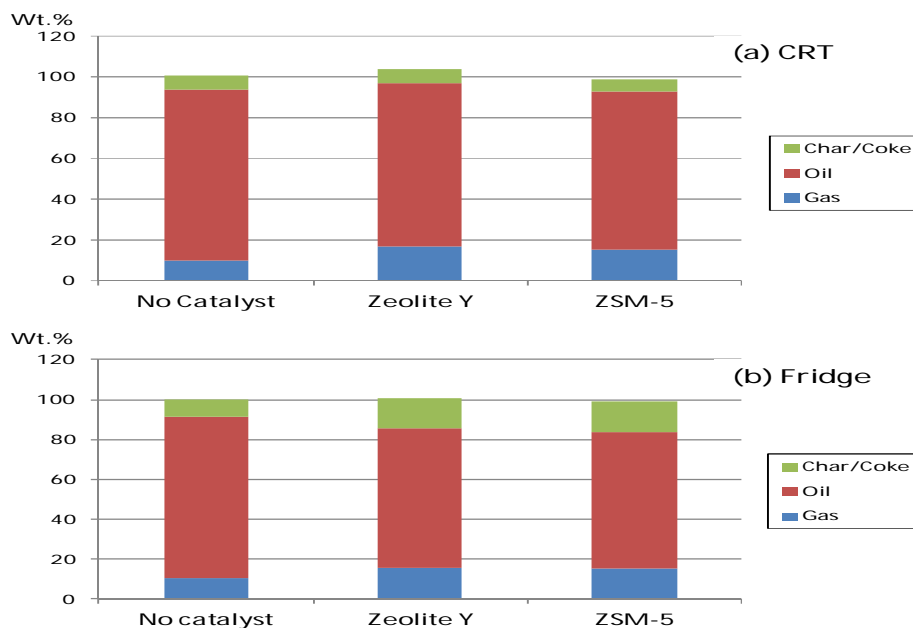


Figure 4.3-1 Product yield from the pyrolysis and pyrolysis-catalysis of CRT and Fridge plastics with Zeolite Y and ZSM-5 catalysts.

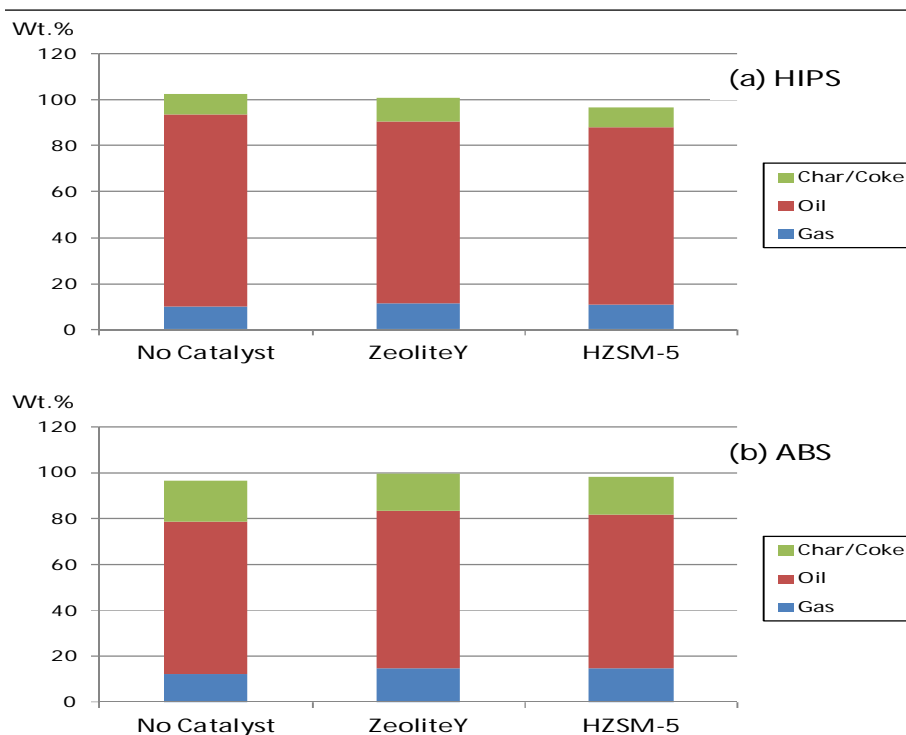


Figure 4.3-2 Product yield from the pyrolysis and pyrolysis-catalysis of HIPS and ABS plastics with Zeolite Y and ZSM-5 catalysts.

The product mass balances were all close to 100 wt%, with the main product being the pyrolysis oil, especially for CRT and fridge in Figure 4.3-1. High oil yield and, use of three dry-ice cooled condensers system had helped to improve the mass balance. Similarly, mass balance >95% reported in the pyrolysis of PS and PS or styrene containing WEEE [5-7].

The bulk component of the plastic used in this work content PS or styrene in their main polymeric structure. Hence, Marczewski et al. [8], described the chemistry of PS transformation. They identified two main routes for the transformation of polystyrene as scheme 1 and 2. This begins with the transformation of the polymeric chain into the radical, cationic or anionic state (scheme 1).

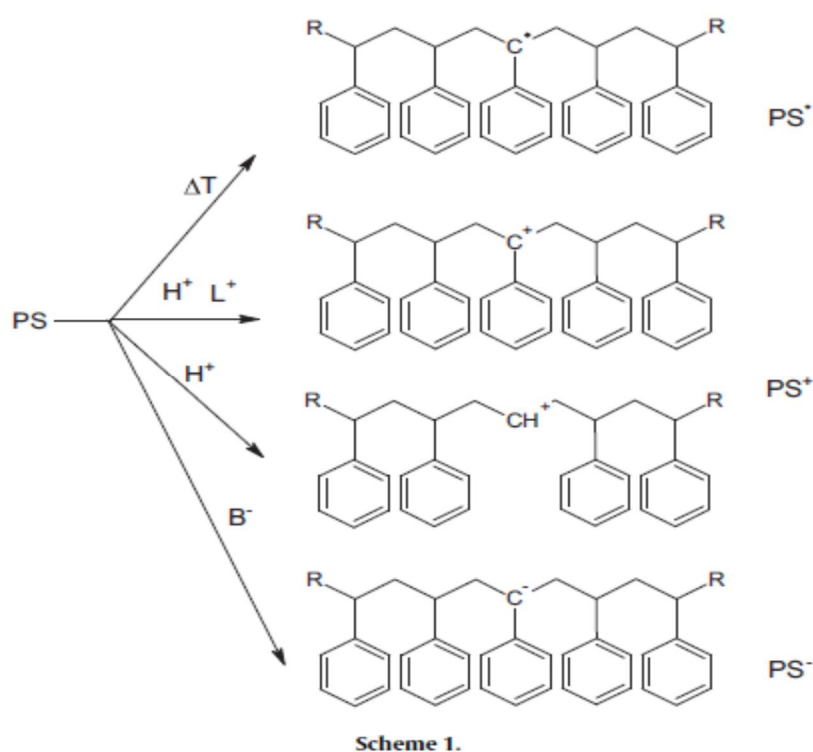


Figure 4.3-3 Degradation or transformation of Polystyrene scheme 1 [8]

Thermal activation results in the radical species formation while cationic or anionic species counterparts a specific catalyst. Hence, a Lewis acid catalyst would remove a hydride anion (H^-) from the benzylic position in PS with III order cation formation [9]. Consequently, Bronsted acid type of catalyst does protonate the aromatic ring attached to the aliphatic chain of the PS resulting in benzene elimination (dealkylation reaction) and formation of a polycation [10]. But, the basic catalyst activates PS through protonation [11]. The β -cleavage of C-C bond located in the aliphatic chain meanwhile is the next step of the transformation. Thus, new radical, anions or cations activate in the further reaction are then formed (scheme 2) [8].

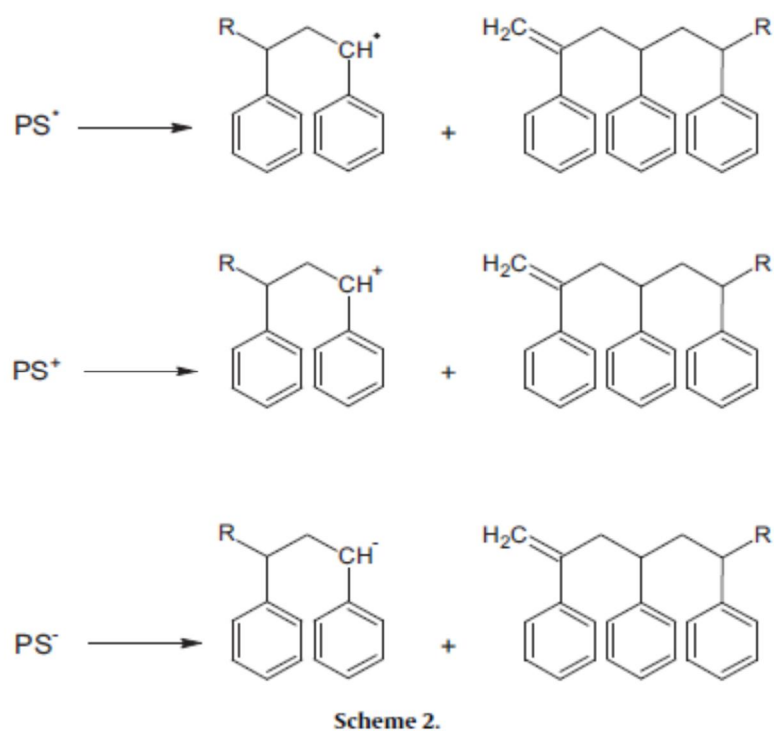


Figure 4.3-4 Degradation or transformation of Polystyrene scheme 2 [8].

Consequently, the radical, anions or cations undergo depolymerization leading to styrene and shorter polymer being II order radicals, cations or anions.

Table 4.3-1 Gas composition for the pyrolysis and pyrolysis-catalysis of HIPS and ABS plastic waste with Zeolite Y and ZSM-5 catalysts

Gas Composition (Vol. %)	High-impact polystyrene (HIPS)			Acrylonitrile-Butadiene-styrene (ABS)		
	No	Y zeolite	ZSM-5 zeolite	No	Y zeolite	ZSM-5 zeolite
	Catalyst			Catalyst		
H ₂	60.6	31.0	37.3	69.7	45.7	49.5
CH ₄	16.6	20.8	8.80	12.9	18.4	11.8
C ₂ H ₄	5.90	18.3	33.1	3.70	9.30	13.5
C ₂ H ₆	6.90	7.00	3.60	5.60	6.50	5.10
C ₃ H ₆	4.20	11.2	13.8	2.60	17.2	15.1
C ₃ H ₈	2.70	7.60	0.00	2.00	0.00	0.00
C ₄ H ₈	1.60	3.80	2.30	2.20	1.20	3.30
C ₄ H ₁₀	1.40	0.50	1.00	1.40	1.60	1.70
C ₂ -C ₄	22.8	48.2	53.9	17.5	35.9	38.7
Alkanes	27.6	35.9	13.2	19.8	26.6	18.6
Alkenes	11.7	33.3	49.2	8.50	28.0	31.9

Table 4.3-2 Gas composition for the pyrolysis and pyrolysis-catalysis of CRT and Fridge plastic wastes with Zeolite Y and ZSM-5 catalysts.

Gas composition (Vol. %)	Television & PC monitor plastics (CRT)			Refrigerator plastics (Fridge)		
	No Catalyst	Y zeolite	ZSM-5 zeolite	No Catalyst	Y zeolite	ZSM-5 zeolite
H ₂	37.6	28.1	35.2	35.1	21.7	19.2
CH ₄	26.7	16.2	11.6	16.1	19.7	10.9
C ₂ H ₄	10.9	19.5	21.8	12.8	21.8	32.3
C ₂ H ₆	9.20	7.50	5.50	11.8	8.70	5.6
C ₃ H ₆	7.80	19.3	19.5	12.7	15.9	23.1
C ₃ H ₈	2.00	6.20	0.00	2.70	6.40	0.00
C ₄ H ₈	3.20	1.70	4.3	5.20	3.30	6.30
C ₄ H ₁₀	2.60	1.40	2.1	3.70	2.40	2.60
C ₂ -C ₄	35.7	55.7	53.2	48.8	58.5	69.8
Alkanes	40.5	31.3	19.2	34.3	37.2	19.1
Alkenes	21.9	40.5	45.6	30.7	41.0	61.7

Table 4.3-1 shows that the main gases were hydrogen, methane and ethane and lower concentrations of other hydrocarbons. However, without the presence of a catalyst, the CRT plastics produced an oil yield of 84.0 wt%. But with the zeolite catalysis produced a decrease in oil yield to 80.0 wt% for the Y zeolite and 77.5 wt% for the ZSM-5 catalysts. There was a consequent increase in gas yield, mainly the alkene gases, particularly ethene and propene. Similar results were found for the Fridge plastics. The char included the carbonaceous pyrolysis char and ash derived from the metal contamination. The ash content of the fridge sample (Table 4.2-1) was high

at 13.8wt.% which would transfer to the solid char product resulting in a higher solid residue; result for the fridge sample compared to the CRT sample which only had 1.30wt.% ash content.

Figure 4.3-2 and Table 4.3-2 shows the product yield and gas composition respectively for the pyrolysis and pyrolysis-catalysis of high impact polystyrene (HIPS) and acrylonitrile-butadiene-styrene (ABS) with the Y zeolite and ZSM-5 catalysts. As with the WEEE plastics, the largest product for uncatalyzed pyrolysis was the pyrolysis oil at 84.0 wt% for HIPS and 66.5 wt% for ABS. The influence of the addition of a zeolite catalyst to the process was to decrease the oil yield and increase the gas yield for the HIPS. But there was less of an effect on the overall product distribution for the ABS plastics. Table 4.3-2 shows there were some changes in gas composition in the presence of the catalysts, in relation to increased concentrations of alkene gases, mainly ethene and propene. The char from HIPS and ABS would contain some of the residual antimony trioxide added as a synergist with the organo-bromine fire retardant compounds. The presence of the fire retardant would also influence the yield of oil from pyrolysis and also increase the char from the pyrolysis of the plastic. The elemental analysis of the HIPS and ABS (Table 4.2-1) shows that the bromine content, from the addition of brominated flame retardant, was significantly higher for the ABS sample (11.8 wt%) compared to the HIPS sample (7.6 wt%). The flame retardant mechanism of brominated flame retardants operates through the release of bromine free radicals at a lower temperature of thermal decomposition than the host plastic, preventing the formation of flammable gases. High energy OH and H radicals, formed during combustion, are removed by reaction with the released

brominated species in the gas flame phase [12]. The reaction considerably slows or prevents the combustion process, thus reducing heat generation and consequently the production of further pyrolysis vapours which later condense to produce the pyrolysis oil. Also, the presence of brominated flame retardants in waste plastics has been shown to increase the yield of char [13]. Therefore, the higher bromine content would produce more charring reactions resulting in a higher solid product yield and also lower oil yield for the ABS compared to the HIPS.

4.4 Oil Composition

The pyrolysis oils were analysed using GC-FID 430 Varian as described in chapter 3 section 3.6.3.2. This section discusses the oil composition produced by various pyrolysis experiment run.

Figure 4.4-1 shows the single ring to four-rings aromatic compounds present in the oils derived from the pyrolysis and the pyrolysis-catalysis of CRT and Fridge plastics with the Y zeolite and ZSM-5 catalysts. The oils are dominated by single ring aromatic compounds with lower concentrations of 2-4 ring polycyclic aromatic hydrocarbons (PAH). The addition of the catalysts resulted in only a slight increase in the single ring aromatic compounds in the product oils. Similarly, Figure 4.4-2 shows aromatic compound distribution according to their ring number for HIPS and ABS plastics. The same trend observed as in CRT and Fridge with the addition of both zeolites catalysts. However, Figure 4.4-3 shows that the relative concentrations of the main aromatic compounds present in the oil showed significant differences due to the effects of the catalysts. Styrene dominated the uncatalysed pyrolysis oil. Also present in high concentration are single ring toluene and ethylbenzene.

At lower concentration were two-ring naphthalene, alkylated naphthalenes and three or more ring PAH such as pyrene. Similarly, Figure 4.4-4 the relative proportion of the main aromatic compound for HIPS and ABS plastics pyrolysed oils. The influence of the zeolites catalysts was in the same trend as in CRT and Fridge .

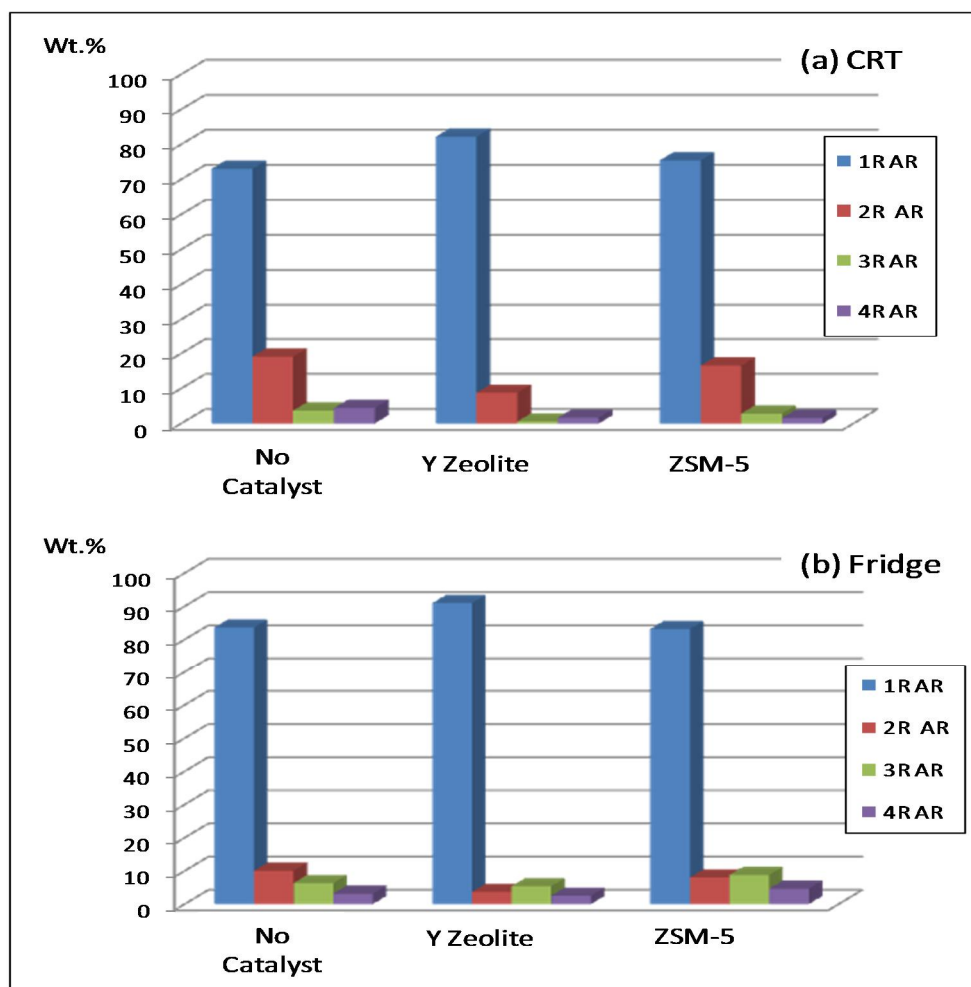


Figure 4.4-1 Aromatic compounds (AR) composition for oil from pyrolysis of CRT and Fridge plastics (1R = single ring; 2R = two rings; 3R = three rings; 4R = four rings aromatic compounds)

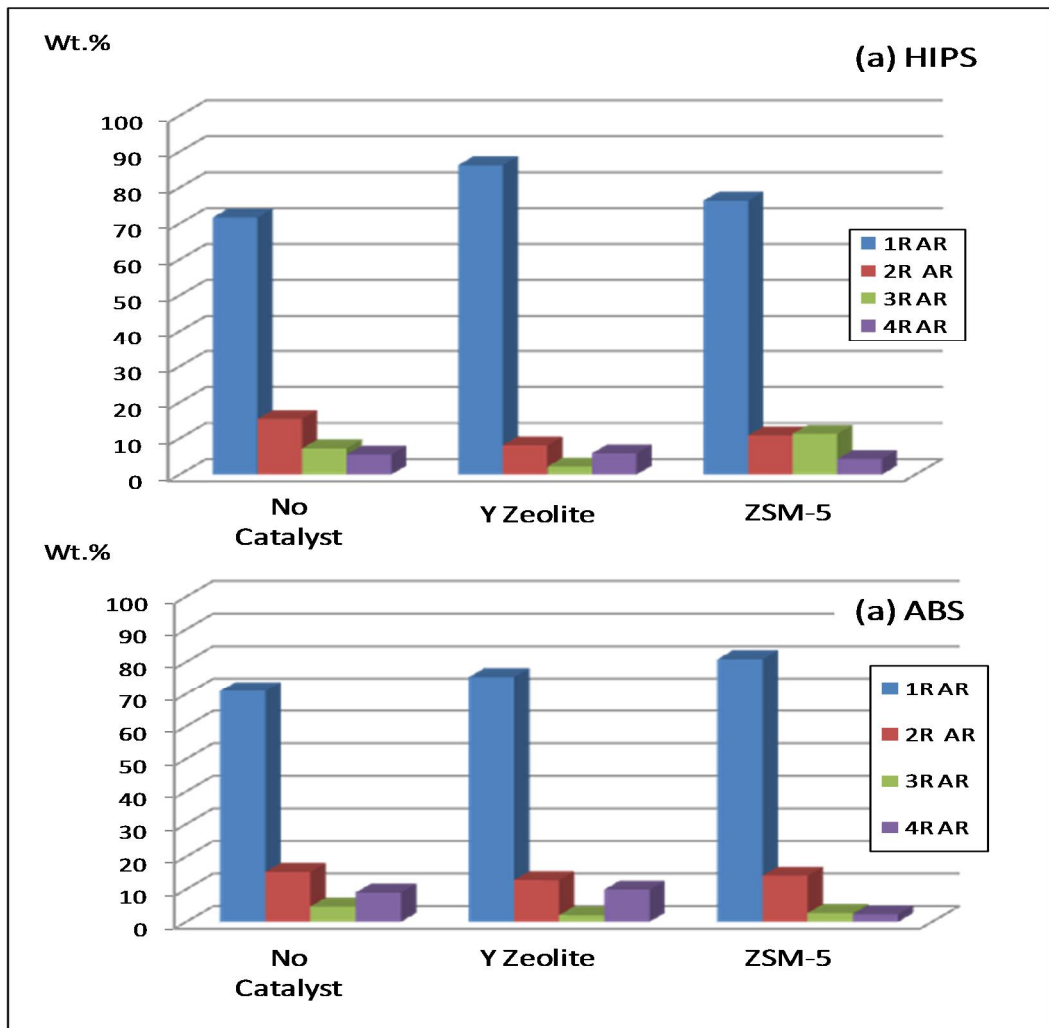


Figure 4.4-2 Aromatic compounds (AR) composition for oil from pyrolysis of HIPS and ABS plastic (1R = single ring; 2R = two rings; 3R = three rings; 4R = four rings aromatic compounds)

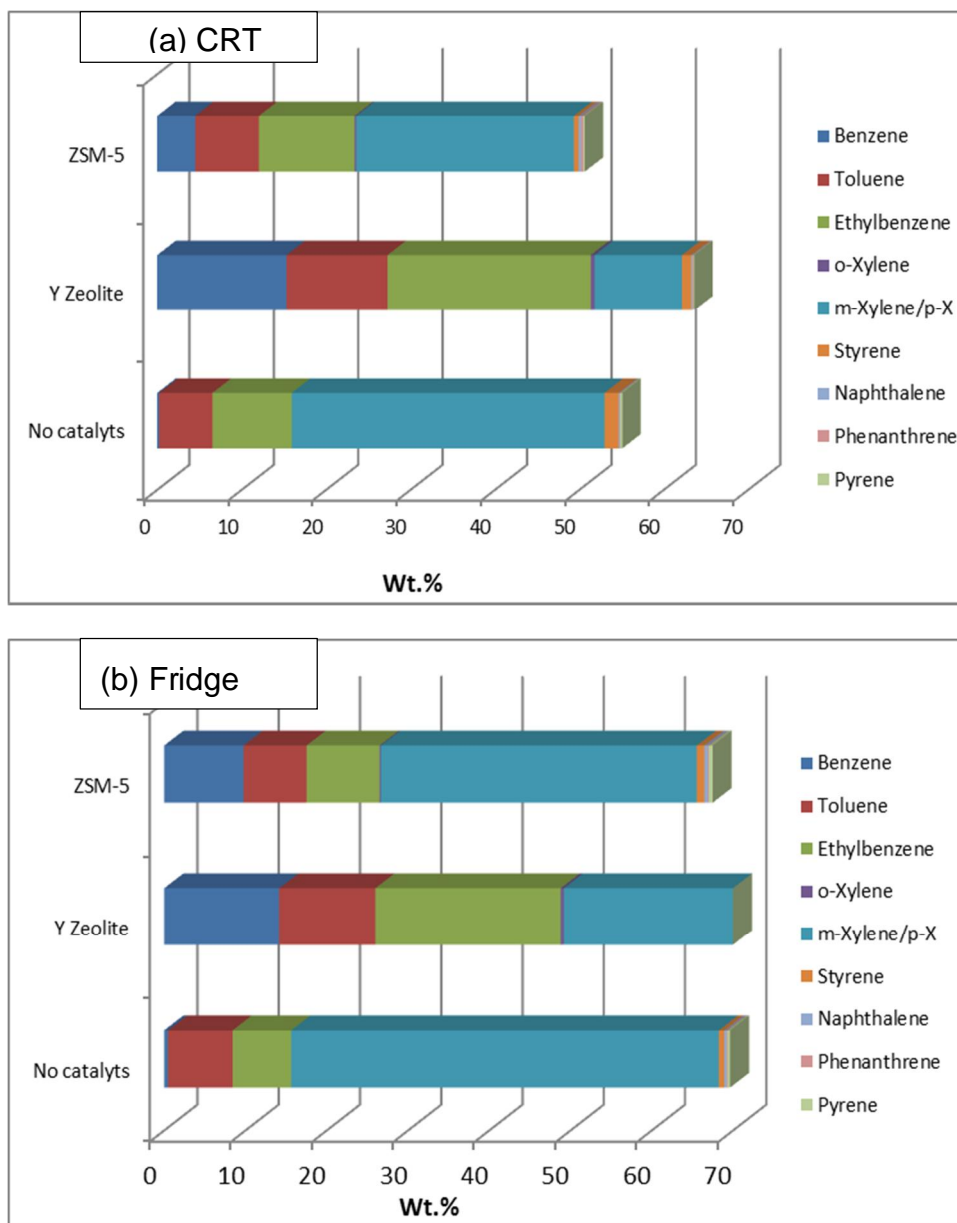


Figure 4.4-3 Relative proportions of the main aromatic compounds in the oil derived from the pyrolysis of CRT and Fridge plastics

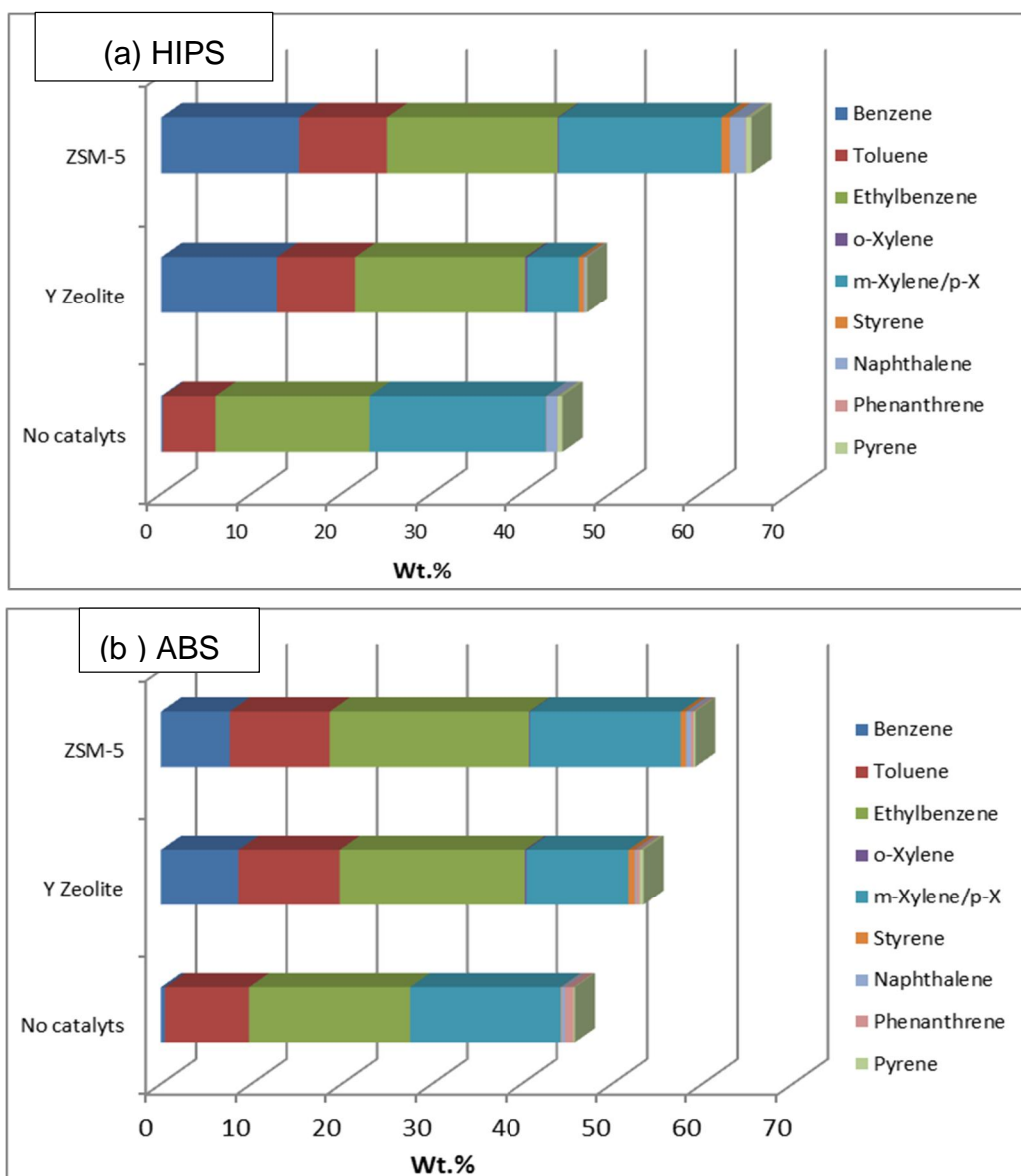


Figure 4.4-4 Relative proportions of the main aromatic compounds in the oil derived from the pyrolysis of HIPS and ABS plastic

The addition of the Y zeolite to the CRT pyrolysis-catalysis process for both the CRT and the Fridge plastics resulted in a marked decrease in styrene concentration in the product oil and a consequent marked increase in benzene and toluene. The influence of the zeolite ZSM-5 catalyst on the pyrolysis of the CRT and fridge plastics was less than that of the Y zeolite catalyst, with less reduction of the styrene concentration and a lower increase in toluene.

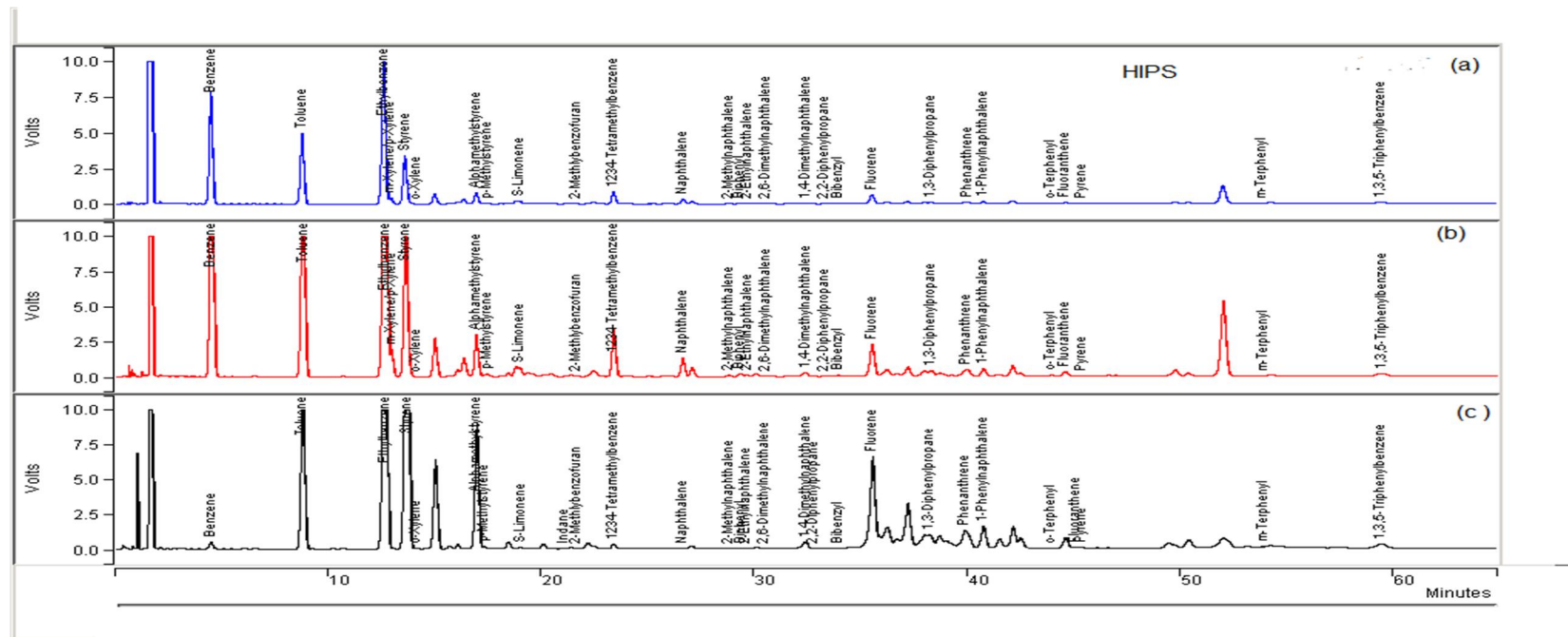


Figure 4.4-5 Gas Chromatograms for (a) the product oil from pyrolysis catalysis of HIPS with ZSM-5 zeolite catalyst, (b) the product oil from pyrolysis catalysis of HIPS with Y zeolite catalyst and (c) the pyrolysis oil derived from uncatalysed pyrolysis of HIP

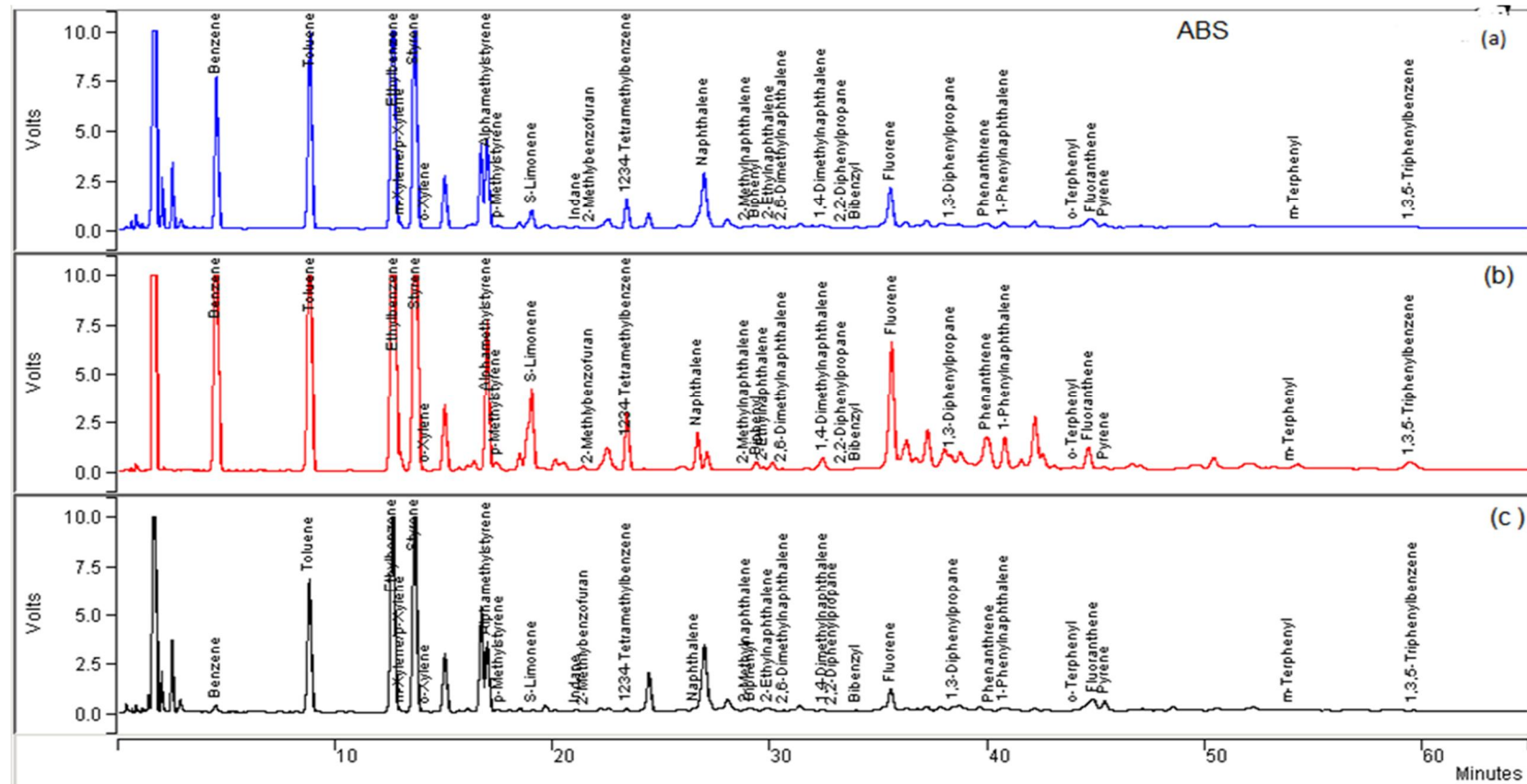


Figure 4.4-6 Gas Chromatograms for (a) the product oil from pyrolysis catalysis of ABS with ZSM-5 zeolite catalyst, (b) the product oil from pyrolysis catalysis of ABS with Y zeolite catalyst and (c) the pyrolysis oil derived from uncatylsed pyrolysis of ABS

Figure 4.4-5 and Figure 4.4-6 shows GC/FID chromatograms for the pyrolysis oil derived from HIPS in the absence of a catalyst and also the product oil from the pyrolysis of HIPS and ABS with the Y zeolite and the ZSM-5 zeolite respectively. The results were, on the whole, similar to those found in the CRT and Fridge plastics, the uncatalysed pyrolysis oils containing high concentrations of single ring aromatic compounds (Figure 4.4-2) which were mainly styrene, directly derived from the styrene-based high impact polystyrene and acrylonitrile-butadiene-styrene and the toluene and ethylbenzene. The addition of the Y zeolite and ZSM-5 catalysts produced increased concentrations of mainly benzene, and toluene, with ethylbenzene and styrene also present. Comparison of the results from the HIPS and ABS suggest, as expected that the CRT and Fridge plastics were mainly composed of HIPS and ABS plastics. However, the real-world WEEE waste plastics derived from the computer and television plastic casings (CRT) and the refrigerators and freezers would also contain other plastics.

The Y zeolite has different characteristics compared to the ZSM-5 zeolite, with the Y zeolite having a pore size of 7.8 Å and a Si/Al ratio of 5.4 and the zeolite ZSM-5 a pore size of 5.6 Å and Si/Al ratio of 40. The lower silica/alumina ratio of the Y zeolite at 5.4 results can increase the relative surface concentration of aluminium compared to the ZSM-5 zeolite with a much higher Si/Al ratio of 40. The consequence of high aluminium content for the Y-zeolite results in a higher surface acidity of the catalyst which in turn results in a higher catalytic activity [14, 15]. The catalytic active sites are producing increased conversion to aromatic products [16]. Zeolites are known as solid acid catalysts because they can have strongly acidic protons

uniformly distributed throughout the internal volume of the catalyst channels. The manipulation of the silica/alumina ratio influences both the number and strength of the acid sites. The Y zeolite also had a larger pore size of 7.8 Å, compared to the ZSM-5 zeolite catalyst at 5.6 Å, the pore size influencing the size of molecules that can enter the three dimensional zeolite structure and react with the active catalyst sites.

Pyrolysis has been suggested to be a promising processing path for the treatment of WEEE plastics but generates oil with a high content of bromine, derived from the brominated flame retardants added to the plastic [17-19]. Zeolite catalysts have been used to reduce the amount of bromine in the product pyrolysis oil [19, 20]. Thus, other researchers have investigated the influence of zeolite catalysts on the pyrolysis of waste plastics and their influence on the composition of the product oil. Aguado et al. [21] used a two-stage pyrolysis–catalysis reaction system to process low-density polyethylene with a zeolite HZSM-5 catalyst and reported a high conversion to alkene gases (73.5 wt.% at 450 °C). The liquid products (16.4 wt.%) contained a high proportion of aromatic and branched hydrocarbons in the gasoline range (C₅–C₁₂). Miskolczi et al. [22], investigated the catalytic pyrolysis of a mixture of polyethylene and polystyrene waste plastics in a batch reactor. The liquid products were reported to consist of a wide range of hydrocarbons (C₅–C₂₈), with polyethylene producing linear non-branched hydrocarbons and polystyrene producing aromatic compounds including ethylbenzene, styrene, toluene and benzene. Lee [23], also investigated the catalytic pyrolysis of a mixture of polyethylene and polystyrene in a stirred batch reactor using spent FCC (zeolite based fluid catalytic cracking (FCC) catalyst). The presence of

styrene and ethylbenzene in high concentrations was reported, and their concentrations were dependent on reaction time, and the relative composition of polyethylene and polystyrene. Lopez et al. [24], used a ZSM-5 zeolite catalyst (Si/Al ratio of 50) in the pyrolysis processing of mixed plastics (18.0wt.% polystyrene) and showed that the uncatalysed oil contained aliphatic compounds derived from the linear plastics and also aromatic compounds which were mainly toluene, ethylbenzene and styrene. The influence of the ZSM-5 catalyst was reported to reduce significantly the styrene concentration and increase the concentration of toluene, ethylbenzene and xylenes.

Ates et al. [16], investigated the batch reactor catalytic pyrolysis of the plastic fraction produced from municipal solid waste using a range of different catalysts. They reported that the Si-Al ratio influenced the production of aromatic compounds in the product oil, with zeolite ZSM-5 catalysts with a Si-Al ratio of 12.6 producing higher aromatic content product oils compared to a β -zeolite with a Si-Al ratio of 17.1. Lee [25], investigated the influence of different types of zeolite catalyst on the upgrading of pyrolysis oil/wax derived from the pyrolysis of the plastic fraction of the municipal solid waste. Comparison of a ZSM-5 zeolite catalyst (Si-Al ratio of 30) and a Y zeolite (Si-Al ratio of 80) showed that the ZSM-5 catalyst with the lower Si-Al ratio produced an oil with 78.9 wt% aromatic compared to the Y zeolite at 31.95 wt% aromatics. The raw oil/wax produced from the pyrolysis of the municipal solid waste plastics had negligible aromatic content. It should also be noted that the zeolite catalysts had different surface areas (ZSM-5 at $400 \text{ m}^2 \text{ g}^{-1}$ and Y zeolite at $780 \text{ m}^2 \text{ g}^{-1}$), and would have different pore structures in addition

to the differences in Si-Al ratio. Therefore, the results of Lee [25], suggest that surface acidity has more influence on the aromatic forming catalytic reactions of the pyrolysis degradation products than the catalyst surface area and wider pore size as found in the Y zeolite.

The main polymeric structure found in the high impact polystyrene, acrylonitrile-butadiene-styrene and WEEE plastics would be based on the polystyrene structure. The mechanism for the degradation of polystyrene in the presence of zeolite catalysts has been discussed by several authors [26-29]. Serrano et al. [29], suggest that the catalytic cracking of polystyrene may proceed through a complex combination of different reactions. Thermal pyrolysis is represented by random scission of the polystyrene polymer to produce polymer radicals. However, acid catalysis involves degradation of the polystyrene at Bronsted active sites to produce carbenium ions which undergo further scission and hydrogen transfer [29]. Cross-linking reactions of the polymer degradation products may also occur and also cracking, and hydrogenation of the thermally produced styrene may occur on the catalyst [30]. Antonakou et al. [26], undertook catalytic pyrolysis of waste plastics containing HIPS (compact disc waste) in the presence of a zeolite ZSM-5 catalyst. They reported that styrene concentration was reduced from 75.75 wt. % in the thermal pyrolysis oil to 64.82 wt. % for the catalytic pyrolysis, with an increase in benzene. They suggested that the thermal degradation of polystyrene started with random initiation to form polymer radicals. But in the presence of the catalysts degradation is extended in the form of cracking and hydrogenation reactions resulting in decreased styrene concentration. Lopez et al. [27], also suggested that the styrene produced from thermal pyrolysis

further degraded to other hydrocarbons via secondary reactions in the presence of the catalyst. Puente et al. [28], investigated the catalytic pyrolysis of polystyrene and polystyrene-polybutadiene using an FCC catalyst (fluid catalytic cracking catalyst from the petroleum refining industry). Miskolczi et al. [22], have described FCC catalyst as being mainly Y zeolite typified by a faujasite type crystal structure with open pores. The open pores are allowing larger molecules to enter the catalyst structure to increase reaction on the catalyst sites. The concentrations of styrene obtained by Puente et al. [28], in the presence of fresh FCC catalyst showed a marked reduction, decreasing from 75.59 wt% to 14.90 wt% for the catalytic pyrolysis of polystyrene, with increased formation of toluene, benzene and ethyl benzene. They also suggest the key degradation mechanism in the presence of a zeolite catalyst is via polymer thermal cracking, surface oligomerisation of styrene molecules and further cracking, in parallel to hydrogen transfer reactions. Audisio et al. [31], investigated the thermal degradation of polystyrene in the presence of several catalysts, including a Y zeolite. They reported that the main degradation products from the non-catalytic pyrolysis of catalytic pyrolysis of polystyrene with the Y zeolite were benzene, ethylbenzene, toluene, α -methyl styrene and indane. They proposed several reaction schemes to describe the thermal degradation of polystyrene to give the reaction products. For example, benzene was proposed to be formed via the catalytic addition of hydrogen to the aromatic ring producing polymeric ions which further react through one route to produce benzene and a polymer ion as a result of β -scission.

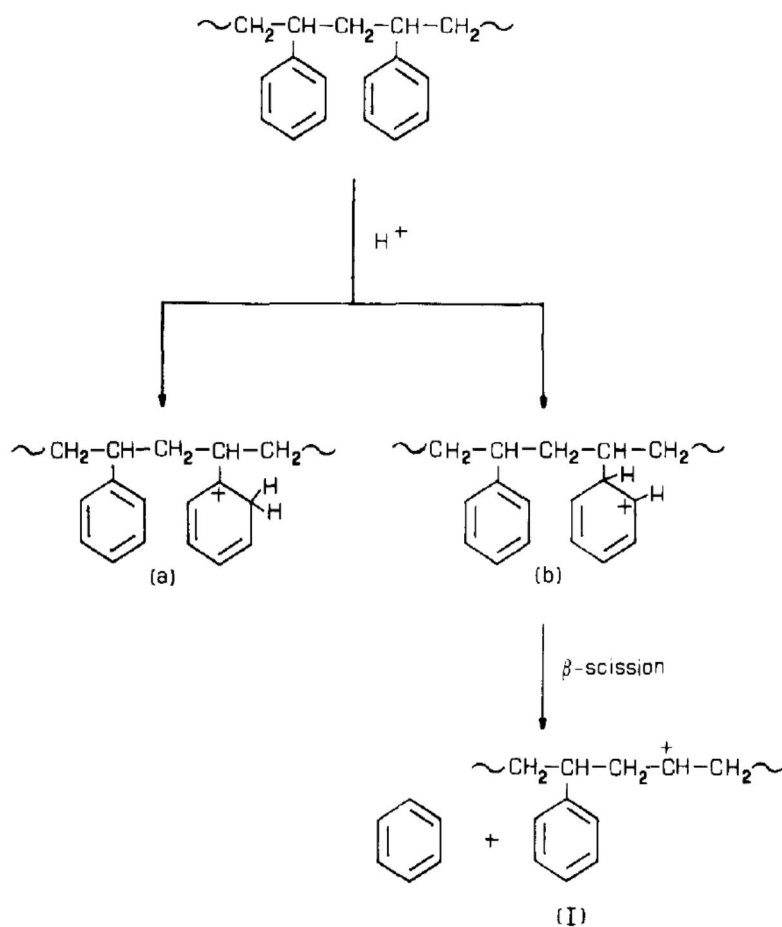


Figure 4.4-7 Catalytic addition of H on aromatic ring give rise to two ions (a) and (b); after β -scission of ion (b) benzene is produced and polymer ion (I)[31].

However, ions (a) from Figure 4.4-7 could undergo a β -scission to produce a polymer ion (II) with the charge on the last carbon atom and a cyclo-diene substituted polymer. Hence the polymer ion (II) could undergo an internal rearrangement by an H^- ion shift followed by β -scission to give α -methyl styrene or undergo β -scission to produce styrene as illustrated by Figure 4.4-8 [31].

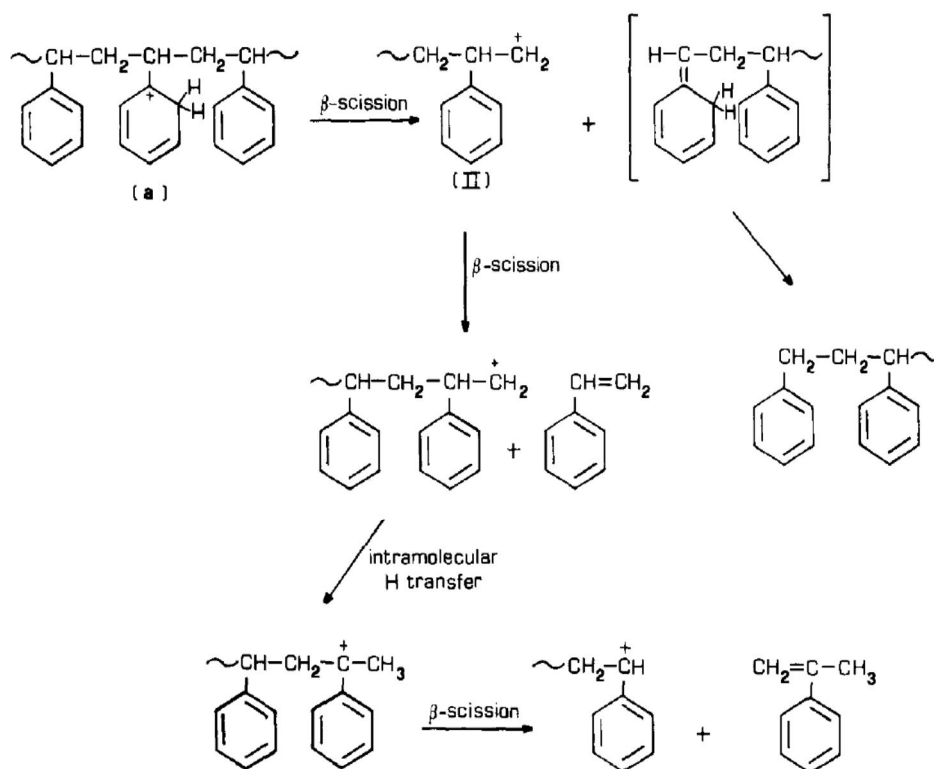


Figure 4.4-8 The ion (a) undergo β -scission or internal rearrangement by H^+ ion shift follows by β -scission to produced styrene or and α -methyl styrene respectively.[31].

Jung et al. [32], investigate the effect of Ca based additives on halogen removal from thermal degradation of ABS containing flame retardants using a fluidized bed reactor. They performed pyrolysis at a temperature range of 430 to 510 °C and, used bench scale reactor equipped with the char separation system. Oil yield markedly reduced to a range of 45 to 64 wt. % from about 77 wt. % as the additive was added. Similarly, the total bromine and chlorine content in the oil reduced to about 0.05 and 0.04 wt. % respectively as Ca (OH)₂ was added. They suggested that gaseous strong acidic halide (HBr and HCl) are captured by Ca(OH)₂ additive, this yielded calcium halide and water. Fast pyrolysis of a waste fraction of HIPS containing brominated flame retardant was performed by Jung et al. [33] in a fluidized bed reactor. They

used Ca-based additives on the removal of bromine at a pyrolysis temperature of 422 to 480 °C. The total bromine content in pyrolysis oil was decreased to 1.3 and 2.7 wt.%. This happens as $\text{Ca}(\text{OH})_2$ and oyster shell were added respectively from 5 wt.% in absent of additives.

In this work, the Y zeolite which has more catalytically active sites and the larger pore size results in the higher conversion of the pyrolysis volatile material to other products compared to the ZSM-5 catalyst. In particular, the larger pore size of the Y zeolite allows the larger molecular size pyrolysis products derived from the polystyrene polymer, including larger polymer fragments and styrene to enter the pores of the catalyst to react at the catalyst sites to reduce styrene concentration. In addition, because of the lower Si-Al ratio of the Y zeolite equating to increased surface aluminium concentration and higher surface acidity of the catalyst which in turn results in a higher catalytic activity higher levels of styrene degradation were found compared to the ZSM-5 zeolite catalyst.

4.5 Summary

The research reported here shows that pyrolysis of plastics produced from commercial waste electrical and electronic equipment produces a mainly oil product containing mostly styrene. The influence of the addition of a zeolite catalyst to the process was mainly dependent on the Si-Al characteristics of the zeolite catalyst used. Zeolite catalyst with a lower Si-Al ratio (Y zeolite) produced a higher conversion of the styrene to other aromatic products, particularly benzene and toluene. Comparison of the catalytic pyrolysis of high impact polystyrene (HIPS) and acrylonitrile-butadiene-styrene (ABS) with

the WEEE plastics results suggests that the WEEE plastics consisted of mostly, but not exclusively HIPS and ABS plastics.

References

1. Zhang, P., Song, L., Lu, H., Wang, J. and Hu, Y., *The influence of expanded graphite on thermal properties for paraffin/high density polyethylene/chlorinated paraffin/antimony trioxide as a flame retardant phase change material*. Energy Conversion and Management, 2010. **51**(12): p. 2733-2737.
2. Gale, P.J., *Mass spectrometric studies of the reactivity of antimony trioxide with halogenated flame retardants in the pyrolysis of plastics*. International Journal of Mass Spectrometry and Ion Processes, 1990. **100**: p. 313-322.
3. Aguado, J., D. Serrano, and J. Escola, *Catalytic Upgrading of Plastic Wastes*. Feedstock Recycling and Pyrolysis of Waste Plastics: Converting Waste Plastics into Diesel and Other Fuels, 2006: p. 73-110.
4. Aguado, J., Serrano, D.P., Miguel, G.S., Escola, J.M. and Rodriguez, J.M., *Catalytic activity of zeolitic and mesostructured catalysts in the cracking of pure and waste polyolefins*. Journal of analytical and applied pyrolysis, 2007. **78**(1): p. 153-161.
5. Liu, Y., Qian, J. and Wang, J. *Pyrolysis of polystyrene waste in a fluidized-bed reactor to obtain styrene monomer and gasoline fraction*. Fuel Processing Technology, 2000. **63**(1): p. 45-55.
6. Brebu, M., Uddin.M.A., Muto, A., Sakata, Y. and Vasile, C., *The role of temperature program and catalytic system on the quality of acrylonitrile-butadiene-styrene degradation oil*. Journal of analytical and applied pyrolysis, 2002. **63**(1): p. 43-57.
7. Bhaskar, T., Murai, K., Matsu, T., Brebu, M.A., Uddin, M.A., Muto, A., Sakata, Y. and Murata, K., *Studies on thermal degradation of acrylonitrile-butadiene-styrene copolymer (ABS-Br) containing brominated flame retardant*. Journal of analytical and applied pyrolysis, 2003. **70**(2): p. 369-381.
8. Marczewski, M., Kaminskwa, E., Marczewska, H., Godek, M., Rokicki, G. and Sokolowski, J., *Catalytic decomposition of polystyrene. The role of acid and basic active centers*. Applied Catalysis B: Environmental, 2013. **129**: p. 236-246.
9. Karmore, V. and G. Madras, *Thermal degradation of polystyrene by Lewis acids in solution*. Industrial & engineering chemistry research, 2002. **41**(4): p. 657-660.

10. Lin, R. and White, R. L. *Acid-catalyzed cracking of polystyrene*. Journal of applied polymer science, 1997. **63**(10): p. 1287-1298.
11. Lin, R. and R. White, *Catalytic cracking of polystyrene*. Preprints of Papers, American Chemical Society, Division of Fuel Chemistry, 1996. **41**(CONF-960807--).
12. Rahman, F., Langford, K.H., Scrimshaw, M.D. and Lester, J.N., *Polybrominated diphenyl ether (PBDE) flame retardants*. Science of the Total Environment, 2001. **275**(1): p. 1-17.
13. Cunliffe, A.M. and Williams, P.T. *Pyrolysis of flame retardant brominated polyester composites*. Environmental Technology, 2004. **25**(12): p. 1349-1356.
14. Campbell, I.M., *Catalysis at surfaces*1988: Springer Science & Business Media.
15. Venuto, P.B. and E.T. Habib Jr, *Fluid catalytic cracking with zeolite catalysts*.MARCEL DEKKER, INC. New York 1979.
16. Ateş, F., Miskolczi, N, and Borsodi, N. *Comparision of real waste (MSW and MPW) pyrolysis in batch reactor over different catalysts. Part I: Product yields, gas and pyrolysis oil properties*. Bioresource technology, 2013. **133**: p. 443-454.
17. Hall, W.J. and Williams, P.T., *Fast pyrolysis of halogenated plastics recovered from waste computers*. Energy & Fuels, 2006. **20**(4).
18. Hall, W.J. and Williams, P.T., *Analysis of products from the pyrolysis of plastics recovered from the commercial scale recycling of waste electrical and electronic equipment*. Journal of analytical and applied pyrolysis, 2007. **79**(1): p. 375-386.
19. Hall, W.J. and Williams, P.T., *Removal of organobromine compounds from the pyrolysis oils of flame retarded plastics using zeolite catalysts*. Journal of analytical and applied pyrolysis, 2008. **81**(2): p. 139-147.
20. Mitan, N.M., Brebu, M., Bhaskar, T., Muto, A. and Sakata, Y., *Individual and simultaneous degradation of brominated high impact polystyrene and brominated acrylonitrile-butadiene-styrene and removal of heteroelements (Br, N, and O) from degradation oil by multiphase catalytic systems*. Journal of Material Cycles and Waste Management, 2007. **9**(1): p. 56-61.
21. Aguado, J., Serrano, D.P., San Miguel, G., Castro, M.C. and Madrid, S., *Feedstock recycling of polyethylene in a two-step thermo-catalytic reaction system*. Journal of analytical and applied pyrolysis, 2007. **79**(1): p. 415-423.

22. Miskolczi, N., Bartha, L. and Deák, G., *Thermal degradation of polyethylene and polystyrene from the packaging industry over different catalysts into fuel-like feedstocks*. *Polymer Degradation and Stability*, 2006. **91**(3): p. 517-526.
23. Lee, K.-H., *Composition of aromatic products in the catalytic degradation of the mixture of waste polystyrene and high-density polyethylene using spent FCC catalyst*. *Polymer Degradation and Stability*, 2008. **93**(7): p. 1284-1289.
24. López, A., De Marco, I., Cabellero, B.M., Laresgoiti, M.F., Adrados, A. and Aranzabai, A., *Catalytic pyrolysis of plastic wastes with two different types of catalysts: ZSM-5 zeolite and Red Mud*. *Applied Catalysis B: Environmental*, 2011. **104**(3): p. 211-219.
25. Lee, K.-H., *Effects of the types of zeolites on catalytic upgrading of pyrolysis wax oil*. *Journal of Analytical and Applied Pyrolysis*, 2012. **94**.
26. Antonakou, E., Kalogiannis, K.G., Stephanidis, S.D., Triantafyllidis, K.S., Lappas, A.A. and Achilias, D.S., *Pyrolysis and catalytic pyrolysis as a recycling method of waste CDs originating from polycarbonate and HIPS*. *Waste Management*, 2014. **34**(12): p. 2487-2493.
27. Lopez, A., de Marco, I., Cabellero, B.M., Adrados, A. and Laresgoiti, M.F., *Deactivation and regeneration of ZSM-5 zeolite in catalytic pyrolysis of plastic wastes*. *Waste management*, 2011. **31**(8): p. 1852-1858.
28. de la Puente, G., Arandes, J.M. and Sedran, U.A. *Recycled plastics in FCC feedstocks: specific contributions*. *Industrial & engineering chemistry research*, 1997. **36**(11): p. 4530-4534.
29. Serrano, D., Aguado, J. and Escola, J. *Catalytic conversion of polystyrene over HMCM-41, HZSM-5 and amorphous SiO₂-Al₂O₃: comparison with thermal cracking*. *Applied Catalysis B: Environmental*, 2000. **25**(2): p. 181-189.
30. Lee, S., Yoon, J.H., Kim, J.R. and Park, D.W., *Catalytic degradation of polystyrene over natural clinoptilolite zeolite*. *Polymer degradation and stability*, 2001. **74**(2): p. 297-305.
31. Audisio, G., Bertini, F., Beltrame, P.L. and Carniti, P., *Catalytic degradation of polymers: Part III—Degradation of polystyrene*. *Polymer Degradation and Stability*, 1990. **29**(2): p. 191-200.
32. Jung, S.-H., Kim, S.-J. and Kim, J.-S. *Thermal degradation of acrylonitrile–butadiene–styrene (ABS) containing flame retardants using a fluidized bed reactor: The effects of Ca-based additives on halogen removal*. *Fuel Processing Technology*, 2012. **96**: p. 265-270.

33. Jung, S.-H., Kim, S.-J. and Kim, J.-S. *Fast pyrolysis of a waste fraction of high impact polystyrene (HIPS) containing brominated flame retardants in a fluidized bed reactor: The effects of various Ca-based additives (CaO, Ca(OH)₂ and oyster shells) on the removal of bromine.* Fuel, 2012. **95**(1).

Chapter 5 : INFLUENCE OF ZEOLITE CATALYST CHARACTERISTICS ON THE CATALYTIC PYROLYSIS OF WASTE HIGH-DENSITY POLYETHYLENE

5.1 Introduction

The addition of catalysts to the pyrolysis of waste plastics can play a critical role in the thermochemical process in terms of promoting targeted reactions, reducing reaction temperature and improving the whole process efficiency [1]. Consequently, most research has centered on the use of zeolite catalysts such as HZSM-5, MCM, NH₄Y and NaY since these are often used in petroleum refineries for upgrading crude oil [2, 3] [4]. Keane [5] has suggested that the shape selectivity micropore-size properties and surface acidity of zeolite catalysts can be manipulated to produce narrow ranges of hydrocarbons. While there are many studies on the use of zeolite catalysts for pyrolysis-catalysis processing of waste plastics, there are few about the relation of the physical properties of the catalyst to the yield and composition of the product oils and gases. Zeolite catalysts are crystalline, alumina-silicates with an open cage/framework structure consisting of AlO₄ and SiO₄ tetrahedral crystal structure with a defined pore size with a defined microporous structure. Due to the poor resolution of propane and propene using GC analysis, the results has been presented at a sum of the two, C₃ hydrocarbon gases. However, a detailed analysis of the proportion of C₂ and C₄ hydrocarbon indicate that propane would be the major product. The Y-type zeolite (faujasite) consists of a cage-like structure with pores comprised of 12-membered rings with a pore diameter of ~7.4 Å and, the ZSM-5 zeolite

structure consists of 5 membered rings with a pore diameter of $\sim 5.4 \text{ \AA}$. The properties of the zeolite catalysts can be varied in terms of their surface area and silica: alumina ratio which may in turn influence the range of products formed during the catalytic pyrolysis of waste plastics. The silica: alumina ratio is known to influence the surface acidity of the zeolites with low Si: Al ratios producing higher surface acidity compared to higher Si: Al ratios[6].

In this chapter, the use of five different Y type zeolite catalysts and three different ZSM-5 zeolite catalysts for the two-stage pyrolysis-catalysis of waste high-density polyethylene has been investigated. The work focused on the influence of the zeolite catalysts on the yield and composition of the product oils and gases. In particular, emphases were made about the aromatic composition of the product oils.

The plastic sample used in this study was waste high-density polyethylene (HDPE) has been earlier described in chapter 3. Five of the catalysts were of the zeolite Y type, and three were of the ZSM-5 type. Table 5.1-1 show the characteristic of the zeolite catalysts. The three Y zeolites catalysts had different surface areas, but with similar silica: alumina ratios at $\sim 5.2:1$. whereas, the two other Y catalysts had a different silica: alumina ratios. The three ZSM-5 zeolite catalysts had similar surface areas, between 450 and 467 $\text{m}^2 \text{ g}^{-1}$, but with different Si: Al ratios of 23:1, 50:1 and 80:1.

Table 5.1-1 Characteristics of zeolite catalysts used

Catalyst properties	Z-1	Z-2	Z-3	Z-4	Z-5	Z-6	Z-7	Z-8
Zeolite Structure	Y-Zeolite	Y-Zeolite	Y-Zeolite	ZSM-5	ZSM-5	ZSM-5	Y-Zeolite	Y-Zeolite
Surface area (m ² g ⁻¹)	705	853	935	450	452	467	937	888
Silica: Alumina ratio	5.1:1	5.1:1	5.2:1	23:1	50:1	80:1	30:1	80:1

The plastic samples (2 g) were pyrolyzed in the fixed bed two-stage batch reactor described in Chapter 3. The plastic sample was heated from ambient temperature to 500 °C at a heating rate of 10 °C min⁻¹. The zeolite catalyst was maintained at a bed temperature of 500 °C. The catalyst (2 g) was mixed with 2 g of 2 mm sized quartz sand and was supported on quartz wool in the second stage reactor. For comparison, where no catalyst was used, quartz sand (4 g) was substituted for the catalyst. In this chapter, the zeolite catalysts are designated as Z-1, Z-2, Z-3, Z-4, Z-5, Z6, Z-7 and .Z-8.

Table 5.1-2 Product yield and gas composition from the pyrolysis-catalysis of waste HDPE with different zeolite catalysts

Product	HDPE	Z-1 (Y-Zeolite)	Z-2 (Y-Zeolite)	Z-3 (Y-Zeolite)	Z-4 (ZSM-5)	Z-5 (ZSM-5)	Z-6 (ZSM-5)	Z-7 (Y-Zeolite)	Z-8 (Y-Zeolite)
Oil (wt. %)	75.0	59.5	59.0	45.4	44.0	50.0	53.5	63.00	63.00
Gas (wt. %)	25.5	38.3	43.9	50.9	49.8	49.7	47.0	37.97	40.83
Char wt. (%)	-	-	-	-	-	-	-	-	-
MB (wt. %)	100.5	97.8	102.9	96.3	93.8	99.7	100.5	100.9	103.8

- Negligible

5.2 Influence of Zeolite Y characteristics on the catalytic degradation of HDPE wastes

The work examines the influence of both surface area and the silica-alumina ratio of Y zeolite in the catalytic degradation of the waste HDPE. Thus, the influence of the zeolite Y catalyst's surface area was discussed separately in section 5.3.1.1 and influence of silica: alumina ratio was discussed in 5.3.1.1. The zeolite Y catalyst surface area was considered here to study its influence on the products yield and composition.

5.2.1 Influence of zeolite Y catalysts surface area on the catalytic degradation of waste HDPE

5.2.1.1 Product Yields

Table 5.1-2 shows the product yield and gas compositions from the pyrolysis-catalysis of the waste high-density polyethylene with the different types of the zeolite catalyst. For the uncatalysed pyrolysis (with sand in the second reactor), the yield of oil was 75.0 wt. % and 25.5 wt. % gas and with negligible char. In the presence of all of the zeolite catalysts, there was a marked reduction in oil yield and a consequent increase in gas yield. The main gases which were increased by the addition of the zeolite catalyst were the C₂-C₄ hydrocarbons, produced by cracking of the HDPE pyrolysis gases. The Y zeolite catalysts exhibited a decreasing oil yield and increasing gas yield in relation to the increasing surface area of these catalysts with an increase in surface area from 705 m² g⁻¹ to 853 m² g⁻¹ and to 935 m² g⁻¹. But for Si: Al ratio variation in Y zeolite catalysts, only gases show a rise in yield with an

increase in the ratio as similar oil yield were obtained for both catalysts. For the ZSM-5 zeolite catalysts, which had a similar surface area ($\sim 450\text{-}467\text{ m}^2\text{ g}^{-1}$) the oil yield showed an increase and gas yield a decrease, the catalyst with the lowest Si:Al ratio (Z-4) exhibiting the lowest oil yield.

The main gases produced were hydrogen, methane and $\text{C}_2 - \text{C}_4$ hydrocarbons. The production of hydrocarbons is known to result from scission of the polymer chain of the HDPE [7]. The Y zeolite catalysts showed an increase in C_3 and C_4 hydrocarbons as the surface area of the Y zeolite catalyst increased. For the ZSM-5 catalysts with similar surface area but increasing Si: Al ratio, the methane, C_2 and C_3 hydrocarbon gases showed a decrease in yield as the Si: Al ratio was increased, but for the C_4 hydrocarbons there was an increase. However, a similar trend was observed for Y zeolite with different Si: Al ratio, the rise in C_4 hydrocarbon and decrease in methane, C_2 , and C_3 Hydrocarbon.

5.2.1.2 Gas composition

Table 5.2-1 Gas composition from Y zeolite with varying surface area

Gas components	No catalyst	Z-1	Z-2	Z-3
H ₂ (vol. %)	11.7	9.98	11.0	13.1
CH ₄ (vol. %)	11.2	13.5	11.2	10.2
C ₂ H ₄ (vol. %)	14.7	10.1	6.90	8.00
C ₂ H ₆ (vol. %)	9.61	6.35	5.35	4.94
C ₃ H ₆ + C ₃ H ₈ (vol. %)	31.9	39.9	37.7	34.2
C ₄ H ₈ (vol. %)	18.9	17.9	20.3	22.2
C ₄ H ₁₀ (vol. %)	2.09	2.30	7.60	7.40
C ₂ -C ₄ (vol. %)	77.2	76.5	77.8	76.8
CV(MJ/m ³)	74.3	76.6	80.4	79.3

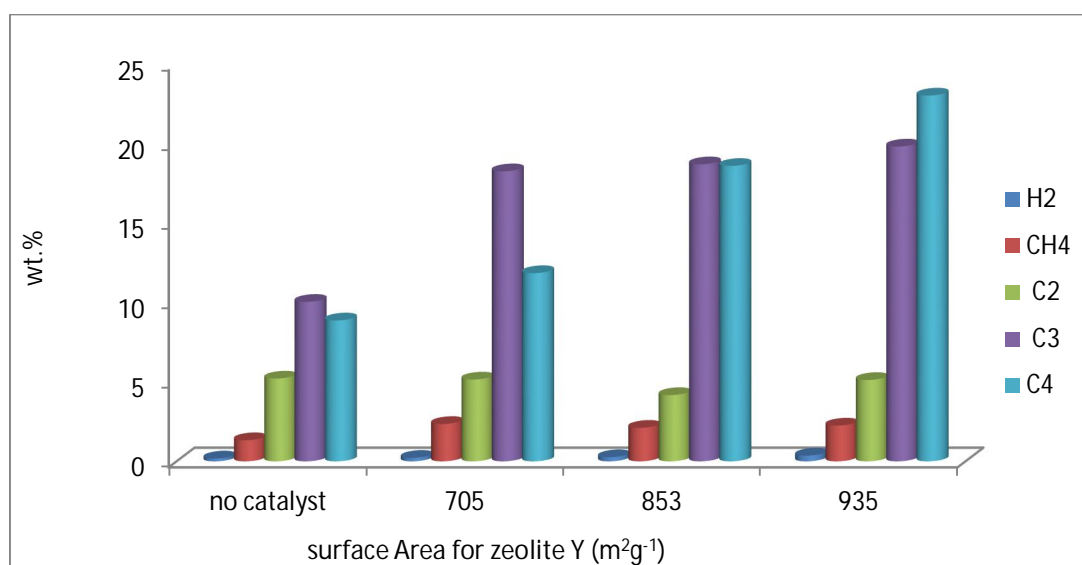


Figure 5.2-1 Gases produced from non-catalytic and catalytic pyrolysis of HDPE waste with Y zeolite with varying surface area

Figure 5.2-1 shows the gas yield for pyrolysis of waste HDPE in the presences of three zeolite Y catalysts with different surface area Z1 (705 m²g⁻¹), Z2 (853 m²g⁻¹) and Z3 (935 m²g⁻¹). The gas yield increases with the increases in the

surface area, and the gas composition gives the same trend with the three Y catalysts. The increase in the gas yield with the introduction of catalysts was reported by other authors [1 2 8-10]). Tables 5.3-1 shows the gas composition in volume % while Figure 6.3-1 gives gas composition in wt.%. The hydrogen gas, methane and C₂ hydrocarbons show a less significant rise from non-catalysed pyrolysis run as the catalysts are introduced. However, the C₃ and C₄ hydrocarbons gases are the main gases produced and increased with increase in surface area of the catalysts. The total gross heating value refer here as calorific value (CV) computed in MJ/m³ in Table 5.2-1 shows an increase with the addition of the catalyst. Likewise, the calorific values of the product gas increased with the surface area for 705 m² g⁻¹ and 853 m² g⁻¹, but it stabilized at the same value for higher surface area 935 m² g⁻¹. The trend in CV is a reflection of the composition of high calorific value gases as observed in both tables above indicating increase in the higher molecular weight hydrocarbon gases. The high-value caloric value is desirable for high valued fuel gases.

5.2.1.3 Oil composition

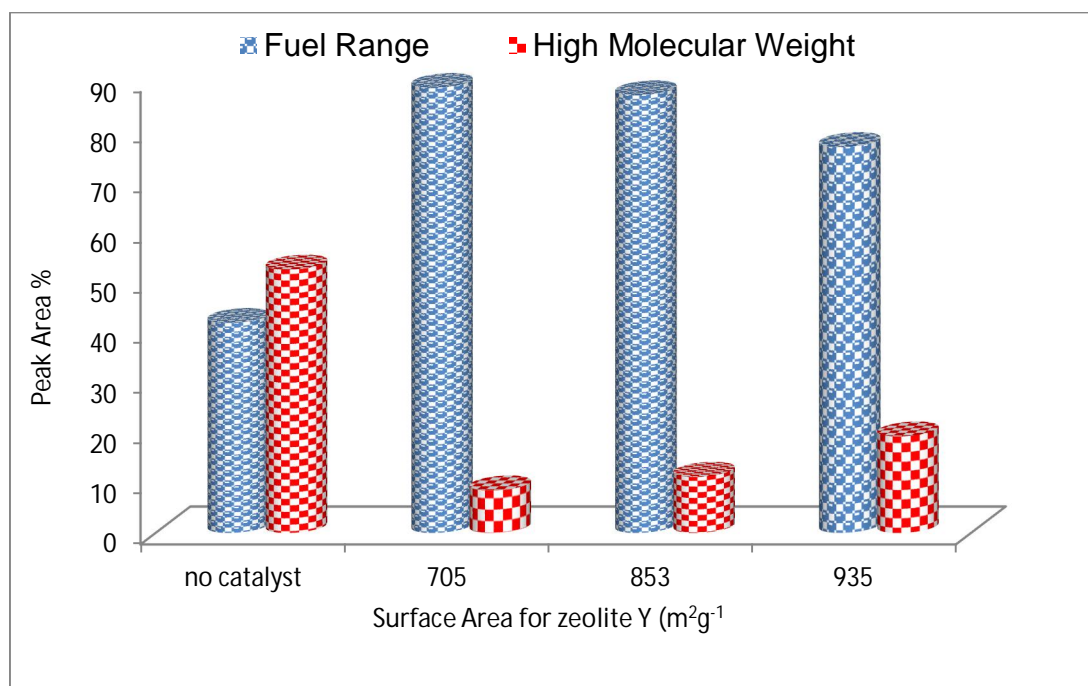


Figure 5.2-2 Fuel range (C₅ – C₁₅) and high molecular weight (C₁₆₊) hydrocarbons from the pyrolysis-catalysis of HDPE in relation to surface areas of Y-zeolite catalysts

Figure 5.2-2 shows the fuel range hydrocarbons in the product oil. The fuel range hydrocarbons defined as C₅-C₁₅ hydrocarbons and the high molecular weight, i.e. as C₁₆₊ hydrocarbons. In the absence of any catalyst (where sand was used as a blank), there was ~55wt% of the condensed oil of high molecular weight hydrocarbons. However, when the zeolite catalysts were introduced, there was a marked decrease in C₁₆₊ higher molecular weight hydrocarbons and a corresponding marked increase in the C₅-C₁₅ hydrocarbons. In some experimental run, the C₅-C₁₅ hydrocarbons reached more than 90.0 wt% of the product oil. Hence, that showed that the two-stage

pyrolysis-zeolite catalysis of waste plastic was effective in producing a useful product oil, similar to that produced from petroleum refining.

Examination of Figure 5.2-2 shows that for the zeolite Y with increasing surface area (705, 853 and 935 $\text{m}^2 \text{g}^{-1}$) there was less conversion to the lower molecular weight fuel range hydrocarbons. The higher surface area (Z-3) zeolite catalyst at 935 $\text{m}^2 \text{g}^{-1}$ showing the lowest conversion to fuel range hydrocarbons.

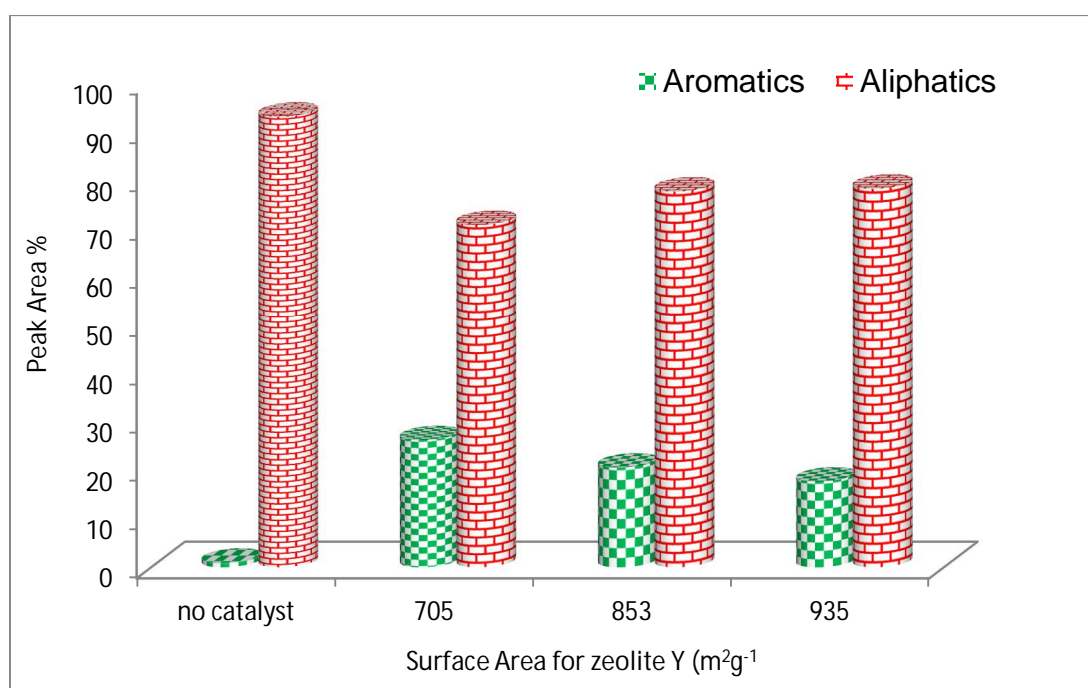


Figure 5.2-3 Aliphatic and aromatic content of the product oil from the pyrolysis-catalysis of HDPE in relation to surface areas of Y-zeolite catalysts

Figure 5.2-3 shows the aliphatic and aromatic content of the product oil from the pyrolysis-catalysis of waste high-density polyethylene in the presence of the various Y-zeolite catalysts with varying surface area. The uncatalyzed pyrolysis of high-density polyethylene produced a mainly aliphatic oil consisting of alkanes, alkenes and alkadienes, with only a low proportion of

aromatic compounds as has been reported by others [11]. For the Y-zeolite catalysts, there was a decrease in aromatic content with an increase in surface area of the catalyst.

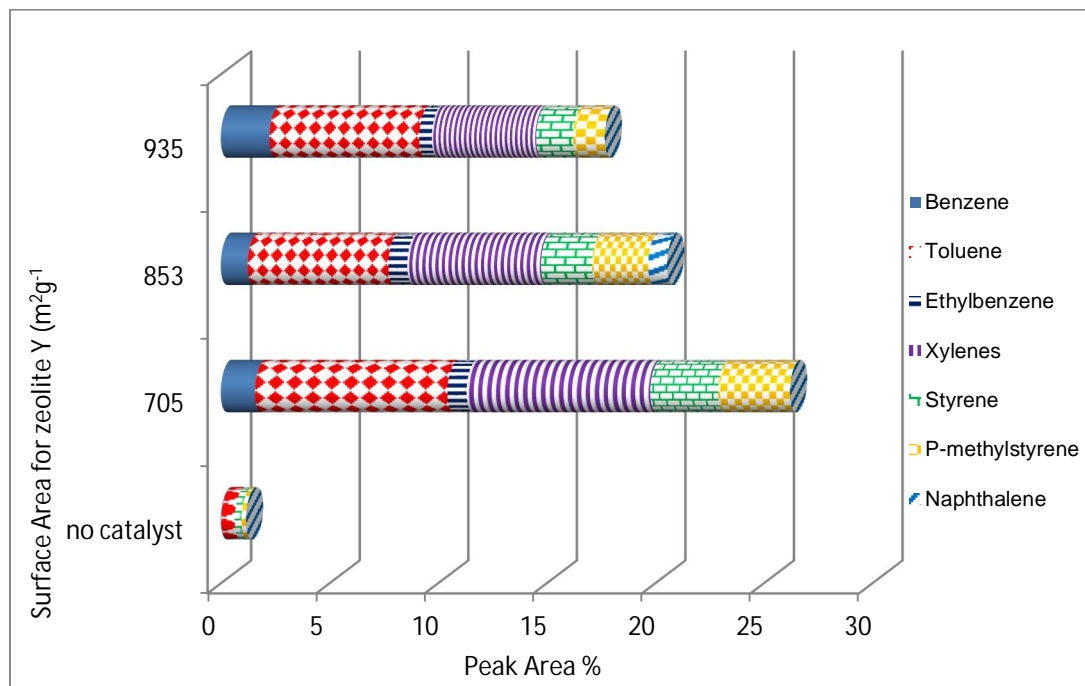


Figure 5.2-4 Yields of selected aromatic compounds in the oils produced from the pyrolysis-catalysis of HDPE in relation to surface areas of Y-zeolite catalysts

Figure 5.2-4 shows the yields of selected aromatic compounds in the oils produced by the pyrolysis and pyrolysis-catalysis of waste high-density polyethylene with different zeolite catalysts. In the absence of a catalyst, there were only low concentrations of aromatic compounds as also shown in Figure 5.2-3. However, when the zeolite catalysts were introduced to the pyrolysis-catalysis reactor system, the concentration of single ring and two-ring aromatic hydrocarbons increased markedly. The aromatic content decreases with the rise in the surface area of the Y zeolite catalyst. Kumar et al. [7], have reviewed the pyrolysis and catalytic pyrolysis of high-density polyethylene.

They reported that the catalytic pyrolysis of polyethylene polymer chain is rapidly depolymerised by the reaction on acid sites on the catalyst reducing the high molecular weight of the polymer to produce a high fraction of low molecular weight hydrocarbons. They suggest that the catalytic reaction process involves a range of reactions, including rearrangement, hydrogenation, dehydrogenation, cyclisation which results in the formation of aromatic compounds, increased C₅-C₁₀ hydrocarbons and increased C₃ and C₄ hydrocarbons in the gas phase as was found in this work. In addition to the surface acidity, the physical properties of the zeolite catalyst such as surface area, pore size, pore volume, pore size distribution and pore structure are all important factors in determining the catalytic activity of the zeolite catalyst [7]. The defined pore size of zeolite catalyst allows hydrocarbons of different molecular size to enter the channels and pores of the catalyst and selectively react with the active sites of the catalyst. However, it has been noted that the large molecular size molecules produced from the pyrolysis of waste plastics have limited diffusion into the pores of zeolite catalyst [7].

Serrano et al. [1], have reviewed the catalytic pyrolysis of polyalkene plastics to fuels and chemicals and have suggested that the reaction mechanism for thermal pyrolysis is very different from that of catalytic pyrolysis. Thermal cracking of polyalkenes such as high-density polyethylene involves random polymer chain scission through initiation, propagation and termination leading to the formation of a range of alkanes, alkenes and alkadienes of molecular weights from C₁ – C₆₀ [1]. The formation of aromatic compounds is, therefore low. However, in the presence of a catalyst, carbenium and carbonium ions are produced on the acid sites of the catalyst followed by isomerization,

oligomerization, cyclization, aromatization and cracking. Catalytic cracking reactions, therefore, lead to increased formation of branched, cyclic and aromatic hydrocarbons. Figure 5.2-5 [1] illustrates the range of reaction pathways for the catalytic pyrolysis of polyalkenes.

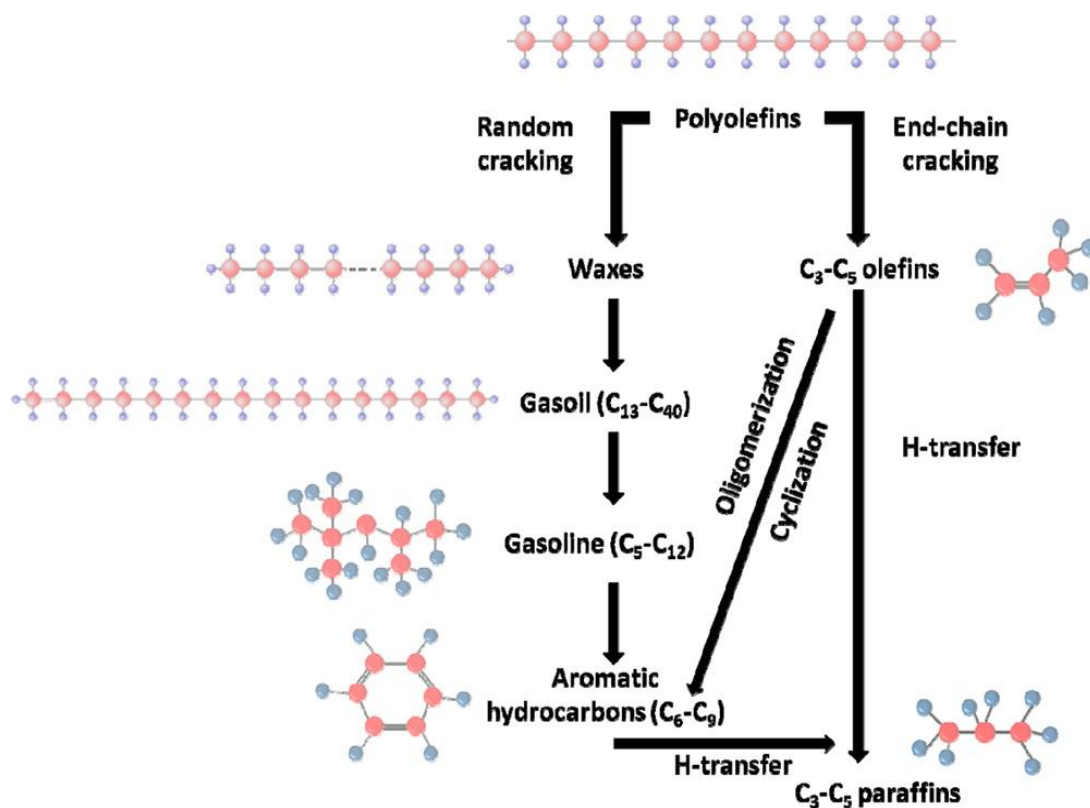


Figure 5.2-5 Reaction pathways for the catalytic cracking of waste plastics [1]
The product oils were analysed for their boiling point range distribution using gas chromatography which enables the simulated distillation of the oils to be determined (ASTM D2887).

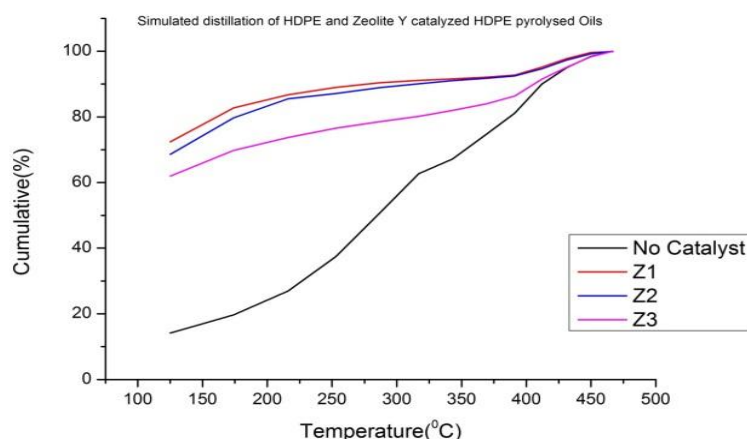


Figure 5.2-6 Simulated distillation of pyrolysis oils from the pyrolysis-catalysis of HDPE in relation to surface areas of Y-zeolite catalysts.

Figure 5.2-6 shows the simulated distillation curves for the product oils from pyrolysis-catalysis of HDPE in the presence of the Y zeolite with varying surface area. The non-catalytic oil product showed that a significant part (greater than 50%) of the oils have a boiling range of greater than 317 °C and only 14% below 150 °C. However, the catalytic degradation product oils show a shift to lower boiling points, reflecting the shift in molecular weight range as seen in Figure 5.3-2. Muhammad et al. [12], noted that boiling range distribution for gasoline would be >95% below 150 °C. Nevertheless, for the catalytic product oils, the boiling point range fraction below 150 °C was between 62.0% and 73.0%. The Y zeolite catalysts used for the catalytic pyrolysis of waste HDPE, show a major improvement in the distillation range of the product oils suggesting a boiling point range similar to petroleum-derived kerosene or diesel fuel.

5.2.1.4 Summary

The influence of surface area of the three Y zeolites investigated show reduction in the low molecular weight hydrocarbons with an increase in the surface area. The high-value fuel hydrocarbon gases improved with the addition of the catalyst and was further enhanced with an increase in surface area. Likewise, aromatic compounds obtained in the pyrolyzed oil show a similar trend, i.e. decrease in aromatic content and single ring aromatic compounds with the increase in the surface area.

5.2.2 Influence of silica: alumina ratio of the Y zeolite on catalytic degradation of waste HDPE

In this section influence of the silica: alumina ratio of the Y zeolite catalyst was considered. The product yields results, and its discussion was shown in the prior section 5.1. Thus, in this section influence of the silica; alumina ration on the following; gas composition, the distribution of fuel range and high molecular weight compounds; aliphatic and aromatic compounds distribution; distribution of selected aromatic compounds and simulated distillation properties are presented and discussed

5.2.2.1 Gas Composition

Table 5.2-2 Gas composition from HDPE pyrolysis using Y zeolite catalysts with varying Si: Al ratio area

	No catalyst	Z-1	Z-7	Z-8
H ₂ (vol. %)	11.7	9.98	8.29	6.57
CH ₄ (vol. %)	11.2	13.5	4.43	3.50
C ₂ H ₄ (vol. %)	14.7	10.1	20.7	21.4
C ₂ H ₆ (vol. %)	9.61	6.35	4.50	3.31
C ₃ H ₆ + C ₃ H ₈ (vol. %)	31.9	39.9	45.4	45.7
C ₄ H ₈ (vol. %)	18.85	17.9	11.5	15.9
C ₄ H ₁₀ (vol. %)	2.09	2.30	5.10	3.73
C ₂ -C ₄ (vol. %)	77.2	76.5	87.2	89.9
CV (MJNm ⁻³)	74.3	76.6	76.1	89.9

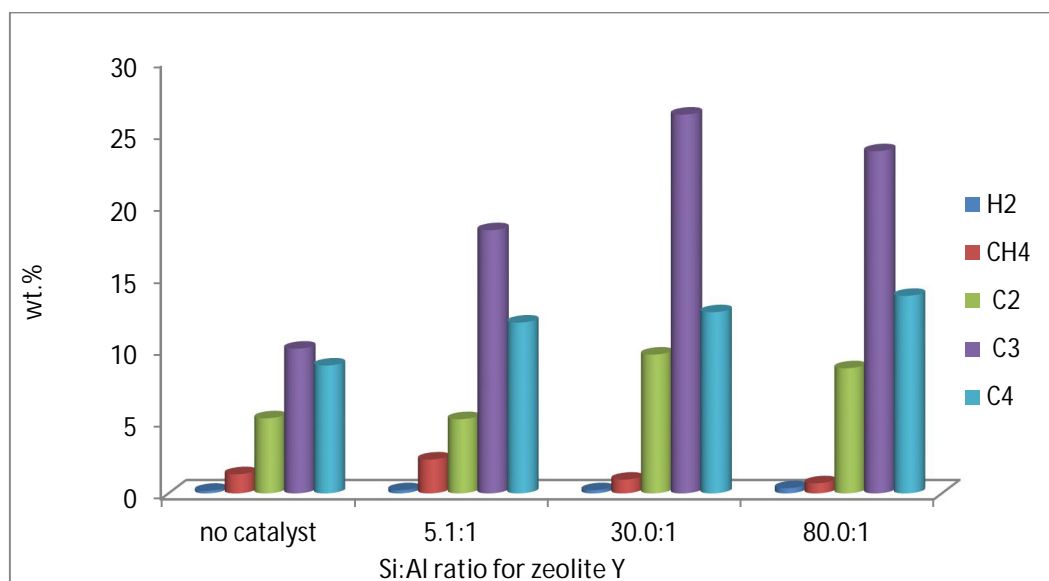


Figure 5.2-7 Gases produced from non-catalytic and catalytic pyrolysis of HDPE with Y zeolite with varying Si: Al ratio

Tables 5.2-3 shows the gas yield for pyrolysis of waste HDPE in the presences of three zeolite Y catalysts with different silica: alumina ratio. The gas yield increases with the addition of the catalysts for the pyrolysis of HDPE waste. The initial gas showed an increase for low silica-alumina ratio Z-1 (38.3 wt.%), but eventually remained fairly stable at the higher ratio Z-7 (37.9 wt.%) and Z-8 (40.8 wt.%). The low Si: Al is an indicator for high catalytic activity as reported [13-15]. Tables 6.3-2 shows the gas composition in volume % while Figure 5.2-7 gives gas composition in wt. %. The gas composition shows a trend with a lower molecular mass hydrocarbons increase with low in Si: Al ratio, with the corresponding reduction in C₃ and C₄ hydrocarbons. Thus, the lower hydrocarbon gases composition rose with the corresponding reduction in Si: Al ratio, the rise perhaps might be due to increase in catalyst activities with Si: Al [10 13 14]. But dwindling increases of C₃ and C₄ hydrocarbons was observed for high Si: Al ratio. The high surface area of the two catalysts (937 m² g⁻¹ and 888 m² g⁻¹) might have contributed to the catalytic degradation of the polymer observed. Likewise, a total gross heating value referred here as caloric value (CV) is shown in Table 5.2-3. The calorific values rose with the addition of the catalyst and improved with increasing silica-alumina ratio. The calorific values show a similar trend as the composition of the gases as observed in both Table 5.2-3 and Figure 5.2-7 above. The productions of high-value calorific value gases are desirable from waste plastics and add value to product yield.

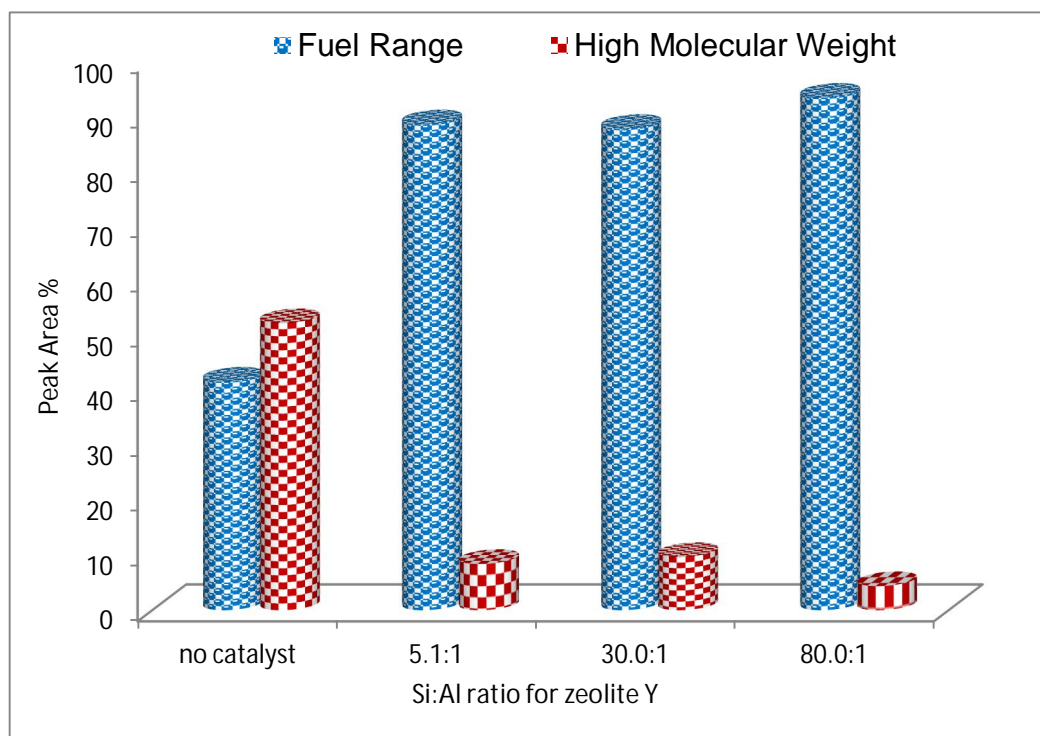


Figure 5.2-8 Fuel range (C₅ – C₁₅) and high molecular weight (C₁₆₊) hydrocarbons from HDPE in relation to Si:Al ratio of zeolite Y catalysts

Figure 5.2-8 shows the fuel range (C₅-C₁₅) hydrocarbons in the product oil from non-catalytic and Y zeolite with varying Si: Al ratio catalyzed pyrolysis run. Likewise, the high molecular weight (i.e. C₁₆₊ hydrocarbons) are presented in the figure. Thus, for a non-catalytic run as shown in section 5.3.1.1, also there was ~55.0wt% of the condensed oil of high molecular weight hydrocarbons. Nevertheless, a marked decrease in C₁₆₊ higher molecular weight hydrocarbons was observed when the Y zeolite catalysts were introduced. Thus, as obtained in the previous section, there was a consistent rise in the C₅-C₁₅ hydrocarbons with catalyst addition. However, for zeolite Y with 80:1 Si: Al (Z-8), the C₅-C₁₅ hydrocarbons reached 90.0wt% of the product oil. The higher Si: Al ratio shows a lower concentration of

aluminium in the catalyst. But, the low concentration of aluminium in the catalyst signifies lower surface acidity [13, 14]. The significance of a lower surface acidity is that the catalyst has lower catalytic activity for the conversion of the plastic HDPE linear polyalkene polymer to low molecular weight compounds [13]. Thus, the zeolite Y (Z-8) catalyst has the potential low catalytic activity, but the higher C₅-C₁₅ hydrocarbons (93.4 %) obtained might be due to both its lower surface area (888 m² g⁻¹) and micropore volume (0.315 cm³ g⁻¹) [13]. Consequently as highlighted before, that the two-stage pyrolysis-zeolite catalysis of waste plastic was effective in producing a useful product oil. However, low surface area might have played a role as observed in Section 5.3.1.1. So, a Z-1 catalyst with both low silica-alumina ratio (5.1:1) and surface area (705 m² g⁻¹), recorded nearly the same fuel range hydrocarbon (88.56 %) as Z-7 with both high Si:Al (30:1) and surface area (937 m² g⁻¹) yielded 87.7 wt.%. Then, it can be presumed that low surface area and high Si: Al in zeolite Y could favour the rise in the yield of desired fuel range hydrocarbons.

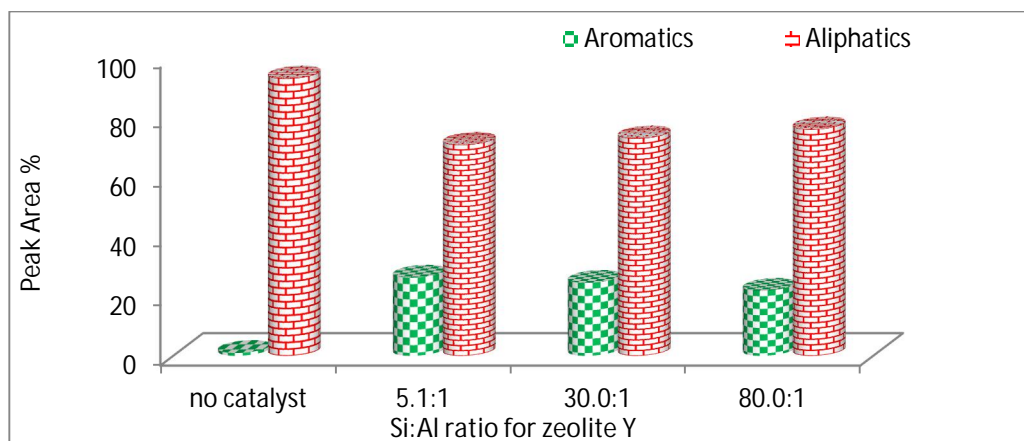


Figure 5.2-9 Aliphatic and aromatic content of the product oils from HDPE in relation to Si:Al ratio of zeolite Y catalysts

Figure 5.2-9 shows the aliphatic and aromatic content of the product oil from the pyrolysis-catalysis of waste high-density polyethylene in the presence of the various Y zeolite with varying silica: alumina ratio. The pyrolysis with no catalyst of high-density polyethylene produced a primarily aliphatic oil containing of alkanes, alkenes and alkadienes, with only a little proportion of aromatic compounds as has been reported by others [11]. Consequently, there was a decrease in aromatic content with an increase in silica: alumina ratio of the Y zeolite catalysts. The lower surface acidity associated with lower silica: alumina ratio in catalyst cause lower catalytic activity. Thus, this could be the main reason for the decrease in the conversion of the plastic HDPE linear polyalkene polymer to aromatic compounds [13]

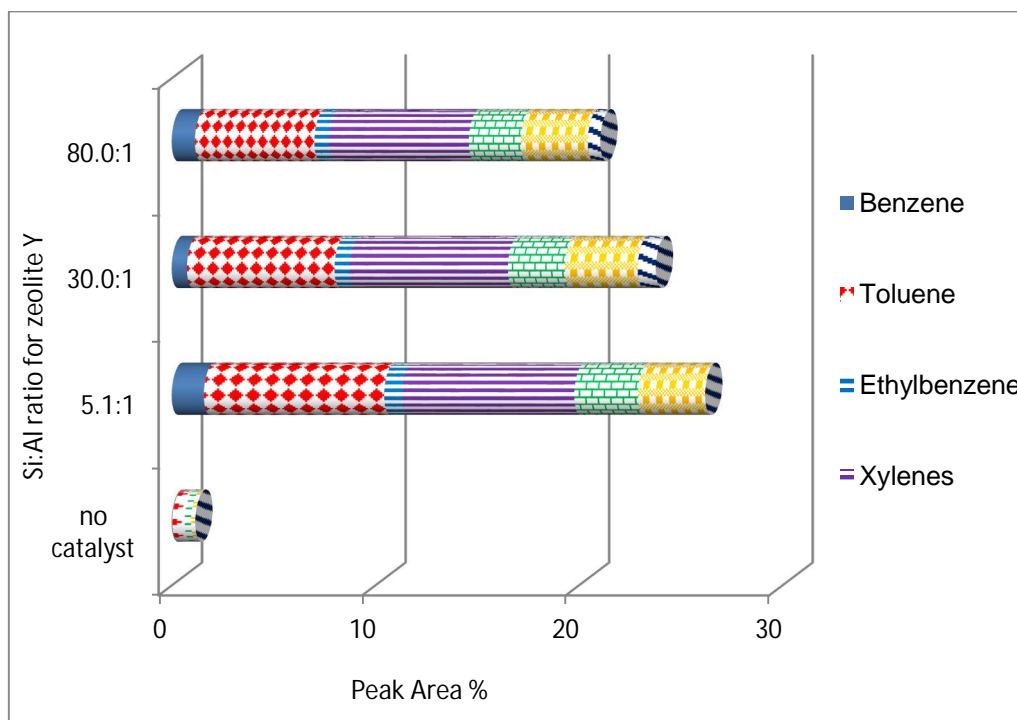


Figure 5.2-10 Yields of selected aromatic compounds in the oils from HDPE in relation to Si:Al ratio of zeolite Y catalysts

Similar to the findings in Section 5.2 in this work, Figure 5.2-8 shows the yields of selected aromatic compounds in the oils produced by the pyrolysis and pyrolysis-catalysis of waste high-density polyethylene with Y zeolite catalysts (with different Si: Al ratio). In the absence of a catalyst, there were only low concentrations of aromatic compounds as also shown in Figure 5.3-9. But, the concentration of single ring and two-ring aromatic hydrocarbons increased markedly, when the zeolite catalysts were introduced to the pyrolysis-catalysis reactor system. The selected aromatics compound considered here are mainly single ring aromatics. The catalyst with high catalytic activity (Z1) produced a higher concentration of benzene, toluene, ethylbenzene and styrene. Consequently, the amount of these selected aromatics compounds decreases with increase in the silica-alumina ratio. Hence, these could be

explained in term of a decrease in the catalytic acidity with increase in silica-alumina ratio.

The products oil from both non-catalytic and catalytic pyrolysis of waste HDPE were analysed for their fuel properties by simulated distillation using gas chromatography to determine the boiling range distribution of the oils.

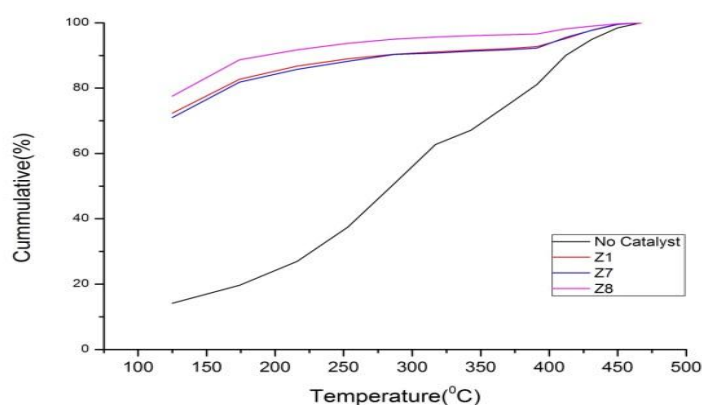


Figure 5.2-11 Simulated distillation of uncatalyzed pyrolysis oils from the pyrolysis-catalysis of HDPE in relation to Si:Al ratio of Y-zeolite catalysts

The Figure 5.2-11 shows the boiling range distribution of the product oil. The non-catalytic oil showed that a substantial part (greater than 50%) of the oils have a boiling range of greater than 317 °C and only 14% below 150 °C. However, the catalytic degradation product oils show a shift to lower boiling points, reflecting the shift in molecular weight range as seen in Figure 5.3-8. Muhammad et al. [12], noted that the boiling range distribution of gasoline would be >95.0% below 150 °C. But, for the catalytic product oils, the boiling point range fraction below 150 °C was between 73.0% and 76.0%.

5.2.2.2 Summary

The influence of the silica-alumina ratio of the three Y zeolites investigated shows a reduction in the low molecular weight hydrocarbons and aromatic compound contents with an increase in the silica-alumina ratio. However, the single ring aromatic compounds obtained in the pyrolyzed oil decrease with an increase in the silica-alumina ratio. The decrease in catalytic activity which comes with the increase in silica-alumina ratio perhaps might be the reason for the decrease in single ring aromatic compounds. But, catalyst (Z-8) with the least catalytic activity and high silica-alumina ratio shows better activity due to perhaps its high surface area and low micropore volume.

5.2.3 Influence of silica: alumina ratio of the ZSM-5 zeolite on catalytic degradation of waste HDPE

In this section influence of the silica: alumina ratio of the ZSM-5 zeolite catalyst was considered. The product yields were considered in the prior section 5.2. Thus, in this section influence of the silica; alumina ratio on the gas composition, distribution of fuel range and high molecular weight compounds; aliphatic and aromatic compounds distribution; distribution of selected aromatic compounds and simulated distillation properties are presented and discussed.

5.2.3.1 Products Yield

Table 5.1-2 shows the gas yield for pyrolysis of waste HDPE in the presences of three ZSM-5 catalysts with different silica: alumina ratio. The gas yield from thermal run increases with the introduction of the catalysts for the pyrolysis of HDPE waste. However, the gas yield slightly varied with the

increase in Si: Al ratio (from 49.8 to 47.0 wt. %). The gas is slightly reduced with increasing Si: Al. Thus, the result might be explained in terms of low catalytic activity with the increase in Si: Al ratio.

5.2.3.2 Gas Composition

Table 5.2-3 Gas composition from ZSM-5 with varying Si: Al ratio catalyzed degradation of HDPE waste

	No catalyst	Z-4	Z-5	Z-6
Si:Al	nd	23:1	50:1	80:1
H ₂ (vol. %)	11.7	9.68	4.75	11.4
CH ₄ (vol. %)	11.2	13.6	6.75	6.90
C ₂ H ₄ (vol. %)	14.7	10.7	7.45	24.1
C ₂ H ₆ (vol. %)	9.61	6.62	3.56	6.03
C ₃ H ₆ + C ₃ H ₈ (vol. %)	31.9	40.8	41.5	44.6
C ₄ H ₈ (vol. %)	18.9	15.4	24.2	6.29
C ₄ H ₁₀ (vol. %)	2.09	3.34	11.8	1.19
C ₂ -C ₄ (vol. %)	77.2	76.8	88.5	82.2
CV (MJMm ⁻³)	74.3	72.1	79.1	81.8

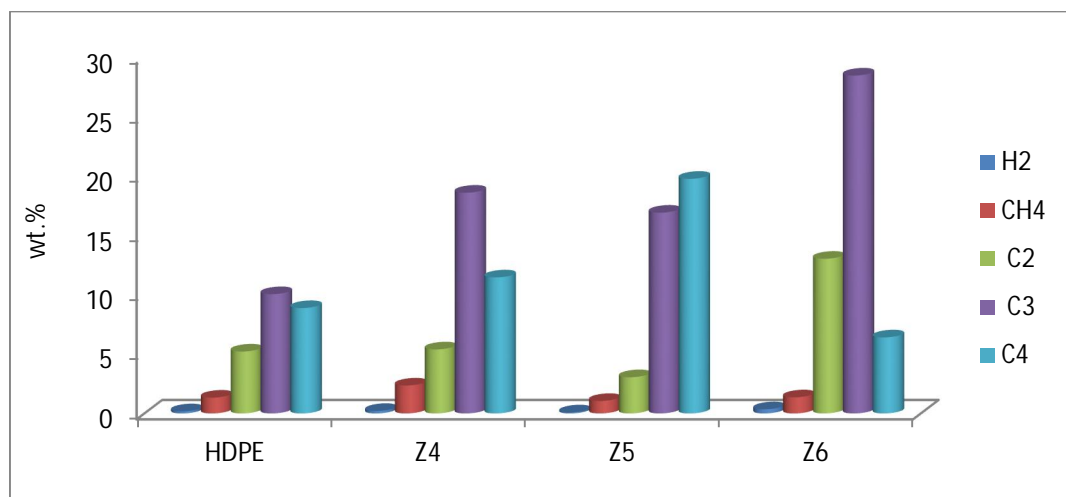


Figure 5.2-12 Gases produced from non-catalytic and catalytic pyrolysis of HDPE waste with ZSM-5 with varying Si: Al ratio

Tables 5.2-3 shows the gas composition in volume % while Figure 5.2-12 gives gas composition in wt. %. Mordi et al. [16], the investigation found that ZSM-5 catalysts give rise to products lighter than C₁₄. The authors obtained a higher amount of hydrocarbon gases 54.0%. They ascribed that to the occurrence of 10-membered ring sinusoidal and straight intersecting channels in the HSZM-5. However, they also pointed out that the cracking initiation took place on the external surface of the zeolite or at the pore mouth., since the polymer is too large to enter the pore. These starting degradation products were subsequently converted over the catalyst through secondary reactions, giving rise to the reported selectivity. The total gross heating values refer here as calorific value (CV) computed in MJ/m³ in Table 5.2-3 shows rise with the introduction of the catalyst. Similarly, the calorific values rise with the silica; alumina ratio as lower molecular weight hydrocarbon gases decrease with low

catalysts activity associated with higher Si: Al ratio. The improvement in the calorific value of the gases with the introduction of the catalyst (except for Z-1) was a reflection of the composition of high caloric value gases as detected in both Table 5.3-3 and Figure above. The high-value calorific value is known to be desirable as a product of waste plastic pyrolysis.

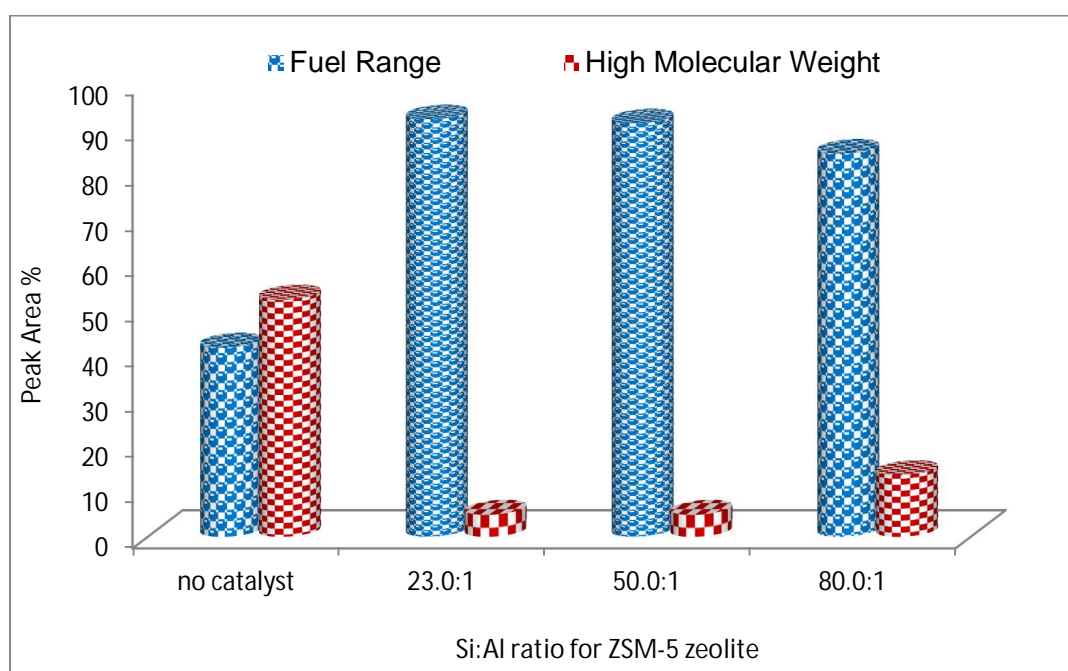


Figure 5.2-13 Fuel range (C₅ – C₁₅) and high molecular weight (C₁₆₊) hydrocarbons from the pyrolysis-catalysis of HDPE in relation to Si:Al ratio of ZSM-5 zeolite catalysts

Figure 5.2-13 shows the fuel range (C₅-C₁₅) hydrocarbons in the product oil from non-catalytic and zeolite ZSM-5 with varying Si: Al ratio catalyzed pyrolysis run. Similarly, the high molecular-weight hydrocarbons (i.e. C₁₆₊) are presented in the figure. Thus, for a non-catalytic run as shown other section above, there was ~55.0wt% of the condensed oil of high molecular weight hydrocarbons. Nevertheless, a marked decrease in C₁₆₊ higher molecular

weight hydrocarbons was observed when the ZSM-5 catalysts with varying Si: Al ratios were introduced. Hence, as obtained in an earlier section, a consistent increase in the C₅-C₁₅ hydrocarbons with catalyst addition was observed. Among the ZSM-5 catalyst with Si: Al ratios of 23:1, 50:1 and 80:1, zeolite Z-4 which has the lowest Si: Al ratio produced the highest conversion of the HDPE pyrolysis gases to fuel range C₅-C₁₅ hydrocarbons. The lower Si: Al ratio indicates a higher concentration of aluminium in the catalyst. Venuto and Habib [14] and Campbell [17] have reported that a higher content of aluminium in zeolite catalysts produces a higher surface acidity through the formation of strongly acidic protons on the surface, and within the pores and channels of the zeolite catalyst. For example, Ates et al. [13] reported that a zeolite ZSM-5 catalyst with and Si:Al ratio of 12.6, produced a higher content of aromatic hydrocarbons in the product oil compared to a zeolite ZSM-5 catalyst with a Si: Al ratio of 17.1 for the pyrolysis-catalysis of municipal solid waste plastic. Kumar et al. [7], have also reported that the aluminium content in the zeolite influences the acid site density which has a marked influence on cracking reactions of high molecular weight hydrocarbons such as the pyrolysis gases produced from high-density polyethylene.

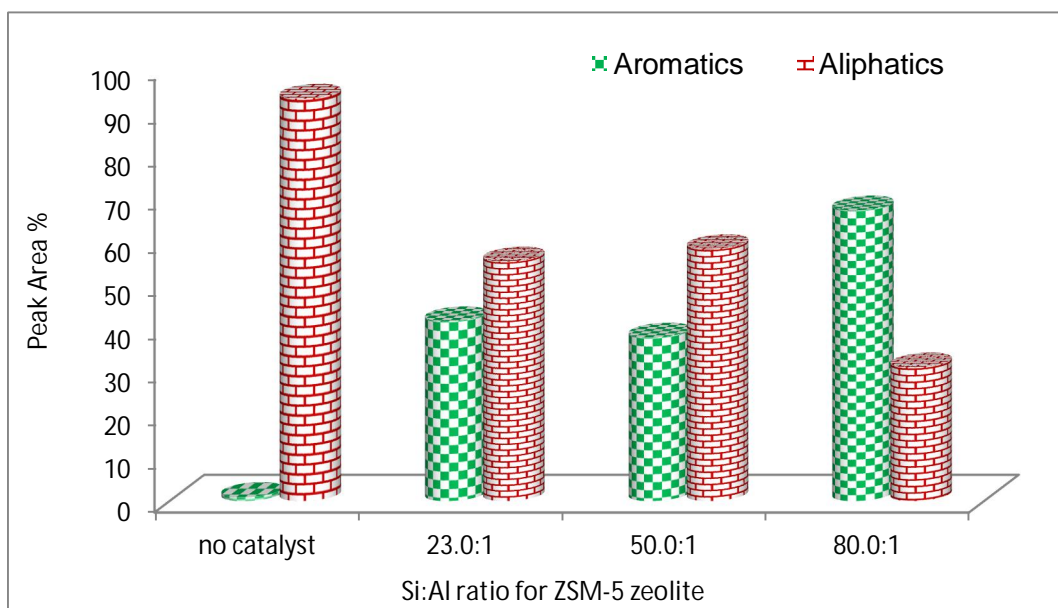


Figure 5.2-14 Aliphatic and aromatic content of the product oil from the pyrolysis-catalysis of HDPE in relation to Si:Al ratio of ZSM-5 zeolite catalysts

Figure 5.2-14 Shows the aliphatic and aromatic content of the product oil from the pyrolysis-catalysis of waste high-density polyethylene in the presence of the various ZSM-5 zeolite catalyst. Examination of Figure 5.2-14 shows that the highest conversion to aromatic compounds was formed by the zeolite Z-8 with the highest Si: Al ratio (80:1) which represents the lowest acidity.

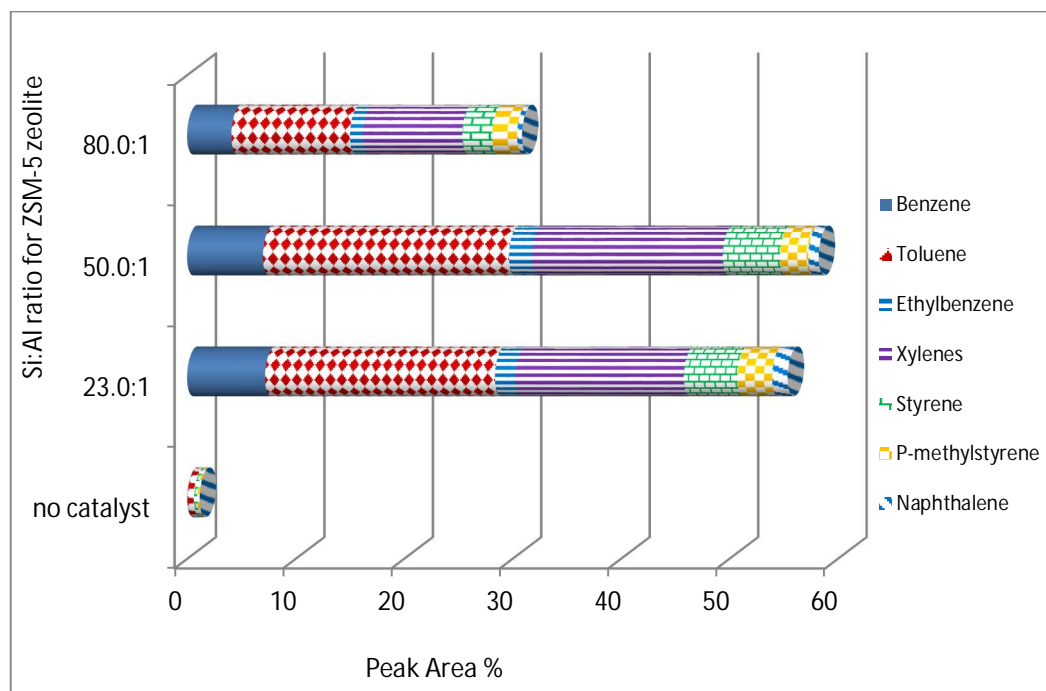


Figure 5.2-15 Yields of selected aromatic compounds in the oils produced from the pyrolysis-catalysis of HDPE in relation to Si:Al ratio of ZSM-5 zeolite catalysts

Accordingly, as also obtained in the section above sections, Figure 5.2-15 shows the yields of selected aromatic compounds in the oils produced by the pyrolysis and pyrolysis-catalysis of waste high-density polyethylene with different zeolite catalysts. In the absence of a catalyst, there were only low concentrations of aromatic compounds as also shown in Figure 5.2.15. But, when the ZSM-5 catalysts were introduced to the pyrolysis-catalysis reactor system, the concentration of single ring and two-ring aromatic hydrocarbons increased markedly. Liu et al. [18], performed catalytic degradation of HDPE over a clay catalyst compared with the catalysts in a fixed bed batch reactor. They proposed catalytic degradation mechanisms of HDPE over the different solid catalysts as shown below in Figure 5.3-16. Thus, they considered HZSM-5 with strong acidic sites and microporous structure, as beneficial for the production of olefins by β -scission reaction via a carbenium mechanism.

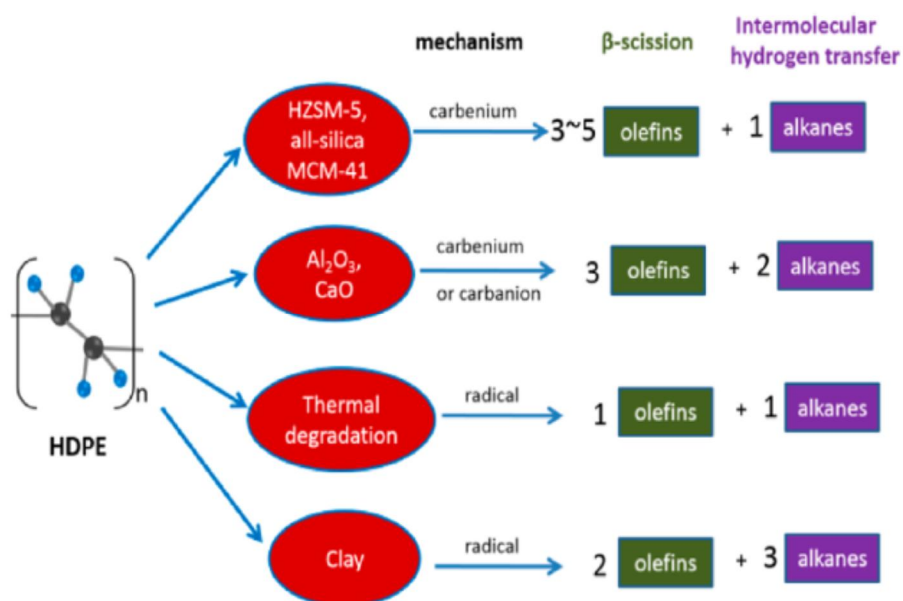


Figure 5.2-16 Mechanistic diagram for catalytic degradation of HPDE

A similar trend was observed in this work for a catalytic run. Conversely, the trend for thermal (non-catalytic) degradation shows resemblance with their proposed mechanism that was the free radical mechanism.

The product oils were analysed for their boiling point range distribution using gas chromatography which enables the simulated distillation of the oils to be determined (ASTM D2887).

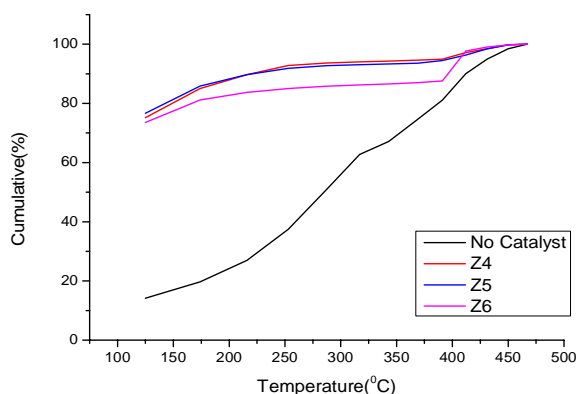


Figure 5.2-17 Simulated distillation of uncatalyzed pyrolysis oil and pyrolysis-catalysis derived the oil from the pyrolysis-catalysis of HDPE in relation to Si:Al ratio of ZSM-5 zeolite catalysts

The non-catalytic oil showed that a substantial part (greater than 50%) of the oils have a boiling range of greater than 317 °C and only 14% below 150 °C. However, the pyrolysis-catalytic product oils show a shift to lower boiling points, reflecting the shift in molecular weight range as seen in Figure 6.3-13. Compared to the boiling point range distribution of gasoline, which gives >95.0% below 150 °C [12] the catalytic product oils, the boiling point range fraction below 150 °C was between 74.0% and 77.0%.

The HZSM-5 zeolite catalysts used for the waste HDPE show a major improvement in the distillation range of the product oils suggesting a boiling point range similar to petroleum-derived kerosene or diesel fuel.

5.2.3.3 Summary

The influence of the silica-alumina ratio of the three zeolites ZSM-5 considered show reduction in the low molecular weight hydrocarbons and aromatic compound contents with an increase in the silica-alumina ratio. However, the single ring aromatic compounds obtained in the pyrolyzed oil

also increase with the increase in the silica-alumina ratio. Thus, low silica-alumina ratio enhanced the catalytic activity of the ZSM-5 catalyst for production of more volatile hydrocarbon and the aromatic compound. The fuel properties investigated shows improvement with the introduction of the catalyst.

The influence of the silica-alumina ratio of the three Y zeolites investigated show reduction in the low molecular weight hydrocarbons and aromatic compound contents with an increase in the silica-alumina ratio

5.3 Comparing influence of Zeolite Y and ZSM-5 catalysts

In this section influence of the silica: alumina ratio of the ZSM-5 zeolite catalyst and zeolite Y was considered. The product yields were shown in the previous section 5.1 Thus, in this Section the influence of different zeolite structure with similar Si: Al ratios (80:1) silica; alumina ratio on the gas composition, distribution of fuel range and high molecular weight compounds; aliphatic and aromatic compounds distribution; distribution of selected aromatic compounds and simulated distillation properties are presented and discussed

5.3.1 Gas Composition

Table 5.3-1 Gas composition from Y zeolite and ZSM-5 catalysed degradation of HDPE waste

	No catalyst	Z6	Z8
H ₂ (vol. %)	11.7	11.4	6.57
CH ₄ (vol. %)	11.2	6.90	3.50
C ₂ H ₄ (vol. %)	14.7	24.1	21.4
C ₂ H ₆ (vol. %)	9.61	6.03	3.31
C ₃ H ₆ + C ₃ H ₈ (vol. %)	31.9	44.6	45.6
C ₄ H ₈ (vol. %)	18.9	6.29	15.9
C ₄ H ₁₀ (vol. %)	2.09	1.19	3.73
C ₂ -C ₄ (vol. %)	77.2	82.2	89.9
CV (MJ m ⁻³)	74.3	81.8	89.9

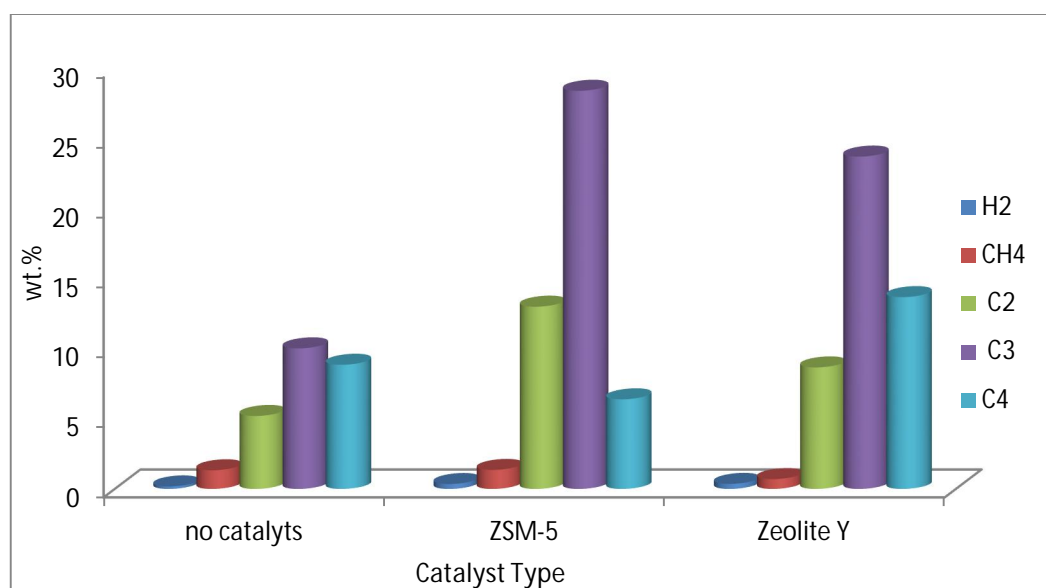


Figure 5.3-1 Gases produced from non-catalytic and catalytic pyrolysis of HDPE waste with Y zeolite and ZSM-5

Tables 5.3-1 shows the gas yield for pyrolysis of waste HDPE in the presence of zeolite Y (Z-8) and ZSM-5 (Z-6) catalysts with same silica: alumina ratio. The gas yield increases with the addition of the catalysts for the pyrolysis of HDPE waste. The zeolite Y gives higher gas yield (63.0 wt. %) than the ZSM-5 (47.0 wt. %). Tables 5.3-4 shows the gas composition in volume % while Figure 5.3-1 gives gas composition in wt. %. However, the total gross heating value or the calorific value (CV) computed in MJ/m³ in Table 5.3-1 shows an increase with the addition of the catalysts, but Y zeolite catalyst gives highest calorific values. Hence, the CV of the product gases shows a reflection of the composition of highly combustible fuel gases as observed in Table 5.3-1 and Figure 5.3-1 above. This high-value fuel gases can be burnt as a mixture to provide energy for the pyrolysis-catalysis plant and separated and sold as individual gases

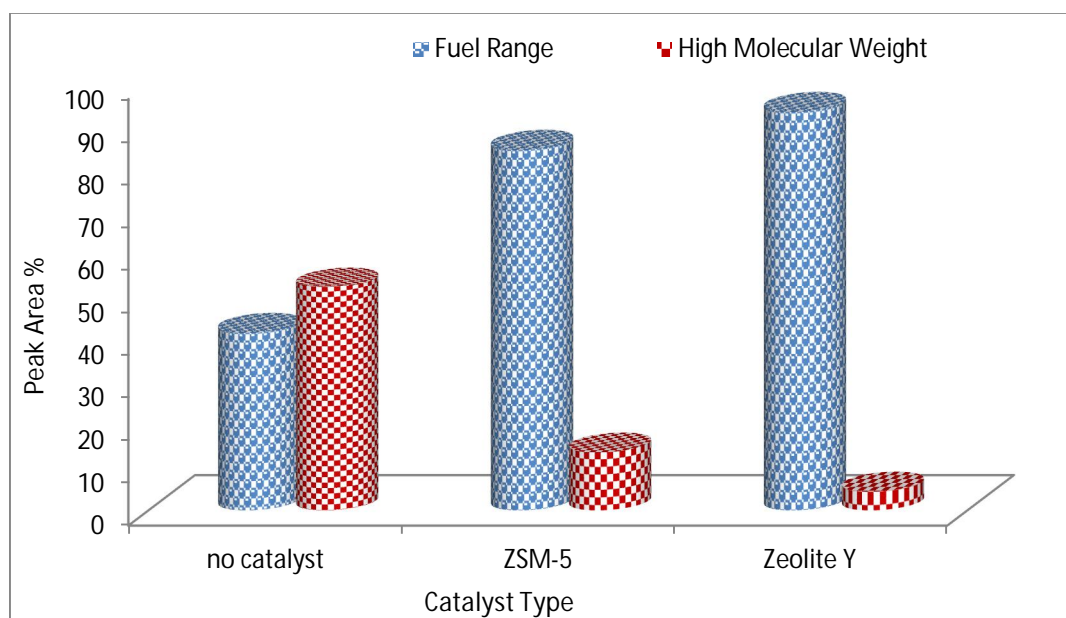


Figure 5.3-2 Fuel range (C₅ – C₁₅) and high molecular weight (C₁₆₊) hydrocarbons from the pyrolysis-catalysis of HDPE in relation to zeolite structure

Figure 5.3-2 shows the fuel range (C_5 - C_{15}) hydrocarbons in the product oil from un-catalytic, zeolite ZSM-5 and Y zeolite catalyzed pyrolysis run. Equally, the high molecular weight (i.e. C_{16+} hydrocarbons) are presented in the figure. Thus, for a non-catalytic run as shown in previous sections, there was ~55.0wt% of the condensed oil of high molecular weight hydrocarbons. However, a noticeable decrease in C_{16+} higher molecular weight hydrocarbons was observed when both zeolite catalysts were introduced. Thus, as found in earlier sections, there was a steady rise in the C_5 - C_{15} hydrocarbons with catalyst addition. However, for zeolite Y with 80:1 Si: Al (Z8), the C_5 - C_{15} hydrocarbons reached more than 90wt% of the product oil, but ZSM-5 (Z6) produce 84.6 wt.%. The large pores of zeolite Y allow heavy oil penetrate and proper acidic properties compared to ZSM-5 made it possible to reform PE pyrolyzed oil to gasoline and low coke [15, 19].

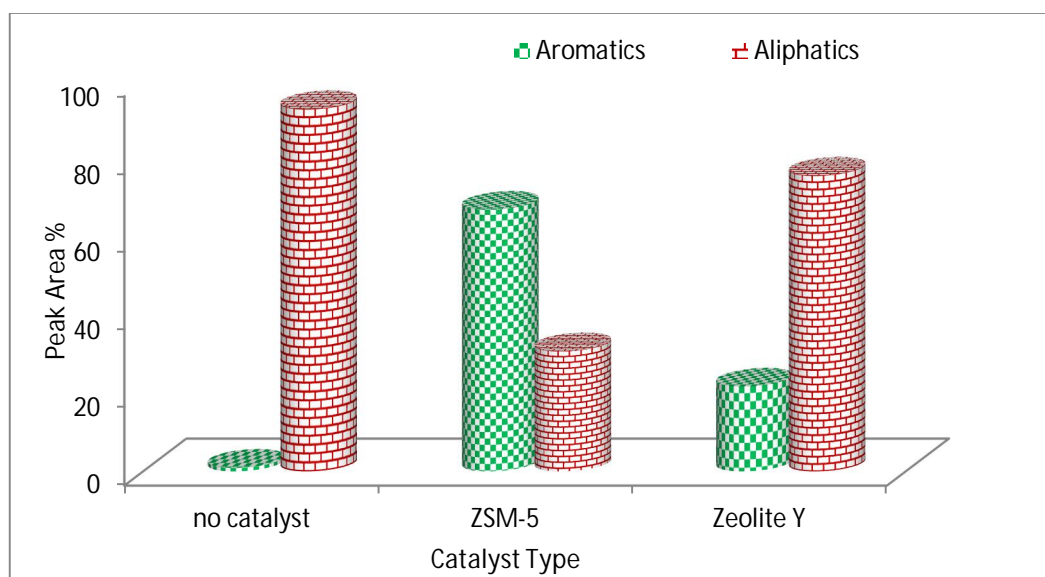


Figure 5.3-3 Aliphatic and aromatic content of the product oil from the pyrolysis-catalysis of HDPE in relation to zeolite structure

Figure 5.3-3 shows the aliphatic and aromatic content of the product oil from the pyrolysis-catalysis of waste high-density polyethylene in the presence of the various Y zeolite (Z-8) and ZSM-5 (Z-6) catalysts. The uncatalyzed pyrolysis of high-density polyethylene produced a mainly aliphatic oil consisting of alkanes, alkenes and alkadienes, with only a low proportion of aromatic compounds as has been reported by others [11].

For the ZSM-5 zeolite catalysts, there was an increase in aromatic content compared with Y catalyst. But the findings of greater concentration of aromatics hydrocarbons with zeolite Y catalyst compared to ZSM-5 was reported elsewhere [2]. Likewise, Muhammad et al. [20], reported pyrolysis of WEEE that Y zeolite with lower silica –alumina ratio produced a higher conversion of the styrene to other aromatics products, particularly benzene and toluene. Thus, the introduction of the ZSM-5 zeolite catalysts produced a much higher conversion of plastics to aromatic compounds compared to the Y zeolite catalyst.

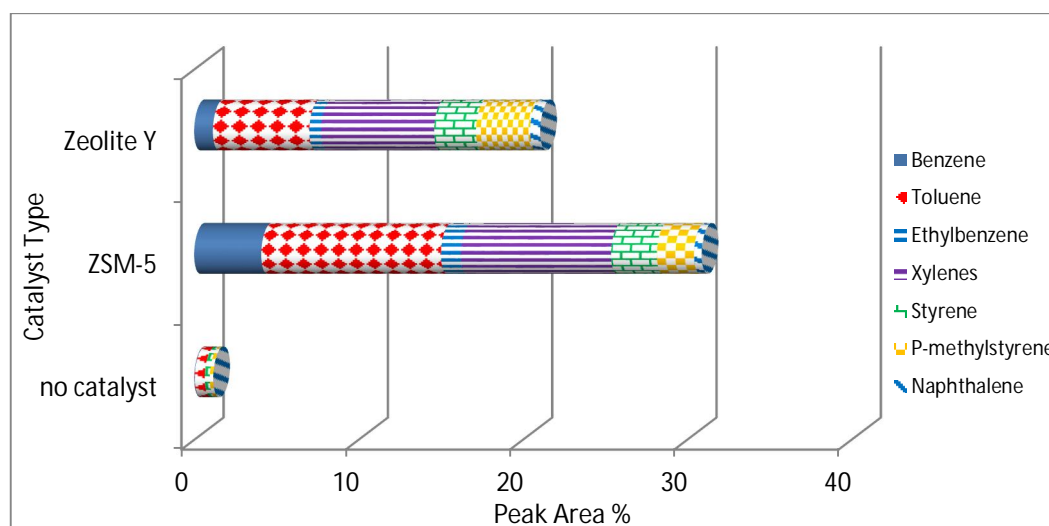


Figure 5.3-4 Yields of selected aromatic compounds in the oils produced from the pyrolysis of HDPE in relation to zeolite structure

Figure 5.3-4 shows the yields of selected aromatic compounds in the oils produced by the pyrolysis and pyrolysis-catalysis of waste high-density polyethylene with different zeolite catalysts. In the absence of a catalyst, there were only low concentrations of aromatic compounds as also shown in Figure 5.3.4. But, when the zeolite catalysts were introduced to the pyrolysis-catalysis reactor system, the concentration of single ring and two-ring aromatic hydrocarbons improved evidently. For the Y zeolites, the concentration of the aromatic compounds produced was less than that for the ZSM-5 catalysts. Notably, the concentration of benzene, toluene and xylenes was significantly higher for the product oil using the Y zeolite compared to the ZSM-5 zeolite catalyst. Lopez et al. [21], investigated the pyrolysis and pyrolysis-catalysis of mixed plastics at 500 °C using zeolite ZSM-5 catalyst and, also reported the presence of increased concentrations of benzene, toluene and styrene with the introduction of the catalyst.

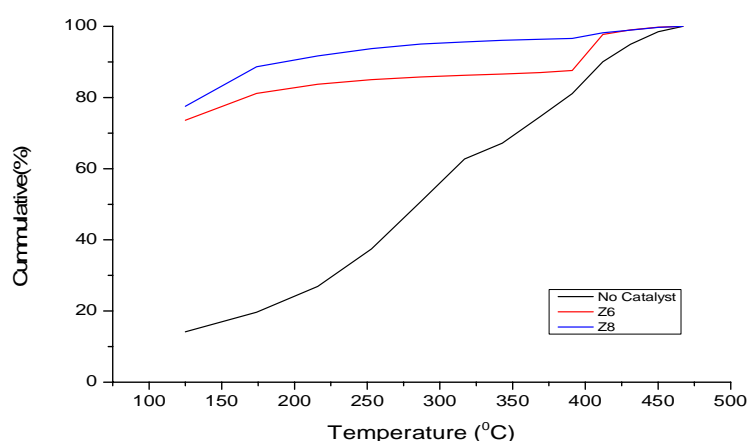


Figure 5.3-5 Simulated distillation of uncatalyzed pyrolysis oil and pyrolysis-catalysis derived the oil from the pyrolysis-catalysis of HDPE in relation to zeolite structure.

The product oils were analysed for their boiling point range distribution using gas chromatography which enables the simulated distillation of the oils to be determined (ASTM D2887). The Figure 5.3-5 shows the simulated distillation curves for the product oils from pyrolysis-catalysis of HDPE in the presence of the Y zeolite and the zeolite ZSM-5 catalyst compared to the simulated distillation of the uncatalysed oil as showed in Figure 5.3-5. The non-catalytic oil showed that a significant fraction (greater than 50%) of the oils have a boiling range of greater than 317 °C and only 14% below 150 °C. However, the catalytic degradation product oils show a shift to lower boiling points, reflecting the shift in molecular weight range as seen in Figure 5.3-19.

Both zeolite catalysts show a major improvement in the distillation range of the product oils suggesting a boiling point range similar to petroleum-derived kerosene or diesel fuel.

5.4 Summary

The influence of zeolite Y and zeolite ZSM-5 catalysts on the products from the catalytic pyrolysis of high-density polyethylene (HDPE) has been investigated. The zeolite catalysts had different characteristics including, surface areas and silica: alumina ratios in addition to the different crystal structures of Y and ZSM-5 zeolites. The pyrolysis products included oil, gas and negligible char. The quantity of oil produced from non-catalysed pyrolysis of HDPE was more than 74 wt%, and the gases consisted of hydrogen, methane and C₂-C₄ hydrocarbons. When the catalysts were introduced, there was a decrease of between 15.0-30.0 wt. percent in oil yield. However, there was a corresponding increase in gas yield ranging between 38-50wt. percent

which increased with catalyst surface area. The catalysed oil was enriched in benzene ethylbenzene, xylenes, styrene and toluene. The catalyst with the higher surface area produced a lower conversion of the higher molecular weight material to single aromatic ring compounds compared to the zeolite Y catalyst with the lower surface area .

Overall, the results suggest that there is some influence of the surface area and the Si: Al ratio on the conversion of HDPE to more valuable products such as fuel range hydrocarbons and chemicals. However, in this study, the zeolite catalysts were obtained commercially and consequently, the composition of the catalysts could not be controlled to enable a thorough study of the influence of only surface area or the Si: Al ratio. For example, within each set of Y zeolite or ZSM-5 zeolite, there was some variation in the catio, for example, H^+ or NH_4^+ , variation in Na_2O content and differences in micropore and mesopore volumes.

References

1. Serrano, D.P., Aguado, J. and Escola, J.M., *Developing Advanced Catalysts for the Conversion of Polyolefinic Waste Plastics into Fuels and Chemicals*. *Acs Catalysis*, 2012. **2**(9): p. 1924-1941.
2. Bagri, R. and Williams, P.T. *Catalytic pyrolysis of polyethylene*. *Journal of analytical and applied pyrolysis*, 2002. **63**(1): p. 29-41.
3. Serrano, D., Aguado, J., Escola, J.M., Rodriguez, J.M., Morselli, L. and Orsi, R., *Thermal and catalytic cracking of a LDPE-EVA copolymer mixture*. *Journal of analytical and Applied Pyrolysis*, 2003. **68**: p. 481-494.
4. Kaminsky, W., Predel, M. and Sadiki, A. *Feedstock recycling of polymers by pyrolysis in a fluidised bed*. *Polymer Degradation and Stability*, 2004. **85**(3): p. 1045-1050.
5. Keane, M.A., *Catalytic transformation of waste polymers to fuel oil*. *ChemSusChem*, 2009. **2**(3): p. 207-214.
6. Hildebrandt, R. and Skala, H., *High-temperature acidity measurements and correlation with catalyst activity*. *Journal of Catalysis*, 1968. **12**(1): p. 61-71.
7. Kumar, S., Panda, A.K. and Singh, R., *A review on tertiary recycling of high-density polyethylene to fuel*. *Resources, Conservation and Recycling*, 2011. **55**(11): p. 893-910.
8. Park, D., Hwang, E.Y., Kim, J.R., Choi, J.K., Kim, Y.A. and Woo, H.C., *Catalytic degradation of polyethylene over solid acid catalysts*. *Polymer degradation and stability*, 1999. **65**(2): p. 193-198.
9. Sharratt, P., Lin, Y.H., Garforth, A.A. and Dwyer, A., *Investigation of the catalytic pyrolysis of high-density polyethylene over a HZSM-5 catalyst in a laboratory fluidized-bed reactor*. *Industrial & engineering chemistry research*, 1997. **36**(12): p. 5118-5124.
10. Neves, I.C., Botelho, G., Machado, A.V., and Rabelo, P., *The effect of acidity behaviour of Y zeolites on the catalytic degradation of polyethylene*. *European polymer journal*, 2006. **42**(7): p. 1541-1547.
11. Williams, P.T. and Williams, E.A. *Fluidised bed pyrolysis of low density polyethylene to produce petrochemical feedstock*. *Journal of Analytical and Applied Pyrolysis*, 1999. **51**(1-2): p. 107-126.
12. Muhammad, C., Onwudili, J.A. and Williams, P.T., *Thermal Degradation of Real-World Waste Plastics and Simulated Mixed*

Plastics in a Two-Stage Pyrolysis-Catalytic Reactor for Fuel Production. Energy & Fuels, 2015. **29**(4): p. 1601-1609.

13. Ateş, F., Miskolczi, N., and Borsodi, N., *Comparison of real waste (MSW and MPW) pyrolysis in batch reactor over different catalysts. Part I: Product yields, gas and pyrolysis oil properties.* Bioresource technology, 2013. **133**: p. 443-454.
14. Venuto, P.B. and Habib Jr, E.T., *Fluid catalytic cracking with zeolite catalysts.* 1979. Marcel Dekker, Inc. New York
15. Aguado, J., Serrano, D.P. and Escola, J.M. *Fuels from Waste Plastics by Thermal and Catalytic Processes: A Review.* Industrial & Engineering Chemistry Research, 2008. **47**(21).
16. Mordi, R.C., Fields, R. and Dwyer, J. *Thermolysis of low density polyethylene catalysed by zeolites.* Journal of analytical and applied pyrolysis, 1994. **29**(1): p. 45-55.
17. Campbell, I.M., *Catalysis at surfaces*1988: Springer Science & Business Media. Berlin.
18. Liu, M., Zhuo, J.K., Xiong,S.J., and Yao,Q., *Catalytic Degradation of High-Density Polyethylene over a Clay Catalyst Compared with Other Catalysts.* Energy & Fuels, 2014. **28**(9): p. 6038-6045.
19. Songip, A.R., Masuda,T.,Kuwahara, H. and Hashimoto, K., *Test to screen catalysts for reforming heavy oil from waste plastics.* Applied Catalysis B: Environmental, 1993. **2**(2): p. 153-164.
20. Muhammad, C., Onwudili, J.A. and Williams, P.T. *Catalytic pyrolysis of waste plastic from electrical and electronic equipment.* Journal of Analytical and Applied Pyrolysis, 2015.
21. López, A., De Marco, I., Cabellero, B.M., Laresgoiti, M.F., Adrados, A. and Aranzabal, A., *Catalytic pyrolysis of plastic wastes with two different types of catalysts: ZSM-5 zeolite and Red Mud.* Applied Catalysis B: Environmental, 2011. **104**(3): p. 211-219.

Chapter 6 : THERMAL DEGRADATION OF REAL-WORLD WASTE PLASTICS AND SIMULATED MIXED PLASTIC FOR FUEL PRODUCTION

This chapter discussed the results of thermal degradation of real-world waste plastics and simulated plastic in a two-stage pyrolysis-catalysis bench scale reactor for fuel production.

6.1 Introduction

Muhammad et al [1], reported a suggestion that an optimum reactor configuration for the catalytic pyrolysis of waste plastic will be a two-stage reactor, with a first stage of pyrolysis followed by catalysis in a second stage reactor [2]. They further stated the advantages includes greater control and optimization of temperature for each stage process, particular suitability for mixed plastic wastes. It is particularly suitable for the mixed plastic where any residue or dirt remains in the first pyrolysis stage, protection of the catalyst from carry-over of particulates that may deactivate the catalyst. Likewise, it will improvement the contact between pyrolysis products and catalyst, and ease of recycling of the used catalyst. Series of authors have investigated the catalytic pyrolysis of plastics using different reactor type, reaction condition and catalyst. Nevertheless, the large majority of studies of couple pyrolysis-catalysis of plastic have been with single, pure polymer plastics; there are fewer studies on the pyrolysis-catalysis process using real-world post consumer mixed plastic waste.

However, in this work real-world, post-consumer plastic waste has been processed using a two stage, pyrolysis-catalysis reactor discussed in chapter 3 section 3.3. They are processed using an HZSM-5 catalyst to produce high-quality liquid fuel containing fuel range hydrocarbons. Also, pure, single-polymer plastics in the form of PE, PP, PS, and PET were also processed in the pyrolysis-catalysis reactor system. Likewise, a simulated mixture of the four plastics was also processed to determine if there was any interaction between the plastic products during the process that might influence the composition of the product oils and gases.

Table 6.1-1 Composition of waste plastics used for research

Waste	HDPE (Wt. %)	LDPE (Wt. %)	PP (Wt. %)	PS (Wt. %)	PET (Wt. %)	PVC (Wt. %)	Others (Wt. %)	Reference
Slovenia P-MSW ¹	65 ²	-	9	9	10	1	6	[3]
Synthetic mixture	34.57	34.58 ³	9.57	9.57	10.64	1.07	-	[3]
South Taiwan P-MSW	38	24	34	1	-	3	-	[4]
Synthetic mixture	33	22	33	11	-	-	-	[5]
Synthetic mixture	68 ²	-	16	16	-	-	-	[6]
Hungary P-MSW	59.1 ²	-	25	7.2	-	-	8.7 ⁴	[7]
Synthetic mixture	40 ²	-	35	18	4	3	-	[8]
Synthetic mixture	30	-	30	20	5	10	5	[9]

¹ Plastics from MSW

² Comprises, HDPE & LDPE

³ Equal quantities of LDPE & LLDPE

⁴ Comprises PET, PVC, PA & ABS

The proportion of the four plastic in the simulated mixture based on a short review of the literature (Table 6.1-1) [3],[4-9]. The range of waste plastic used in this work was selected to reflect the range of the main plastic polymers found or researched in municipal solid waste plastics

6.2 Mixed plastic Characterization

The plastic samples were characterized using thermogravimetric analysis as described in chapter 3 section 3.4.2.

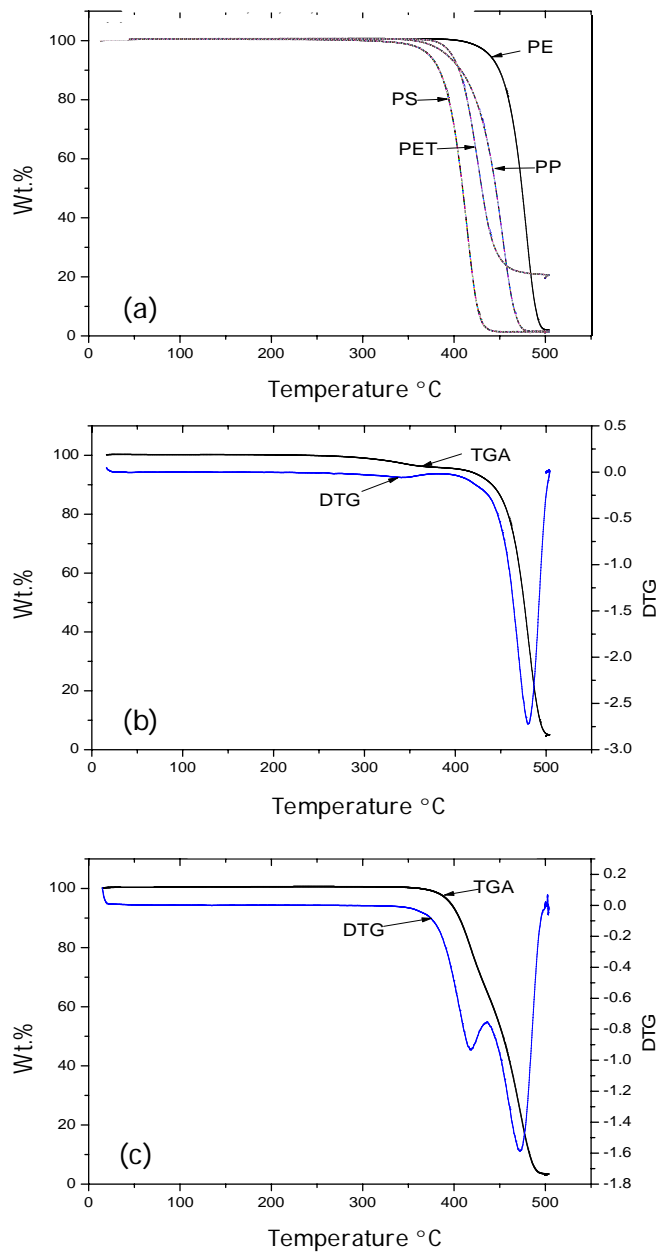


Figure 6.2-1 Thermogravimetric Analysis for (a) Virgin Plastics, (b) Real-world mixed plastics (MP) and (c) Simulated mixed plastic (SMP)

The plastic samples were characterised to study the thermal degradation of the plastics with increasing temperature of pyrolysis. Figure 6.2-1a shows the TGA and thermograms of individual virgin plastics. Figure 6.2-1b the TGA

and DTG the real-world mixed plastic (MP), and Figure 6.2-1c the TGA and DTG of the simulated mixture of plastic (SMP).

The TGA thermograms of the individual plastic polymers in the Figure above, showed that polystyrene gave the main degradation peak at a lower temperature (~420 °C), lower than the other polymers and that polyethylene had the highest degradation temperature (~480 °C). The order of thermal degradation was PS < PET < PP < PE. The mass loss thermograms for the real-world mixed plastic waste showed a DTG single peak at 480 °C, which is consistent with its reported composition of mainly polyalkene plastics. The simulated mixture of plastics showed two areas of weight loss on the TGA, as shown by the two DTG peaks indicating weight loss attributed to the PS and PET composition at the lower temperature (~420 °C) and the PE and PP content at the higher temperature (470 °C).

6.3 Product Yield

Panels a and b Figure 6.3-1 show the product yield obtained from the uncatalyzed and catalyzed pyrolysis of the real-world mixed plastic, simulated plastic mixture and the four virgin plastics respectively. Virgin plastic polystyrene gave a maximum oil yield of ~ 97.0 wt. % for uncatalyzed pyrolysis with catalysed PET producing the lowest oil yield (38.50 wt. %), with a significant production of char. Park et al [10], investigated the pyrolysis and catalytic pyrolysis of polystyrene in a semi batch reactor and reported an oil yield of 96.7 wt. % at a reaction temperature of 480 °C for noncatalytic, thermal pyrolysis. Similarly, Achilias et al. [11], reported an oil yield of 91.8 wt. % for the pyrolysis of polystyrene in a fixed bed reactor at 510 °C.

Polyethylene and polypropylene gave high wax yields of over 80 wt. %; similar results have reported for the thermal pyrolysis of polyalkene plastics[12].

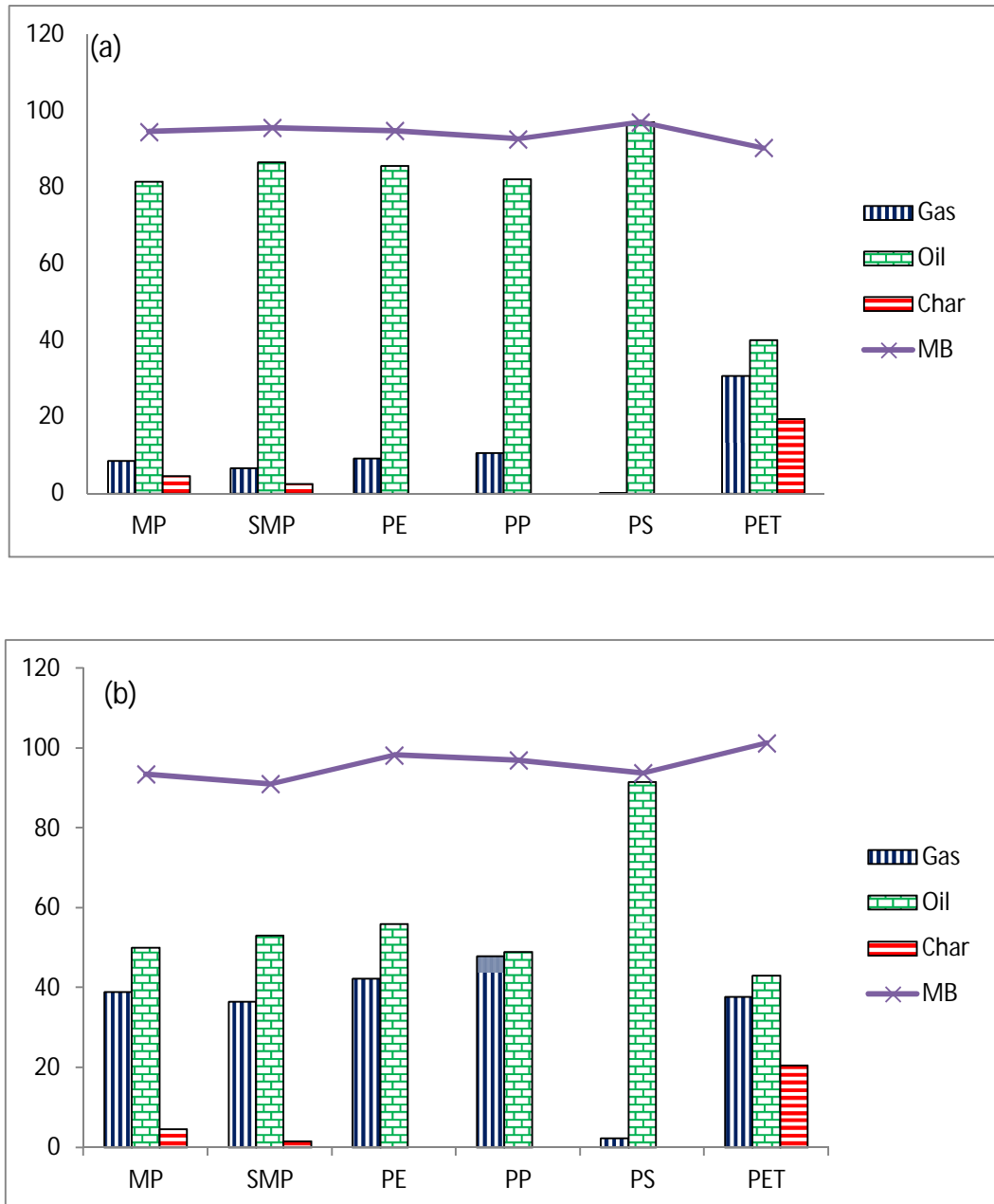


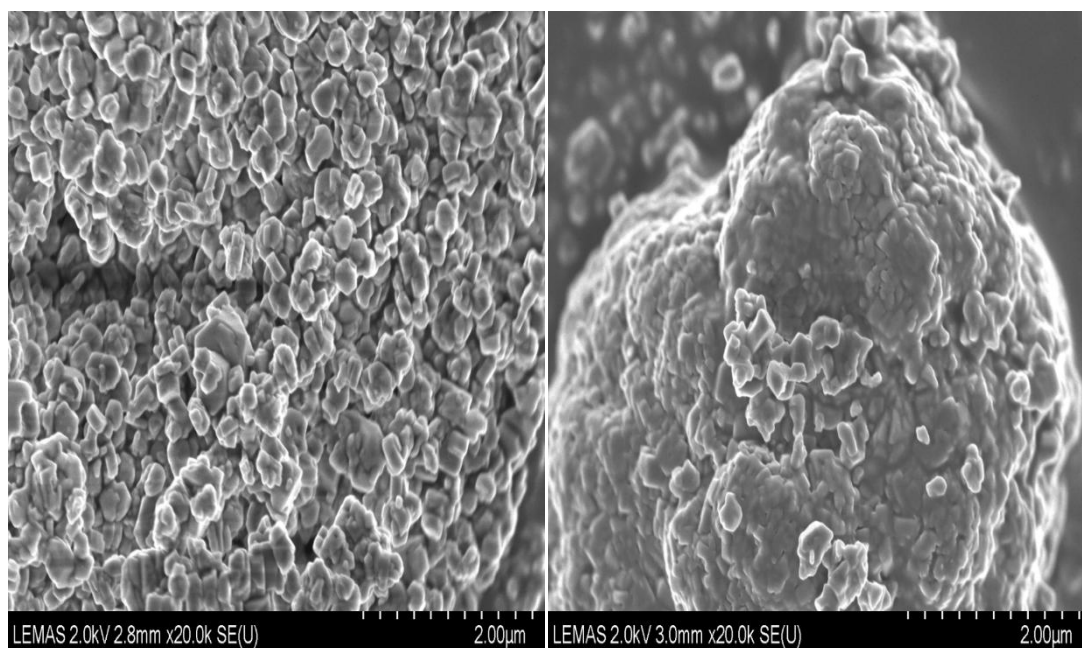
Figure 6.3-1 Product yield and mass balance (MB) for non-catalytic (a) and catalytic (b) pyrolysis of real world plastics (MP), the simulated mixture of plastics (SMP) and virgin plastics (PE, PP, PS, PET).

The liquid products from the uncatalyzed pyrolysis of real-world mixed plastic (MP) and the simulated mixture of plastics gave product yields similar to that found for polyethylene and polypropylene, reflecting the dominance of these polymers in the plastic mixtures investigated. However, the mixed plastics also produced some char, which reflects the content of PET in the mixtures. The overall mass balances for the experiments are shown in Figure 6.3-1 and show that high mass closures were achieved.

The addition of the Zeolite HZSM-5 catalyst to the second-stage catalytic reactor produced a marked increase in gas production from the pyrolysis-catalysis of the plastics with a resultant reduction in oil yield. The exception was for the polystyrene that maintained a high yield of oil (91.5 wt. %) in the presence of the catalyst. Similar observations on the influence of catalyst on the plastic pyrolysis were reported by Aguado et al. [13] and Lopez et al. [8, 14]. For example Lopez et al.[8], investigated the catalytic pyrolysis of packaging plastic waste in a semi-batch reactor at 400 °C using a zeolite HZSM-5 catalyst. They obtained a product yield for the non-catalytic experiment of 79.3 wt. % liquid, 17.7 wt. % gas and 3.00 wt. % char, which changed to 56.9 wt. % liquid, 40.4 wt. % gas and 3.20 wt. % char in the presence of the catalyst. Ateş et al. [7], also reported a reduction in the oil produced by the catalytic pyrolysis of municipal solid waste derived plastics when zeolite HZSM-5 catalyst was added to the process of catalytic pyrolysis.

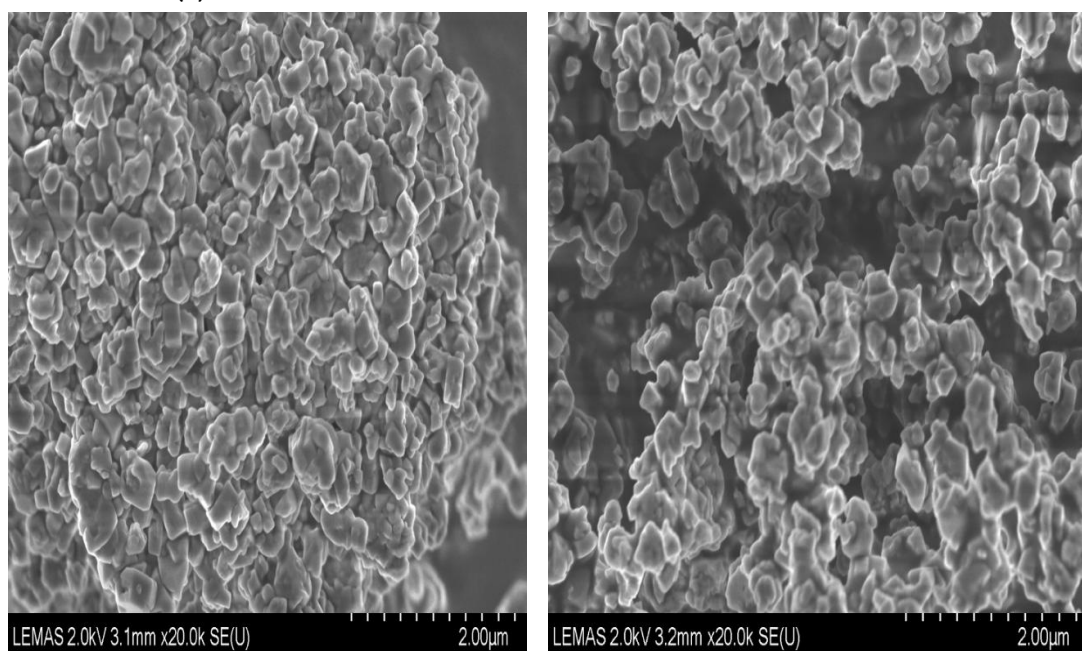
The mass of carbon deposited on the catalyst during pyrolysis determined by temperature programmed oxidation (TPO) which showed that the carbon deposition was only 0.48 wt. % of the mass of reacted catalyst. Similarly,

scanning electron microscopy observation of the reacted catalysts are shown in Figure 6.3-2 for the fresh HZSM-5 (Figure 6.3-2 a), reacted HZSM-5 with HDPE (Figure 6.3-2 b); reacted HZSM-5 with MP (Figure 5.3-2 c) and reacted HZSM-5 with HDPE 5 (Figure 6.3-2 d). The SEM observation of the reacted catalyst after the pyrolysis-catalysis experiments did not reveal any significant carbon deposition on the catalyst surface.



(a) Fresh HZSM-5

(b) HZSM-5 spent for HDPE



(c) HZSM-5 spent for MP

(d) HZSM-5 spent for SMP

Figure 6.3-2 SEM analysis of the fresh and reacted HZSM-5 after pyrolysis for the plastic samples

Kumar et al. [15], reported that low acidity zeolite catalysts, with a high Si:Al ratio (similar to this work), would produce lower coke formation than a high acidity, low Si:Al ratio catalyst, but with the disadvantage that the lower

acidity means that the catalyst is less effective in cracking hydrocarbons compared to a high acidity catalyst.

6.4 Gas Composition:

This section described the gas composition from various pyrolysis experiments carry out.

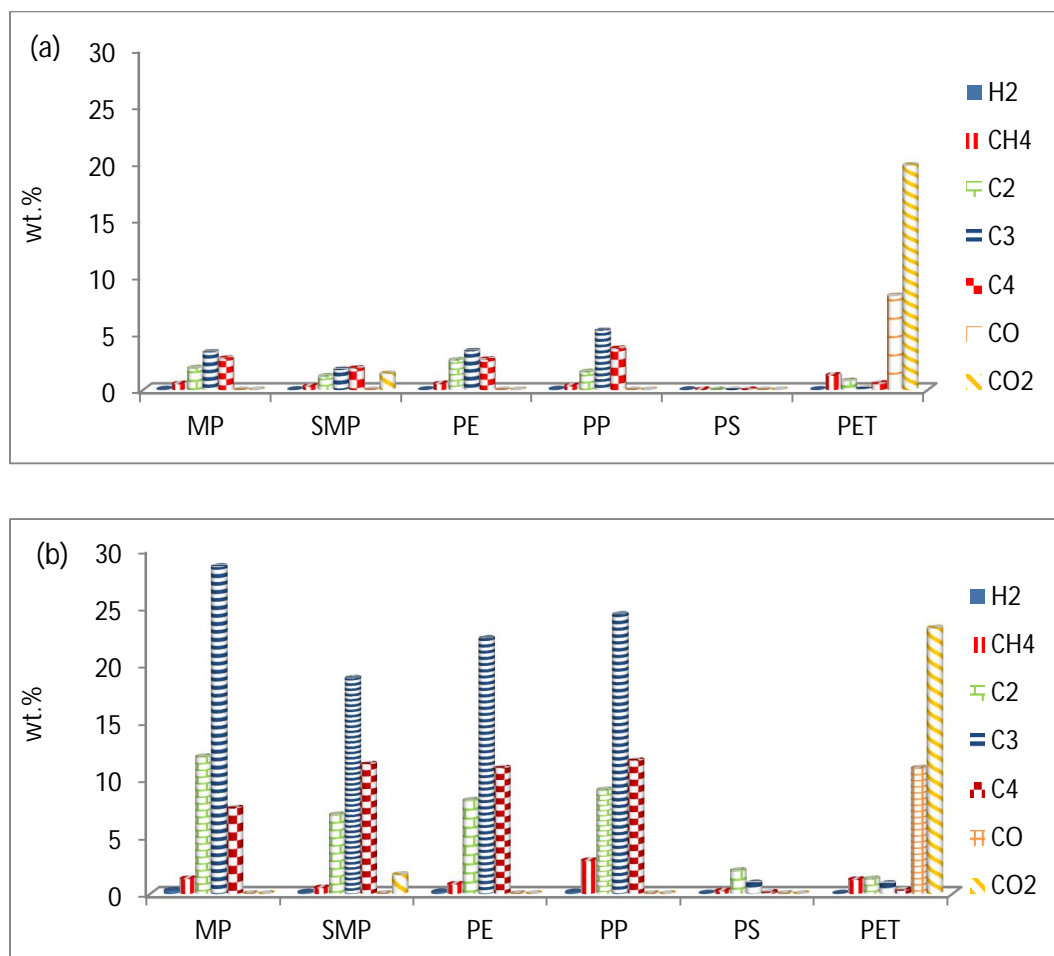


Figure 6.4-1 Gases produced from (a) non-catalytic (b) catalytic pyrolysis of real world plastics (MP), the simulated mixture of plastics (SMP) and virgin plastics (PE, PP, PS, PET).

Figure 6.3-1 shows that the addition of the zeolite HZMS-5 catalyst to the second stage of the reactor system produced a marked rise in gas yield. Thus, Figure 6.4-1 shows the concentration of the product gases with and without

the zeolite catalyst for the pyrolysis and pyrolysis-catalysis of the real world plastics (MP) the simulated mixture of plastics (SMP), and the virgin plastics (PE, PP, PS, PET). Likewise, Figure 6.4-1a shows that the main gases produced during the thermal pyrolysis of MP, SMP, PE and PP in the absence of the catalyst were C_2 (mainly ethene with lower concentrations of ethane), C_3 (mainly propene) and C_4 gases (mainly butene). These plastic samples consisted of mainly polyalkene polymer structures. But, the polyalkenes plastic are thermally degraded via a random scission process to produce mainly alkene gases C_2H_4 , C_3H_6 , and C_4H_8 , and to a lesser extent the alkanes gases, C_2H_6 , C_3H_8 , and C_4H_{10} [16]. The pyrolysis of polystyrene produced little gas. For PET, the main gases were carbon dioxide, formed from the decarboxylation of the PET and CO, as well formed through decarboxylation of polymer or reaction between carbon dioxide and char [16].

The addition of the zeolite HZSM-5 catalyst showed a marked rise in the yield of the $C_2 - C_4$ hydrocarbon gases, but particularly C_3 for the pyrolysis-catalysis of the MP, SMP, PE and PP plastics (Figure 6.4-1b). The yield and composition of the product gases from the pyrolysis-catalysis of PS and PET (Figures 6.3-1b and 6.4-1 b) showed only a small influence when the Zeolite catalysts were introduced to the process. Other researchers have reported the observed enhanced production of hydrocarbon gases with the introduction of a zeolite catalyst.[2, 14, 15, 17]. For example, Lopez et al. [14], reported that the main gases derived from the thermal processing of a mixture of plastics (PE, PP, PS, PET, PVC) were methane, ethene, ethane, and C_3 - C_4 gases. The C_3 - C_4 hydrocarbons were the highest product gases. They also reported

the presence of CO and CO₂ derived from the PET in the plastic mixture. The introduction of a zeolite HZSM-5 catalyst to their process produced an overall increase in gas yield, including C₃-C₄ hydrocarbon gases.

Table 6.4-1 Possible Interaction of plastics during pyrolysis of the simulated mixture of plastics compared with the expected gas composition based on the proportions of the individual plastics.

	Thermal Actual Gas Yield (Wt. %)	Expected Gas Yield (Wt. %)
Hydrogen	0.02	0.02
Methane	0.27	0.47
C ₂ Hydrocarbons	1.18	1.83
C ₃ Hydrocarbons	1.78	2.73
C ₄ Hydrocarbons	1.88	2.12
Carbon monoxide	<0.10	0.74
Carbon dioxide	1.41	1.78
	Catalytic Actual Gas Yield (Wt. %)	Expected Gas Yield (Wt. %)
Hydrogen	0.13	0.12
Methane	0.50	1.01
C ₂ Hydrocarbons	6.87	6.54
C ₃ Hydrocarbons	18.76	16.73
C ₄ Hydrocarbons	11.27	8.11
Carbon monoxide	<0.10	0.98
Carbon dioxide	1.65	2.08

Table 6.4-1 shows the gas concentration of the gases produced from pyrolysis and pyrolysis-catalysis of the simulated mixture of plastics compared with the

expected gas composition based on the proportions of the individual plastics. The gas composition for the simulated mixture of plastics showed a yield of the C₂, C₃ and C₄ gases was higher than expected based on the proportions of each gas generated by the individual virgin polymers, which suggests some interaction between the individual virgin plastics in the mixture. The yield of carbon monoxide and carbon dioxide from the pyrolysis and pyrolysis-catalysis was lower than would be expected, suggesting an interaction of the mixture of plastics.

Jing et al. [18], used a closed batch reactor to investigate the pyrolysis 50:50 ratio mixture of low-density polyethylene and polypropylene and also reported an interaction between the polymers. The yield of gases, specifically the yield of alkane gases, C₂H₆, C₃H₈ and C₄H₁₀, was increased compared to that expected from the proportions of the individual plastics. Williams and Williams [12], also showed that for several different plastics, mixing the individual plastic with polystyrene produced a clear interaction between the plastics, resulting in increased yield of alkene gases.

6.5 Oil Composition:

This section described the gas composition from various pyrolysis experiments carry out.

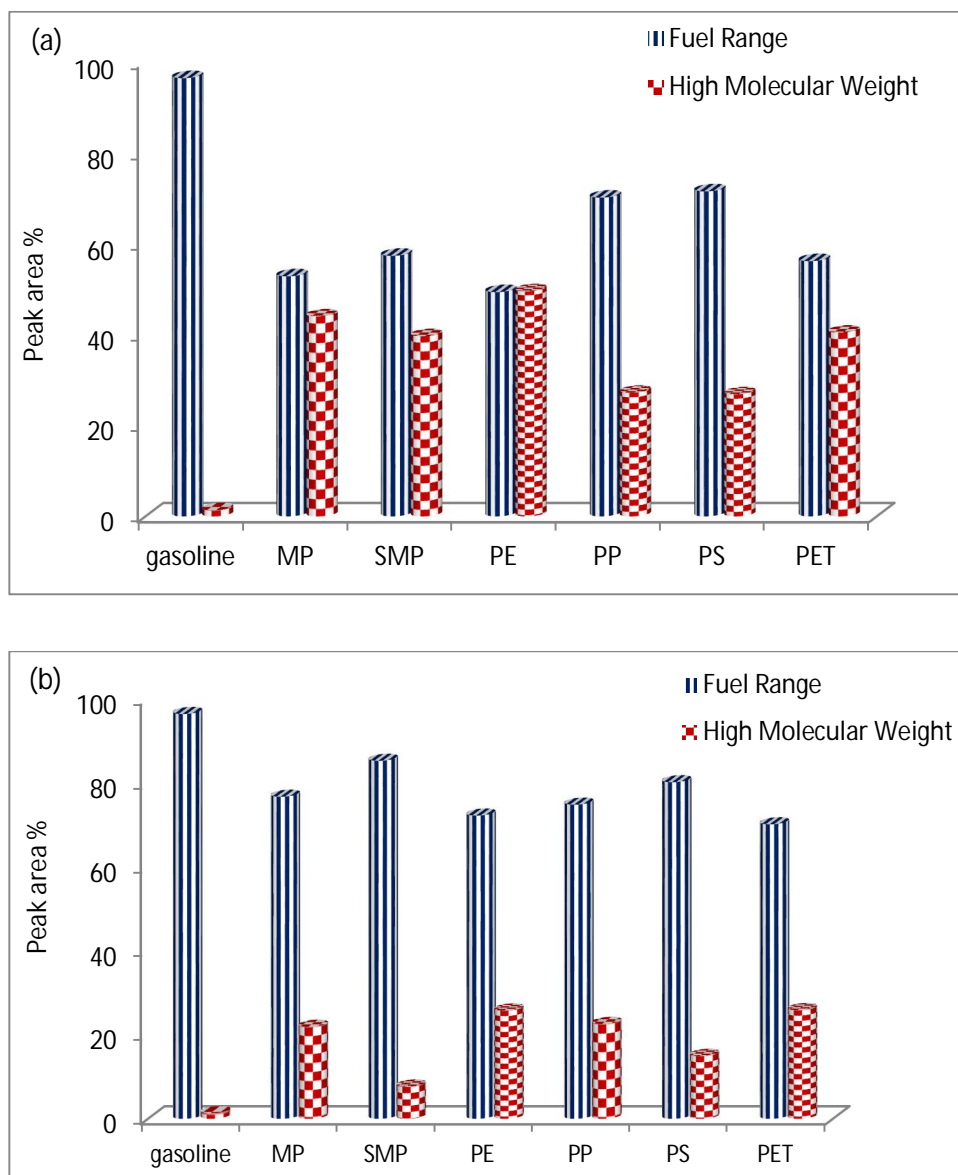


Figure 6.5-1 Influence of HZSM-5 on the distribution of fuel range (F.R.) and high molecular weight (HMWt) compounds in non-catalysed (a) and catalysed (b) product oil from processing MP, SMP and virgin plastics (PE, PP, PS, PET) in comparison to gasoline

The product yield from the pyrolysis-catalysis of the plastics shown in Figure 6.3-1 showed a decrease in oil yield when the Zeolite catalyst

introduced to the second stage of the pyrolysis/catalysis process. However, the composition of the oils was greatly influenced by the presence of the catalyst. Thus, Figure 6.5-1 shows the influence of the addition of zeolite HZSM-5 catalyst addition on the fuel range (i.e. C₅-C₁₅) and the high molecular weight (i.e. C₁₆₊) hydrocarbon compounds, for the uncatalyzed (a) and catalyzed (b) product oils, respectively. The results of the fuel range and high molecular weight hydrocarbons were compared to standard gasoline hydrocarbons. The uncatalyzed pyrolysis of the plastic samples showed a high proportion of fuel range hydrocarbons, but also significantly a high content of the high molecular weight hydrocarbons from C₁₆ and above. However, in the presence of the catalyst, the fuel range hydrocarbons dominate the composition of the product oil. Sakata et al. [19], investigated the pyrolysis and catalytic pyrolysis of polyethylene and polypropylene for several different catalysts, including zeolite ZSM-5. For the processing of polyethylene, they reported a pyrolysis oil yield of 69.3 wt. % which decreased to 49.8 wt.% when zeolite ZSM-5 catalyst was present, with a corresponding rise in gas yield from 9.60 wt. % to 44.3 wt. %. They also reported for polypropylene an oil yield of 80.1 wt.% for thermal pyrolysis that decreased to 47.0 wt. % with the zeolite catalyst and gas yield increased from 6.6 wt. % to 50.0 wt. %. They attributed the changes to be due to the strong surface acidity of the zeolite ZSM-5 catalyst that promoted the degradation and or cracking of the heavier hydrocarbons into lighter hydrocarbons. Although the oil yield was reduced with the catalyst, Sakata et al.[19] showed that the majority of the hydrocarbons in the product oil had a carbon number distribution in the

gasoline range compared to the uncatalyzed pyrolysis oil with a significantly higher carbon number distribution.

The product oils from the thermal pyrolysis and catalytic pyrolysis of the plastic samples were analyzed for their fuel properties by simulated distillation using gas chromatography to determine the boiling range distribution of the oils. The results are shown in Figure 6.5-2.

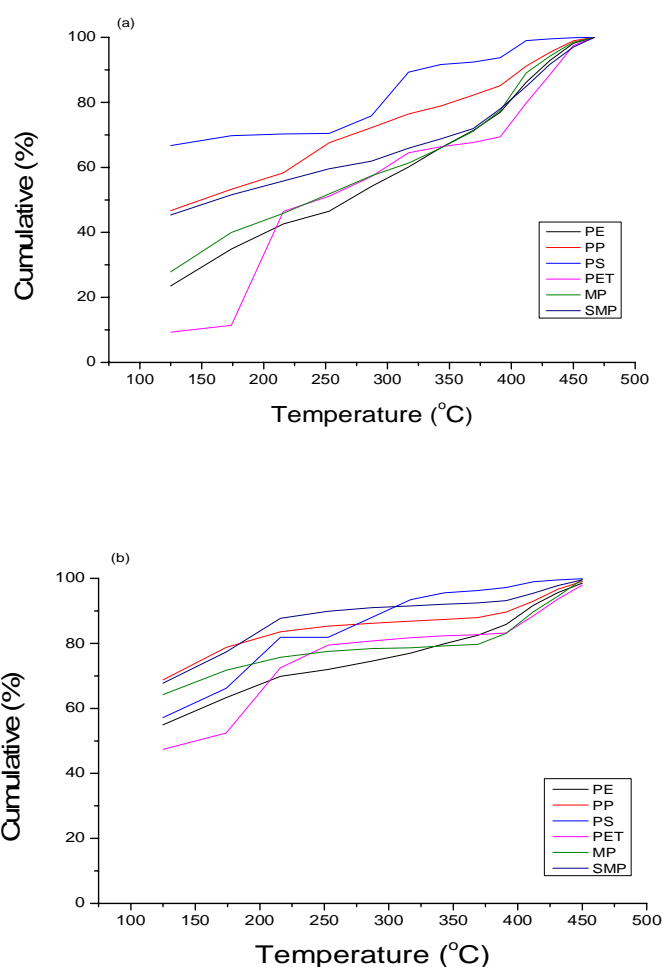


Figure 6.5-2 Simulated distillation of (a) the uncatalyzed pyrolysis oil and (b) the pyrolysis-catalysis product oils.

The uncatalyzed oils showed that a significant fraction of the oils has a boiling point range of greater than 250 °C; however, the catalytic pyrolysis product

oils show a shift to lower boiling points, reflecting the shift in molecular weight range as shown in Figure 6.5-1. Although there was an improvement in the properties of the product oils in the presence of the catalyst, boiling range distributions for gasoline would be >95% below 150 °C. However, for the pyrolysis–catalysis product oils, the boiling range fraction below 150 °C was between 50% and 70%.

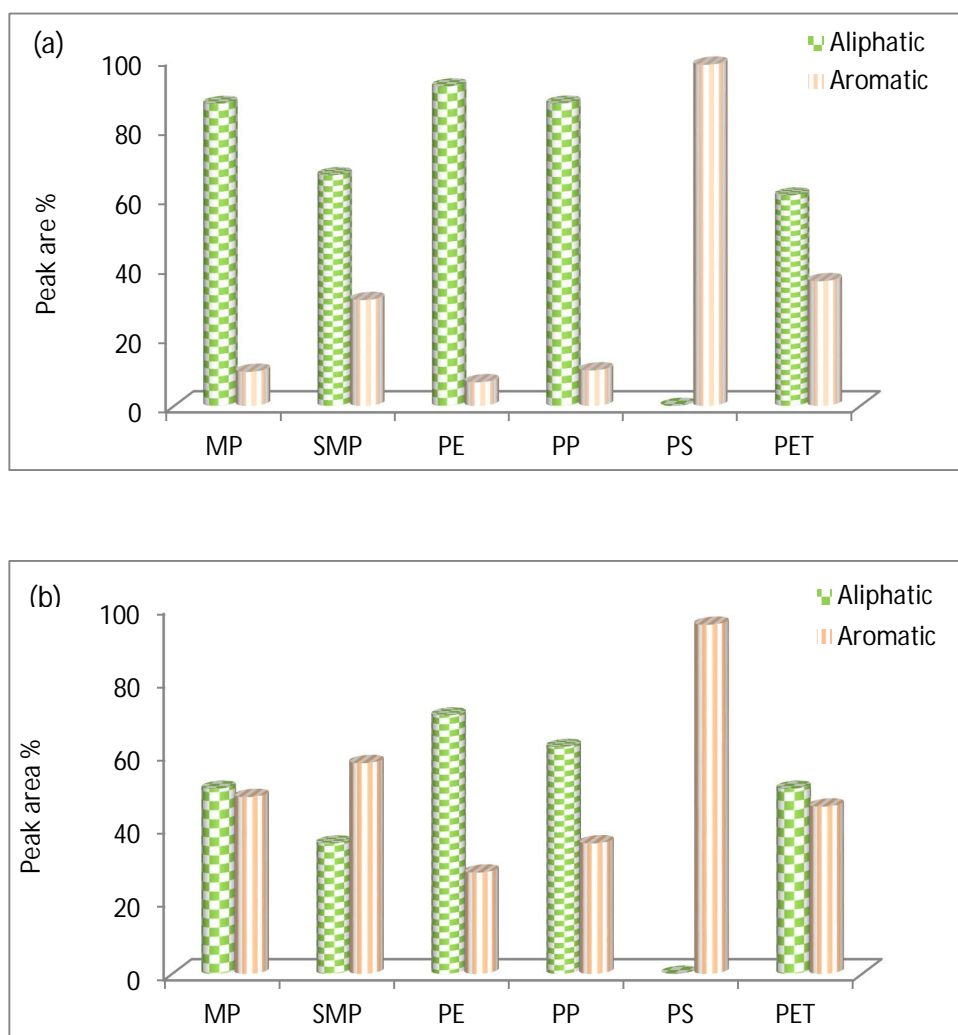


Figure 6.5-3 Distribution of aliphatic and aromatics hydrocarbons in (a) non-catalysed and (b) catalysed (b) product oil from processing of real world plastics (MP), the simulated mixture of plastics (SMP) and virgin plastics (PE, PP, PS, PET).

The hydrocarbon composition of the oils produced from the pyrolysis and pyrolysis-catalysis of the plastic samples presented as fuel range (C_5 - C_{15}) and the high molecular weight (C_{16+}) hydrocarbons shown in Figure 6.5-1. It may also be presented in terms of their aromatic and aliphatic content. Thus, the Figure 6.5-3 shows the composition of the product oils from pyrolysis (a) and, also the pyrolysis-catalysis (b) of the three categories of plastics. The plastics include real-world plastics (MP), the simulated mixture of plastics (SMP) and virgin plastics (PE, PP, PS, PET). Accordingly, for the plastic samples containing the polyalkene polymers (MP, SMP, PE, PP), the oil produced from pyrolysis was mainly aliphatic in nature. However, the polystyrene and polyethylene terephthalate produced an aromatic oil derived from the aromatic nature of the polymer structure. The polyethylene and polypropylene pyrolysis oil would be expected to be almost wholly aliphatic in content, but there was some aromatic content. These aromatics present may be due to the cracking reactions over the sand placed in the second stage reactor (for the uncatalysed experiments), also resulting in an extended time in the hot zone of the reactor. Abbas-Abadi et al. [20], have reported an aromatic content of 10% in the pyrolysis oil from pyrolysis of polypropylene in a semi-batch reactor. Jung et al. [21], too reported an aromatic content of ~25 wt.% for the pyrolysis of polypropylene using a fluidised bed reactor, at 668 °C (a higher temperature than used in this work). Both Abbas-Abadi et al. [20] and Jung et al. [21] reported increasing aromatic content in the product oils with increasing temperature. The PET produced an oil which consisted of a mainly aromatic content with benzoic acid detected in large quantities (~30 wt. %). Jing et al. [18], in their work proposed a mechanistic model as shown in Figure 5.5-5.

The model considers only the main reactions (chain initiation, intermolecular hydrogen transfer, intramolecular hydrogen transfer, and β -scission) to evaluate the interaction between PP and LDPE.

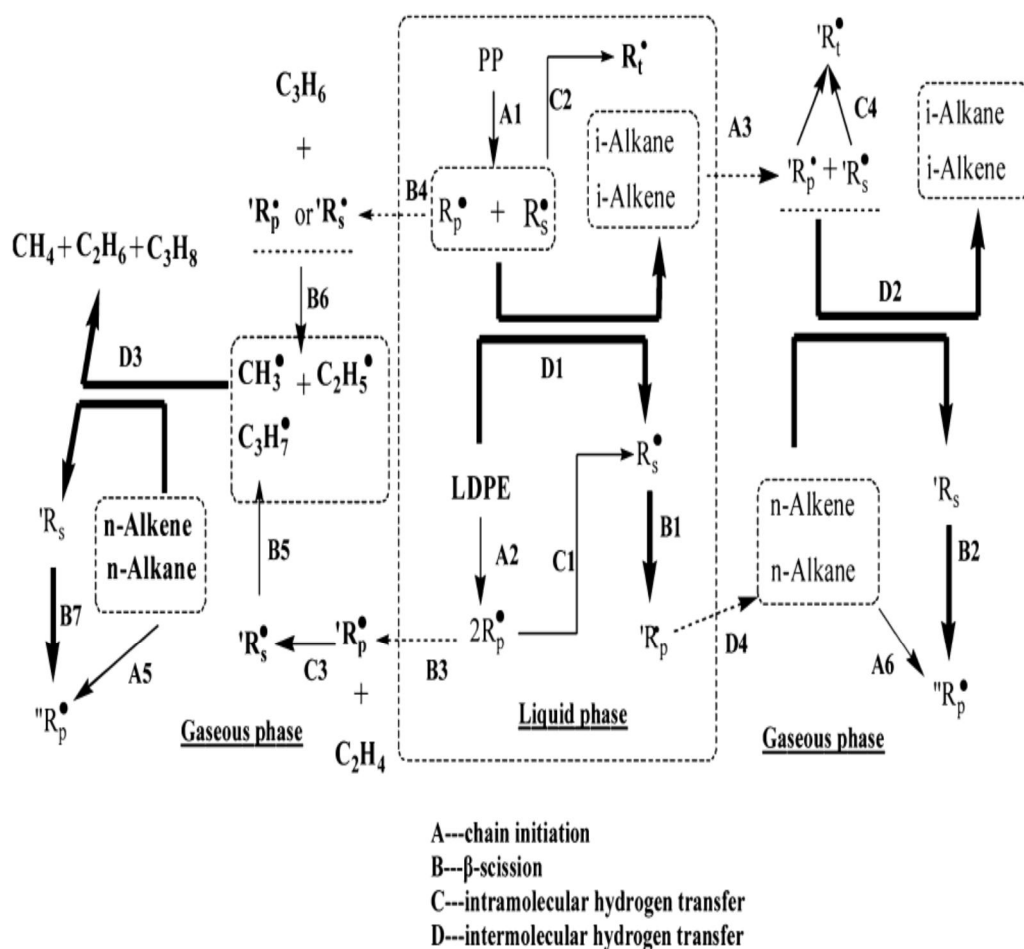


Figure 6.5-4 Jing et. al.[18] proposed interaction scheme by enhanced intermolecular hydrogen transfer.

The model revealed that there were more radical from thermal degradation of PP in Figure 6.5-4 (feature A1) than the thermal degradation of PE (feature A2) in the initial process. Decomposition of PP provides PE with more radical (R_p or R_s) which after intermolecular hydrogen transfer from PE and a β -scission, respectively (feature D1 and B1), the reaction path of PE taken. Consequently, the initial reaction of PE degradation is enhanced by chain

transfer reaction with R_p or R_s . The model further shows that PP radicals (R_p or R_s) abstract hydrogen from PE or their cracked products (D1, D2 and so on) to form i-alkanes or i-alkenes. Whereas PE and their cracked products degrade to form shorter-chain n-alkanes or n-alkenes by β -scission, followed by intermolecular hydrogen transfer (feature B1 and D4).

When the zeolite HZSM-5 catalyst was introduced into the process, the aromatic content of the product oils increased significantly with a decline in the aliphatic content of the oils. The polyalkene plastics, PE and PP, and the MP and SMP plastic mixtures, (both of which were dominated by PE and PP), produced oils with a marked rise in aromatic content in the presence of the zeolite ZSM-5 catalyst. For aromatic containing polymers, polystyrene and polyethylene terephthalate, the product oils from the thermal pyrolysis had a higher aromatic content which further increased when the catalyst was present in the process. The benzoic acid found in the oil from the thermal pyrolysis of PET was reduced in the presence of the zeolite catalyst being cracked to mainly toluene.

Kumar et al. [15], discussed broadly on the thermo catalytic degradation mechanism of the polymer. They emphasized that it is a well-known fact, that the thermal cracking of plastic occurs by a radical mechanism, where the effect of heat forms the initiating radicals. Conversely, Kumar et al. [15], regard catalytic cracking of polymer to proceed generally through carbenium ions. They consider that the ion are produced by the abstraction of H^- ion from the polymer (as catalyst acts as Lewis acid), or the addition of H^+ to it (catalyst acts as Bronsted acid) as an initial step. But further cracking of the fragment formed in the first cracking reactions occur, into lower molecular weight

hydrocarbons at the active sites of the catalyst. Therefore, the unstable primary fragments are cracked in further decomposition reaction. Kumar et al. [15], identified the following elemental reactions to take place both in thermal and thermo-catalytic cases.

(a) Initiation

(b) Formation of secondary radicals

- Depolymerization, formation of monomers;
- Favorable and unfavorable hydrogen transfer reaction;
- Intermolecular hydrogen transfer (formation of paraffins and dienes);
- Isomerization via vinyl groups;

(c) Termination by disproportionation or recombination of radical.

The details of the elementary reactions discussed below;

(a) Initiation

Thermo-catalytic degradation initiation mechanism is partly radical [15]. Hence, the cracking of C-C bond occurs by homolytic cracking of C-C bonds, in regions with structural faults or distortion of the electron cloud. Kumar et al [15], cited that thermal decomposition of HDPE as initially proceeds basically by random scission mechanisms. However, catalytic cracking proceeds through a carbenium ion from a polymer or the addition of proton in the polymer macromolecule in the initial step of the reaction [22]. The Figure 6.5-6 below shows that initial step for the reaction of HDPE.

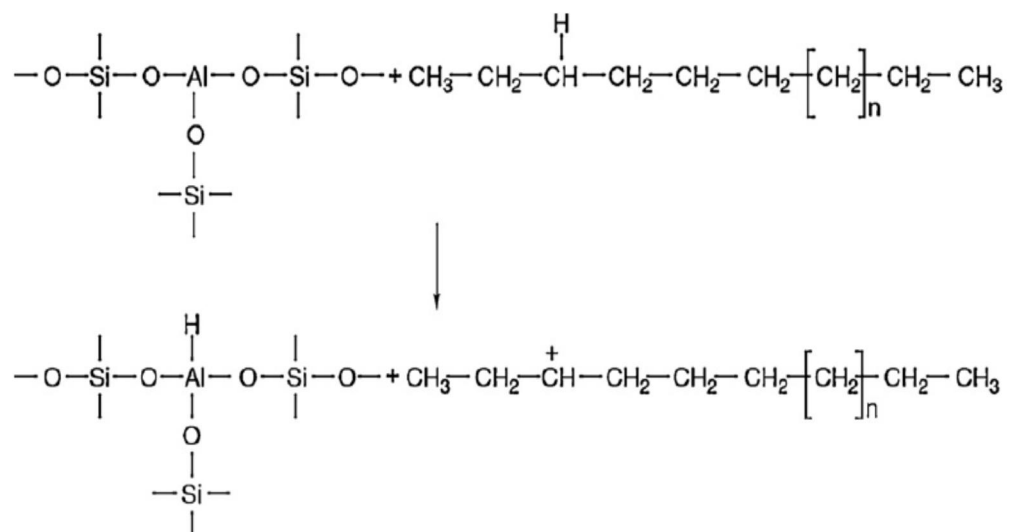


Figure 6.5-5 Initiation mechanism of HDPE via carbenium ion [15]

Consequently, C-C bond dissociation is the more probable in initiation step, this happens as the C-C bond (347 KJ/mol.) is weaker than the C-H bond (413 KJ/mol.). However, both C-C bond and C-H bond dissociated at high temperatures, and almost only C-C bond does so at low temperature. So, the initial step in thermal degradation is random scission to unstable hydrocarbon radicals [24]. Hence, smaller differences were found between thermal and thermo-catalytic degradation with respect to yields and structure of products at higher temperatures (450-500 °C) than that at a lower temperature (400-420 °C)[15]. Kumar et al. [15], summoned that the concentration of isoparaffin and olefins increased with decreasing temperature, They suggest that it as a result of the increase in further degradation of branched hydrocarbons, and which is greater than that of non-branched with increasing temperature. Hence, similar phenomena could be observed in the case of catalysts

possessing a weak hydrogenation property accompanied by considerable acidity because the olefin intermediates formed are isomerized in greater ratio on the acidic sites of catalysts. On the other hand, the probability of isomerization, but catalysts activity is decreasing with decreasing of the catalyst.

(b) Formation of unstable secondary compounds

The unstable secondary compounds of lower molecular weight formed from unstable molecular fragments (radicals and ions). These are formed in the initiating reaction as a result of further decomposition reaction with uncracked macromolecules of polymer or radicals and ions. Figure 6.5-7 shows the different reactions that occur in a second step; these include β -scission, isomerization of carbon framework, isomerization of the double bond and hydrogen transfer reactions.

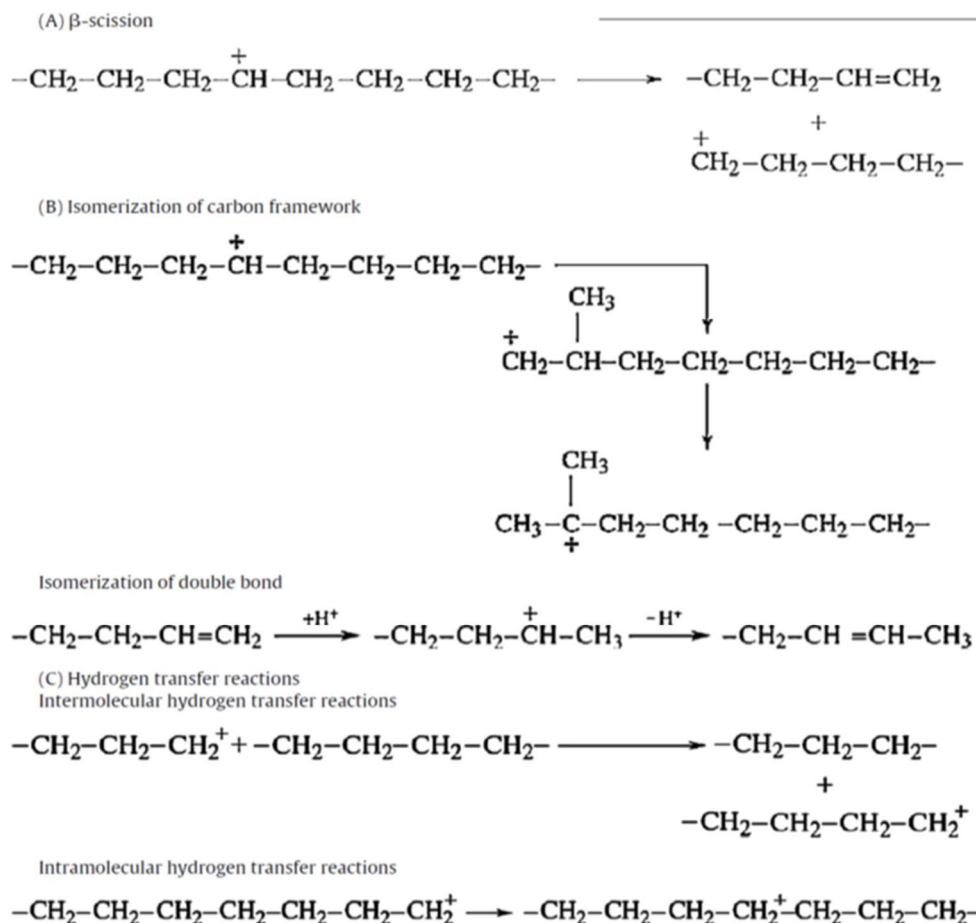


Figure 6.5-7 the different reactions in the second step of the polymer degradation mechanism[15].

But, the different radicals formed in the thermal pyrolysis, from random scission are capable of stabilizing themselves either by H-abstraction or β -scission, all of which form stable molecules [15]. However; temperature determines which reaction would be favored for stabilization. Thus, at low temperature (200-300 °C) abstraction is the preferred route for radical stabilization leading to higher hydrocarbons. Then, at high temperature (300 °C) other reactions such as intermolecular H-transfer and intramolecular H-transfer, β -scission, etc. become important. So, some lighter hydrocarbons beyond 300 °C are formed due to intermolecular H-transfer followed by a β -

scission. Dimers, trimers, tetramers, pentamers, etc. are produced via 1, 5 H-transfer. Hujjuri et al. [23], reported that β -scission and or depolymerization is responsible for the production of lower molecules at 400-500 °C. So, lighter hydrocarbons beyond 300 °C are formed due to intermolecular H-transfer. Kumar et al. [15], noted that the formation of aromatic by Diels-Alders reaction is possible at a higher temperature. The primary unstable fragment reacts with alkenes. Thus, polyenes might be the precursor of benzene.

(c) Termination with recombination or disproportionation

Recombination or disproportionation of an unstable fragment from primary and secondary cracking could stabilize these products. Consequently, due to the recombination the molecular weight and branching of products might be significantly increased. Likewise, cyclization, aromatization or polycondensation are other ways of termination. These reactions above result in forming cyclic alkenes, alkenes, mono and polynuclear arenes or coke [15]. Figure 6.5-8 shows cyclization and aromatization as a termination strip of the degradation products of polymer.

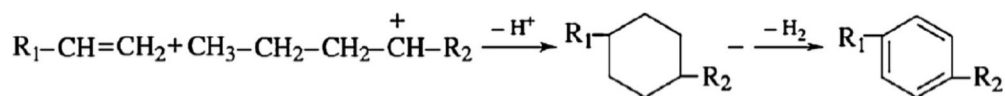


Figure 6.5-6 Cyclization and aromatization as termination step for degradation mechanism of the polymer

Zeolite catalysts are known to produce aromatic hydrocarbons during catalytic pyrolysis of plastics because of the properties of surface area, porosity, and silica: alumina ratio. The silica: alumina ratio influences the surface acidity of the catalyst with lower ratios (higher relative surface alumina concentration)

producing an increase in the surface acidity of the catalyst [24]. For zeolite catalyst, surface acidity equates with catalytic activity, and the manipulation of the pore size of the zeolite structure enables reaction selectivity. It has been shown that low silica:alumina ratio catalysts with consequently higher surface acidity and surface catalytic activity produce oils with increased content of aromatic compounds from the pyrolysis–catalysis of PE using different zeolite catalysts [6, 25]. The zeolite HZSM-5 catalyst used in this work had a Si: Al ratio of 50, which is relatively high, and consequently the catalysts had a relatively lower surface acidity and catalyst activity for aromatic hydrocarbon production. The influence of the pore size of zeolite catalysts is through the restriction of the size of the hydrocarbon molecule which can enter the pore structure and participate in catalytic reactions of cracking and reformation which produce the aromatic hydrocarbons [24]. Therefore, any large molecular weight materials which are formed from the pyrolysis of the plastic would have to be thermally decomposed on the catalyst surface before they could enter the controlled pore size of the catalyst. Kumar et al [15], have discussed, in detail, the role of catalysts, including zeolite catalysts, in the mechanism of catalytic thermal degradation of plastics. They summarized the main steps of catalytic pyrolysis as diffusion on the catalyst surface, adsorption, chemical reaction, desorption from the catalyst, and diffusion in the liquid phase.

Table 6.5-1 Evaluation of possible Interaction of plastics during pyrolysis of the simulated mixture of plastics using aliphatic and aromatic components

	Thermal	
	Actual	Expected
	(Peak area %)	(Peak area %)
Aliphatic	66.49	79.84
Aromatic	30.53	18.63
	Catalytic	
	Actual	Expected
	(Peak area %)	(Peak area %)
Aliphatic	35.53	58.45
Aromatic	57.47	38.75

Table 6.5-1 shows the aliphatic and aromatic hydrocarbon content of the product oil for the pyrolysis and pyrolysis–catalysis of the simulated mixed plastics (SMP) compared with the expected content based on the proportions of the individual plastics. The aromatic and aliphatic content of simulated plastic and collective yield of the individual plastics that make up the simulated plastics compared, and evaluated for a possible interaction between the plastics. The aromatic hydrocarbon content in the oils from the pyrolysis and pyrolysis–catalysis of the simulated mixed plastics was significantly higher than expected from the proportions derived from the individual virgin plastics. This increase in aromatic content in the product oils suggests there is some interaction of the individual virgin plastic that composed the SMP. Jing et al [18], reported that for pyrolysis of a 30:70 mixture ratio of PE and PP. They found there was an increase in the aromatic content of the product oil

compared to the expected concentration of aromatics derived from the proportions of the individual plastics, suggesting significant interaction. Williams and Williams [12], mixed polystyrene in binary mixtures with HDPE, LDPE, PP, PVC, and PET and analyzed the product oil from pyrolysis of the mixtures. It was reported that the concentration of single-, two-, and three-ring aromatic hydrocarbons in the product oil was influenced by the interaction of each plastic with the polystyrene.

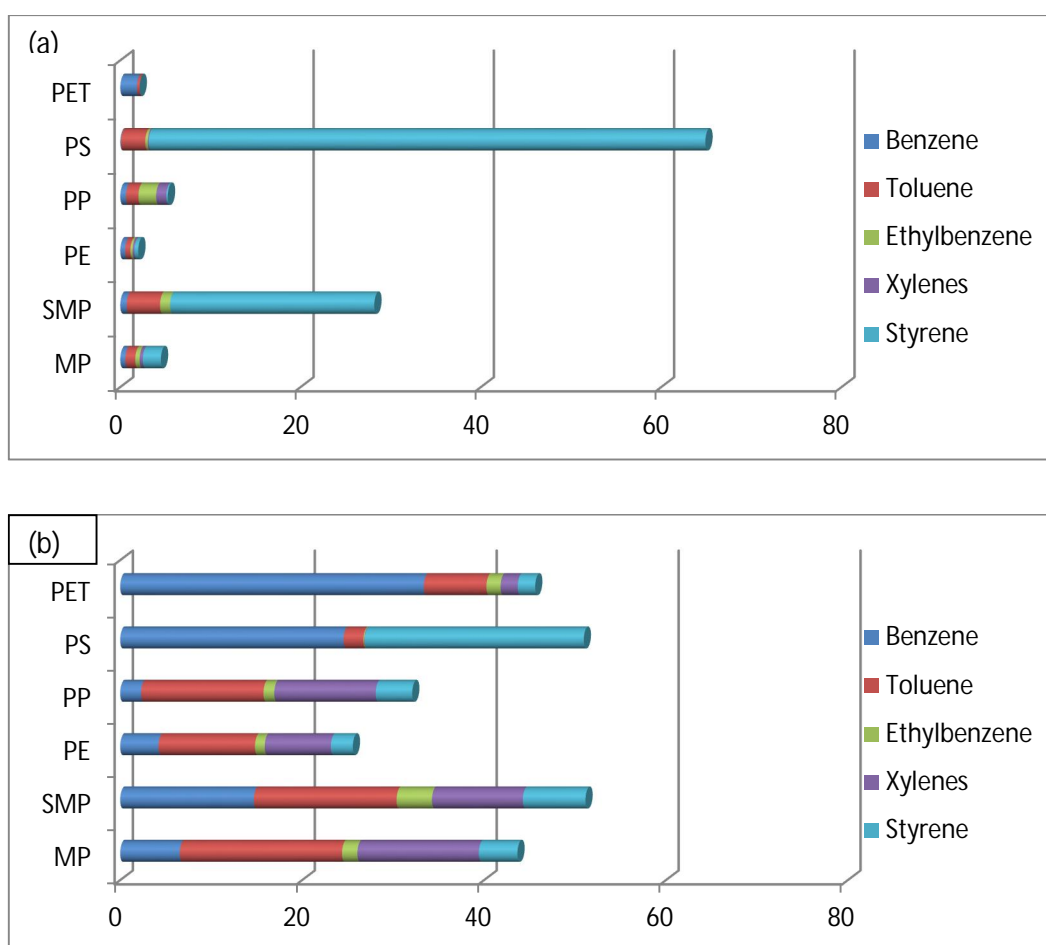


Figure 6.5-7 Yields of some selected aromatic compounds in (a) non-catalysed and (b) catalysed (b) product oil from processing of real world plastics (MP), the simulated mixture of plastics (SMP) and, virgin plastics (PE, PP, PS, PET).

The aromatic hydrocarbons in the product oils from the pyrolysis and pyrolysis–catalysis of the plastic samples are shown in Figure 6.5-9a, b. The results are expressed in terms of the peak area in relation to the gas chromatogram obtained from the analysis. The results show that the uncatalyzed pyrolysis oil (Figure 6.5-9a) for the polystyrene contained mainly styrene, derived from the polystyrene polymer. Park et al [10], have also reported high concentrations of styrene for thermal pyrolysis of polystyrene, for example, 76.31 wt. % styrene was reported at a pyrolysis temperature of 450 °C. The simulated plastic mixture also contained significant amounts of styrene, but more than would be expected based on the simulated composition, suggesting that there was some interaction between the plastics. Lopez et al [14], investigated the pyrolysis and pyrolysis–catalysis of a mixture of plastics and reported a higher than expected content of styrene, as also reported here for the simulated mixture of plastics. Lopez et al [14], also suggested that other mechanisms such as secondary reactions could result in the higher styrene content.

The main aromatic compounds produced from catalytic pyrolysis of the plastic samples with zeolite HZSM-5 catalyst shows (Figure 6.5-9b). They are mainly single-ring aromatic compounds with benzene, toluene, ethylbenzene, xylenes, and styrene accounting for a significant proportion as reported by others [2 14 26]. Benzene produced in high yield for the pyrolysis–catalysis of the plastic samples, but particularly for PET and for SMP as the catalyst was introduced, while styrene yields reduced. The reduction of styrene concentration in the presence of a zeolite catalyst has been attributed to the

carbenium nature of the acid catalyzed decomposition of polystyrene leading to the formation of aromatic products other than styrene [27]. For a simulated mixture of plastics processed at 500 °C, Lopez et al [14], reported toluene concentrations (% peak area) of 8.1% for pyrolysis which increased to 17.5% in the presence of a zeolite ZSM-5 catalyst, ethylbenzene increased from 5.0% to 9.6%, and xylenes increased from <3.0% to 13.8%. Bagri and Williams[28] investigated the pyrolysis and pyrolysis–catalysis of polystyrene in a fluidized bed reactor using a zeolite ZSM-5 catalyst. The uncatalyzed pyrolysis oils were found to contain large amounts of styrene. However, the addition of zeolite catalyst resulted in a marked decrease in styrene concentration in the product oils and increased concentrations of monoaromatic compounds. Lin and White [29], also reported that the thermal degradation of polystyrene produces high yields of styrene, but catalytic pyrolysis with ZSM-5 catalyst markedly reduced styrene concentration and increased the production of benzene; in addition, ethyl benzene and toluene were also formed at lower concentrations. Similarly, Aguado et al. [30], investigated the influence of the operating variables on the catalytic conversion of a polyolefin mixtures over HMCM-41 and nanosized n-HZSM-5. They proposed reaction pathway as shown by Figure 6.5-10

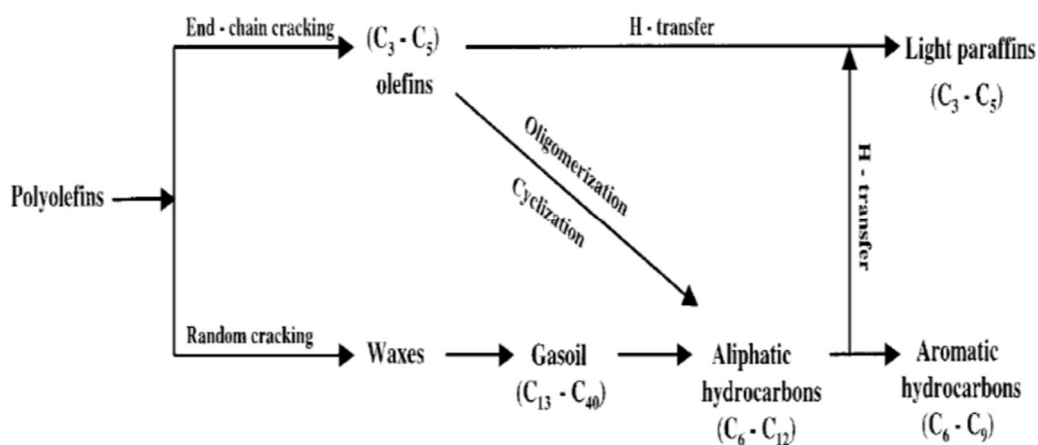


Figure 6.5-8 Aguado et. al,[30] proposed reaction pathways in the (catalytic) conversion of polyolefins mixtures

Consequently, due to the addition of n-HZSM-5 zeolite, the cracking takes place on the external surface of the crystal, yielding mainly light olefin as the primary products coming from the an-end-chain scission mechanism. The olefins undergo subsequent oligomerization and cyclization reactions, leading to heavier aliphatic hydrocarbons. Likewise, aromatic are formed from hydrogen transfer reaction from the aliphatic products to gaseous olefins and favor the transformation of olefins into paraffin. However, cracking the polyolefins on HMCM-41 crystal occur mainly within its mesopores yielding waxes as the primary products, but the contribution from thermal degradation cannot be discarded.

Summary

A two-stage pyrolysis–catalysis fixed bed reactor was used to investigate the product yield, composition, and hydrocarbon distribution from the pyrolysis of plastics. And the pyrolysis–catalysis of real-world mixed plastics, simulated mixed plastic, and four virgin plastics in the presence of a zeolite HZSM-5 catalyst. For the uncatalyzed pyrolysis of the plastics, a high yield of oil/wax was obtained for the plastic material in the range of 81–97 wt. %. The yield of oil/wax decreased with the addition of a catalyst to between 44 and 51 wt. %, depending on the plastic, with a resultant increase in gas yield. However, the composition of the pyrolysis–catalysis oils significantly increased in aromatic hydrocarbon content. Accordingly In addition, the composition of the oils shifted from high molecular weight hydrocarbons (C₁₆₊) to fuel range hydrocarbons (C₅–C₁₅), with a high content of single-ring aromatic hydrocarbons such as benzene, toluene, ethylbenzene, xylenes, and styrene. The yield and composition of the products obtained from the pyrolysis and pyrolysis–catalysis of the simulated mixture of plastics (PE, PP, PS, PET) were compared with those obtained from the expected results based on the individual plastic data. The results showed that there was interaction between the plastics in the simulated plastic mixture resulting in a yield of the C₂, C₃, and C₄ gases that was higher than expected in the proportions of each gas generated by the individual virgin polymers. Also, the aromatic hydrocarbon content of the oils from the simulated mixture of plastics (SMP) was also higher than expected.

References

1. *Muhammad, C., Onwudili, J.A. and Williams, P.T., Thermal Degradation of Real-World Waste Plastics and Simulated Mixed Plastics in a Two-Stage Pyrolysis-Catalytic Reactor for Fuel Production. Energy & Fuels, 2015. 29(4): p. 1601-1609.*
2. *Serrano, D.P., Aguado, J. and Escola, J.M., Developing Advanced Catalysts for the Conversion of Polyolefinic Waste Plastics into Fuels and Chemicals. Acs Catalysis, 2012. 2(9): p. 1924-1941.*
3. *Bajus, M. and Hájeková, E., Thermal cracking of the model seven components mixed plastics into oils/waxes. Petroleum & Coal, 2010. 52(3): p. 164-172.*
4. *Lin, Y.-H., Production of valuable hydrocarbons by catalytic degradation of a mixture of post-consumer plastic waste in a fluidized-bed reactor. Polymer Degradation and Stability, 2009. 94(11): p. 1924-1931.*
5. *Lee, K.-H. and Shin, D.-H. Characteristics of liquid product from the pyrolysis of waste plastic mixture at low and high temperatures: Influence of lapse time of reaction. Waste Management, 2007. 27(2).*
6. *Pinto, F., Costa, P., Gulyurtlu, I. and Cabrita, I., Pyrolysis of plastic wastes. 1. Effect of plastic waste composition on product yield. Journal of Analytical and Applied Pyrolysis, 1999. 51(1-2).*
7. *Ateş, F., Miskolczi, N. and Borsodi, N. Comparison of real waste (MSW and MPW) pyrolysis in batch reactor over different catalysts. Part I: Product yields, gas and pyrolysis oil properties. Bioresource technology, 2013. 133: p. 443-454.*
8. *Lopez-Uriónabarrenechea, A., de Marco, I., Cabellero, B.M., Laresgoiti, M.F. and Adrados, A., Catalytic stepwise pyrolysis of packaging plastic waste. Journal of Analytical and Applied Pyrolysis, 2012. 96(0): p. 54-62.*
9. *Brebu, M., Bhaskar, T., Murai, A., Sakata, Y. and Uddin, M.A., The effect of PVC and/or PET on thermal degradation of polymer mixtures containing brominated ABS. Fuel, 2004. 83(14): p. 2021-2028.*
10. *Park, J.J., Park, K., Kim, J.S., Maken, S., Song, H., Shin, H., Park., J.W. and Choi, M.J., Characterization of styrene recovery from the pyrolysis of waste expandable polystyrene. Energy & fuels, 2003. 17(6): p. 1576-1582.*

11. Achilias, D.S., Kanellopoulou, I., Panagiotis, M., Antonakou, E. and Lappas, A.A., *Chemical recycling of polystyrene by pyrolysis: potential use of the liquid product for the reproduction of polymer. Macromolecular Materials and Engineering*, 2007. **292**(8): p. 923-934.
12. Williams, P.T. and Williams, E.A. *Interaction of plastics in mixed-plastics pyrolysis. Energy & Fuels*, 1999. **13**(1): p. 188-196.
13. Aguado, J., Serrano, D.P. and Escola, J.M., *Fuels from Waste Plastics by Thermal and Catalytic Processes: A Review. Industrial & Engineering Chemistry Research*, 2008. **47**(21).
14. López, A., de Marco, I., Cabellero, B.M., Laresgoiti, M.F., Adrados, A. and Aranzabal, A., *Catalytic pyrolysis of plastic wastes with two different types of catalysts: ZSM-5 zeolite and Red Mud. Applied Catalysis B: Environmental*, 2011. **104**(3): p. 211-219.
15. Kumar, S., Panda, A.K. and Singh, R. *A review on tertiary recycling of high-density polyethylene to fuel. Resources, Conservation and Recycling*, 2011. **55**(11): p. 893-910.
16. Williams, P.T., *Yield and composition of gases and oils/waxes from the feedstock recycling of waste plastic. Feedstock Recycling and Pyrolysis of Waste Plastics: Converting Waste Plastics into Diesel and Other Fuels*, 2006: p. 285-313.
17. Aguado, J., Serrano, D.P., San Miguel, G., Castro, M.C. and Madrid, S., *Feedstock recycling of polyethylene in a two-step thermo-catalytic reaction system. Journal of analytical and applied pyrolysis*, 2007. **79**(1): p. 415-423.
18. Jing, X., Zhao, Y., Wen, H. and Xu, Z., *Interactions between low-density polyethylene (LDPE) and polypropylene (PP) during the mild cracking of polyolefin mixtures in a closed-batch reactor. Energy & Fuels*, 2013. **27**(10): p. 5841-5851.
19. Sakata, Y., Uddin, M.A. and Muto, A., *Degradation of polyethylene and polypropylene into fuel oil by using solid acid and non-acid catalysts. Journal of Analytical and Applied Pyrolysis*, 1999. **51**(1): p. 135-155.
20. Abbas-Abadi, M.S., Mehdi, N., Yaganeh, H. and McDonald, A.G., *Evaluation of pyrolysis process parameters on polypropylene degradation products. Journal of Analytical and Applied Pyrolysis*, 2014. **109**: p. 272-277.
21. Jung, S.-H., Chio, M.H., Kang, B.S. and Kim, J.S., *Pyrolysis of a fraction of waste polypropylene and polyethylene for the recovery of*

- BTX aromatics using a fluidized bed reactor. Fuel Processing Technology, 2010. 91(3): p. 277-284.*
22. Chan, J. and S. Balke, *The thermal degradation kinetics of polypropylene: Part III. Thermogravimetric analyses. Polymer degradation and stability, 1997. 57(2): p. 135-149.*
 23. Hujuri, U., Ghoshal, A.K. and S. Gumma, S., *Temperature-dependent pyrolytic product evolution profile for low-density polyethylene from gas chromatographic study. Waste management, 2010. 30(5): p. 814-820.*
 24. Venuto, P.B. and E.T. Habib Jr, *Fluid catalytic cracking with zeolite catalysts. 1979. Marcel Dekker, Inc. New York.*
 25. Al-Salem, S., Lettieri, P., and Baeyens, J., *Recycling and recovery routes of plastic solid waste (PSW): A review. Waste management, 2009. 29(10): p. 2625-2643.*
 26. Bagri, R. and Williams, P.T., *Catalytic pyrolysis of polyethylene. Journal of analytical and applied pyrolysis, 2002. 63(1): p. 29-41.*
 27. Serrano, D., Aguado, J. and Escola, J. *Catalytic conversion of polystyrene over HMCM-41, HZSM-5 and amorphous SiO₂-Al₂O₃: comparison with thermal cracking. Applied Catalysis B: Environmental, 2000. 25(2): p. 181-189.*
 28. Bagri, R. and Williams, P.T., *Fluidised-bed catalytic pyrolysis of polystyrene. Journal of the Institute of Energy, 2002. 75(505): p. 117-123.*
 29. Lin, R. and White, R. L., *Acid-catalyzed cracking of polystyrene. Journal of applied polymer science, 1997. 63(10): p. 1287-1298.*
 30. Aguado, J., Serrano, D.P., Sotelo, J.L., Van Gneken, R. and Escola, J.M., *Influence of the operating variables on the catalytic conversion of a polyolefin mixture over HMCM-41 and nanosized HZSM-5. Industrial & engineering chemistry research, 2001. 40(24): p. 5696-5704.*

Chapter 7 : PYROLYSIS-CATALYSIS OF REAL-WORLD WASTE PLASTICS AND FUTURE SIMULATED MIXED PLASTIC FOR VALUABLE PRODUCTION FUELS AND CHEMICAL FEEDSTOCK

7.1 Introduction

The use of fluid cracking catalyst (FCC) in the oil industries is well established, and the cost of the catalyst is very high. The quantity of spent FCC catalyst thrown away as solid waste has risen significantly in recent years due to the high demand for light and high-quality transportation fuels as well as the changes in feedstock [1]. Thus, the disposal of this type of waste which has been classified as hazardous material in many countries is problematic. So, the use of spent FCC for waste plastic pyrolysis could prove to be a great idea for sustainability. Pu et al. [1], suggested that the utilization of spent FCC catalyst as a raw material in the production of other valuable products is an attractive option, which takes the environmental regulations and economic benefit into consideration. Lee et al. [3], performed a study on the comparison of plastic types for catalytic degradation of waste plastics into a liquid product with spent FCC catalyst in stirred semi-batch operation at 400 °C reaction temperature. Four plastic materials HDPE, LDPE, PP and PS, were considered for product rate and liquid product distribution during catalytic degradation. The authors found that the polyolefin plastics (both PE and PP) produced a liquid yield of between 80-85 %, but polystyrene gave higher liquid and less gas. Thus, the degradation temperature influenced the accumulative liquid product weight by catalytic degradation. Similarly, they showed for all

polyolefin plastics there was a tendency for similar molecular weight distribution of the liquid product. But for PS the liquid products showed an aromatic content of 97% or over and the C₈ aromatic components was about 75%.

This work was based on the predicted future plastic wastes from a review work reported by Delgado et al. [4]. The authors carried out a comprehensive assessment of the environmental advantages and drawbacks of existing and emerging polymer recovery processes, and arrived at a future plastic waste composition. The future municipal solid waste (MSW) generation in Europe was considered and simulated mixed plastic waste was prepared and used for the study. The plastic sample could be known as future simulated mixed plastics (FSMP). Five plastics samples considered in this work were as follows; high-density polyethylene (HDPE), low-density polyethylene (LDPE), polypropylene (PP), polystyrene (PS), polyethylene terephthalate (PET) and simulated mixed plastic prepared from plastics as described by Delgado et al.[4]; and real-world mixed plastics were as earlier described in chapter 3. The proportion of each was as follows; PE 62.0% (HDPE 19.0% and LDPE 43.0%), PP (8.0%), PS (15.0%) and PET (15.0%). However, the catalytic pyrolysis performed in the work used spent FCC catalyst as the main catalyst. The spent FCC catalyst properties have been detailed in chapter 3 section 3.3.3 of this work. The Influence of catalyst loading on the future simulated mixed plastic was carried out. Three pyrolysis temperatures were considered 400 °C, 500 °C and 600 °C.

The catalysts used was spent FCC catalyst, Table 7.1-1 show the characteristic of the catalysts.

Table 7.1-1 Characteristics of spent FCC and the zeolite catalysts used

Catalyst properties	FCC
Zeolite Structure	FCC-Zeolite
Surface area ($\text{m}^2 \text{g}^{-1}$)	148.1
Silica: Alumina ratio	16.4
Cation	-
Na_2O (%)	0.14
Micropore Volume ($\text{cm}^3 \text{g}^{-1}$)	0.032
Mesopore volume ($\text{cm}^3 \text{g}^{-1}$)	-
Pore radius (\AA)	-

For each experiment, 2 g of plastic was pyrolyzed in the fixed bed two-stage batch reactor as described in Chapter 3. The plastic sample was heated from ambient temperature to 500 °C at a heating rate of 10 °C min⁻¹. In order to study the effect of the different catalyst (spent FCC) amount, the catalyst was maintained at a bed temperature of 500 °C. The pyrolysis temperature of 500 °C and nitrogen flow rate 200 ml min⁻¹ maintained throughout all the experimental run. The catalyst bed was prepared by mixing 2 g each catalyst and 2 g of 2 mm sized quartz sand and was supported on quartz wool in the second stage reactor. For comparison, where no catalyst was used, quartz sand (4 g) was substituted for the catalyst. In this work, FCC1 denotes 1g spent FCC and 3 g quartz sand while FCC2 denotes 2 g FCC spent and 2 g quartz sand.

Table 7.1-2 Catalyst and quartz sand mixing proportion

	No catalyst	FCC1	FCC2
Quartz (g)	4	3	2
Catalyst (g)	0	1	2

Results

The various result obtained from the influence of spent FCC loading on pyrolysis of FSMP are discussed in this section.

7.2 Product Yields

Figure 7.1-1 shows the product yield from the pyrolysis and pyrolysis-catalysis of the real-world mixed plastics (MP) and future simulated mixed plastic (FSMP) as well as the five individual virgin plastics .The results of the non-catalytic pyrolysis of these plastics have been discussed earlier. However, the FSMP, HDPE and LDPE, which are the new sample, the yields are given in Table 7.2-1. Lee et al. [3], also observed HDPE, LDPE and PP produced less liquid and more gas than the PS. A similar result was reported for thermal degradation of real-world waste plastics and simulated mixed plastic in a two-stage pyrolysis-catalysis reactor for fuel production [5]. Elordi et al. [6], investigated the cracking on a spent FCC of polyethylene in a conical spouted bed reactor at 500 °C reaction temperature. The authors used HDPE cracked over the spent FCC catalyst and HY zeolite and tested both catalysts mixture agglomerated with bentonite.They observed for thermal cracking of HDPE at 500 °C temperature, waxes (liquid) were the main products as obtained in this work and reported by other [3].

Table 7.2-1 Products Yields for FSMP, HDPE and LDPE thermal pyrolysis

Non-cat	SMP	HDPE	LDPE
Gas (wt. %)	10.3	1.78	9.32
Oil (wt. %)	79.0	98.0	87.5
Char (wt.)	3.5	0.00	0.00
MB (wt. %)	92.8	99.8	96.8

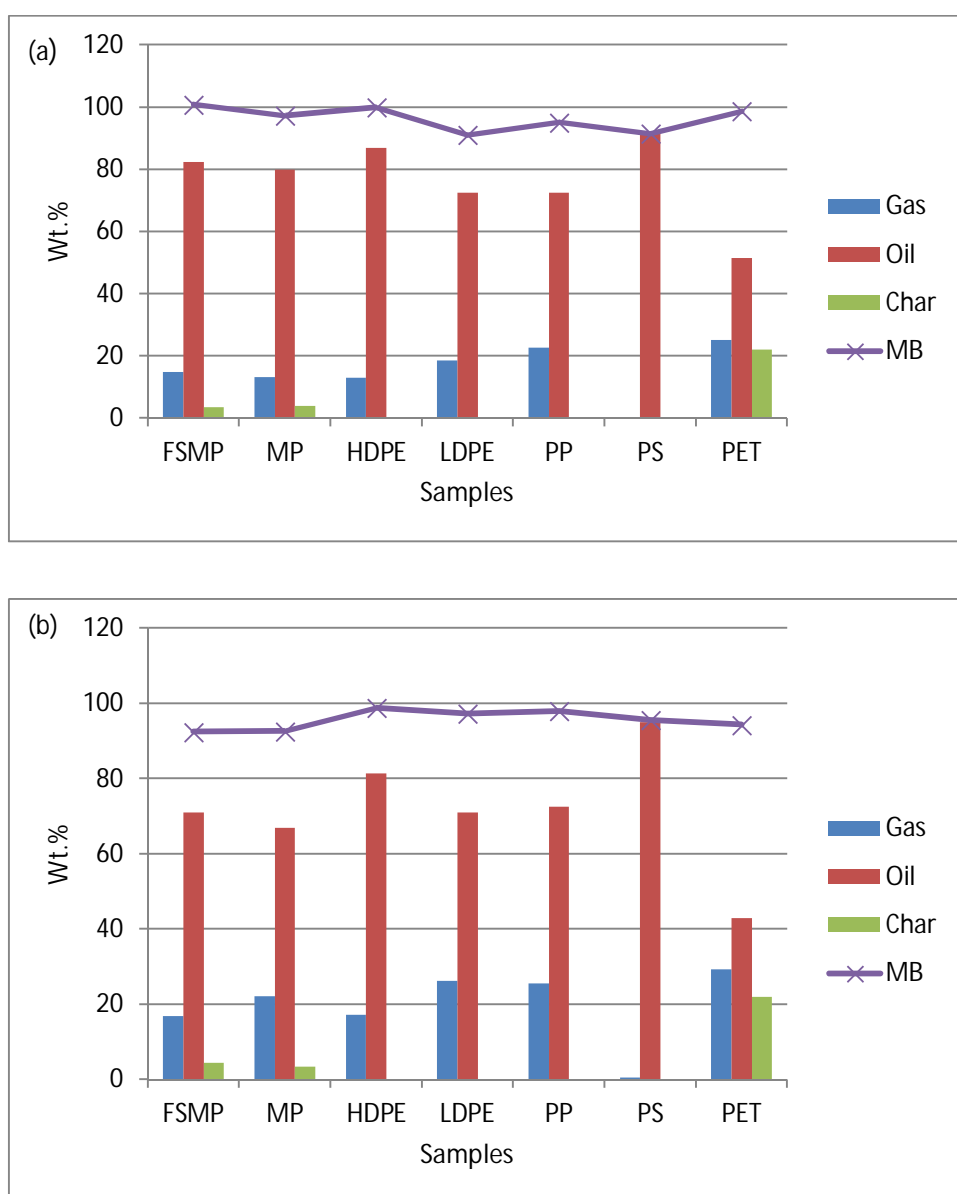


Figure 7.2-1 Product yield for (a) FCC1 and (b) FCC2 catalytic pyrolysis of real-world (MP), the future simulated mixture of plastics (SMP), and virgin plastics (HDPE, LDPE, PP, PS and PET)

Bajus and Hájeková [7] investigated thermal cracking of the model seven components of mixed plastics into oils/waxes in a batch reactor temperatures from 350 to 500 °C. The author obtained the highest liquid product yield at 450 °C for polyolefin and mixed plastics of 85.0 wt.% for PP and lowest yield 75.4 wt.% for mixed plastics (LDPE / HDPE /LLDPE /PP /PVC / PS/ PET). The presence of PET and PVC in the mixed plastic that evolved volatile product (gas phase) contribute to low liquid products. Accordingly, a similar trend was observed in this work as the liquid product from thermal pyrolysis of FSMP (79 wt.%) than HDPE, LDPE, PP and PS. However, the liquid products reduced and gas products rose with introduction of the spent FCC catalyst as showed in the Figure 7.2-1 (b) and (c). Therefore, in the presence of the spent FCC catalysts amount, there was a marked reduction in oil yield and a subsequent increase in gas yield. The decrease in liquid products and subsequent rise in gas products with the introduction of catalyst was reported before [8, 9] [6] [10]. Similarly, the reduction in liquid products and rise in gas products was found to increase with the amount of the catalysts used for the plastics as reported elsewhere [6 11 12].

Gas composition

Tables 7.2-2, 7.2-3 and 7.2-4 (vol.%) and Figure 7.2-2 (wt.%) shows the concentration of the product gases with and without the spent FCC catalyst for the pyrolysis and pyrolysis-catalysis of the real world plastics (MP), the future simulated mixture of plastics (FSMP) and the virgin plastics (HDPE, LDPE, PP, PS, PET). However, Figure 7.2-1 (a) shows that the main gases produced during the thermal pyrolysis of MP, FSMP, HDPE, LDPE and PP in the absence of the spent FCC catalyst were C₂ (mainly ethene with lower

concentrations of ethane), C₃ (mainly propene) and C₄ gases (mainly butene). Hence, these plastic samples consisted of mostly polyolefin polymer structures. Nevertheless, the polyolefin plastic is thermally degraded via a random scission process to produce mainly alkene gases C₂H₄, C₃H₆, and C₄H₈, and to a lesser extent the alkanes gases, C₂H₆, C₃H₈, and C₄H₁₀ [13]. Likewise, the main gases that increased by the addition of the spent FCC catalyst were the C₂-C₄ hydrocarbons. The gases were produced by cracking of the plastics, but carbon monoxide (CO) and carbon dioxide (CO₂) were formed by FSMP and PET samples. The CO and CO₂ yield were influenced by the introduction of the catalyst.

Table 7.2-2 Gas Product composition for thermal pyrolysis of FSMP, HDPE and LDPE plastics

Not-cat	FSMP	HDPE	LDPE
H ₂ (vol. %)	4.55	14.8	5.31
CH ₄ (vol. %)	8.72	11.1	12.0
C ₂ H ₄ (vol. %)	12.8	19.9	18.7
C ₂ H ₆ (vol. %)	6.14	9.44	11.6
C ₃ H ₆ + C ₃ H ₈ (vol. %)	17.1	28.5	33.0
C ₄ H ₈ (vol. %)	6.43	8.45	11.9
C ₄ H ₁₀ (vol. %)	4.18	7.82	7.43
CO (vol. %)	14.8	0	0
CO ₂ (vol. %)	25.6	0	0
CV (MJ m ⁻³)	45.5	69.6	77.1
C ₃ -C ₄ (vol. %)	46.5	74.2	82.7

Note; (the data for PP, MP, PS and PET are given in Chapter 6)

Table 7.2-3 Gas Product composition for FCC1 catalyzed pyrolysis of MP, FSMP and five virgin plastics

FCC1	FSMP	MP	HDPE	LDPE	PP	PS	PET
H ₂ (vol. %)	4.46	5.28	8.19	4.44	2.26	100	1.91
CH ₄ (vol. %)	6.11	9.3	6.98	6.72	5.73	0	3.89
C ₂ H ₄ (vol. %)	9.88	12.8	11.8	10.4	5.05	0	3.64
C ₂ H ₆ (vol. %)	3.84	7.20	5.81	6.02	5.76	0	0
C ₃ H ₆ + C ₃ H ₈ (vol. %)	26.6	41.1	41.3	45.8	45.3	0	1.08
C ₄ H ₈ (vol. %)	11.2	15.9	17.3	18.4	26.5	0	0.85
C ₄ H ₁₀ (vol. %)	9.71	8.47	8.65	8.27	9.39	0	0
CO (vol. %)	12.2	0	0	0	0	0	46.7
CO ₂ (vol. %)	16.0	0	0	0	0	0	41.9
CV (MJ m ⁻³)	61.7	82.7	82.7	86.3	92.5	12.1	11.5
C ₃ -C ₄ (vol. %)	61.3	85.4	84.8	88.8	92.0	0	5.56

Table 7.2-4 Gas Product composition for FCC2 catalyzed pyrolysis of MP, FSMP and five virgin plastics

FCC2	FSMP	MP	HDPE	LDPE	PP	PS	PET
H ₂ (vol. %)	5.47	6.63	6.58	4.31	2.00	49.8	2.42
CH ₄ (vol. %)	4.72	7.62	6.43	5.38	5.81	8.29	3.84
C ₂ H ₄ (vol. %)	9.08	11.2	11.37	8.42	4.86	15.8	3.42
C ₂ H ₆ (vol. %)	2.94	5.61	5.03	4.65	5.49	0.00	0.00
C ₃ H ₆ + C ₃ H ₈ (vol. %)	30.5	43.3	47.8	40.2	37.2	21.6	1.62
C ₄ H ₈ (vol. %)	13.6	16.9	15.2	24.1	30.9	4.50	1.66
C ₄ H ₁₀ (vol. %)	6.64	8.72	7.54	12.9	13.8	0.00	0.00
CO (vol. %)	10.9	0.00	0.00	0.00	0.00	0.00	41.6
CO ₂ (vol. %)	16.2	0.00	0.00	0.00	0.00	0.00	45.4
CV (MJ m ⁻³)	62.7	83.7	83.8	90.8	95.1	43.7	12.2
C ₃ -C ₄ (vol. %)	62.7	85.8	86.9	90.3	92.2	41.9	6.77

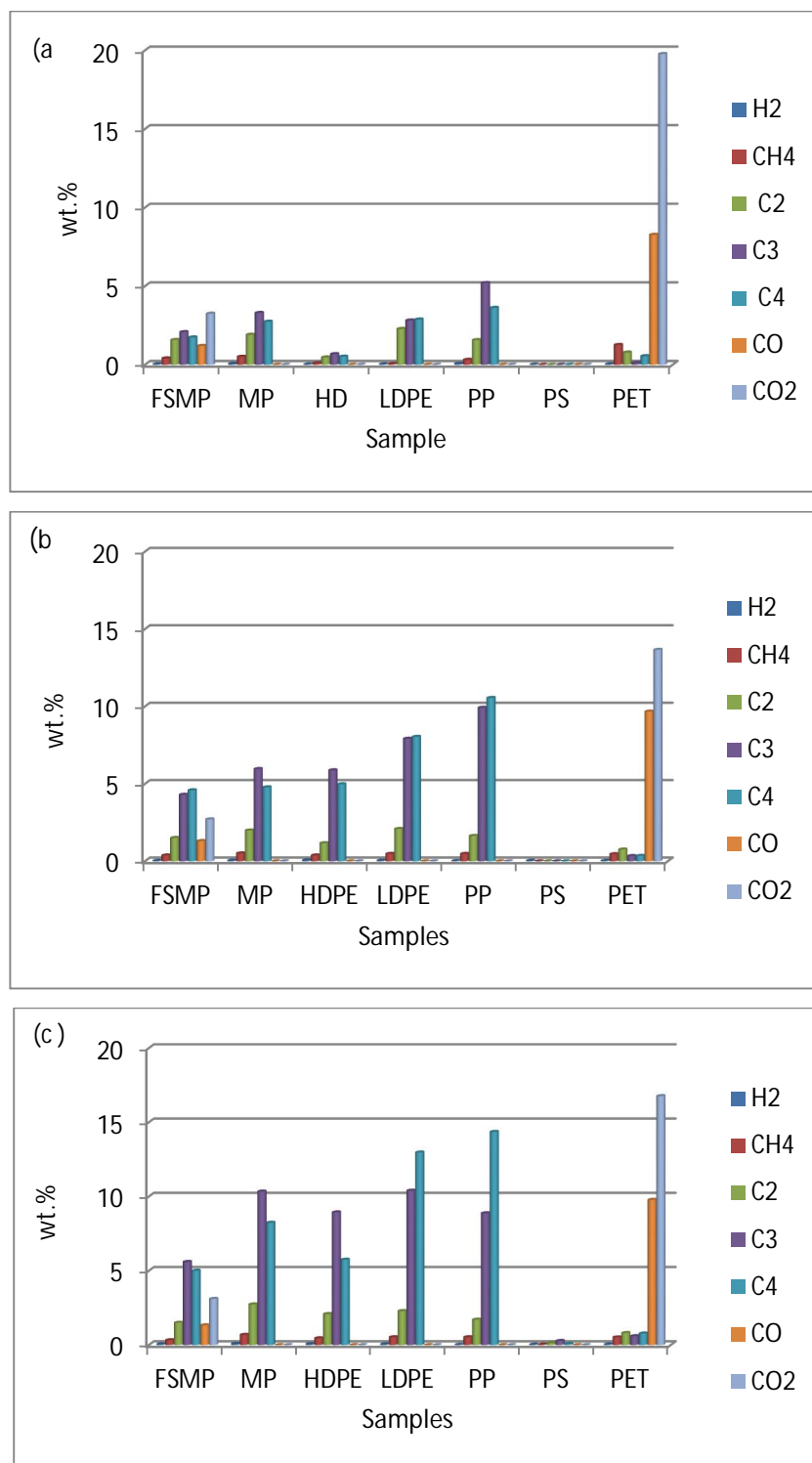


Figure 7.2-2 Gases produced from non-catalytic (a) FCC1 (b) and FCC2 catalyzed (c) pyrolysis of real-world (MP), the future simulated mixture of plastics (FSMP), and virgin plastics (HDPE,LDPE,PP,PS and PET)

Similarly, the calculated calorific value (CV) obtained shows the same trend as the gas composition. Thus, the CV rises with the introduction of the catalyst

and further enhance with the amount of the catalyst. Huang et al.[11], reported work using ZSM-5, MOR, USY, MCM-41, ASA as fluidizing cracking catalysts. They performed thermochemical conversion of polymer wastes into hydrocarbon fuels over various FCC on fluidized bed reactor. The authors observed that the zeolite catalyst yielded high volatile than the non-zeolite catalyst. The bulk of the volatile product were the gas phase with less than 6.00 wt. % liquid collected. They suggested two of the catalysts show similarities between them, ZSM-5 and MOR with C₁-C₄ and C₅-C₉ yielded 58.7 wt. % and 26.3 wt. % respectively. A similar trend was observed in this work as shown in Figure 7.3-2 (a) and (b) that show FCC catalysed gas products. The rise in gas with the amount of FCC could be due to the number of acid sites. The number of the acid sites may be easily augmented by increasing the amount of catalyst used or by decreasing the silica-alumina ratio [14]. Therefore, the results obtained reflect the different cracking effect of the FCC that differs with the amount of the catalyst. Elordi et al. [6], obtained from catalytic pyrolysis of HDPE higher yield of butenes and propylene with the low yield of C₂ and other gases. The authors finding are similar to what was obtained in this work. Abbas-Abadi et al. [10], reported an evolution of pyrolysis process parameters on PP degradation over FCC in stirred reactor at varying temperature 420-510 °C.

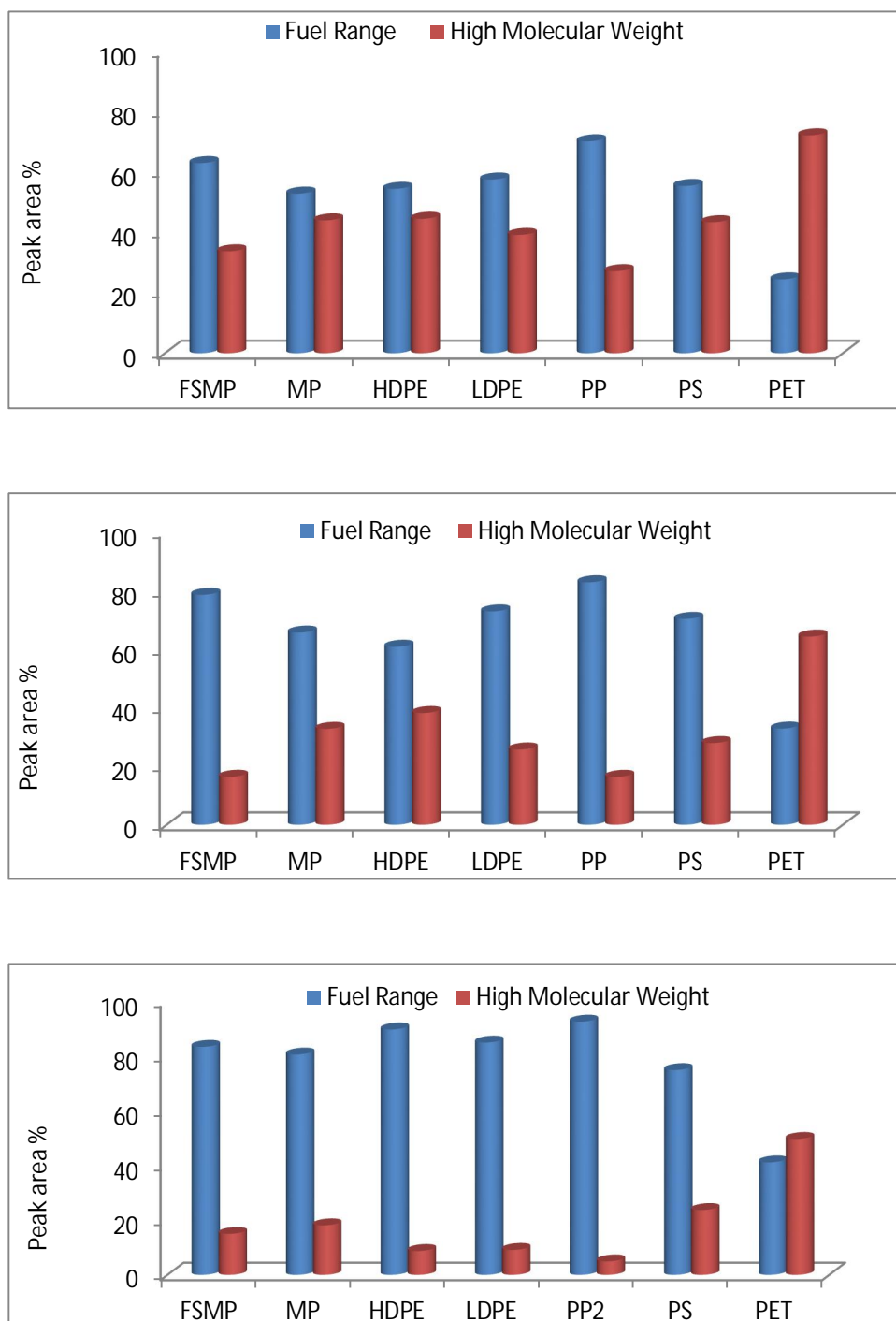


Figure 7.2-3 Distribution of fuel range and high molecular weight hydrocarbons for (a) non-catalytic (b) FCC1 and (c) FCC2 catalytic pyrolysis of MP, FSMP and virgin plastics

The liquid products were analysed using GC/FID. Thus, from the product yield for the pyrolysis-catalysis of the plastics shown in Figure 7.2-1, oil yield reduced when the spent FCC catalyst introduced to the second stage of the

pyrolysis/catalysis process. Conversely, the composition of the liquid products was greatly influenced by the presence of the catalyst. Accordingly, Figure 7.2-3 shows the influence of the addition of spent FCC catalyst addition on the fuel range (i.e. C_5-C_{15}) and the high molecular weight (i.e. C_{16+}) hydrocarbon compounds, for the uncatalyzed (a) 1g FCC (FCC1) (b) and 2g FCC (FCC2) catalyzed (c) product oils, respectively. The uncatalyzed pyrolysis of the plastic samples gave a high amount of fuel range hydrocarbons, but also considerably a high content of the high molecular weight hydrocarbons from C_{16} and above. The benzoic acid detected in high concentration for PET pyrolysis was included in high molecular weight compounds. Thus the high yield of high molecular weight compound from thermal pyrolysis of PET was mainly due to high yield of benzoic acid. Though, in the presence of the catalyst, the fuel range hydrocarbons dominate the composition of the product oil [14-16]. The improvement in fuel range hydrocarbon with the introduction of catalyst, further increase with the amount of spent FCC as shown in Figure 7.2-3 (b) and (c) for FCC1 and FCC2 respectively. So, increase in the available activity sites of the catalyst with the amount of FCC might cause the rise in its activities and production of lighter molecular weight compounds [14] . The high molecular weight hydrocarbons from C_{16} and above were for both amount of catalysts reduced in the corresponding order with the increase in fuel range. Likewise, there was a drastic reduction in benzoic acid for PET with the introduction of a catalyst.

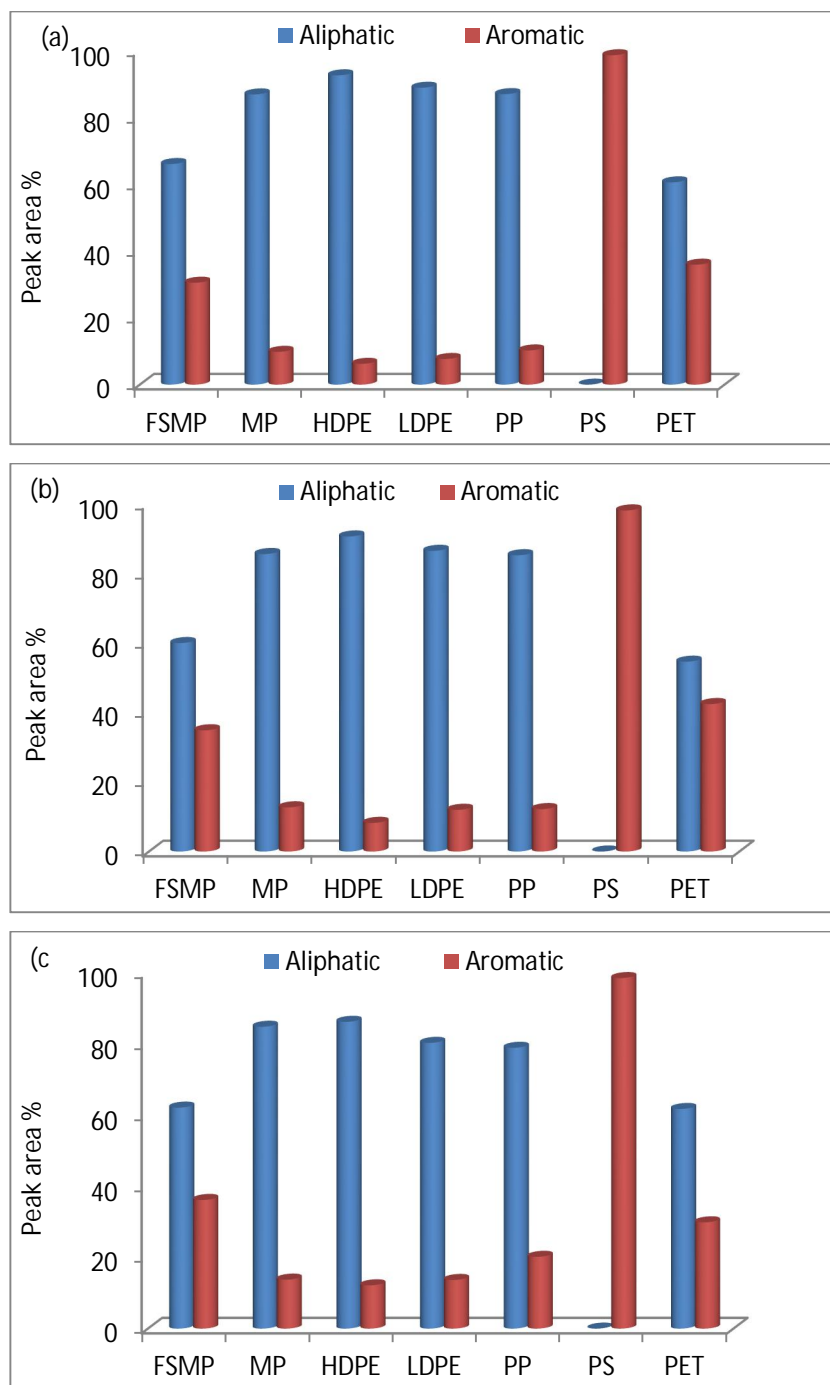


Figure 7.2-4 Distribution of aliphatic and aromatic hydrocarbons for (a) non-catalytic (b) FCC1 (c) FCC2 pyrolysis of MP, SMP, and virgin plastics (HDPE,LDPE,PP,PS and PET).

The distribution of the hydrocarbon compounds obtained from the pyrolysis process was also compared in term of aliphatic and aromatic compound distribution. Figure 7.2-4 shows the distribution of the oil product composition in terms of the aliphatic and aromatic content. The polymeric structure of the

plastic also play a role on the composition of oil products. For the polyolefins plastics (MP, FSMP, PE, PP) oil from pyrolysis was mainly aliphatic in nature. But, the polystyrene and polyethylene terephthalate produced an aromatic oil derived from the aromatic nature of the polymer structure. The polyethylene and polypropylene pyrolysis oil would be more probable to be almost solely aliphatic in content, but there was some aromatic content. These aromatics present may be due to the cracking reactions over the sand placed in the second stage reactor (for the thermal experiments), also resulting in an extended time in the hot zone of the reactor. Jing et al. [17], reported that in a closed batch reactor, there was increase in aromatics for pyrolysed LDPE:PP mixture when proportion of PP was higher than LDPE 30:70 ($3.34 \pm 0.47\% \text{H}^\alpha$), whereas lower LDPE:PP mixture 70:30 yields low aromatics ($0.95 \pm 0.05 \text{H}^\alpha$). The authors suggested on interaction mechanism, in would which probable, the intermolecular H transfer and LDPE/PP mixture increases alkene content by enhancing β -scission. Then the higher alkene content accelerates aromatics formation by unimolecular cyclisation reactions, followed by dehydrogenation or Diels-Alder reactions. The aliphatic and aromatic distribution were influenced with the introduction of the spent FCC catalyst. Lin [18] reported FCC catalytic degradation of post-consumer plastic waste suggested that FCC and ZSM-5 are likely to form a plastic/zeolite complex and consequently proceed via the scission reaction to further produced the volatile products.

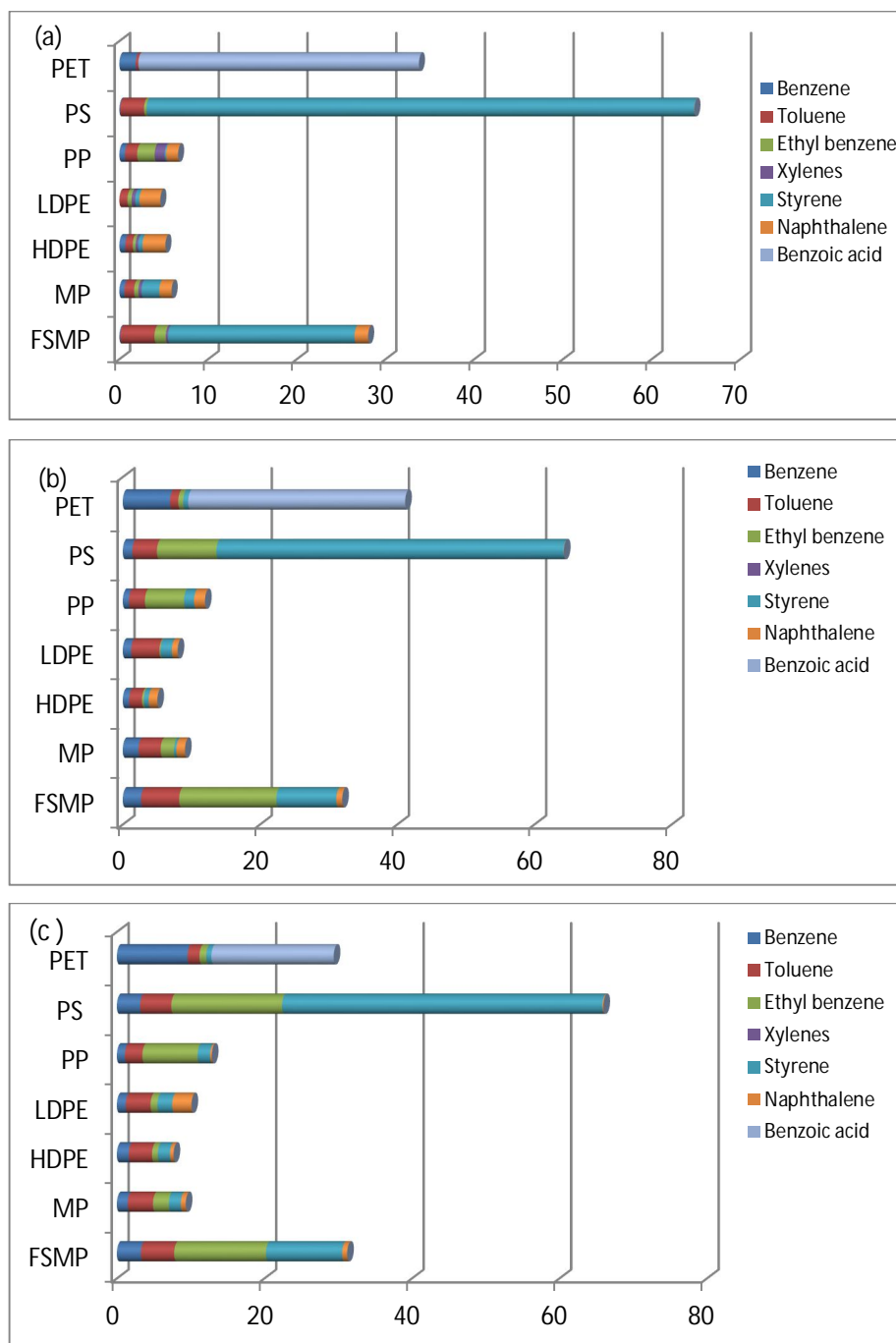


Figure 7.2-5 Yield of some selected aromatic compounds for (a) non-catalytic (b) FCC1 (c) FCC2 pyrolysis of real-world (MP), the future simulated mixture of plastics (FSMP), and virgin plastics (HDPE,LDPE,PP,PS and PET)

However, the introduction of the catalyst resulted in an increase in aromatics and PAH compounds as shown in Figure 7.2-5 (b). Similarly, the production of the aromatics compound were further enhanced with the amount of the FCC catalyst used as shown in Figure 7.2-5 (c). The increase in aromatics with the

introduction of the catalyst was reported by others [3, 19-22]. Lee et al. [3], reported that a higher yield of the aromatics was obtained in their work from spent FCC pyrolysis of mixed plastics compared to thermal degradation. The authors suggested these were due to cyclization of olefin within pores of the catalyst due to shape selectivity. The higher aromatics obtained for LDPE than HDPE in this work agree with Lee et al. [3]. Thus, the authors suggested that pyrolysis of waste LDPE the olefinic intermediates from primary cracking of the polymer were reacted more readily to the paraffin by hydrogenation and aromatic by cyclization than waste HDPE [3]. The bulk product of PS was aromatics and shows similar findings with 97.0% aromatic yields for PS by Lee et al.[3]. The styrene was the primary product of thermal PS pyrolysis as reported by others [16]. The introduction of the spent FCC catalyst significantly reduced the styrene content and increased benzene, toluene and ethyl benzene which was further increased with the quantity of the catalyst. These catalytic effects on the styrene yield was obtained by other researchers [16]. The bulk of the benzoic acid was produced in the thermal pyrolysis of PET. The benzoic acid produced was significantly reduced with the catalytic cracking and was converted into mainly benzene. The conversion of the benzoic acid to mainly benzene and another aromatic was further improved with the quantity of the spent FCC used. Hence, it would seem that the enhanced yield of all the aromatic compounds considered in the Figure 7.2-5 with the increased quantity of the spent FCC was largely due to increase in available catalysts sites.

Fuel properties of product oils

The product oils from the uncatalyzed pyrolysis and catalytic pyrolysis of the plastic samples were analyzed for their fuel properties by simulated distillation. The gas chromatography was used for simulated distillation to determine the boiling range distribution of the product oils. The results of boiling range distribution are shown in Figure 7.2-6.

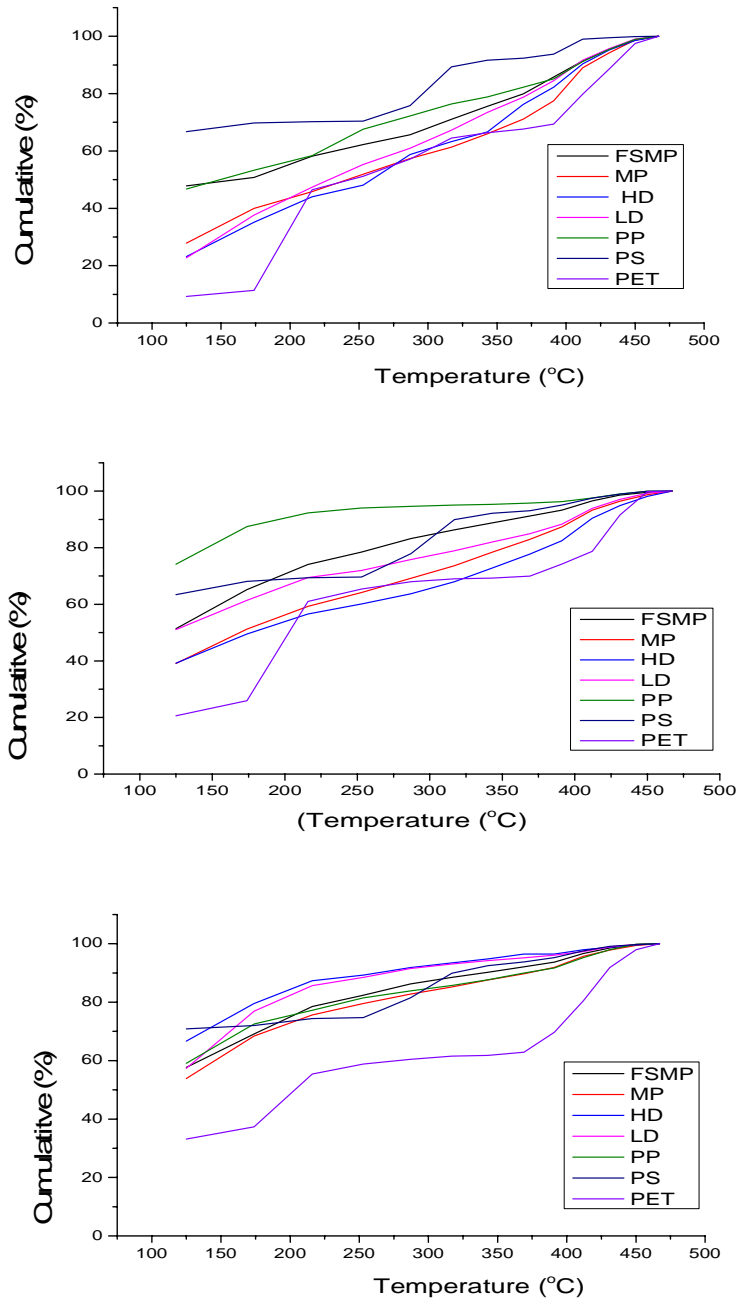


Figure 7.2-6 Simulated distillation of for (a) non-catalytic (b) FCC1 (c) FCC2 pyrolysis of real-world (MP), the future simulated mixture of plastics (FSMP), and virgin plastics (HDPE,LDPE,PP,PS and PET)

The boiling point range distribution for non-catalytic product oil showed in Figure 7.2-6 (a) have a significant boiling point range of greater than 250 °C. But, the boiling point range distribution was significantly influenced with the

addition of the spent FCC catalyst as shows in Figure 7.2-6 (b) and (c). The boiling point distribution was further greatly influenced with the quantity of spent FCC used.

Summary

The influence of spent FCC catalyst on pyrolysis-catalysis of real-world waste plastics and future simulated mixed plastic for valuable production of fuels and chemical feedstock was investigated. The main product of pyrolysis obtained is hydrocarbon gases, liquid oil and a trace amount of char. The quantity of oil produced from uncatalyzed future simulated mixed plastics was 79.0 wt.% and real-world waste plastics 81.5 wt.%, and the gases consisted of hydrogen, methane, C₂-C₄ hydrocarbons for both, but additional gases i.e. CO and CO₂ were also produced. However, when the catalyst was introduced, there were a decrease of between 9-15 wt. percent in oil yield with a corresponding increase in gas yield ranging from 6-15 wt. % that increased with catalyst amount. The oil from catalytic test was enriched in single ring aromatic compounds i.e. benzene, ethyl benzene, xylenes, styrene and toluene. In addition, the results include the interaction between the individual plastic that make up the simulated mixed plastic.

References

1. Pu, X., Luan, J.-N. and Shi, L., *Reuse of Spent FCC Catalyst for Removing Trace Olefins from Aromatics*. Bulletin of The Korean Chemical Society, 2012. **33**(8): p. 2642-2646.
2. Aguado, J., Serrano, D.P. and Escola, J.M., *Fuels from Waste Plastics by Thermal and Catalytic Processes: A Review*. Industrial & Engineering Chemistry Research, 2008. **47**(21).
3. Lee, K.-H., Noh, N.S., Shin, D.H. and Seo, Y., *Comparison of plastic types for catalytic degradation of waste plastics into liquid product with spent FCC catalyst*. Polymer Degradation and Stability, 2002. **78**(3): p. 539-544.
4. Delgado, C., Barruetabena, L., Salas, O. and Wolf, O., *Assessment of the Environmental Advantage and Drawbacks of Existing and Emerging Polymers Recovery Processes*. Joint Research Center Scientific and Technical Report, 2007. jrc37456: p. 264.
5. Muhammad, C., Onwudili, J.A. and Williams, P.T. *Thermal Degradation of Real-World Waste Plastics and Simulated Mixed Plastics in a Two-Stage Pyrolysis-Catalytic Reactor for Fuel Production*. Energy & Fuels, 2015. **29**(4): p. 1601-1609.
6. Elordi, G., Olazar, M., Castano, P., Artetxe, M. and Bilbao, J., *Polyethylene cracking on a spent FCC catalyst in a conical spouted bed*. Industrial & Engineering Chemistry Research, 2012. **51**(43): p. 14008-14017.
7. Bajus, M. and Hájeková, E. *Thermal cracking of the model seven components mixed plastics into oils/waxes*. Petroleum & Coal, 2010. **52**(3): p. 164-172.
8. Bagri, R. and Williams, P.T. *Fluidised-bed catalytic pyrolysis of polystyrene*. Journal of the Institute of Energy, 2002. **75**(505): p. 117-123.
9. Aguado, J., Serrano, D.P., Miguel, G.S., Escola, J.M. and Rodriguez, J.M., *Catalytic activity of zeolitic and mesostructured catalysts in the cracking of pure and waste polyolefins*. Journal of Analytical and Applied Pyrolysis, 2007. **78**(1): p. 153-161.
10. Abbas-Abadi, M.S., Mehdi, N., Yaganeh, H. and McDonald, A.G., *Evaluation of pyrolysis process parameters on polypropylene degradation products*. Journal of Analytical and Applied Pyrolysis, 2014. **109**: p. 272-277.

11. Huang, W.-C., Huang, M.S., Huang, C.F., Chen, C.C. and Ou, K.L., *Thermochemical conversion of polymer wastes into hydrocarbon fuels over various fluidizing cracking catalysts*. Fuel, 2010. **89**(9).
12. Houshmand, D., Roozbehani, B. and Badakhshan, A., *Thermal and Catalytic Degradation of Polystyrene with a Novel Catalyst*. International Journal of Science & Emerging Technologies, 2013. **5**(1).
13. Williams, P.T. and Williams, E.A., *Fluidised bed pyrolysis of low density polyethylene to produce petrochemical feedstock*. Journal of Analytical and Applied Pyrolysis, 1999. **51**(1): p. 107-126.
14. Ohkita, H., Nisshiyama, R., Tochiyama, Y., Mizushima, T., Kakuta, N., Morioka, Y., Ueno, A., Namiki, Y. and Tanifuji, S., *Acid properties of silica-alumina catalysts and catalytic degradation of polyethylene*. Industrial & engineering chemistry research, 1993. **32**(12): p. 3112-3116.
15. Williams, P.T. and Brindle, A.J., *Catalytic pyrolysis of tyres: influence of catalyst temperature*. Fuel, 2002. **81**(18): p. 2425-2434.
16. Muhammad, C., Onwudili, J.A. and Williams, P.T., *Catalytic pyrolysis of waste plastic from electrical and electronic equipment*. Journal of Analytical and Applied Pyrolysis, 2015.
17. Jing, X., Zhao, Y., Wen, H., and Xu, Z., *Interactions between low-density polyethylene (LDPE) and polypropylene (PP) during the mild cracking of polyolefin mixtures in a closed-batch reactor*. Energy & Fuels, 2013. **27**(10): p. 5841-5851.
18. Lin, Y.-H., *Production of valuable hydrocarbons by catalytic degradation of a mixture of post-consumer plastic waste in a fluidized-bed reactor*. Polymer Degradation and Stability, 2009. **94**(11): p. 1924-1931.
19. Serrano, D., Aguado, J., Escola, J.M., Morselli, L. and Orsi, R., *Thermal and catalytic cracking of a LDPE-EVA copolymer mixture*. Journal of analytical and Applied Pyrolysis, 2003. **68**: p. 481-494.
20. Bagri, R. and Williams, P.T., *Catalytic pyrolysis of polyethylene*. Journal of analytical and applied pyrolysis, 2002. **63**(1): p. 29-41.
21. Aguado, J., Serrano, D.P., San Miguel, G., Castro, M.C. and Madrid, S., *Feedstock recycling of polyethylene in a two-step thermo-catalytic reaction system*. Journal of analytical and applied pyrolysis, 2007. **79**(1): p. 415-423.
22. Lopez, A., de Marco, I., Cabellero, B.M., Adados, A. and Laresgoiti, M.F., *Deactivation and regeneration of ZSM-5 zeolite in catalytic*

pyrolysis of plastic wastes. Waste management, 2011. **31**(8): p. 1852-1858.

23. Williams, P.T., *Yield and composition of gases and oils/waxes from the feedstock recycling of waste plastic*. Feedstock Recycling and Pyrolysis of Waste Plastics: Converting Waste Plastics into Diesel and Other Fuels, 2006: p. 285-313.

Chapter 8 : INFLUENCE OF CATALYST BED TEMPERATURE AND CATALYST TYPE ON PYROLYSIS OF FUTURE SIMULATED MIXED PLASTICS (FSMP)

8.1 Introduction

The use of the catalyst in the pyrolysis of waste plastic has been well documented [1-12]. However, there are few works among catalytic pyrolysis of plastic that investigate the influence of catalyst types and catalyst bed temperature in a two stage pyrolysis-catalysis process. Boxiong et al. [11], performed pyrolysis of waste tyres with zeolite USY and ZSM-5 catalysts over a fixed bed reactor. The authors investigated the influence of the catalytic temperature on the yield of the product of pyrolysis-catalysis of waste tyres. Boxiong et al. [11], reported that an increase of catalytic temperature enhances gas yield at the expense of oil yield. Achilias et al. [13], reported work on the chemical recycling of plastics waste made from polyethylene (HDPE and LDPE) and polypropylene in fixed bed reactor at 450 °C reaction temperature. The authors obtained low gas yield for catalytic pyrolysis of model HDPE, LDPE and PP using acidic FCC catalyst, as well as on waste products. The low gas yield was attributed to the low pyrolysis temperature for all the plastics used. Williams and Brindle[14] investigated catalytic pyrolysis of tyres in a two stage pyrolysis-catalysis and considered the influence of catalyst temperature using zeolite Y and ZSM-5 catalysts. The catalyst was found to reduce the yield of oil with a consequent increase in the gas and formation of coke on the catalyst[14]. Zhang et al. [15], performed catalytic co-pyrolysis of biomass and different plastics (PE, PP and PS) to improve hydrocarbon yields in a fluidized bed reactor using spent FCC catalyst, zeolite ZSM-5 and γ -Al₂O₃. Thus, Zhang et al. [15], reported that the

spent FCC catalyst gave maximum carbon yield of petrochemicals (71.0%) at 600 °C pyrolysis temperature.

This work based on a review work reported by Delgado et al. [16] and a detailed description of the plastics used and preparation are given in Chapter 7. The future municipal solid waste (MSW) generation in Europe as reported by Delgado et al. [16]. The catalytic pyrolysis carried out in the work makes use of spent FCC catalyst and fresh zeolite catalysts that include two zeolite Y catalysts and one ZSM-5 catalyst. Table 8.1-1 show the characteristic of the zeolite catalysts. The two Y zeolites catalysts had both different silica-alumina ratio and surface area, but one Y zeolite catalyst (ZY-2) had the same silica-alumina ratio with ZSM-5 zeolite catalyst (ZS-1) of 80:1.

For each experiment 2g of plastic was pyrolyzed in the fixed bed two-stage batch reactor as described in Chapter 3. The plastic sample was heated from ambient temperature to 500 °C at a heating rate of 10 °C min⁻¹ and the second stage (catalyst bed) was maintained at a temperature of 500 °C before the heating of plastic started. Equally, when the influence of catalyst type and bed temperature were considered, the catalyst bed temperature maintained at either 500 °C or 600 °C. The pyrolysis temperature of 500 °C and nitrogen flow rate 200 ml min⁻¹ was maintained throughout all the experiments. The catalyst bed was prepared as Table 8.1-1. In this chapter, the zeolite catalysts are designated as ZY-1 and ZY-2 for the Y-zeolites catalysts, ZS-1 for ZSM-5 catalyst and FCC for spent FCC catalyst.

Table 8.1-1 Catalyst and quartz sand mixing proportion

	No catalyst	FCC	ZY-1	ZY-2	ZS-1
Quartz (g)	4	2	2	2	2
Catalyst (g)	-	2	2	2	2

8.2 Influence of FCC bed temperature

In this section influence of the spent FCC catalyst bed temperature was considered.

8.2.1 Product Yields

Figure 8.2.-1 shows the product yield from the pyrolysis and pyrolysis-catalysis of the future simulated mixed plastic (FSMP) at 400 °C catalyst bed temperature.

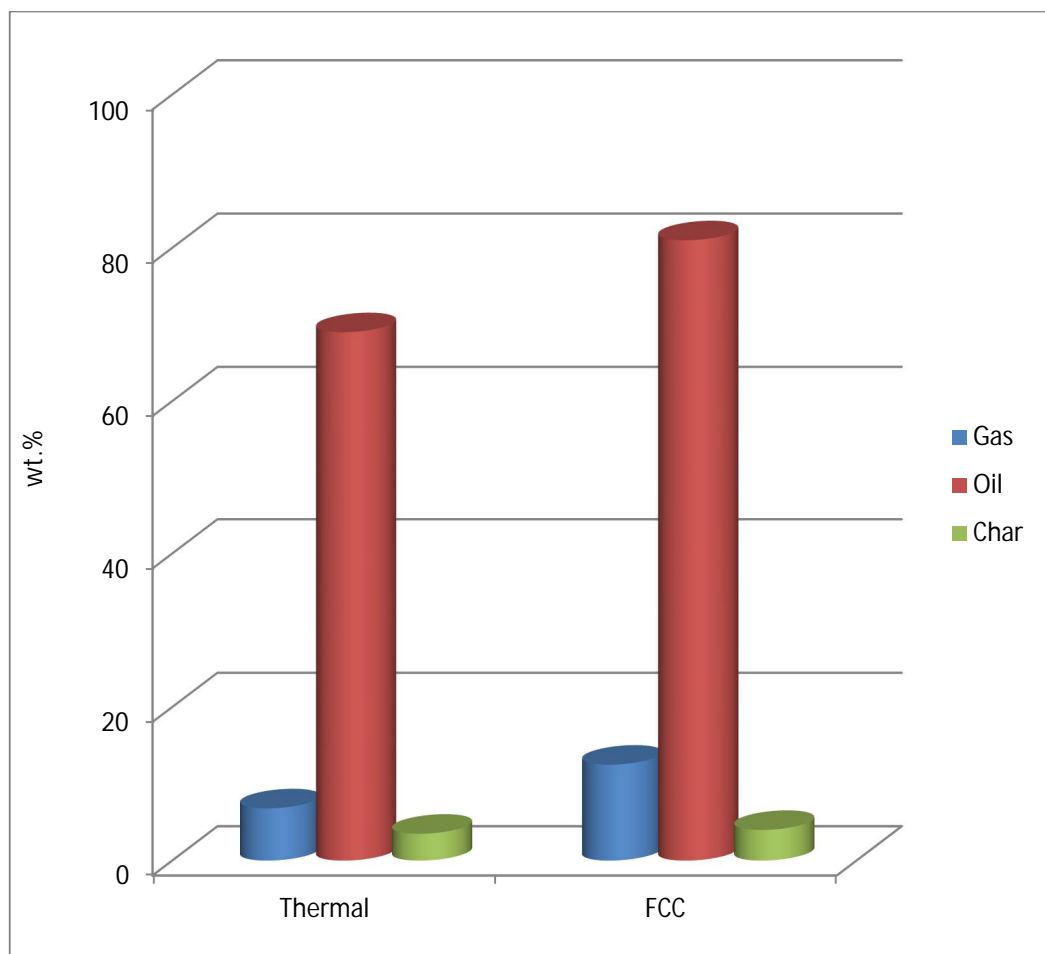


Figure 8.2-1 Product yield for non-catalytic and catalytic pyrolysis of the future simulated mixture of plastics (FSMP) at 400 °C

However, oil yield for thermal pyrolysis at a bed temperature of 400 °C (69.0 wt%) was lower than FCC catalysed (81.0 wt%), this might be as a result of a sudden drop in temperature from 500 °C to a catalyst bed temperature of 400 °C. As a result of a sudden drop in the temperature from a pyrolysis temperature of 500 °C to a catalyst bed temperature of 400 °C leading to condensation of melted plastic in the cooler bed temperature clearly shows a decrease in oil yield for non-catalytic run. This occurrence of a trend might indicate that the influence of temperature was more pronounced than the influence of the catalyst. Aguado et al. [17], reported the overall conversion of plastic in the first stage of thermo-catalytic conversion of LDPE solely

controlled by the temperature in the thermal reactor and were not affected by the presence of a catalyst in the second stage. Therefore, the authors found that when the reaction was conducted at 425 °C, only 53-55 wt. % of the original plastic was collected as hydrocarbon products in the condenser or gas sampling bag. So the remaining 45-47 wt. % was unable to pass through the reaction system and stayed in the thermal reactor as a liquid oil. .But a remarkable rise in conversion values (90-95 wt. %) was obtained at 450 °C, and the reaction was completed at 475 °C. The two-stage reactor Aguado et al. [17], used was an upward draft, and the nitrogen flow rate was 39 ml min⁻¹ unlike the down draft system and 20 ml min⁻¹ nitrogen employed in this work. The Figure 8.2-2 shows the schematic diagram of two-stage reactor used by Aguado et al. [17].

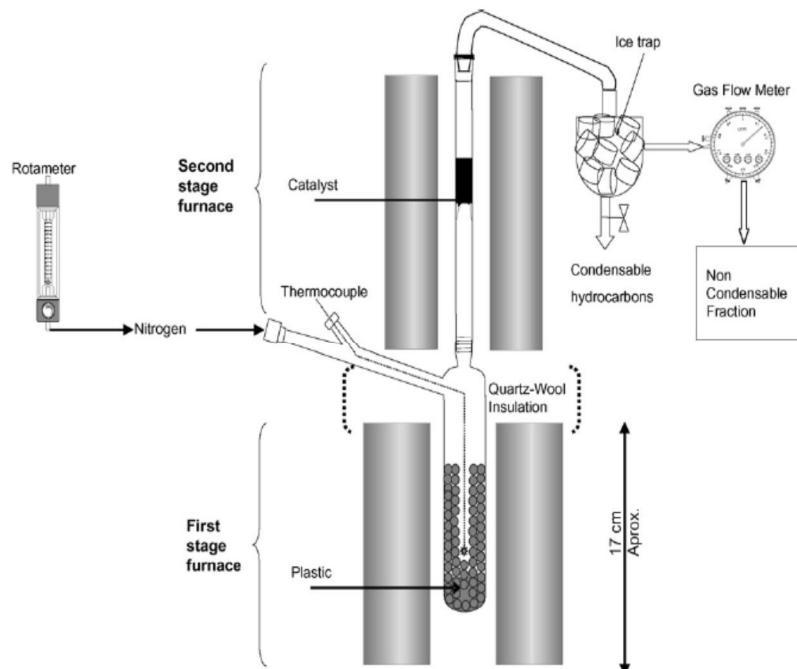


Figure 8.2-2 **A schematic representation of two stage reaction system by Aguado et al. [17].**

Accordingly, in this work the flow rate and delivery system gases to move downwards by nitrogen flow. The pyrolysis temperature was 500 °C. Thus, the plastic would almost entirely pyrolyze. Accordingly many researchers reported the strong influence of both catalyst and bed temperature in decreasing oil yield and a corresponding increase in gas yield [9, 14]. Venuto et al. [18], reported that the activity of modern zeolite cracking catalyst has improved to the point where, for the most part, only 1 to 4 seconds of contact time are required to effect substantially complete a non-aromatic portion of the feed. Lee et al. [19], suggested that the yields of gas and liquid from catalytic degradation strongly depended on the type of plastics. Thus, the overall performance of the spent FCC on the degradation of FSMP was dependant of the proportion of the individual virgin plastic that made up the mixture.

8.2.2 Gas composition

The main gases produced during the thermal pyrolysis of FSMP at 400 °C bed temperature were C₂ (mainly ethene with lower concentrations of ethane), C₃ (mainly propene) and C₄ gases (mainly butene), carbon monoxide and carbon dioxide as shown in Table 8.2-1. So that the gas yield of hydrocarbon product depended on the bed temperature. Therefore, even at a bed temperature of 400 °C, the spent FCC catalyst prevented the condensation of the melted plastic and rather transferred hydrocarbons to oil products.

Table 8.2-1 Gas Product composition for FCC catalyzed pyrolysis of FSMP at different catalyst bed temperature

	Thermal	FCC
	400 °C	400 °C
H ₂ (vol. %)	5.99	5.16
CH ₄ (vol. %)	0.99	3.36
C ₂ H ₄ (vol. %)	7.61	6.28
C ₂ H ₆ (vol. %)	3.92	2.48
C ₃ H ₆ + C ₃ H ₈ (vol. %)	11.76	23.34
C ₄ H ₈ (vol. %)	4.66	15.54
C ₄ H ₁₀ (vol. %)	6.50	9.30
CO (vol. %)	22.23	10.12
CO ₂ (vol. %)	36.35	24.41
CV (MJ m ⁻³)	34.94	58.95
C ₃ -C ₄ (vol. %)	34.44	56.94

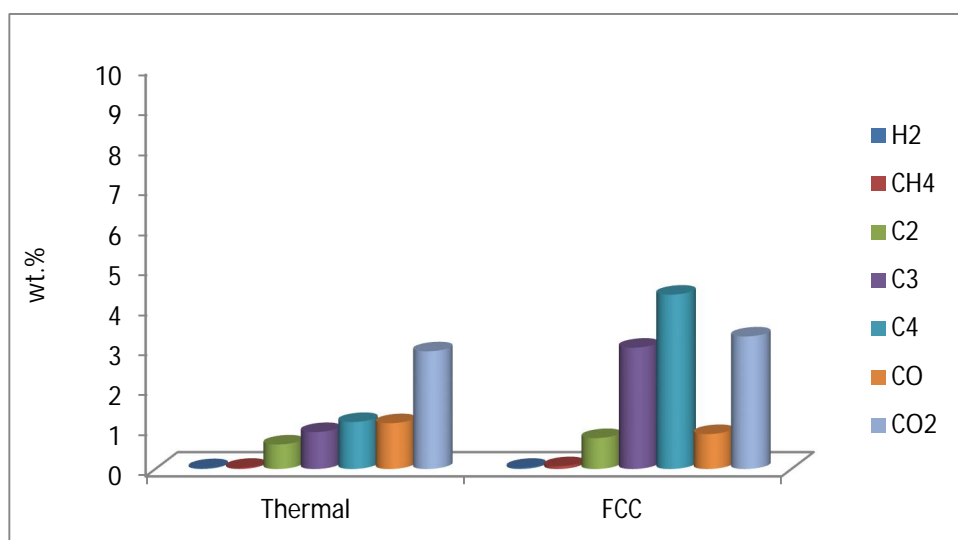


Figure 8.2-3 Gas composition from non-catalytic (a) and catalytic (b) pyrolysis of the future simulated mixture of plastics (FSMP)

The FSMP consist of mainly polyolefin i.e. HDPE, LDPE and PP (more than 65 wt.%), and they are known to thermally degraded via a random scission to produce mainly alkenes gases C_2H_4 , C_3H_6 , and C_4H_8 , and to a smaller range the alkanes gases, C_2H_6 , C_3H_8 , and C_4H_{10} [20]. Table 8.2-1 and Figure 8.2-3 shows the concentration of the product gases with and without the spent FCC catalyst for the pyrolysis and pyrolysis-catalysis of the future simulated mixture of plastics (FSMP) at 400 °C bed temperature. The pyrolysis of polystyrene is known to produced a small quantity of gas while PET is the source of CO_2 by decarboxylation and CO formed through decarboxylation of polymer or reaction between carbon dioxide and char [20]. Thus, FSMP gas production is affected by both PS and PET that are part its constituents, so low gas yield and the presence of CO and CO_2 are due to the present of PS and PET respectively. The yield of gas rises with the introduction of the catalyst, so also do the constituent gases, C_3 , C_4 , and CO_2 which show a significant rise. Zhang et al. [15], reported that the degradation of plastic is an endothermic reaction; thus, the olefin yield increases with the increasing temperature. Aguado et al. [17], observed the selectivities by carbon atom number exhibited by the hydrocarbon products produced at different temperature (425-475 °C) in the absece of catalyst; yield of light species at 425 °C were 16.0% and increased to 37.0% at higher temperature of 475 °C. However, cracking over n-HZSM-5 at 450 °C (C_1 - C_4) fraction reached 77.0%. The authors attributed this increase to high acidic properties of the catalyst.

Product oils composition

The product oils were characterized using data from GC/FID analysis into fuel range and high molecular weight compounds. The distribution of the fuel range and high molecular weight for FSMP at 400 °C different bed temperature is shown in Figure 8.2-4.

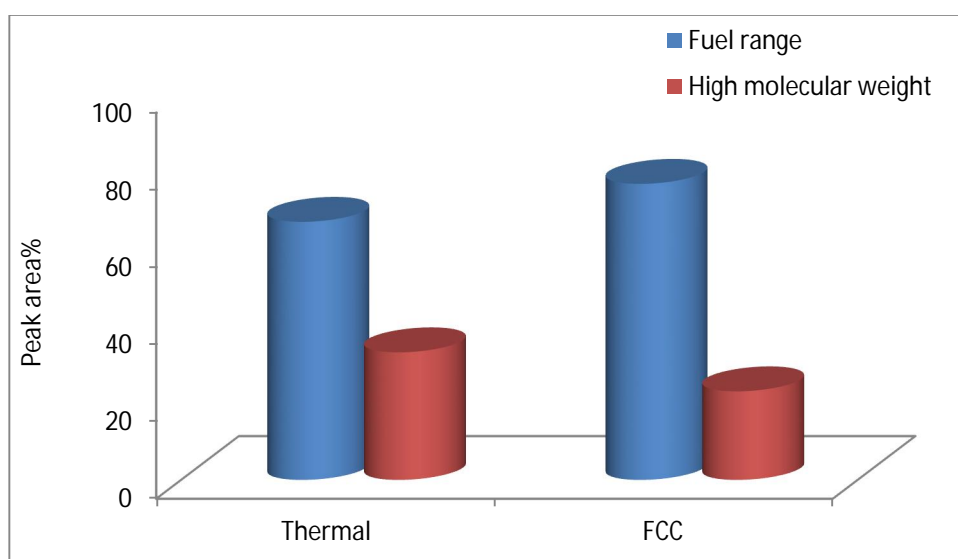


Figure 8.2-4 **Distribution of Fuel range (C₅ – C₁₅) and high molecular weight (C₁₆₊) hydrocarbons for (a) non-catalytic and (b) catalytic pyrolysis of the future simulated mixture of plastics (FSMP) at 400 °C**

The high molecular weight compounds distribution reduced with the introduction of catalyst and a corresponding increase in fuel range hydrocarbons was observed. The spent FCC with low Si: Al showed mild activity with its high available acidic sites. The low catalyst bed temperature did not significantly enhance fuel range hydrocarbon production. Escola et al. [21], reported work on conversion of PE into transportation fuels by the combination of thermal cracking and catalytic hydro-reforming over Ni supported on hierarchical beta zeolite. The authors obtained for thermal cracking of LDPE in a stirred autoclave reactor at 400 °C mostly hydrocarbon

within the range of gasoline (C_5 - C_{12} , 48.4%) and light diesel C_{13} - C_{18} , 35.5%) , with the remaining hydrocarbon being gases (C_1 - C_4 , 0.4%) and heavy diesel (C_{19} - C_{40} , 15.7%). Accordingly, these hydrocarbon fractions are suggested cannot be used in a straightforward way as transportation fuels due to the high amount of olefins that might lead toward the formation of gum in the engines as well as during storage. The same can be said of the oil produced from both the catalytic and thermal runs at a bed temperature of 400 °C in this work.

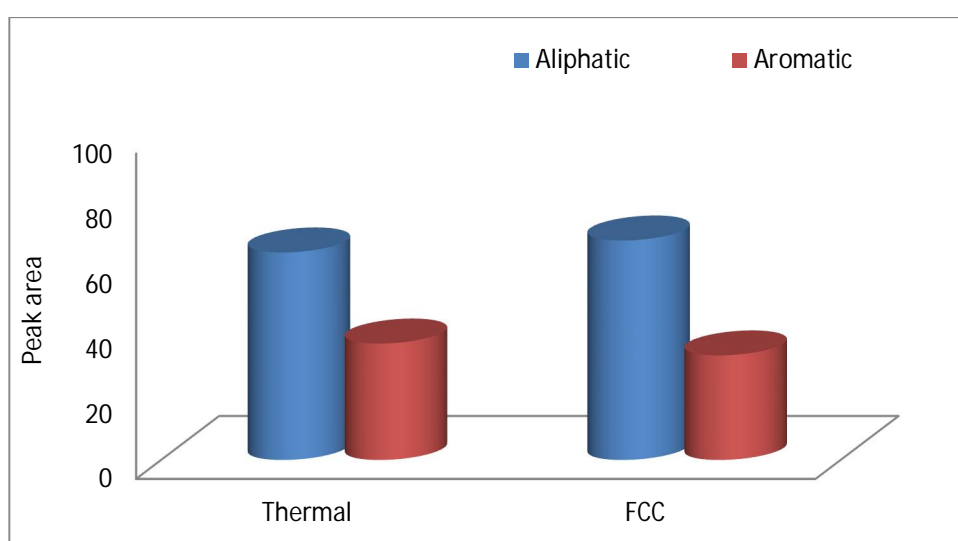


Figure 8.2-5 **Distribution of aliphatic and aromatics hydrocarbon for (a)non-catalytic and (b) catalytic pyrolysis of the future simulated mixture of plastics (FSMP)**

Figure 8.2-5 shows the distribution of the oil product composition in terms of the aliphatic and aromatic content from pyrolysis process of FSMP at 400 °C catalyst bed temperature. The polymeric structure of the plastic that made up the future simulated mixed plastics might also play a role in the distribution as more than 65.0% of the mixture made up polyolefins plastics. Thus, the oil from pyrolysis was mainly aliphatic in nature. Nevertheless, the polystyrene and polyethylene terephthalate component of the mixture were expected to contribute an aromatic oil derived from the aromatic nature of the polymer structure. Those aromatic compounds present were suggested to come from

the cracking reactions over the sand placed in the second stage reactor (for the thermal experiments), also resulting in an extended time in the hot zone of the reactor. The aliphatic compound distribution showed modest rise (63.8 to 67.4%) with the introduction of FCC catalyst and a decrease in aromatic yield (35.8 to 32.1%). These further demonstrate that the low catalyst bed temperature did not support good catalyst activity. Escola et al. [21], obtained very low aromatic yield in the hydrocarbon mixtures at 400 °C cracking temperature in a stirred autoclave reactor. The authors regard the low aromatics compound observed not suitable for use in the transportation fuel mixture, as the presence of a higher amount of aromatics in the gasoline enhances the desired research octane number (RON).

The fuel property of the product oils was investigated using gas chromatography to determine the boiling range distribution of the product oils. The boiling range distribution results are shown in Figure 8.2-6. The product oils from thermal pyrolysis showed that a higher fraction of the oils has a boiling point range greater than 300 °C, compared to those obtained in the presence of spent FCC. However, the spent FCC catalysed products oil show an only modest shift to lower boiling points, reflecting little appreciable shift in molecular weight range as observed in Figure 8.2-4.

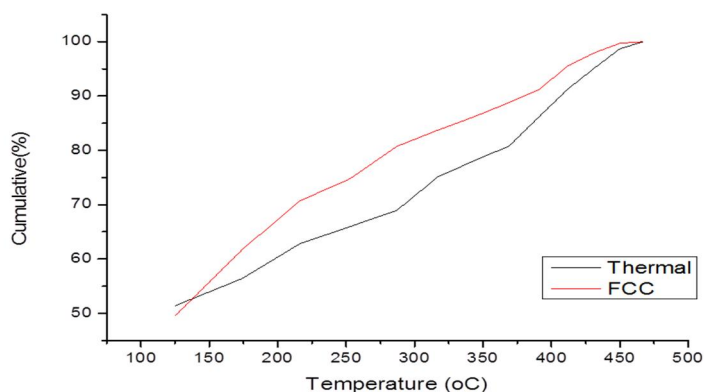


Figure 8.2-6 **Simulated distillation of (a) thermal and (b) catalytic pyrolysis product oils from FSMP.**

8.3 The influence of catalyst type and bed temperatures for the pyrolysis-catalysis on the future simulated mixed plastic

The preceding section shows that while the spent catalyst resulted in the better conversion of plastic samples at 400 °C bed temperature, the yield of fuel range compounds showed only a slight improvement. Therefore, the other catalyst were tested at 500 °C and 600 °C bed temperature. Thus, in this section, the spent FCC catalyst and three fresh zeolites catalysts were used to study pyrolysis-catalysis of future simulated mixed plastic (FSMP). The four catalysts described in Table 7.1-1 all designated as follows; ZY-1 and ZY-2 for the Y-zeolites catalysts, ZS-1 for ZSM-5 catalyst and FCC for spent FCC catalyst.

8.3.1 Product Yields

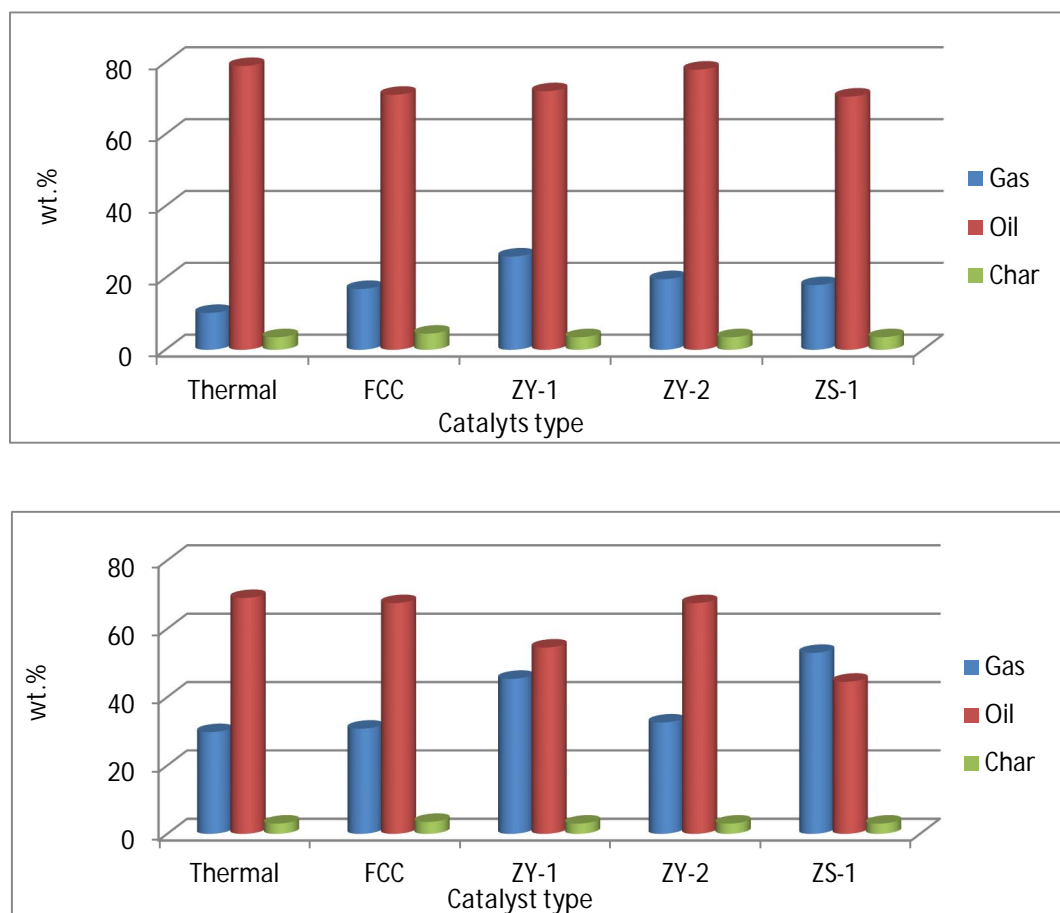


Figure 8.3-1 **Product yield for non-catalytic and catalytic pyrolysis of the future simulated mixture of plastics (FSMP) at (a) 500 °C and (b) 600 °C catalyst bed temperature**

Figure 8.3.-1 shows the product yield from the pyrolysis and pyrolysis-catalysis of the future simulated mixed plastic (FSMP) at different catalyst bed temperatures.

Considering FCC performance over the three temperatures tested, the uncatalyzed pyrolysis of FSMP at between the temperature of 500 °C gave the maximum oil yield of 79.0 wt.% compared to a bed temperature of 600 °C and 400 °C. The increase in bed temperature led to increasing in gas yield, particularly visible at 500 °C and 600 °C. For example, in the non-catalytic run,

gas yield increased from 6.81 to 10.27 wt.% as the bed temperature increased from 400 °C to 500 °C. There was a 3-fold increase in gas yield after bed temperature increased from 500 °C to 600 °C for a non-catalytic run. Similarly, gas yield increased slightly when bed temperature was increased from 400 °C to 500 °C, but nearly doubled when bed temperature increased from 500 °C to 600 °C. Accordingly, similar gas and oil yields were obtained for both catalytic and non-catalytic runs when the temperature was 600 °C. This effect of the bed temperature might indicate that the influence of temperature was more pronounced than the influence of catalyst at 600 °C. In Figure 8.3-1. The thermal pyrolysis of FSMP at 500 °C gave the highest oil yield of 79.0 wt.%, with ZS-1 catalysed FSMP at 600 °C producing the lowest oil yield (44.5 wt.%), The oil product yield decreased with both catalyst addition and increases in bed temperature, with a corresponding increase in gas products. Similar results have been reported in the literature [9, 14, 15]. The zeolite ZS-1 had a low surface area ($467 \text{ cm}^3 \text{ g}^{-1}$) and low available acidic catalytic site as a result of high Si:Al ratio (80:1), however it exhibit higher activity to produce less oil (44.7%) at 500 °C temperature and highest gas product (52.9%) at 600 °C bed temperature. Therefore, the yield of gas rose markedly at the expense of oil yield with the increase in catalyst bed temperature. Thus, the same trend in increased gas yield was obtained for ZY-1 (25.9 to 45.3 wt.%), ZY-2 (19.7 to 32.6 wt.%) and FCC (16.9 to 30.8 wt.%) as the bed temperature was increase from 500 to 600 °C. The data obtained suggest that the bed temperature also had an effect on the thermal pyrolysis. The increase in gas yield with an increase in catalyst bed temperature was reported in the literature [11, 14].

8.3.2 Gas composition

Table 8.3-1 Gas Product composition for thermal and catalytic pyrolysis of FSMP with different catalyst type at 500 °C bed temperature

500 °C	Thermal	FCC	ZY-1	ZY-2	ZS-1
H ₂ (vol. %)	4.55	5.47	15.7	22.3	14.3
CH ₄ (vol. %)	8.72	4.72	9.97	5.27	6.38
C ₂ H ₄ (vol. %)	12.8	9.08	9.96	9.81	11.9
C ₂ H ₆ (vol. %)	6.14	2.94	4.80	3.06	3.70
C ₃ H ₆ + C ₃ H ₈ (vol. %)	17.1	30.5	26.9	24.0	29.0
C ₄ H ₈ (vol. %)	6.34	13.6	12.6	7.75	9.37
C ₄ H ₁₀ (vol. %)	4.18	6.64	4.68	5.04	6.10
CO (vol. %)	14.8	10.9	5.82	7.88	6.32
CO ₂ (vol. %)	25.5	16.2	9.66	15.0	12.9
CV (MJ m ⁻³)	45.5	62.7	59.0	49.5	57.9
C ₃ -C ₄ (vol. %)	46.5	62.7	58.9	49.6	60.0

Table 8.3-2 Gas Product composition for thermal and catalytic pyrolysis of FSMP with different catalyst type at 600 °C bed temperature

600 °C	Thermal	FCC	ZY-1	ZY-2	ZS-1
H ₂ (vol. %)	10.6	9.91	31.8	12.6	9.46
CH ₄ (vol. %)	15.4	14.6	16.7	10.7	7.44
C ₂ H ₄ (vol. %)	23.1	17.7	8.80	8.98	21.7
C ₂ H ₆ (vol. %)	6.80	5.88	6.41	3.69	3.40
C ₃ H ₆ + C ₃ H ₈ (vol. %)	17.7	21.4	16.1	14.2	25.6
C ₄ H ₈ (vol. %)	4.65	5.72	5.57	4.15	4.64
C ₄ H ₁₀ (vol. %)	3.74	4.64	7.65	2.61	4.51
CO (vol. %)	8.92	7.75	4.49	37.2	19.7
CO ₂ (vol. %)	9.17	12.5	2.49	5.93	3.55
CV (MJ m ⁻³)	52.7	54.7	33.3	67.2	50.8
C ₃ -C ₄ (vol. %)	55.9	55.3	44.5	33.6	58.8

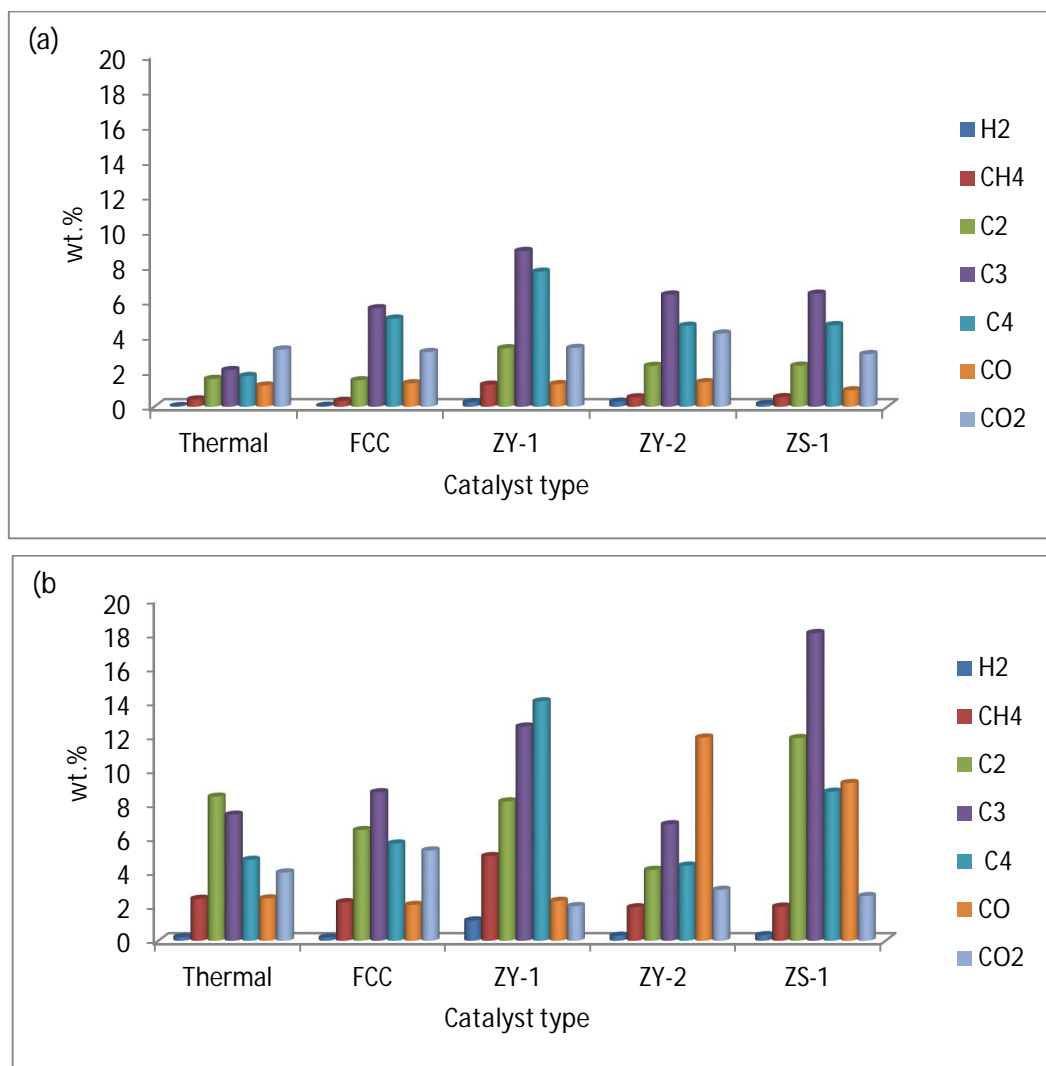


Figure 8.3-2 **Gas composition from non-catalytic and catalytic pyrolysis of the future simulated mixture of plastics (SMP) at (a) 500 °C and (b) 600 °C catalyst bed temperature**

Tables 8.3-1, 8.3-2, Figures 8.3-2 and 8.3-2, shows the concentration of the product gases for the pyrolysis and pyrolysis-catalysis of FSMP using different catalysts at 500 or 600 °C bed temperatures. The thermal pyrolysis product gases consisted of mainly alkenes gases C_2H_4 , C_3H_6 , and C_4H_8 , and to a smaller range of the alkanes gases, C_2H_6 , C_3H_8 , and C_4H_{10} . The gases produced increased with the temperature rise. Thus, the gas yield were further enhanced with the introduction of the catalyst so that at 500 °C bed

temperature, the FCC catalyst (Si:Al, 16.4) with strong acidic site produce the highest yield of C₂-C₄ hydrocarbons (62.7 vol.%), while low acidic ZY-2 catalysts (Si: Al, 80.1) produced low yield of C₂-C₄ (49.7vol.%). However, ZY-1 with stronger acidic properties (Si:Al, 5.2) produced more H₂ and CH₄ (15.7vol,%, 9.97 vol.%) than FCC H₂ and CH₄ (5.47vol.%, 4.72 vol.%). Similarly, ZS-1 with the same acidic strength as ZY-2 show better catalytic activity with a higher yield of C₂-C₄ hydrocarbons (60.0 vol, %), lower H₂ and CH₄ (14.3 vol.%, 6.38 vol.%). The calorific values of the hydrocarbons increase with the introduction of the catalyst. Accordingly, at 600 °C bed temperature there was a corresponding increase in hydrocarbon, CO and CO₂ gases with the introduction of catalysts. However, there was some variation from what was observed at 500 °C bed temperature. ZY-1 recorded lower C₂-C₄ hydrocarbons yields of 44.51vol.% and 33.64vol.% respectively than thermal run 55.93 vol.%. Accordingly, the calorific value (52.7 Mj m⁻³) of the gas products decrease with the introduction of the catalyst with spent FCC gave slightly improved calorific value of 54.7 Mj m⁻³. Likewise, there was the corresponding rise in H₂ gas for ZY-1 catalyzed pyrolysis of FSMP at 600°C catalytic cracking temperature. Lin and Yang [22], reported C₁-C₄ hydrocarbon distribution from spent FCC commercial equilibrium catalyzed the conversion of commingled polymer over a temperature range of 340-460 °C. The authors observed an increase in C₂-C₄ hydrocarbon with the rise in temperature of 18.2% to 28.7%, but methane and ethane were detected only at the higher temperatures. Huang et al. [6], observed that change in the hydrocarbon yield with temperature was similar, for all catalysts tested, with faster rates observed at higher temperatures. Lopez et al. [23], reported work on deactivation and regeneration of ZSM-5 in the catalytic pyrolysis of plastic

wastes using a semi-batch reactor at 440 °C. The authors observed that fresh catalyst enhanced the production of C₃ and C₄ fractions compared to the thermal pyrolysis; but in the case of spent and regenerated ZSM-5, the production of C₄ fraction was even higher than in the fresh zeolite pyrolysis, while C₃ fraction was lower in the former cases. However, Lopez et al. [23], obtained similar results for spent catalyst and thermal pyrolysis as C₃ and C₄ are added (43.8 and 42.6 wt.% respectively) and was lower than those observed with fresh and regenerated ZSM-5 (57.0 and 57.1 wt.% respectively) and suggested that ZSM-5 promotes the production of such fractions.

8.3.3 Product oils composition

Similarly, the product oils were characterized using data from GC/FID analysis into fuel range (C₅ – C₁₅) and high molecular weight (C₁₆₊) compounds. The distribution of the fuel range and high molecular weight compounds for FSMP pyrolyzed using different catalysts at 500 °C, or 600 °C catalytic cracking temperature was shown in Figure 8.3-3.

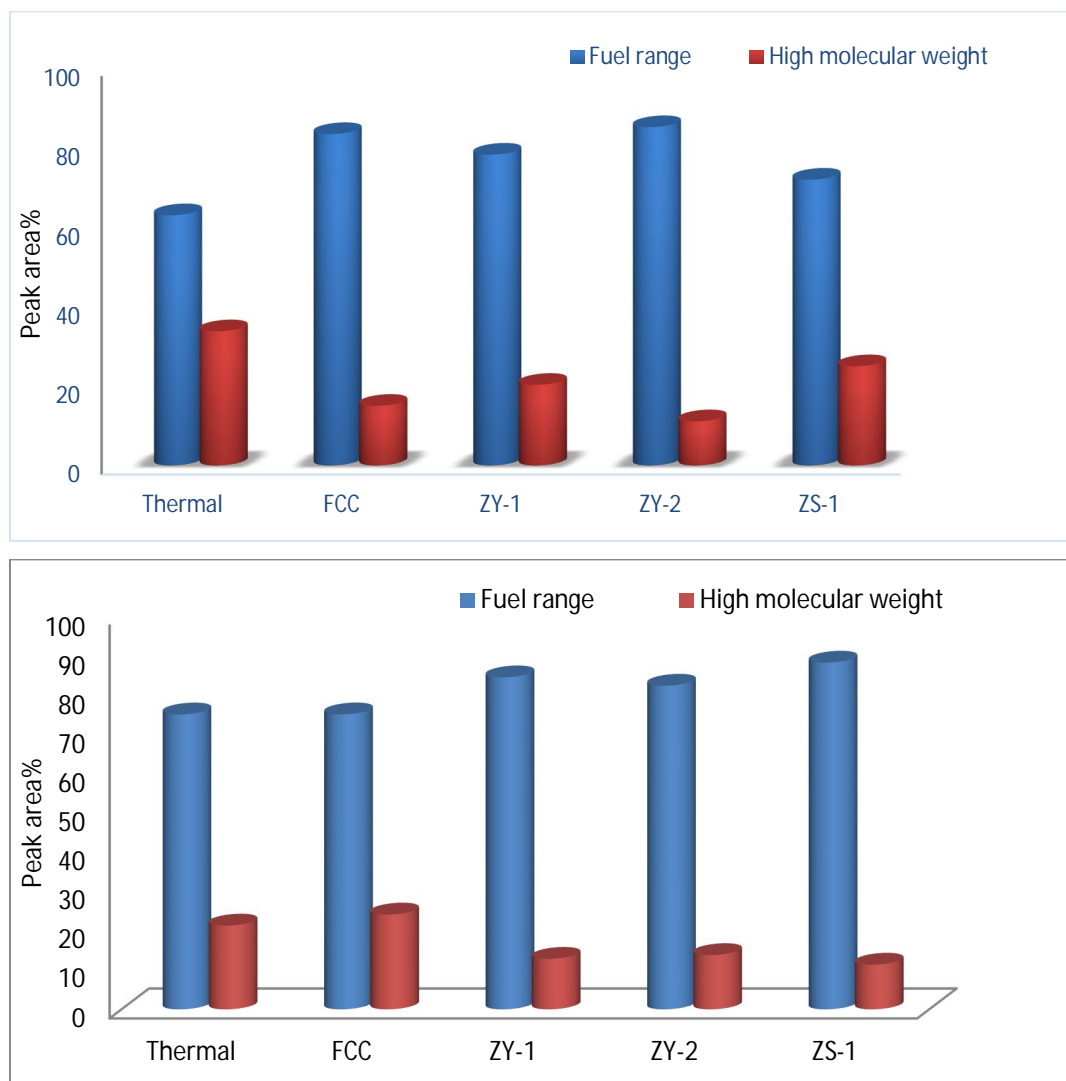


Figure 8.3-3 **Distribution of Fuel range ($C_5 - C_{15}$) and high molecular weight (C_{16+}) hydrocarbons for non-catalytic and catalytic pyrolysis of the future simulated mixture of plastics (FSMP) at (a) 500 °C and (b) 600 °C catalyst bed temperature**

The fuel range hydrocarbons increased with catalysts introduction from 62.9 to 85.1 %. The spent FCC at 500 °C catalytic cracking temperature competed with fresh zeolite catalysts and recorded the second highest yield (83.4%). The small acidic ZY-2 catalyst gave the best fuel range hydrocarbons yield (85.1%) better than ZS-1 with the same available acidic sites (Si: Al 80.1). Thus, a general trend was observed at a 500 °C catalytic cracking temperature

as high molecular weight compounds were cracked into fuel range compounds. However, there was a reoccurrence of the increase in fuel range compounds and decrease in high molecular compounds at 600 °C cracking temperature. But, this was true for all comparative to 500 °C cracking temperatures. Nevertheless, spent FCC and ZS-1 showed an increase in high molecular weight compounds and reduction in fuel range compounds at 600 °C temperature when compared to their activity at 500 °C cracking temperature. Lopez-Uriónabarrenechea et al. [24], noted that Serrano et al. [25], suggested the pyrolysis of polyolefins over the ZSM-5 catalyst leads to the reactions through an end-chain scission pathway, yielding light hydrocarbons as primary products, instead of the typical polyolefin random scission pathway that takes place in thermal pyrolysis.

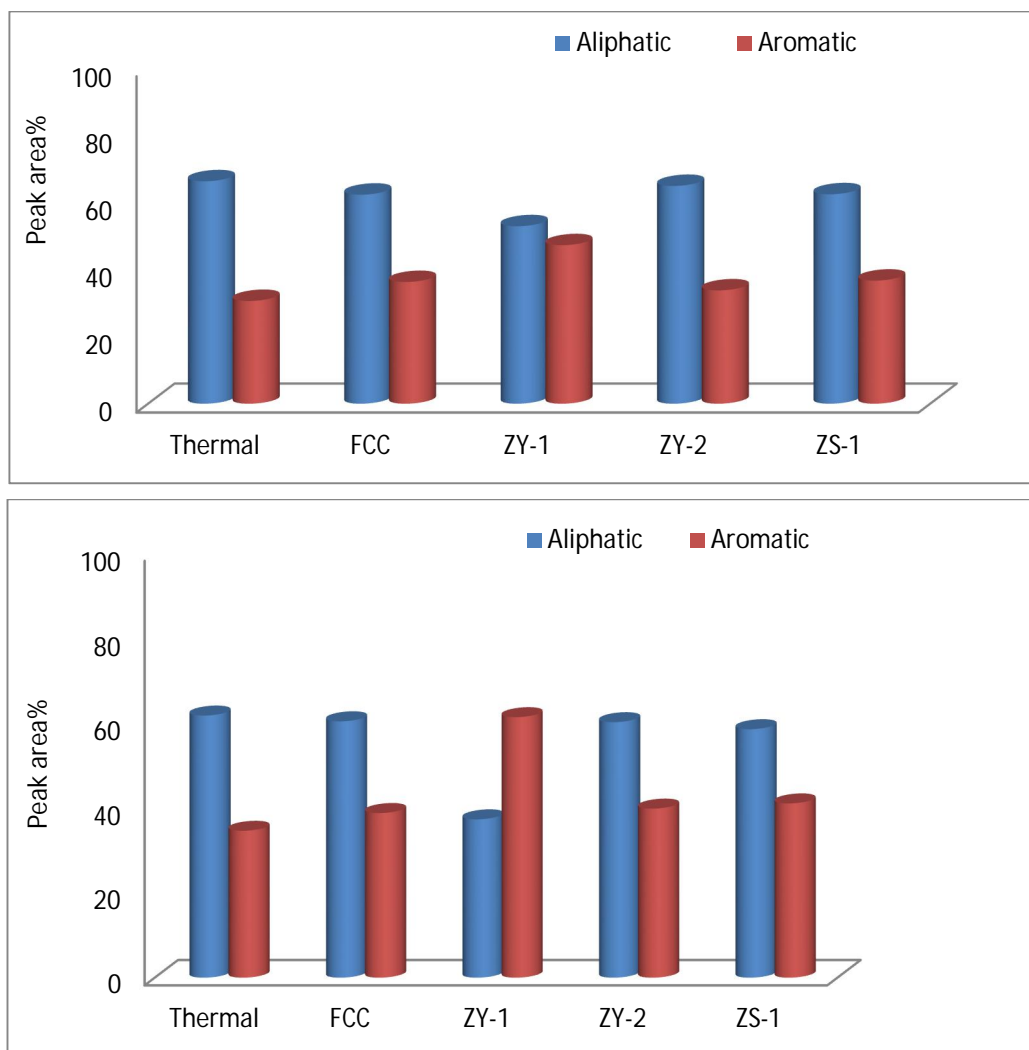


Figure 8.3-4 **Distribution of aliphatic and aromatics hydrocarbon for non-catalytic and catalytic pyrolysis of the future simulated mixture of plastics (FSMP) at (a) 500 °C and (b) 600 °C catalyst/sand bed temperature**

The distribution of the hydrocarbon compounds obtained from the pyrolysis process of SMP at different catalyst bed temperature were also compared in terms of aliphatic and aromatic compound distribution. These are shown in Figure 8.3-4. The results show that the composition of oils relative to catalyst bed temperature for the plastics were all influenced by the introduction of the catalyst. The various catalysts show their different influence at the two catalyst bed temperatures. There was also influence from the composition of the plastic sample as mentioned in section 8.2. The aromatic content of the

product oil was affected by both the catalyst type and bed temperature. So, the catalyst with the less silica-alumina ratio (ZY-1) and also higher available acidic catalytic sites gave highest aromatics yield at both bed temperatures (47.1% and 61.4% respectively for 500 °C and 600 °C). Similarly, the aromatic yield rises with an increase in temperature for all the catalysts. The spent FCC with medium acidic property due to its low silica and alumina ratio, compete favourably with other fresh zeolite catalysts recording higher (36.2%) aromatic yield than ZY-2 (33.7%) with more Si:Al ratio and low acidic catalytic site at 500 °C. However, at the higher bed temperature of 600 °C spent FCC recorded slightly lower aromatic yield (38.8%) than zeolite ZY-2 (39.8%). Likewise, the zeolite ZS-1 (ZSM-5) showed enhanced aromatic compounds production compared to ZY-2 (zeolite Y) with both having same Si: Al ratio at 500 °C catalyst bed temperature. However, at higher catalyst bed temperature of 600 °C, both catalysts ZS-1 (41.0%) and ZY-2 (39.8%) show improved aromatic compounds production and with rather a slight increase in ZS-1 aromatic compounds production. Thus, there is evidence from many kinds of literature that the pyrolysis of polyolefins can obtain high aromatics; the formation mechanism is not well agreed [24, 26]. Lopez-Urionabarrenechea et al.[24] and Lapez et al. [26], both suggested mechanism was Diels-Alder reaction followed by dehydrogenation and unimolecular cyclisation followed by dehydrogenation. Jing et al. [27], suggested that higher alkene content during catalytic pyrolysis of polyolefin plastic mixture (LDPE/PP) accelerates aromatic formation by unimolecular cyclisation reactions, followed by dehydrogenation or Diel-Alders reactions. The Si: Al ratio of the catalyst influence the product yield, Rahimi et al. [28],

reported that as the Si: Al ratio increases the yield of BTX decreases over the modified HZSM-5 zeolites.

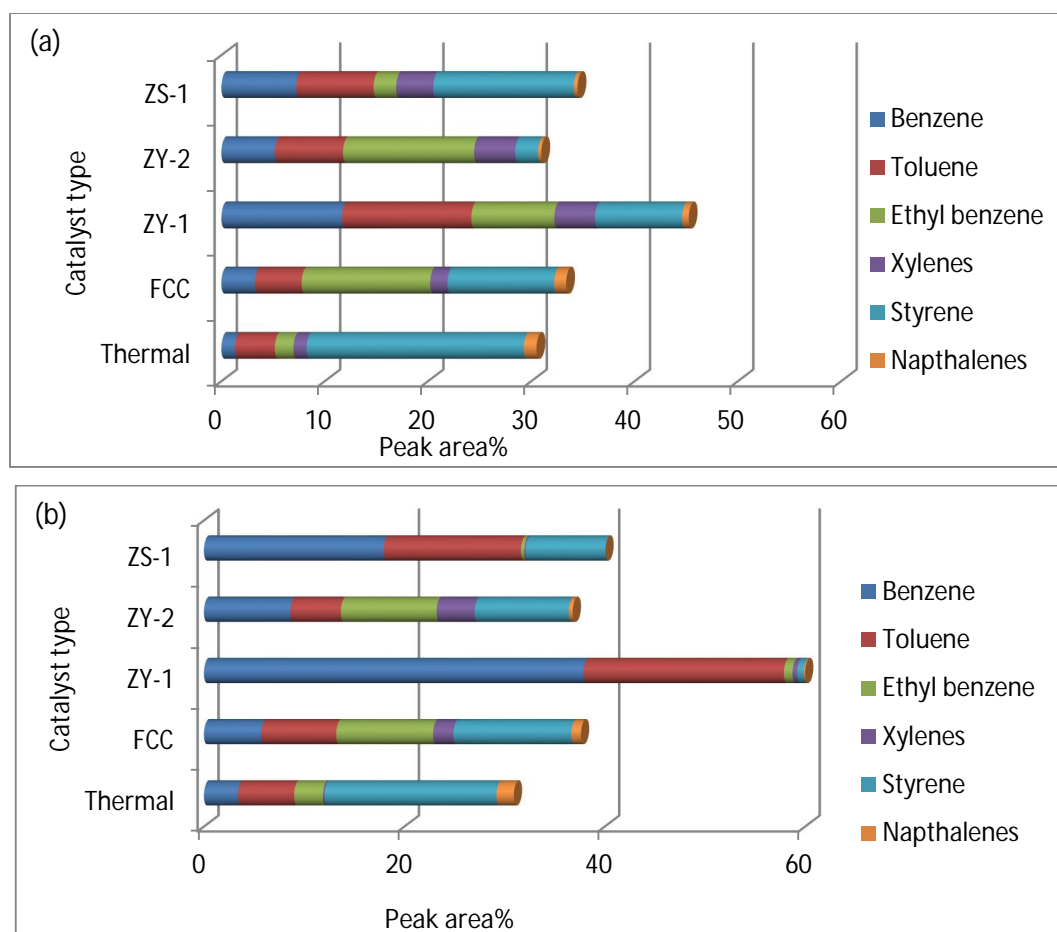


Figure 8.3-5 **Yield of some selected aromatic compounds for non-catalytic and catalytic pyrolysis of the future simulated mixture of plastics (FSMP) at (a) 500 °C and (b) 600 °C catalyst/sand bed temperature**

Figure 8.3-5 shows the peak area % of some specific aromatic hydrocarbons in relation to catalyst type and bed temperature. The percentage peak area yield of styrene for thermal pyrolysis of FSMP was 21.03% for 500 °C and 500 °C catalyst/sand bed cracking temperature, and 17.17% for 600 °C catalyst/sand bed cracking temperature. Williams et al. [29], reported a high yield of styrene with percentage mass yield of derived styrene ($53.0 \pm 1.0\%$) for 500 and 600 °C secondary cracking temperature, and 34.0 for the 700 °C cracking temperature. However, the authors observed during the upgrade of the

product oil the styrene content markedly decreased in concentration as the temperature of the secondary reactor increased from 500 to 700 °C. The reduction of styrene with the styrene dimer and trimer, and from intermolecular transfer followed by β -scission leading to the production of new radicals and alkenes. Williams et al. [29], proposed a Diel-Alder reaction for the formation of PAH from the secondary reaction of alkenes, including the alkene radicals of styrene and styrene oligomers derived from the pyrolysis of PS [29]. The Figure 8.3-6 shows the proposed Diel-Alder reaction proposed.

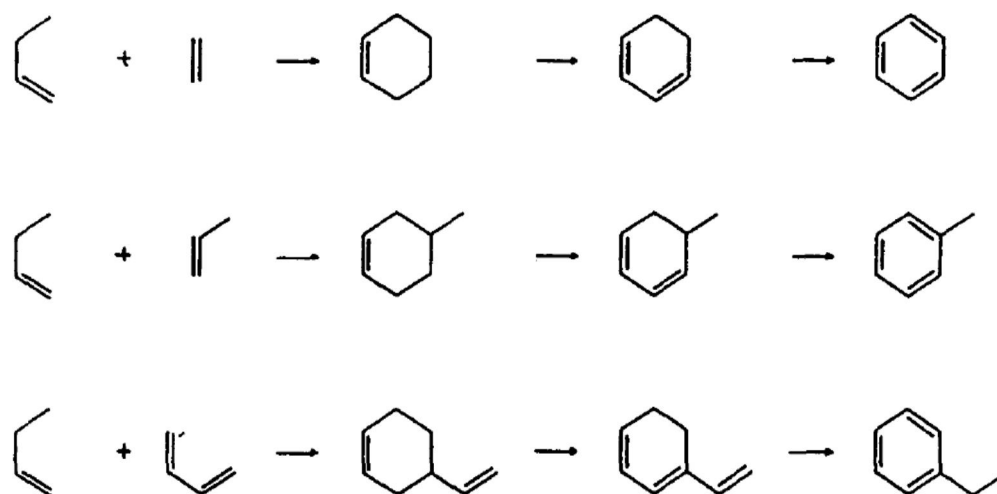


Figure 8.3-6 **Diels-Alder reaction of alkenes [29]**

The fuel properties of the product oils was examined using gas chromatography to determine the boiling range distribution of the product oils. The boiling range distribution results are shown in Figure 8.3-7. The thermal product oils showed that the substantial fraction of the oils have a boiling point range greater than 300 °C, but 600 °C bed temperature recorded a large fraction at a slightly below 300 °C boiling. Accordingly, the catalysed products oil show a shift to lower boiling points, reflecting the shift in molecular weight range as observed in Figure 8.3-3.

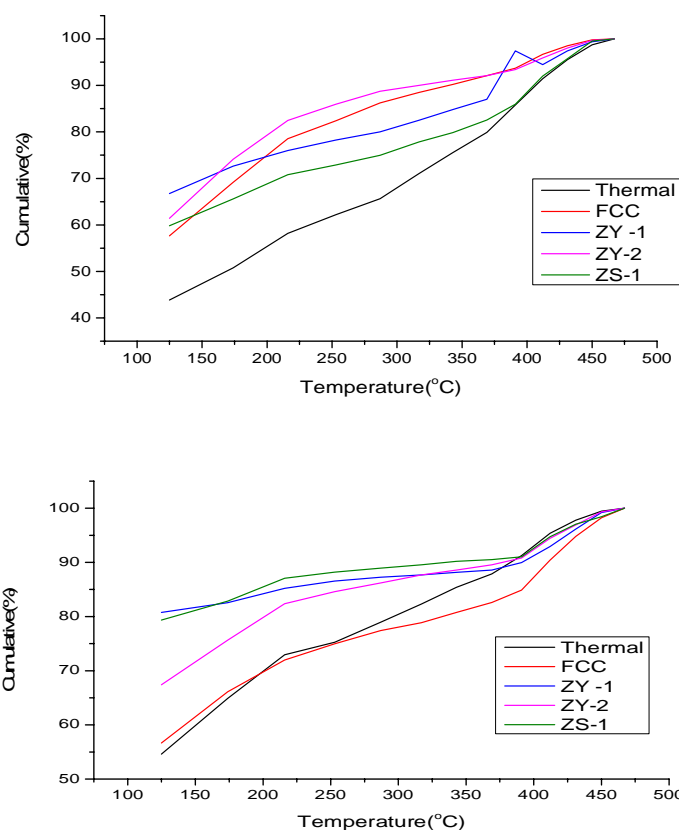


Figure 8.3-7 **Simulated distillation of (a) 500 °C and (b) 600 °C bed temperature thermal and catalytic pyrolysis product oils from FSMP**

The significant boiling range distribution for FCC, ZY-1 and ZY-2 are at a lower boiling range distribution of the product oils.

Other researchers [30] reported that the boiling range distribution for gasoline would be >95% below 150 °C. However, the catalysis product oil was between 50% and 70% at 150 °C boiling range. Hence, there was an improvement for catalysis product oil for 500 °C bed temperatures. However, the 600 °C catalyst bed temperature product oil boiling point range distribution improved slightly with the introduction of FCC catalyst, while the ZY-1, ZY-2 and ZS-1 gave much better boiling range distribution with a range between 70% and

80% below 150 °C. All these showed the resemblance to the preceded molecular weight range distribution shown in Figure 8.3-3.

Summary

The Influence of catalyst bed temperature and type of catalyst on pyrolysis of future simulated mixed plastic (FSMP) for the production of valuable liquid fuels and chemical feedstock was studied. Hence, a sample of spent FCC catalyst was used in a bench batch reactor to investigate the effect of 400 °C catalyst bed temperature for degradation of FSMP. Subsequently, the influence of catalyst type at 500 or 600 °C catalyst bed temperature using the spent FCC, two zeolite Y and one ZSM-5 catalyst was investigated. The main product of both thermal and catalytic pyrolysis obtained was gases, liquid oil and a trace amount of char. The quantity of oil produced from uncatalyzed FSMP was 79.0 wt.%, and oil yield decreased with temperature, whereas the gases consisted of hydrogen, methane, C₂-C₄ hydrocarbons, CO and CO₂. Conversely, once the catalyst was introduced, there were a drastic decrease in oil yield with a corresponding increase in gas yield. With the spent FCC shows significant catalytic activity under the three temperature conditions, gas yield massively increase with the temperature in the presence of the catalyst. The spent FCC shows that at 500 °C bed temperature highest yield of fuel range hydrocarbons (83.4%), and the highest aliphatic hydrocarbons at 400 °C (67.4%) and aromatics at 600 °C (38.8%) respectively. Accordingly, when the influence of catalyst type on pyrolysis of FSMP was considered, oil yields equally decreased with the introduction of catalyst and further decreased with temperature. Similarly, a corresponding increase in gas yield was obtained

with temperature. The caloric value decreases with temperature for thermal and all catalytic above 500 °C pyrolysis temperature. Hence, all the oil products from the catalytic test were enriched in single ring aromatic compounds i.e. benzene, ethyl benzene, xylenes, styrene and toluene. Also, the results show the presence of interaction between the individual plastic that make up the FSMP. The spent FCC compete favourably with the fresh zeolite catalyst in processing the FSMP into valuable gas and liquid products.

References

1. Williams, P.T. and Brindle, J.A., *Catalytic pyrolysis of tyres: influence of catalyst temperature*. Fuel, 2002. **81**(18): p. 2425-2434.
2. Bagri, R. and Williams, P.T., *Catalytic pyrolysis of polyethylene*. Journal of analytical and applied pyrolysis, 2002. **63**(1): p. 29-41.
3. Pinto, F., Costa, P., Gulyurtlu, I. and Cabrita, I., *Pyrolysis of plastic wastes. 1. Effect of plastic waste composition on product yield*. Journal of Analytical and Applied Pyrolysis, 1999. **51**(1-2).
4. Serrano, D.P., Aguado, J. and Escola, J.M., *Developing Advanced Catalysts for the Conversion of Polyolefinic Waste Plastics into Fuels and Chemicals*. Acs Catalysis, 2012. **2**(9): p. 1924-1941.
5. Buekens, A. and Huang, H., *Catalytic plastics cracking for recovery of gasoline-range hydrocarbons from municipal plastic wastes*. Resources, Conservation and Recycling, 1998. **23**(3): p. 163-181.
6. Huang, W.-C., Huang, M.S., Huang, C.F., Chen, C.C. and Ou, K.L. , *Thermochemical conversion of polymer wastes into hydrocarbon fuels over various fluidizing cracking catalysts*. Fuel, 2010. **89**(9).
7. Li, X., Li, J., Zhou, G., Feng, Y., Wang, Y., Yu, G., Deng, S., Huang, J. and Wang, B., *enhancing the production of renewable petrochemicals by co-feeding of biomass with plastics in catalytic fast pyrolysis with ZSM-5 zeolites*. Applied Catalysis A: General, 2014. **481**: p. 173-182.
8. Wu, C., Nahil, M.A., Miskolczi, N., Huang, J. and Williams, P.T., *Processing Real-World Waste Plastics by Pyrolysis-Reforming for Hydrogen and High-Value Carbon Nanotubes*. Environmental science & technology, 2013. **48**(1): p. 819-826.
9. Abbas-Abadi, M.S., Hagganeh, H. and McDonald, A.G., *Evaluation of pyrolysis process parameters on polypropylene degradation products*. Journal of Analytical and Applied Pyrolysis, 2014. **109**: p. 272-277.
10. Houshmand, D., Roozbehani, B. and A. Badakhshan, *Thermal and Catalytic Degradation of Polystyrene with a Novel Catalyst*. International Journal of Science & Emerging Technologies, 2013. **5**(1).
11. Boxiong, S., Chunfei, W., Binbin, G. and Rui, W., *Pyrolysis of waste tyres with zeolite USY and ZSM-5 catalysts*. Applied Catalysis B: Environmental, 2007. **73**(1): p. 150-157.
12. Achilias, D.S., Roupakias, C., Megalokonomos, P., Lappas, A.A. and Antonakou, E.V. , *Chemical recycling of plastic wastes made from*

- polyethylene (LDPE and HDPE) and polypropylene (PP)*. J Hazard Mater, 2007. 149(3): p. 536-42.
13. Achilias, D.S, Roupakias,C., Megalokonomos, P., Lappas, A.A. and Antonakou, E.V., *Chemical recycling of plastic wastes made from polyethylene (LDPE and HDPE) and polypropylene (PP)*. Journal of Hazardous Materials, 2007. **149**(3): p. 536-542.
 14. Williams, P.T. and Brindle, A.J., *Aromatic chemicals from the catalytic pyrolysis of scrap tyres*. Journal of analytical and applied pyrolysis, 2003. **67**(1): p. 143-164.
 15. Zhang, H., Nie, J., Xiao, R., Jin, B., Dong, B., and Xiao, G., *Catalytic Co-pyrolysis of Biomass and Different Plastics (Polyethylene, Polypropylene, and Polystyrene) To Improve Hydrocarbon Yield in a Fluidized-Bed Reactor*. Energy & Fuels, 2014. **28**(3): p. 1940-1947.
 16. Delgado, C., Barruetabena, L., Salas, O. and Wolf, O., *Assessment of the Environmental Advantage and Drawbacks of Existing and Emerging Polymers Recovery Processes*. Join Research Center Scientific and Technical Report, 2007. **jrc37456**: p. 264.
 17. Aguado, J., Serrano,D.P., San Miguel, G.,Castro, M.C. and Madrid, S., *Feedstock recycling of polyethylene in a two-step thermo-catalytic reaction system*. Journal of analytical and applied pyrolysis, 2007. **79**(1): p. 415-423.
 18. Venuto, P.B. and E.T. Habib Jr, *Fluid catalytic cracking with zeolite catalysts*. Marcel Dekker,Inc.New York 1979.
 19. Lee, K.-H., Noh, N.S., Shin, D.H. and Seo,Y., *Comparison of plastic types for catalytic degradation of waste plastics into liquid product with spent FCC catalyst*. Polymer Degradation and Stability, 2002. **78**(3): p. 539-544.
 20. Williams, P.T., *Yield and composition of gases and oils/waxes from the feedstock recycling of waste plastic*. Feedstock Recycling and Pyrolysis of Waste Plastics: Converting Waste Plastics into Diesel and Other Fuels, 2006: p. 285-313.
 21. Escola, J., Aguado, J., Serrano, D.P., Briones, L., Diaz de.,T,J.L., Calvo, R. and Fernandez, E., *Conversion of polyethylene into transportation fuels by the combination of thermal cracking and catalytic hydroreforming over Ni-supported hierarchical beta zeolite*. Energy & Fuels, 2012. **26**(6): p. 3187-3195.
 22. Lin, Y.H. and Yang, M.H.,*Catalytic conversion of commingled polymer waste into chemicals and fuels over spent FCC commercial catalyst in a fluidised-bed reactor*. Applied Catalysis B: Environmental, 2007. **69**(3): p. 145-153.

23. Lopez, A., de Marco, I., Cabellero, B.M., Adados, A. and Laresgoiti, M.F., *Deactivation and regeneration of ZSM-5 zeolite in catalytic pyrolysis of plastic wastes*. Waste management, 2011. **31**(8): p. 1852-1858.
24. Lopez-Urionabarrenechea, A., de Morco, I., Cabellero, B.M. Laresgoiti, M.F. and Adrados, A. *Catalytic stepwise pyrolysis of packaging plastic waste*. Journal of Analytical and Applied Pyrolysis, 2012. **96**(0): p. 54-62.
25. Serrano, D., Guado, J., Escola, J.M., and Rodriguez, J.M., *Influence of nanocrystalline HZSM-5 external surface on the catalytic cracking of polyolefins*. Journal of analytical and applied pyrolysis, 2005. **74**(1): p. 353-360.
26. López, A., De Marco, I., Cabellero, BM, Laresgoiti, MF and Adrados, A, *Influence of time and temperature on pyrolysis of plastic wastes in a semi-batch reactor*. Chemical Engineering Journal, 2011. **173**(1): p. 62-71.
27. Jing, X., Zhao, Y., Wen, H., and Xu, Z., *Interactions between low-density polyethylene (LDPE) and polypropylene (PP) during the mild cracking of polyolefin mixtures in a closed-batch reactor*. Energy & Fuels, 2013. **27**(10): p. 5841-5851.
28. Rahimi, N. and Karimzadeh, R., *Catalytic cracking of hydrocarbons over modified ZSM-5 zeolites to produce light olefins: A review*. Applied Catalysis A: General, 2011. **398**(1): p. 1-17.
29. Williams, P.T., Horne, P.A. and Taylor, D.T., *Polycyclic aromatic hydrocarbons in polystyrene derived pyrolysis oil*. Journal of analytical and applied pyrolysis, 1993. **25**: p. 325-334.
30. Muhammad, C., Onwudili, J.A. and P.T. Williams, *Thermal Degradation of Real-World Waste Plastics and Simulated Mixed Plastics in a Two-Stage Pyrolysis-Catalytic Reactor for Fuel Production*. Energy & Fuels, 2015. **29**(4): p. 1601-1609.

Chapter 9 CONCLUSIONS AND SUGGESTIONS FOR FUTURE WORK

The research presented in this thesis has been divided into several sections. Different commercial zeolite catalysts were tested during the pyrolysis of different single plastics and mixed plastic samples that are often found in municipal solid wastes, in order to produce upgraded liquid fuels and valuable chemicals. A two stage pyrolysis-catalysis reaction system was used to carry out the experiments described in this research work.

The main aim of the work was the improvement of the thermochemical process which focused on catalysis for production of good quality liquid products. A series of different commercial zeolite catalysts and one spent FCC catalyst were used in the experiments. The range of catalysts had different physical characteristics such as surface area and silica-alumina ratios. In addition, some of the catalysts were in powdered form, while others were in the form of pellets.

9.1 General conclusion

The following conclusions were addressed considering the order of the Chapters and results in this research work.

9.1.1 Thermal and Catalytic Pyrolysis of Waste Plastic from Electrical and Electronic Equipment

The effects of two zeolite catalysts, namely Zeolite Y and ZSM-5 were tested on the catalytic degradation of waste electric and electronic equipment (WEEE) plastics, and two main plastic components of WEEE plastics i.e. HIPS

and ABS. The work showed that thermal (non-catalytic) pyrolysis of the styrene-based plastics produced from commercial waste electrical and electronic equipment produced mainly an oil product containing mostly styrene. The influence of the addition of a zeolite catalyst to the process was mainly dependent on the Si-Al characteristics of the zeolite catalyst used. Zeolite catalyst with a lower Si-Al ratio (Y zeolite) produced a higher conversion of the styrene to other aromatic products, notably benzene and toluene. Comparison of the catalytic pyrolysis of high impact polystyrene (HIPS) and acrylonitrile-butadiene-styrene (ABS) with the WEEE plastics results suggests that the WEEE plastics consisted of mostly, but not exclusively HIPS and ABS plastics.

9.1.2 Influence of Zeolite Catalysts Characteristics on the Catalytic Pyrolysis of Waste High-Density Polyethylene

The influence of six zeolites catalysts were tested on the catalytic pyrolysis of waste high-density polyethylene (HDPE) in a two-stage pyrolysis-catalysis fixed bed reactor. The zeolite catalysts used were of different characteristics including, surface areas and silica: alumina ratios in addition to the different crystal structures of Y and ZSM-5 zeolites. The pyrolysis products included oil, gas and negligible char. The quantity of oil produced from non-catalysed pyrolysis of HDPE was more than 74 wt%, and the gases (nearly the balance) consisted of hydrogen, methane and C₂-C₄ hydrocarbons. However, when the influence of catalyst surface area of the catalysts was investigated, there was a decrease of between 15-30 wt. % in oil yield with introduction of the catalysts and a corresponding increase in gas yield ranging between 38-50wt. %. These processes are increased with increase in catalyst surface area. The

catalysed oil was enhanced in the concentration of benzene ethylbenzene, xylenes, styrene and toluene. The catalyst zeolite Y with the higher surface area ($935 \text{ m}^2 \text{ g}^{-1}$) produced a lower conversion of the higher molecular weight material to single ring aromatic compounds compared to the zeolite Y catalyst with the smaller surface area ($705 \text{ m}^2 \text{ g}^{-1}$). The high-value fuel hydrocarbon gases improved with the addition of the catalyst and was further enhanced with an increase in surface area. Likewise, aromatic compounds obtained in the pyrolysis oil show a similar trend, i.e. decrease in aromatic content and single ring aromatic compounds with the increase in the surface area.

Accordingly, when the influence of the silica-alumina ratio of the three Y zeolites was investigated, the results showed reduction in the low molecular weight hydrocarbons and aromatic compound contents with an increase in the silica-alumina ratio. However, the single ring aromatic compounds obtained in the pyrolysis oil decrease with an increase in the silica-alumina ratio. Decrease in catalytic activity which comes with increase in silica-alumina ratio perhaps might be the reason for the decrease in single ring aromatic compounds. But, the catalyst (Z-8) with the least catalytic activity and high silica-alumina ratio shows better activity due to perhaps its high surface area and low micropore volume.

Similarly, as the influence of the silica-alumina ratio of the three zeolites ZSM-5 is considered, the results obtained showed a reduction in the low molecular weight hydrocarbons and aromatic compound contents with an increase in the silica-alumina ratio. However, the single ring aromatic compounds obtained in the oil product also increase with the increase in the silica-alumina ratio. Thus, a small silica-alumina ratio enhanced the catalytic activity of the ZSM-5

catalyst for production of more volatile hydrocarbon and aromatic compound. The fuel properties investigated showed improvement with the introduction of the catalyst.

Overall, the results suggest that there was some influence of the surface area and the Si: Al ratio on the conversion of HDPE to more valuable products such as fuel range hydrocarbons and chemicals. However, in this study, the zeolite catalysts were obtained commercially, and the composition of the catalysts could not be controlled. Therefore, it was not possible to undertake a thorough study of the influence of only surface area or the Si: Al ratio. For example, within each set of Y zeolite or ZSM-5 zeolite, there was some variation in the catio, for example, H^+ or NH_4^+ , variation in Na_2O content and differences in micropore and mesopore volumes.

9.1.3 Thermal degradation of real-world waste plastics and simulated mixed plastic for fuel production

A pyrolysis-catalysis investigation of real-world mixed plastics, simulated mixed plastic (SMP), and four virgin plastics in the presence of a zeolite HZSM-5 catalyst was investigated. A high yield of oil/wax was obtained for the plastic materials in the range of 81–97 wt. % during thermal pyrolysis. The oil product yields decreased with the addition of the catalyst to between 44 and 51 wt. %, depending on the plastic, with a resultant increase in gas yield. However, the composition of the pyrolysis-catalysis oils significantly increased in aromatic hydrocarbon content mainly single-ring aromatic hydrocarbons such as benzene, toluene, ethylbenzene, xylenes, and styrene. While there was a shift of the high molecular weight hydrocarbons

(C₁₆₊) to fuel range hydrocarbons (C₅–C₁₅). The results showed that there was an interaction between the plastics in the SMP mixture resulting in a yield of gases that were higher than expected compared to the proportions of each gas generated by the individual virgin polymers. Also, the aromatic hydrocarbon content of the oils from the simulated mixture of plastics (SMP) was also higher than expected.

9.1.4 Pyrolysis-Catalysis of real-world waste plastics and future simulated mixed plastic (FSMP) for valuable production fuels and chemical feedstock

The influence of spent FCC catalyst on pyrolysis-catalysis of real-world waste plastics and future simulated mixed plastics (FSMP) for valuable production of fuels and chemical feedstock was investigated. Comparison with three fresh zeolites catalysts was also investigated. The main products of pyrolysis obtained are hydrocarbon gases, liquid oil and a trace amount of char. The quantity of oil produced from uncatalyzed simulated (future) mixed plastics was 79 wt.% and real-world waste plastics 81.50 wt.%, and the gases consisted of hydrogen, methane, C₂-C₄ hydrocarbons for both, but additional gases i.e. CO and CO₂ were also produced due to the presence of PET. However, when the catalyst was introduced, there were a decrease of between 9-15 wt. percent in oil yield with a corresponding increase in gas yield ranging from 6-15 wt. % that increased with catalyst amount. The oil from the catalytic test was enriched in single ring aromatic compounds i.e. benzene-ethyl benzene, xylenes, styrene and toluene. In addition, the results show overall include the interaction between the individual plastic that make up the

simulated mixed plastic. Therefore, the spent FCC catalysts showed strong catalytic activity for the pyrolysis of real-world and FSMP for the production of liquid fuels and valuable chemicals.

9.1.5 Influence of catalyst bed temperature and catalyst type on pyrolysis of future simulated mixed plastics (FSMP)

The Influence of catalyst bed temperature and type of catalyst on pyrolysis of future simulated mixed plastic (FSMP) for the production of valuable liquid fuels and chemical feedstock was also investigated. In the previous sections, the catalyst bed temperature was maintained throughout at 500 °C, so in these sets of experiments, the catalyst bed temperature was varied from 400 °C to 600 °C. In these tests, the pyrolysis temperature was still kept at 500 °C. Subsequently, the bed temperature of 400 °C led to a marginal performance with spent FCC, even though results were better (in terms of conversion) compared to the non-catalytic tests, which resulted in the deposition of melted plastics on the cooler bed temperature. Therefore, with the three catalysts, the influence of bed temperature was investigated at 500 °C or 600 °C. The main products of both thermal and catalytic pyrolysis obtained are gases, liquid oil and a trace amount of char. The oil yield from the non-catalytic test decreased with temperature, whereas the gases produced increased. Likewise, gas yield enhanced with an increase in catalyst bed temperature. Invariably, once the catalyst was introduced, there were a drastic decrease in oil yield with a corresponding increase in gas yield, these happened with all the catalysts and with the different bed temperatures. The spent FCC showed significant catalytic activity under the three temperatures but especially at 500 °C and

600 °C. with gas yields massively increasing with temperature in the presence of the catalyst. The test with the spent FCC at 500 °C bed temperature, produced the highest yield of fuel range hydrocarbons (83.38%), whereas the test at 600 °C gave the highest aromatic yields (38.78%) respectively. However, when the influence of the catalyst type on pyrolysis FSMP was considered, the oil yield similarly decreased with the introduction of the catalyst. Also there was a further decrease with increased bed temperature. In addition, a corresponding increase in gas yield was obtained with temperature. The calorific value of the product gases decreased with temperature for thermal and all catalytic above 500 °C pyrolysis temperature due to the enhanced yields of hydrogen and methane compared to the C₂-C₄ hydrocarbon gases. Hence, all the oil products from the catalytic test were enriched in single ring aromatic compounds i.e. benzene, ethyl benzene, xylenes, styrene and toluene. The zeolite Y catalyst with lowest Si:Al ratio performed better than the rest of the catalysts tested, indicating that this property was influential during the pyrolysis-catalysis process investigated. It is fair to say though that the spent FCC competed favourably with the fresh zeolite catalyst in transforming the FSMP into valuable gas and liquid products.

9.1.6 General remarks

In general, it was found that the two-stage pyrolysis-catalysis of waste plastics in a fixed bed reactor at 500 °C reaction temperature as established in this work could be an important technique to treat waste plastics. The use of zeolite catalyst for the catalytic pyrolysis processes has demonstrated that the versatile application of the catalyst could be exploited to upgrade the pyrolysis

oil of waste plastics for more useful applications in the fuels and chemical industry. The silica-alumina ratio of the catalyst has demonstrated the strong influence on the overall properties of the catalyst used. The product oils of pyrolysis-catalysis showed remarkable improvement in quality of both fuel properties (boiling range temperature distribution), aromatics and fuel range hydrocarbons. There was strong evidence that the individual plastics used to prepare simulated mixed plastic interacted among themselves during the thermochemical process, possibly leading to improved overall properties of the product oils and gases. Finally, 500 °C catalyst bed temperature was found to be the optimum reaction temperature for the yield of quality product liquids for pyrolysis-catalysis of waste plastic into liquid fuels.

9.2 Future work

During the development of this research work, some of the initially identified objectives were either removed or modified and, so also additional aims were included according to the experimental results obtained. Therefore, it is suggested to perform certain tasks to achieve some of these goals. A brief description of the future work suggested given below.

9.2.1 Life cycle studies of the catalysts used

The zeolite catalysts tested in this research work using plastics samples as mentioned earlier yielded very low carbon deposition according to TPO studies. Thus, there is the need to investigate the deactivation properties of the catalyst under the optimum reaction condition ascertained in this work. For example, this could be through the repeated reuse of the catalysts or through increasing the reaction residence times. Further TGA/TPO and SEM studies

for the re-used reacted catalyst need to be done to test its potential for regeneration and reuse.

9.2.2 Use of mesoporous zeolite catalyst and metallic doping of the catalyst

The use of mesoporous zeolite catalyst could be suggested to explore the high pore size properties of these catalysts for the production of high-quality liquid products. Likewise, metal doping of the zeolite catalyst could be proposed to improve the catalytic activity of the catalyst. The transition metals such as nickel and Pd could be used to enhance some secondary reactions for high octane number fuel productions.

9.2.3 Pyrolysis-catalysis of contaminated plastics and co-pyrolysis of biomass and plastics

The two-stage pyrolysis-catalysis system used could be a potential success for catalytic degradation of contaminated plastics and co-pyrolysis of biomass and plastics. Hence, in both cases the pyrolysis vapour produced in the top furnace and swept downwardly over catalyst bed will minimize catalyst deactivation potential of the vapour compared to a bed of mixed catalyst and feedstock. Co-pyrolysis of waste plastics and biomass may become a veritable way to obtain liquid fuels with the desired consistent and synergistic properties in the future. Thus, the process might be achieved by carefully determining the appropriate plastic/biomass ratios through rigorous experimentation. The plastics component being more energy dense could provide much needed improvement in the fuel properties in biomass bio-oil.